GRAPHENE-ENHANCED ELECTROCHEMICAL SENSING PLATFORMS

EDITED BY: Aimin Yu, Li Fu and Fatemeh Karimi
PUBLISHED IN: Frontiers in Chemistry

frontiers Research Topics

frontiers

ISSN 1664-8714
ISBN 978-2-88974-112-0
DOI 10.3389/978-2-88974-112-0

About Frontiers

Frontiers is more than just an open-access publisher of scholarly articles: it is a pioneering approach to the world of academia, radically improving the way scholarly research is managed. The grand vision of Frontiers is a world where all people have an equal opportunity to seek, share and generate knowledge. Frontiers provides immediate and permanent online open access to all its publications, but this alone is not enough to realize our grand goals.

Frontiers Journal Series

The Frontiers Journal Series is a multi-tier and interdisciplinary set of open-access, online journals, promising a paradigm shift from the current review, selection and dissemination processes in academic publishing. All Frontiers journals are driven by researchers for researchers; therefore, they constitute a service to the scholarly community. At the same time, the Frontiers Journal Series operates on a revolutionary invention, the tiered publishing system, initially addressing specific communities of scholars, and gradually climbing up to broader public understanding, thus serving the interests of the lay society, too.

Dedication to Quality

Each Frontiers article is a landmark of the highest quality, thanks to genuinely collaborative interactions between authors and review editors, who include some of the world's best academicians. Research must be certified by peers before entering a stream of knowledge that may eventually reach the public - and shape society; therefore, Frontiers only applies the most rigorous and unbiased reviews.
Frontiers revolutionizes research publishing by freely delivering the most outstanding research, evaluated with no bias from both the academic and social point of view. By applying the most advanced information technologies, Frontiers is catapulting scholarly publishing into a new generation.

What are Frontiers Research Topics?

Frontiers Research Topics are very popular trademarks of the Frontiers Journals Series: they are collections of at least ten articles, all centered on a particular subject. With their unique mix of varied contributions from Original Research to Review Articles, Frontiers Research Topics unify the most influential researchers, the latest key findings and historical advances in a hot research area! Find out more on how to host your own Frontiers Research Topic or contribute to one as an author by contacting the Frontiers Editorial Office: frontiersin.org/about/contact

GRAPHENE-ENHANCED ELECTROCHEMICAL SENSING PLATFORMS

Topic Editors:
Aimin Yu, Swinburne University of Technology, Australia
Li Fu, Hangzhou Dianzi University, China
Fatemeh Karimi, Quchan University of Advanced Technology, Iran

Citation: Yu, A., Fu, L., Karimi, F., eds. (2022). Graphene-Enhanced Electrochemical Sensing Platforms. Lausanne: Frontiers Media SA. doi: 10.3389/978-2-88974-112-0

Table of Contents

04 ***Editorial: Graphene-Enhanced Electrochemical Sensing Platforms***
Li Fu, Fatemeh Karimi and Aimin Yu

06 ***Preparation of Graphene Oxide-Embedded Hydrogel as a Novel Sensor Platform for Antioxidant Activity Evaluation of* Scutellaria baicalensis**
Shuai Yan, Yinzi Yue, Li Zeng, Lianlin Su, Min Hao, Wei Zhang and Xiaopeng Wang

13 ***Detection of Imatinib Based on Electrochemical Sensor Constructed Using Biosynthesized Graphene-Silver Nanocomposite***
Zhen Wu, Jingjing Liu, Minmin Liang, Haoyue Zheng, Chuansheng Zhu and Yan Wang

20 ***A Novel Graphene-Based Nanomaterial Modified Electrochemical Sensor for the Detection of Cardiac Troponin I***
Jing Li, Shenwei Zhang, Li Zhang, Yu Zhang, Hua Zhang, Chuanxi Zhang, Xuexi Xuan, Mingjie Wang, Jinying Zhang and Yiqiang Yuan

28 ***Graphene-Assisted Sensor for Rapid Detection of Antibiotic Resistance in* Escherichia coli**
Chunlei Li and Feng Sun

34 ***A Methylene Blue Assisted Electrochemical Sensor for Determination of Drug Resistance of* Escherichia coli**
Rongshuai Duan, Xiao Fang and Dongliang Wang

41 ***Evaluation of Peroxidase in Herbal Medicines Based on an Electrochemical Sensor***
Yinzi Yue, Lianlin Su, Min Hao, Wenting Li, Li Zeng and Shuai Yan

47 ***A New Electrochemical Detection Technique for Organic Matter Content in Ecological Soils***
Jinping Liu, Tao Yang, Jiaqi Xu and Yankun Sun

54 ***Label-free Electrochemical Impedance Spectroscopy Aptasensor for Ultrasensitive Detection of Lung Cancer Biomarker Carcinoembryonic Antigen***
Yawei Wang, Lei Chen, Tiantian Xuan, Jian Wang and Xiuwen Wang

62 ***The Impact of Recent Developments in Electrochemical POC Sensor for Blood Sugar Care***
Wei Li, Weixiang Luo, Mengyuan Li, Liyu Chen, Liyan Chen, Hua Guan and Mengjiao Yu

69 ***Graphene-Assisted Electrochemical Sensor for Detection of Pancreatic Cancer Markers***
Zhenglei Xu, Minsi Peng, Zhuliang Zhang, Haotian Zeng, Ruiyue Shi, wXiaoxin Ma, Lisheng Wang and Bihong Liao

74 ***Recent Development of Graphene Based Electrochemical Sensor for Detecting Hematological Malignancies-Associated Biomarkers: A Mini-Review***
Shougang Wei, Xiuju Chen, Xinyu Zhang and Lei Chen

80 ***Carbon Material Based Electrochemical Immunosensor for Gastric Cancer Markers Detection***
Zhuliang Zhang, Minsi Peng, Defeng Li, Jun Yao, Yingxue Li, Benhua Wu, Lisheng Wang and Zhenglei Xu

frontiers in Chemistry

EDITORIAL
published: 02 December 2021
doi: 10.3389/fchem.2021.815981

Editorial: Graphene-Enhanced Electrochemical Sensing Platforms

Li Fu[1]*, *Fatemeh Karimi*[2] *and Aimin Yu*[3]

[1]Key Laboratory of Novel Materials for Sensor of Zhejiang Province, College of Materials and Environmental Engineering, Hangzhou Dianzi University, Hangzhou, China, [2]Department of Chemical Engineering and Energy, Quchan University of Technology, Quchan, Iran, [3]Department of Chemistry and Biotechnology, Faculty of Science, Engineering and Technology, Swinburne University of Technology, Hawthorn, VIC, Australia

Keywords: sensor, graphene, cancer, soil, antioxidant, drug detection, drug resisitance

Editorial on the Research Topic

Graphene-Enhanced Electrochemical Sensing Platforms

Graphene is a two-dimensional carbon material with very wide applications. Its emergence has had a very significant impact on the field of electrochemical sensing. The most direct impact is about the large number of electrochemical sensors modified with graphene materials have been reported. The purpose of this Research Topic is to attract scientists from different fields to provide individual research on graphene electrochemical sensors. This Research Topic attracted a total of 12 papers, including eight research articles and four mini-reviews. Not surprisingly, this topic has attracted research efforts in different fields, including drug detection, investigation of antioxidant properties, analysis of soil organic matter content and characterization of antimicrobial properties.

The detection of cancer indicators is the most frequent research direction in this Research Topic. Zhang et al. summarized the development of carbon nanomaterials for electrochemical analysis of gastric cancer markers, with particular emphasis on the important work of graphene in recent years. Carcinoembryonic antigen (CEA), carbohydrate antigen (CA) 125, CA19-9, CA72-4 and several miRNAs were presented in detail as the most important gastric cancer markers. Wei et al. summarized the recent development of graphene-based electrochemical sensors for detecting hematological malignancies-associated biomarkers. They highlighted electrochemical sensors in RNA biomarkers and protein-based markers. In addition, this mini-review specifically contains label-free electrochemical sensors for the detection of DNA and CTC markers in blood tumors. A mini-review was also contributed by (Xu et al.). They focused on the analytical application of graphene electrochemical sensors in pancreatic cancer detection. They also discussed the use of CEA detection in pancreatic cancer screening. Due to the specificity of pancreatic cancer, they also discuss the application of graphene-assisted electrochemical sensors in mutant K-Ras gene detection. In addition to the review, this Research Topic also attracted a research paper on cancer indicator detection. Wang et al. reported an integrated electrode system on an FR-4 glass fiber. Graphene electrode has been used as a working electrode. The proposed electrochemical sensor can be used for linear sensing of CEA in the range of 0.2–15.0 ng/ml with a limit of detection of 0.085 ng/ml. From the above studies, it is clear that there is no particularly strong specificity between cancer indicators and cancer, for example, CEA can be used as an indicator for many different cancers. Therefore, for the diagnosis of cancer, a combination of multiple indicators is often required. Therefore, how to establish an electrochemical sensor for multi-indicator detection is an important direction for this technology in the future. This Research Topic not only attracts detection for cancer indicators, but also for cancer drugs. Wu et al. reported a biosynthesized graphene-silver nanocomposite for imatinib detection.

The detection of indicators has a very important place in clinical research. In addition to cancer indicators, troponin I and blood glucose are very important indicators in the clinical diagnosis of myocardial infarction and diabetes, respectively. In this Research Topic, Li et al. reported a silver nanoparticles/MoS_2/reduced graphene oxide electrochemical sensor for cardiac troponin I detection.

OPEN ACCESS

Edited and reviewed by:
Nosang Vincent Myung, University of Notre Dame, United States

***Correspondence:**
Li Fu
fuli@hdu.edu.cn

Specialty section:
This article was submitted to Electrochemistry, a section of the journal Frontiers in Chemistry

Received: *16 November 2021*
Accepted: *18 November 2021*
Published: *02 December 2021*

Citation:
Fu L, Karimi F and Yu A (2021) Editorial: Graphene-Enhanced Electrochemical Sensing Platforms. Front. Chem. 9:815981. doi: 10.3389/fchem.2021.815981

Meanwhile, another mini-review summarizes the application of electrochemical POC sensors in blood glucose detection (Li et al.). The POC blood glucose sensor is a product that has been commercialized, but still has some application disadvantages. Graphene may be able to provide new solutions to these problems.

Graphene has become a platform for evaluating microbial resistance due to its excellent electrical properties and its two-dimensional structure that allows microorganisms to be sequestered. This Research Topic has attracted two articles in this field. Li and Sun reported a graphene-assisted electrochemical sensor for antibiotic resistance detection in *Escherichia coli*. Duan et al. also reported an electrochemical sensor for drug resistance of *Escherichia coli*. However, methylene blue was used as a probe in this work.

In addition to the common electrochemical sensors mentioned above, this Research Topic has attracted three interesting works related to the agricultural and phytological fields. Yue et al. used an electrochemical sensor for peroxidase evaluation in herbal medicines. The reduction of hydrogen peroxide by a graphene-assisted sensor was used as a signal. Yan et al. reported a graphene oxide-embedded hydrogel for antioxidant activity evaluation of *Scutellaria baicalensis*. Liu et al. reported a pioneer work. For the first time, they used graphene-modified electrodes for the detection of organic matter content in the soil.

AUTHOR CONTRIBUTIONS

All authors listed have made a substantial, direct and intellectual contribution to the work, and approved it for publication.

ACKNOWLEDGMENTS

We would like to thank all the authors and reviewers for their dedication and time in this Frontiers Research Topic.

Conflict of Interest: The authors declare that the research was conducted in the absence of any commercial or financial relationships that could be construed as a potential conflict of interest.

Publisher's Note: All claims expressed in this article are solely those of the authors and do not necessarily represent those of their affiliated organizations, or those of the publisher, the editors and the reviewers. Any product that may be evaluated in this article, or claim that may be made by its manufacturer, is not guaranteed or endorsed by the publisher.

frontiers in Chemistry

ORIGINAL RESEARCH
published: 16 April 2021
doi: 10.3389/fchem.2021.675346

Preparation of Graphene Oxide-Embedded Hydrogel as a Novel Sensor Platform for Antioxidant Activity Evaluation of *Scutellaria baicalensis*

Shuai Yan[1,2†], *Yinzi Yue*[3†], *Li Zeng*[3], *Lianlin Su*[4], *Min Hao*[5], *Wei Zhang*[1*] and *Xiaopeng Wang*[2*]

[1] State Key Laboratory of Quality Research in Chinese Medicine, Macau University of Science and Technology, Macau, China, [2] Suzhou TCM Hospital Affiliated to Nanjing University of Chinese Medicine, Suzhou, China, [3] First Clinical Medical College, Nanjing University of Chinese Medicine, Nanjing, China, [4] School of Pharmacy, Nanjing University of Chinese Medicine, Nanjing, China, [5] School of Pharmacy, Zhejiang Chinese Medicine University, Hangzhou, China

OPEN ACCESS

Edited by:
Fatemeh Karimi,
Quchan University of Advanced Technology, Iran

Reviewed by:
Somaye Cheraghi,
Shahid Bahonar University of Kerman, Iran
Mehdi Baghayeri,
Hakim Sabzevari University, Iran

***Correspondence:**
Wei Zhang
wzhang@must.edu.mo
Xiaopeng Wang
wxpeng2004@163.com

[†] These authors have contributed equally to this work

Specialty section:
This article was submitted to Electrochemistry, a section of the journal Frontiers in Chemistry

Received: 03 March 2021
Accepted: 22 March 2021
Published: 16 April 2021

Citation:
Yan S, Yue Y, Zeng L, Su L, Hao M, Zhang W and Wang X (2021) Preparation of Graphene Oxide-Embedded Hydrogel as a Novel Sensor Platform for Antioxidant Activity Evaluation of Scutellaria baicalensis. Front. Chem. 9:675346. doi: 10.3389/fchem.2021.675346

Antioxidation is very important in medicine and food. The current evaluation technologies often have many shortcomings. In this work, an improved electrochemical sensing platform for the evaluation of antioxidant activity has been proposed. A hydrogel was prepared based on graphene oxide, zinc ions, and chitosan. Zinc ions play the role of crosslinking agents in hydrogels. The structure of chitosan can be destroyed by injecting hydrogen peroxide into the hydrogel, and the free zinc ions can diffuse to the surface of the electrode to participate in the electrochemical reaction. This electrochemical sensor can evaluate the antioxidant activity by comparing the current difference of zinc reduction before and after adding the antioxidant. With the help of graphene oxide, this hydrogel can greatly enhance the sensing effect. We conducted tests on 10 real samples. This proposed electrochemical platform has been successfully applied for evaluating the antioxidant activity of *Scutellaria baicalensis,* and the results were compared to those obtained from the 2,2-diphenyl-1-picrylhydrazyl-based traditional analysis technique.

Keywords: antioxidant activity, *Scutellaria baicalensis*, electrochemical analysis, hydrogel, graphene oxide

INTRODUCTION

Antioxidants are substances that effectively inhibit the oxidation of free radicals when present in low concentrations. They can capture excess free radicals, neutralize them, and reduce the damage caused by oxidative stress. Antioxidants can effectively clean up excess free radicals in the body and prevent various diseases (Apak et al., 2018; Moteshakeri et al., 2018; Aghdam et al., 2019; Karimi-Maleh et al., 2021a). Antioxidants can be divided into exogenous antioxidants and endogenous antioxidants. Among them, exogenous antioxidants are the antioxidants that are taken into the human body through food, such as flavonoids, vitamins, hormones, phenolic acids, and esters (Brainina et al., 2019; Karimi-Maleh et al., 2019; Masek et al., 2019; Kurtulbaş et al., 2020).

Many studies have proved that Chinese herbal medicine has antioxidant active ingredients that can clean up and reduce the damage of the free radicals in the organism (Han et al., 2017; Jin et al., 2018; Malekmohammad et al., 2019). At the same time, Chinese herbal medicine

can also effectively enhance immunity. According to the main antioxidant components present, the antioxidants in Chinese herbal medicine can be divided into phenylhexoside, ginsenoside, flavonoids, alkaloids, anthraquinone, and polysaccharides (Karimi-Maleh et al., 2021b). However, evaluating the antioxidant activity of Chinese herbal medicine is still a difficult problem.

So far, the main methods used to evaluate antioxidant activity include the hydrogen atom transfer method, the single-electron transfer method, the chromatographic method, and the electrochemical method (Shabani et al., 2020; Ye et al., 2020; Carp et al., 2021). These methods all have some disadvantages. For example, the hydrogen atom transfer method is when the antioxidants transfer hydrogen atoms to free radicals, making them inactive (Xu et al., 2020; Zhang et al., 2020; Zhou et al., 2020). The advantage of this method is that it can be used to determine water-soluble and oil-soluble substances, but the disadvantage is that the light probe is sensitive and the method is time-consuming (Boudier et al., 2012). The reaction rate of the single-electron transfer method is usually very low, and it takes a long time to complete the detection. Chromatography allows quantification of the antioxidant capacity of OH, H_2O_2, and peroxynitrite. However, this method is not easily adaptable for high-throughput analysis requiring quality control, because it requires multiple injections to measure the ethylene production (Shui and Leong, 2004; Cimpoiu, 2006).

On the other hand, electrochemical methods have attracted a lot of attention because of their rapidity and efficiency (Kilmartin, 2001; Blasco et al., 2007; Teixeira et al., 2013; Apak et al., 2016). The non-radical electrochemical methods include cyclic voltammetry, enzyme voltammetry, and potentiometric analysis (Ghanei-Motlagh et al., 2019; Ghanei-Motlagh and Baghayeri, 2020; Naderi Asrami et al., 2020; Karimi-Maleh et al., 2021c; Nodehi et al., 2021). Electrode poisoning is the reduction of efficiency on the electrode surface due to the deposition of reactants (Karimi-Maleh et al., 2020). Recently, an electrochemical method based on hydrogel has been used for evaluating the antioxidant activity (Fu et al., 2018a,b). This method uses the signal from the metal ions in the hydrogel linkage, which could provide sensitive determination of the antioxidant activity in the whole electrolyte system. In this work, we further developed an advanced hydrogel using chitosan, graphene oxide (GO), and zinc ions. The presence of GO in the hydrogel system accelerates the electron transfer rate of the metal ions during the sensing, which improves the performance of the platform. *Scutellaria baicalensis* Georgi has been used as a real example for evaluating the practical application of the proposed method.

MATERIALS AND METHODS

All materials used in this work were analytical grade. Zinc acetate, acetic acid, ascorbic acid, ascorbic acid, 2,2-diphenyl-1-picrylhydrazyl (DPPH), and gallic acid were purchased from Aladdin Reagent Inc (Chuhuazhi Rd, Shanghai, China). Chitosan (50,000–190,000 Da) was purchased from Sigma-Aldrich (St. Louis, MO, United States). Graphite powder was purchased from Linke ChemTech Co. Ltd. (College Street, Kolkata, India). The morphology of the hydrogel was observed using a field emission scanning electron microscope (FESEM, Apreo, FEI). The x-ray diffraction (XRD) patterns of the sample were collected using an X-ray diffractometer (Broker Philips PW1730). Thermal gravimetric analysis (TGA) was carried out using a TGA instrument (BÄHR-Thermoanalyse GmbH, Altendorfstraße 12 D-32609, Hüllhorst). The Fourier-transform infrared spectroscopy (FTIR) spectra of the sample were characterized using an FTIR spectrophotometer (Bruker vector FTIR).

Preparation of the hydrogel: GO was prepared using a typical Hummers' method (Chen et al., 2013). The prepared GO was

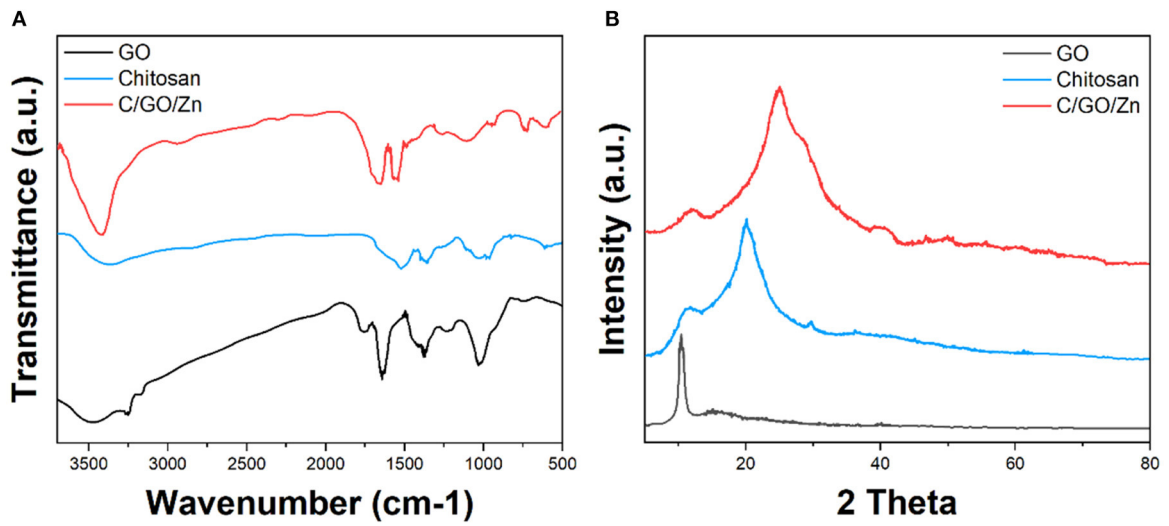

FIGURE 1 | (A) FTIR spectra and **(B)** XRD patterns of GO, chitosan, and C/GO/Zn.

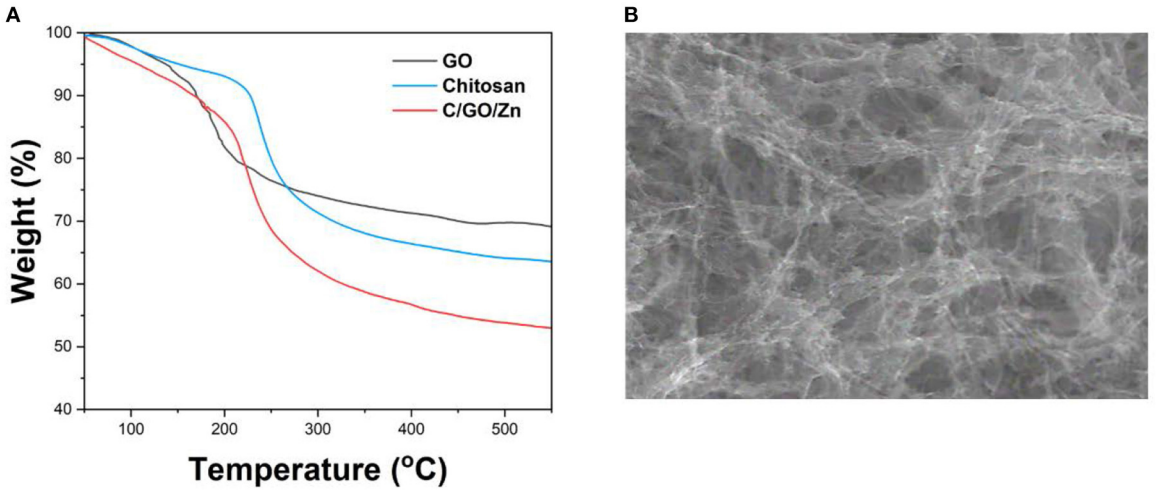

FIGURE 2 | (A) TGA curves of GO, chitosan, and C/GO/Zn. **(B)** SEM image of C/GO/Zn.

dispersed into water to form a 0.5 mg/ml dispersion for further use. For the synthesis of the hydrogel, a certain amount of GO dispersion was added into 10 ml of 1 wt% chitosan solution (in 1% acetic acid) under stirring. Then, 0.1 ml of zinc acetate solution was added as well. After half an hour of stirring, NaOH (0.1 M) was added drop-by-drop until the initiation of the gelation process. The formed hydrogel was denoted as C/GO/Zn. The hydrogel without GO was prepared using a similar process without the addition of GO dispersion. This product was denoted as C/Zn.

Preparation of *Scutellaria baicalensis* extract: A 5 g sample of *Scutellaria baicalensis* powder was weighed and 70% ethanol was added in the mass ratio of 1:30 (powder:solvent). The ultrasonic-assisted extraction method was used for extraction three times, 20 min each time. After filtration, the supernatant was taken as the extract.

Antioxidant activity test: the antioxidant activity test was carried out using two methods. The first one is the DPPH measurement. Typically, 5 mg DPPH was dissolved in 125 ml of C_2H_5OH. Then, 0.8 ml of DPPH solution was mixed with 0.2 ml of the *Scutellaria baicalensis* extract or different concentrations of tocopheryl, and the reaction was kept away from light for 15 min at room temperature. Then, the UV-Vis spectrophotometer was used to determine the spectrophotometry value of the solution, which was determined to be at 514 nm. The second method is the hydrogel-based electrochemical method. Typically, after the addition of the *Scutellaria baicalensis* extract or different concentrations of tocopheryl, a certain amount of H_2O_2 solution was injected. Sonication was conducted for 30 s to accelerate the diffusion. Then, a glassy carbon electrode (GCE), Ag/AgCl (3M), and a Pt wire were inserted into the hydrogel. Either cyclic voltammetry (CV) or differential pulse voltammetry (DPV) was used for measuring the redox of the Zn ions for evaluating the antioxidant activity of the samples.

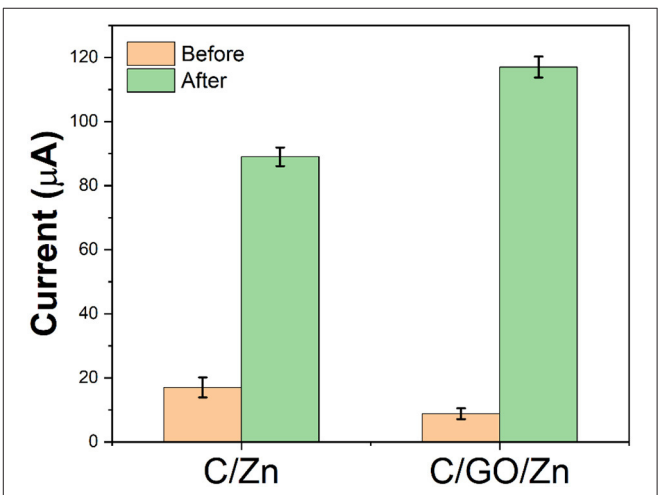

FIGURE 3 | Current value of C/Zn and C/GO/Zn before and after the injection of 0.1 ml H_2O_2 (10%) after 10 min.

RESULTS AND DISCUSSION

Figure 1A shows the FTIR spectra of GO, chitosan, and C/GO/Zn. As shown in the figure, the spectrum of GO shows the peaks located at 1,042, 1,626, 1,725, and 3,397 cm^{-1}, which can be assigned to the stretching vibrations of the C-O, C=C, C=O, and O-H bonds (Strankowski et al., 2016), respectively. The presence of the peaks at 1,042 and 3,397 cm^{-1} indicate the successful formation of GO. The spectrum of chitosan shows a series of peaks between 1,750 and 600 cm^{-1}, indicating the stretching of the C-H, C=O, C=C bonds (Manoratne et al., 2017), while the peaks between 3,000 and 3,500 cm^{-1} can be ascribed to the stretching of the OH group (Lawrie et al., 2007). In addition, the spectrum of C/GO/Zn shows the combination of both the

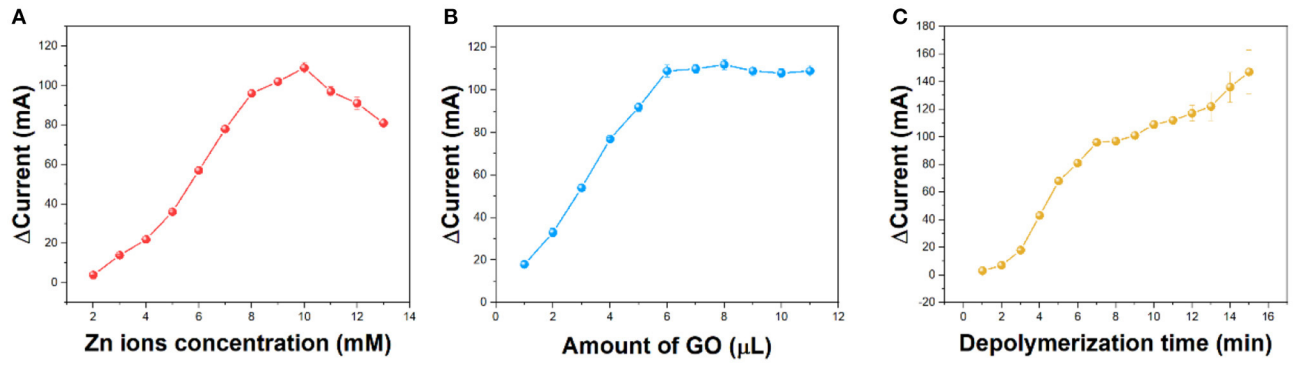

FIGURE 4 | Effect of **(A)** concentration of Zn ions, **(B)** amount of GO dispersion, and **(C)** depolymerization time on the current difference recoded from CV.

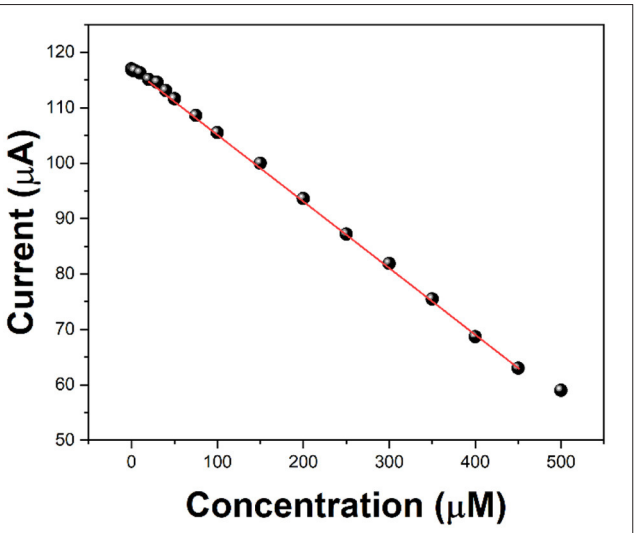

FIGURE 5 | Current value of C/GO/Zn after the injection of 0.1 ml of H_2O_2 (10%) and different concentrations of ascorbic acid.

TABLE 1 | The antioxidant capacity of 10 samples of *Scutellaria baicalensis* detected using the DPPH method and the proposed electrochemical method.

Sample No.	DPPH (mgTrolox/mg)	Electrochemical method (μA)
1	46.21 ± 1.07	40.1
2	37.44 ± 0.78	29.8
3	36.51 ± 2.21	35.2
4	42.01 ± 1.04	33.5
5	44.28 ± 1.22	31.6
6	36.89 ± 1.50	24.7
7	50.36 ± 1.42	22.2
8	31.04 ± 0.94	42.1
9	39.98 ± 0.71	37.5
10	41.20 ± 1.03	36.9

materials, indicating the successful formation of the composite in the hydrogel.

Figure 1B shows the XRD pattern of GO, chitosan, and C/GO/Zn. The pattern of GO shows a typical peak at around 11° due to the plane (200) of GO (Stobinski et al., 2014). The chitosan shows a series of peaks between 10° and 30° due to the polymeric networks (Tang et al., 2003). The C/GO/Zn shows a very similar pattern compared with that of the chitosan. However, we can still observe the appearance of the peak corresponding to the plane (200) of GO.

Figure 2A shows the TGA profiles of GO, chitosan, and C/GO/Zn. It can be seen that the GO shows a poor thermal property, which causes weight loss at <100°C. This weight loss can be ascribed to the evaporation of water. Then, the GO shows a fast decline loss between 150 and 200°C, indicating the reduction of oxygen-containing groups of the sheets plane (Li et al., 2012). The curve of the chitosan shows that the mass loss begins at 230°C and continues until 400°C. It can be due to the depolymerization of chitosan and the degradation of glycosidic units. The further decline of the weight above 400°C can be ascribed to the breakdown of the structure of chitosan (Corazzari et al., 2015). The curve of C/GO/Zn shows that the main weight loss starts at above 205°C. The decline of the thermal stability of the hydrogel can be ascribed to the formation of a network between the two materials. The poor stability of the GO lowers the thermal stability of the hydrogel.

Figure 2B shows the Scanning electron microscopic (SEM) image of the C/GO/Zn hydrogel. It can be seen that the hydrogel shows a very porous structure. This structure can be ascribed to the successful formation of cross-links between zinc ions and chitosan. In addition, the presence of GO in the hydrogel network can be clearly identified.

Since chitosan needs to be dissolved in an acetic acid solution, an acetic acid buffer solution was selected for the preparation of the sensor platform. In the C/GO/Zn hydrogel, zinc ions are used as crosslinking agents to connect chitosan and GO. Therefore, if electrochemical scanning is carried out in the hydrogel, the Zn ion will not be able to move freely from the hydrogel to the electrode surface, hence, the electrochemical response will be low. After the injection of hydrogen peroxide, the free zinc ions in the

hydrogels become more diverse due to the slow destruction of the structure of chitosan by the hydrogen peroxide. These free zinc ions can rapidly diffuse to the electrode surface to participate in the redox reaction. We use −0.6 V as the reduction potential of the zinc ions and reflect the content of free zinc ions in hydrogels according to the current value. At the same time, by comparing the current values before and after the injection of hydrogen peroxide, we can evaluate the damage effect of free radicals on chitosan. It can be seen from **Figure 3** that without GO, a certain amount of hydrogen peroxide produces a current difference of 72 μA. However, with the participation of GO, the same amount of hydrogen peroxide produces a current difference of 109 μA. There are two reasons for this increase in the current difference. First, GO helps the electron transfer of the zinc ions. The second reason is that GO affects the stability of hydrogels, so that more zinc ions will be released in the C/GO/Zn hydrogel under the injection of the same amount of hydrogen peroxide.

Zinc ion addition is a very important factor. If the amount of zinc added is not enough, the hydrogel will not be formed. If there are too many zinc ions, the free zinc ions in the hydrogel will affect the accuracy of the detection. **Figure 4A** shows the effect of different zinc ion concentrations on hydrogels. It can be seen from the figure that zinc ions increase the corresponding current from 2 to 10 mM. Above 10 mM, the difference in the value of current begins to decrease. Therefore, we chose 10 mM zinc ions for the preparation of hydrogels.

The addition of GO is also a very important factor. GO in fewer amounts will not be able to enhance the detected signal. By contrast, too much GO will hinder the formation of the hydrogels. As can be seen from **Figure 4B**, the current intensity increases from 1 to 6 μl and reaches the saturation point. Increasing the amount of GO will only have a small impact. If the amount of GO is more than 11 μl, the C/GO/Zn hydrogel will not be formed. Therefore, 6 μl of GO has been selected for preparation.

The waiting time for the hydrogen peroxide to depolymerize is also important. Sufficient time for depolymerization time can make enough zinc ions participate in the electrochemical reduction. As shown in **Table 1**, the reduction current gradually increases from 1 to 10 min and remains stable. Although increasing the depolymerization world can further increase the current, these tests have large errors. Therefore, we chose 10 min as the depolymerization time.

Ascorbic acid is used as a detection molecule to measure the antioxidant activity evaluation performance of the electrochemical platform. After 5 min of hydrogen peroxide injection, we added different concentrations of ascorbic acid, and then tested it at 10 min. Because ascorbic acid prevents the free radicals from attacking the chitosan molecules further, the reduction current of zinc ions will be reduced. Compared with the current value without ascorbic acid and with ascorbic acid, it can be used to evaluate the antioxidant activity of ascorbic acid. **Figure 5** shows the current values against the addition of 0.5 to 500 μM of ascorbic acid. It can be seen that the increase in the concentration of ascorbic acid lowers the current response. It can be seen that in the range of 2–450 μM, the decrease of the current value presents a linear relationship, so it can be used to evaluate the antioxidant activity of ascorbic acid.

We tested the antioxidant activity of *Scutellaria baicalensis* purchased from 10 different samples. In addition to the electrochemical detection method proposed in this paper, the DPPH method was also used for comparison. In DPPH detection, Trolox was used as the reference material. The antioxidant capacities of these 10 samples were calculated by measuring the absorbance of different concentrations of Trolox and DPPH at the same time. The results are shown in **Table 1**. It can be seen from the table that the antioxidant capacities of the 10 samples of *Scutellaria baicalensis* are not the same. This may be because of the fact that they come from different places of origin or use different processing technologies. Although the two detection techniques cannot be compared horizontally, it can be seen from the comparison of the differences between the samples that the results of the proposed electrochemical detection method are basically consistent with those of the DPPH detection method. In both detection techniques, sample 7 shows the strongest antioxidant activity, while sample 8 shows the weakest.

CONCLUSION

In this work, we proposed an electrochemical platform based on a hydrogel synthesized using graphene, chitosan, and zinc ions. This electrochemical platform can be used for evaluating the antioxidant capacity by monitoring the current change with the reduction of zinc ions. The addition of GO significantly enhances the current response, which could be used for high-sensitivity sensing. The proposed electrochemical platform was successfully used for evaluating the antioxidant capacity of *Scutellaria baicalensis*.

DATA AVAILABILITY STATEMENT

The original contributions presented in the study are included in the article/supplementary material, further inquiries can be directed to the corresponding authors.

AUTHOR CONTRIBUTIONS

SY, WZ, and XW conceived of the study. XW and WZ supervised the development program. SY, MH, and YY collected materials characterization. YY and LZ received and curated samples and analytical records. LS, MH, and SY wrote the manuscript. All authors read and approved the manuscript.

FUNDING

This work was funded by the Macau Young Scholars Program (AM2020020), the Natural Science Foundation of Nanjing University of Chinese Medicine (XZR2020038), the Jiangsu Youth Medical Talents Project (QNRC2016255), and the Fifth Batch of Gusu Health Personnel Training Project in Suzhou (GSWS2020085).

REFERENCES

Aghdam, A. A., Majidi, M. R., Veladi, H., and Omidi, Y. (2019). Microfluidic-based separation and detection of synthetic antioxidants by integrated gold electrodes followed by HPLC-DAD. *Microchem. J.* 149:104059. doi: 10.1016/j.microc.2019.104059

Apak, R., Demirci Çekiç, S., Üzer, A., Çelik, S. E., Bener, M., Bekdeşer, B., et al. (2018). Novel spectroscopic and electrochemical sensors and nanoprobes for the characterization of food and biological antioxidants. *Sensors* 18:186. doi: 10.3390/s18010186

Apak, R., Özyürek, M., Güçlü, K., and Çapanoglu, E. (2016). Antioxidant activity/capacity measurement. 2. Hydrogen atom transfer (HAT)-based, mixed-mode (electron transfer (ET)/HAT), and lipid peroxidation assays. *J. Agric. Food Chem.* 64, 1028–1045. doi: 10.1021/acs.jafc.5b04743

Blasco, A. J., González Crevillén, A., González, M. C., and Escarpa, A. (2007). Direct electrochemical sensing and detection of natural antioxidants and antioxidant capacity *in vitro* systems. *Electroanal. Int. J. Devoted Fundam. Pract. Asp. Electroanal.* 19, 2275–2286. doi: 10.1002/elan.200704004

Boudier, A., Tournebize, J., Bartosz, G., El Hani, S., Bengueddour, R., Sapin-Minet, A., et al. (2012). High-performance liquid chromatographic method to evaluate the hydrogen atom transfer during reaction between 1, 1-diphenyl-2-picryl-hydrazyl radical and antioxidants. *Anal. Chim. Acta* 711, 97–106. doi: 10.1016/j.aca.2011.10.063

Brainina, K., Stozhko, N., and Vidrevich, M. (2019). Antioxidants: terminology, methods, and future considerations. *Antioxidants* 8:297. doi: 10.3390/antiox8080297

Carp, O. E., Moraru, A., Pinteala, M., and Arvinte, A. (2021). Electrochemical behaviour of piperine. Comparison with control antioxidants. *Food Chem.* 339:128110. doi: 10.1016/j.foodchem.2020.128110

Chen, J., Yao, B., Li, C., and Shi, G. (2013). An improved Hummers method for eco-friendly synthesis of graphene oxide. *Carbon* 64, 225–229. doi: 10.1016/j.carbon.2013.07.055

Cimpoiu, C. (2006). Analysis of some natural antioxidants by thin-layer chromatography and high performance thin-layer chromatography. *J. Liq. Chromatogr. Relat. Technol.* 29, 1125–1142. doi: 10.1080/10826070600574911

Corazzari, I., Nisticò, R., Turci, F., Faga, M. G., Franzoso, F., Tabasso, S., et al. (2015). Advanced physico-chemical characterization of chitosan by means of TGA coupled on-line with FTIR and GCMS: thermal degradation and water adsorption capacity. *Polym. Degrad. Stab.* 112, 1–9. doi: 10.1016/j.polymdegradstab.2014.12.006

Fu, L., Wang, A., Lyu, F., Lai, G., Yu, J., Lin, C.-T., et al. (2018a). A solid-state electrochemical sensing platform based on a supramolecular hydrogel. *Sens. Actuators B Chem.* 262, 326–333. doi: 10.1016/j.snb.2018.02.029

Fu, L., Wang, A., Lyv, F., Lai, G., Zhang, H., Yu, J., et al. (2018b). Electrochemical antioxidant screening based on a chitosan hydrogel. *Bioelectrochemistry* 121, 7–10. doi: 10.1016/j.bioelechem.2017.12.013

Ghanei-Motlagh, M., and Baghayeri, M. (2020). Determination of trace Tl (I) by differential pulse anodic stripping voltammetry using a novel modified carbon paste electrode. *J. Electrochem. Soc.* 167:066508. doi: 10.1149/1945-7111/ab823c

Ghanei-Motlagh, M., Taher, M. A., Fayazi, M., Baghayeri, M., and Hosseinifar, A. (2019). Non-enzymatic amperometric sensing of hydrogen peroxide based on vanadium pentoxide nanostructures. *J. Electrochem. Soc.* 166:B367. doi: 10.1149/2.0521906jes

Han, B., Xin, Z., Ma, S., Liu, W., Zhang, B., Ran, L., et al. (2017). Comprehensive characterization and identification of antioxidants in Folium Artemisiae Argyi using high-resolution tandem mass spectrometry. *J. Chromatogr. B* 1063, 84–92. doi: 10.1016/j.jchromb.2017.08.021

Jin, Z., Li, Y., Ren, J., and Qin, N. (2018). Yield, nutritional content, and antioxidant activity of *Pleurotus ostreatus* on corncobs supplemented with herb residues. *Mycobiology* 46, 24–32. doi: 10.1080/12298093.2018.1454014

Karimi-Maleh, H., Alizadeh, M., Orooji, Y., Karimi, F., Baghayeri, M., Rouhi, J., et al. (2021a). Guanine-based DNA biosensor amplified with Pt/SWCNTs nanocomposite as analytical tool for nanomolar determination of daunorubicin as an anticancer drug: a docking/experimental investigation. *Ind. Eng. Chem. Res.* 60, 816–823. doi: 10.1021/acs.iecr.0c04698

Karimi-Maleh, H., Ayati, A., Davoodi, R., Tanhaei, B., Karimi, F., Malekmohammadi, S., et al. (2021b). Recent advances in using of chitosan-based adsorbents for removal of pharmaceutical contaminants: a review. *J. Clean. Prod.* 291:125880. doi: 10.1016/j.jclepro.2021.125880

Karimi-Maleh, H., Farahmandfar, R., Hosseinpour, R., Alizadeh, J., and Abbaspourrad, A. (2019). Determination of ferulic acid in the presence of butylated hydroxytoluene as two phenolic antioxidants using a highly conductive food nanostructure electrochemical sensor. *Chem. Pap.* 73, 2441–2447. doi: 10.1007/s11696-019-00793-y

Karimi-Maleh, H., Karimi, F., Orooji, Y., Mansouri, G., Razmjou, A., Aygun, A., et al. (2020). A new nickel-based co-crystal complex electrocatalyst amplified by NiO dope Pt nanostructure hybrid; a highly sensitive approach for determination of cysteamine in the presence of serotonin. *Sci. Rep.* 10:11699. doi: 10.1038/s41598-020-68663-2

Karimi-Maleh, H., Yola, M. L., Atar, N., Orooji, Y., Karimi, F., Senthil Kumar, P., et al. (2021c). A novel detection method for organophosphorus insecticide fenamiphos: molecularly imprinted electrochemical sensor based on core-shell CO_3O_4@MOF-74 nanocomposite. *J. Colloid Interface Sci.* 592, 174–185. doi: 10.1016/j.jcis.2021.02.066

Kilmartin, P. A. (2001). Electrochemical detection of natural antioxidants: principles and protocols. *Antioxid. Redox Signal.* 3, 941–955. doi: 10.1089/152308601317203495

Kurtulbaş, E., Yazar, S., Ortaboy, S., Atun, G., and Sahin, S. (2020). Evaluation of the phenolic antioxidants of olive (*Olea europaea*) leaf extract obtained by a green approach: use of reduced graphene oxide for electrochemical analysis. *Chem. Eng. Commun.* 207, 920–932. doi: 10.1080/00986445.2019.1630397

Lawrie, G., Keen, I., Drew, B., Chandler-Temple, A., Rintoul, L., Fredericks, P., et al. (2007). Interactions between alginate and chitosan biopolymers characterized using FTIR and XPS. *Biomacromolecules* 8, 2533–2541. doi: 10.1021/bm070014y

Li, Y.-L., Kuan, C.-F., Chen, C.-H., Kuan, H.-C., Yip, M.-C., Chiu, S.-L., et al. (2012). Preparation, thermal stability and electrical properties of PMMA/functionalized graphene oxide nanosheets composites. *Mater. Chem. Phys.* 134, 677–685. doi: 10.1016/j.matchemphys.2012.03.050

Malekmohammad, K., Sewell, R. D., and Rafieian-Kopaei, M. (2019). Antioxidants and atherosclerosis: mechanistic aspects. *Biomolecules* 9:301. doi: 10.3390/biom9080301

Manoratne, C., Rosa, S., and Kottegoda, I. (2017). XRD-HTA, UV visible, FTIR and SEM interpretation of reduced graphene oxide synthesized from high purity vein graphite. *Mater. Sci. Res. India* 14, 19–30. doi: 10.13005/msri/140104

Masek, A., Chrzescijanska, E., Latos, M., and Kosmalska, A. (2019). Electrochemical and spectrophotometric characterization of the propolis antioxidants properties. *Int. J. Electrochem. Sci.* 14, 1231–1247. doi: 10.20964/2019.02.66

Moteshakeri, M., Travas-Sejdic, J., and Kilmartin, P. A. (2018). Effect of holding time on electrochemical analysis of milk antioxidants using PEDOT electrodes. *Int. J. Nanotechnol.* 15, 729–735. doi: 10.1504/IJNT.2018.098441

Naderi Asrami, P., Aberoomand Azar, P., Saber Tehrani, M., and Mozaffari, S. A. (2020). Glucose oxidase/Nano-ZnO/thin film deposit FTO as an innovative clinical transducer: a sensitive glucose biosensor. *Front. Chem.* 8:503. doi: 10.3389/fchem.2020.00503

Nodehi, M., Baghayeri, M., Behazin, R., and Veisi, H. (2021). Electrochemical aptasensor of bisphenol A constructed based on 3D mesoporous structural SBA-15-Met with a thin layer of gold nanoparticles. *Microchem. J.* 162:105825. doi: 10.1016/j.microc.2020.105825

Shabani, E., Zappi, D., Berisha, L., Dini, D., Antonelli, M. L., and Sadun, C. (2020). Deep eutectic solvents (DES) as green extraction media for antioxidants electrochemical quantification in extra-virgin olive oils. *Talanta* 215:120880. doi: 10.1016/j.talanta.2020.120880

Shui, G., and Leong, L. P. (2004). Analysis of polyphenolic antioxidants in star fruit using liquid chromatography and mass spectrometry. *J. Chromatogr. A* 1022, 67–75. doi: 10.1016/j.chroma.2003.09.055

Stobinski, L., Lesiak, B., Malolepszy, A., Mazurkiewicz, M., Mierzwa, B., Zemek, J., et al. (2014). Graphene oxide and reduced graphene oxide studied by the XRD, TEM and electron spectroscopy methods. *J. Electron Spectrosc. Relat. Phenom.* 195, 145–154. doi: 10.1016/j.elspec.2014.07.003

Strankowski, M., Włodarczyk, D., Piszczyk, Ł., and Strankowska, J. (2016). Polyurethane nanocomposites containing reduced graphene oxide, FTIR, Raman, and XRD studies. *J. Spectrosc.* 2016:7520741. doi: 10.1155/2016/7520741

Tang, E., Huang, M., and Lim, L. Y. (2003). Ultrasonication of chitosan and chitosan nanoparticles. *Int. J. Pharm.* 265, 103–114. doi: 10.1016/S0378-5173(03)00408-3

Teixeira, J., Gaspar, A., Garrido, E. M., Garrido, J., and Borges, F. (2013). Hydroxycinnamic acid antioxidants: an electrochemical overview. *BioMed. Res. Int.* 2013:251754. doi: 10.1155/2013/251754

Xu, Y., Lu, Y., Zhang, P., Wang, Y., Zheng, Y., Fu, L., et al. (2020). Infrageneric phylogenetics investigation of Chimonanthus based on electroactive compound profiles. *Bioelectrochemistry* 133:107455. doi: 10.1016/j.bioelechem.2020.107455

Ye, Y., Ji, J., Sun, Z., Shen, P., and Sun, X. (2020). Recent advances in electrochemical biosensors for antioxidant analysis in foodstuff. *TrAC Trends Anal. Chem.* 122:115718. doi: 10.1016/j.trac.2019.115718

Zhang, M., Pan, B., Wang, Y., Du, X., Fu, L., Zheng, Y., et al. (2020). Recording the electrochemical profile of pueraria leaves for polyphyly analysis. *ChemistrySelect* 5, 5035–5040. doi: 10.1002/slct.202001100

Zhou, J., Zheng, Y., Zhang, J., Karimi-Maleh, H., Xu, Y., Zhou, Q., et al. (2020). Characterization of the electrochemical profiles of lycoris seeds for species identification and infrageneric relationships. *Anal. Lett.* 53, 2517–2528. doi: 10.1080/00032719.2020.1746327

Conflict of Interest: The authors declare that the research was conducted in the absence of any commercial or financial relationships that could be construed as a potential conflict of interest.

frontiers in Chemistry

ORIGINAL RESEARCH
published: 22 April 2021
doi: 10.3389/fchem.2021.670074

Detection of Imatinib Based on Electrochemical Sensor Constructed Using Biosynthesized Graphene-Silver Nanocomposite

Zhen Wu[1], *Jingjing Liu*[2], *Minmin Liang*[3], *Haoyue Zheng*[3], *Chuansheng Zhu*[2] *and Yan Wang*[2]*

[1] Day Chemotherapy Unit, Qianfoshan Hospital, The First Affiliated Hospital of Shandong First Medical University, Jinan, China, [2] Hematology Department, Qianfoshan Hospital, The First Affiliated Hospital of Shandong First Medical University, Jinan, China, [3] Shandong First Medical University, Jinan, China

The establishment of a monitoring technique for imatinib is necessary in clinical and environmental toxicology. Leaf extracts of *Lycoris longituba* were used as reducing agent for the one-step synthesis of reduced graphene oxide-Ag nanocomposites. This nanocomposite was characterized by TEM, FTIR, XRD, and other instruments. Then, the graphene/Ag nanocomposite was used as a modifier to be cemented on the surface of the glassy carbon electrode. This electrode exhibited excellent electrochemical sensing performance. Under the optimal conditions, the proposed electrode could detect imatinib at 10 nM−0.28 mM with a low limit of detection. This electrochemical sensor also has excellent anti-interference performance and reproducibility.

Keywords: biosynthesis, imatinib, silver nanoparticle, graphene composite, *Lycoris longituba*

OPEN ACCESS

Edited by:
Li Fu,
Hangzhou Dianzi University, China

Reviewed by:
Yasin Orooji,
Nanjing Forestry University, China
Vahid Arabali,
Islamic Azad University Sari Branch, Iran

***Correspondence:**
Yan Wang
wangyan@vtcuni.com

Specialty section:
This article was submitted to Electrochemistry, a section of the journal Frontiers in Chemistry

Received: *20 February 2021*
Accepted: *19 March 2021*
Published: *22 April 2021*

Citation:
Wu Z, Liu J, Liang M, Zheng H, Zhu C and Wang Y (2021) Detection of Imatinib Based on Electrochemical Sensor Constructed Using Biosynthesized Graphene-Silver Nanocomposite. Front. Chem. 9:670074. doi: 10.3389/fchem.2021.670074

INTRODUCTION

Cancer is one of the most important diseases facing humanity today. Cancer is lethal because its cells are uncontrolled and proliferate indefinitely and spread throughout the body. Cytostatic agents are the most commonly used class of anti-cancer drugs (Karthik et al., 2017; Liu et al., 2018; Muti and Muti, 2018; Zahed et al., 2018). Their purpose is to inhibit the growth of cancer cells. However, the widespread use of cytostatic agents has caused some other effects, such as on environmental toxicology. Among them, imatinib is a specific inhibitor. Imatinib is frequently used in the treatment of chronic myeloid leukemia and gastrointestinal stromal tumors (Cahill et al., 2017; Hochhaus et al., 2017). For example, patients with chronic myeloid leukemia can use 400 mg of imatinib per day. Previous reports have demonstrated that the cytogenetic and molecular response to imatinib is associated with low plasma concentrations in patients with chronic myeloid leukemia (Serrano et al., 2019; Buclin et al., 2020). Therefore, monitoring of imatinib is necessary, both in the clinical and environmental toxicology fields.

Currently, the detection methods for imatinib include UV-vis spectroscopy (Grante et al., 2014), HPLC (Roth et al., 2010), and electrophoresis (Li et al., 2012; Ahmed et al., 2019). Although these methods can be used for the rapid detection of imatinib, they all have their own drawbacks. For example, UV-vis spectroscopy requires a large number of samples. HPLC methods are slower and require large instruments. The detection sensitivity of electrophoresis method is not enough. Therefore, it is necessary to develop a technique for the rapid detection of imatinib. Electrochemical sensors are a fast and sensitive detection technology. It enables highly sensitive detection of electrochemically active substances. Previous studies have demonstrated that imatinib can be oxidized at lower potentials, so assembling an imatinib-based electrochemical sensor is an approach worth investigating.

Conventional electrochemical sensors use carbon electrodes for the detection of target molecules (Fu et al., 2019; Mahmoudi-Moghaddam et al., 2019; Zhou et al., 2020). Carbon electrodes have a stable electrochemical window and do not react easily with other substances. However, the electrochemical signal of ordinary carbon electrodes is weak (Karimi-Maleh et al., 2021a), so it is difficult to meet the demand of highly sensitive detection. Modification on the surface of ordinary carbon electrodes is a common method to improve the electrochemical activity of sensors (Cao et al., 2019; Alam et al., 2020; Fu et al., 2020). Recent studies have shown that modification of carbon nanomaterials on the surface of glassy carbon electrodes can improve the performance (Karimi-Maleh et al., 2020). For example, modification of graphene on the surface of glassy carbon electrodes can increase the electrical conductivity. However, the layer-layer interaction of graphene is so strong that direct modification can cause agglomeration, which in turn reduces the performance of the sensor (Kumar et al., 2019; Jadoon et al., 2020). Surface modification of polymers allows the surface of graphene to be loaded with tubular energy groups. Under the principle of homogeneous charge repulsion, the layer-layers of graphene can be separated from each other. However, the modified graphene also cannot perform very well due to the poor electrical conductivity of the polymer (Liu et al., 2019). Another strategy is to grow nanoparticles between graphene. The graphene lamellae are separated by nanoparticles. This approach is most beneficial for the modification of electrochemical sensors (Karimi-Maleh et al., 2021b). The presence of nanoparticles can increase the electrochemically active surface area. Also, some nanoparticles have electrochemical catalytic properties that can improve the sensitivity of detection.

Graphene-nanoparticle composites are synthesized by many methods. In recent years, the one-step synthesis of graphene-nanoparticle composites using plant extracts has attracted much attention (Nandgaonkar et al., 2014; Keerthi et al., 2018; Khanam and Hasan, 2019). This method does not require polluting reducing agents and easily controls the size of nanoparticles. For example, Song and Shi (2019) reported the synthesis of graphene/Ag nanocomposites using *Shewanella oneidensis*. Weng et al. (2018) reported the synthesis of graphene/Fe nanocomposites using eucalyptus leaves.

In this work, we chose the leaf extract of *Lycoris longituba* as a reducing agent. The graphene/Ag nanocomposites were reduced by a one-step hydrothermal method. We characterized the conforming materials. The synthesized composites were used for surface modification of glassy carbon electrodes and successfully used for electrochemical detection of imatinib. This novel electrochemical sensor allows highly sensitive detection of imatinib.

EXPERIMENTS

All reagents, including KH_2PO_4, Na_2HPO_4 and silver nitrate were purchased from Macklin Co. Ltd. and used without purification. Graphene oxide (GO) was purchased from Nanin Youshan Biotech Co. Ltd. *Lycoris longituba* was purchased from local nursery. The working electrode, counter electrode and reference electrode were glassy carbon electrode (GCE), Pt wire and Ag/AgCl (3M), respectively. Phosphate buffer solution (PBS) was prepared by mixing stock solutions of 0.1 M disodium hydrogen phosphate and sodium dihydrogen phosphate. The electrochemical determination of imatinib was carried out using a CHI760 electrochemical workstation. Differential pulse voltammetry (DPV) was used for electrochemical recording. The scan range was 0–1.2 V. The pulse amplitude was 50 mV. The pulse width was 0.05 s. The pulse period was 0.5 s.

The XRD pattern of sample was collected by a XRD with Cu Kα ($\lambda = 0.1546$ nm) radiation (D8-Advanced, Bruker). Transmission electron microscopy (TEM) image was observed with a JEOL JEM-2100 high-resolution transmission electron microscope. FTIR spectra were collected by a Fourier transform infrared spectroscopy (Nicolet iS5, Thermo Scientific).

To prepare the aqueous extract of *Lycoris longituba*, its crushed leaf (1:20 ratio) was shaken overnight at 200 rpm with water as solvent. Then, the mixture was filtered, and the resulting extract was used for further experiment. Then, 5 mL of the extract

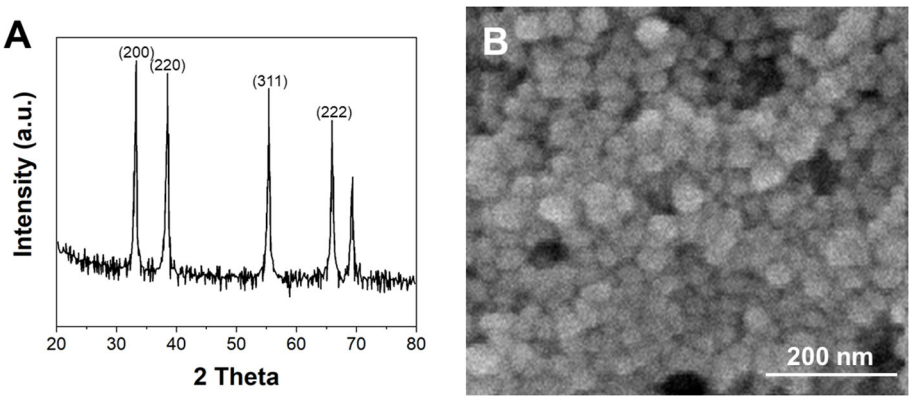

FIGURE 1 | (A) XRD pattern and **(B)** TEM image of biosynthesized G/Ag.

was diluted to 20 mL, and silver nitrate (10 mM) was added to it. This solution was transferred to an autoclave and heated at 120°C for 10 h. The composite was collected after filtration and re-dispersed into water to form a 0.5 mg/mL dispersion (denoted as G/Ag).

RESULTS AND DISCUSSION

Figure 1A shows the XRD pattern of the synthesized G/Ag. It can be seen that four distinct planes of the sample corresponding to (200), (220), (311), and (222) lattice plane of silver face-centered-cube (fcc) crystal (Waterhouse et al., 2001). This result was mated to the reference data in JCPDS file no. 04-0783, suggesting the successful formation of the Ag nanoparticles. Moreover, an additional peak appearing at 26.10° can be also noticed, due to the partial reduced GO sheets to form an ordered crystalline structure (Wang et al., 2013). **Figure 1B** shows the TEM image of the synthesized G/Ag. By the contrast with the background, we can see the layered graphene. On the graphene lamellae we can see the growing Ag nanoparticles. According to the statistics, the average size of Ag nanoparticles is 24 nm.

Figure 2 shows the FTIR spectra of *Lycoris longituba*, and biosynthesized G/Ag. It can be seen that the extract of *Lycoris longituba* exhibited a series bands at range from 700 to 2,000 cm^{-1}. The absorbance peak at 1,322 cm^{-1} is corresponding to the C–O stretching (Ranjana and Mendhulkar, 2015). In addition, the peak located at 883 cm^{-1} can be assigned to the C–N vibrations of the nitroso groups. These two peaks were also found in the biosynthesized G/Ag, suggesting the biomolecules of the *Lycoris longituba* were attached on the composite surface. The intensity of the oxygen containing groups on the G/Ag is relatively low, indicating the reduction of GO during the hydrothermal treatment.

Figure 3A shows the DPV curves of G/Ag/GCE in 10 μM imatinib solution in the pH range between 4.0 and 8.0. It can be seen that the oxidation potential of imatinib shifted to positive direction along with the increase of the pH. **Figure 3B** shows the plot of oxidation potential of imatinib vs. pH value. It can be seen that a slope of 56.9 mV/pH was obtained, suggesting the equal

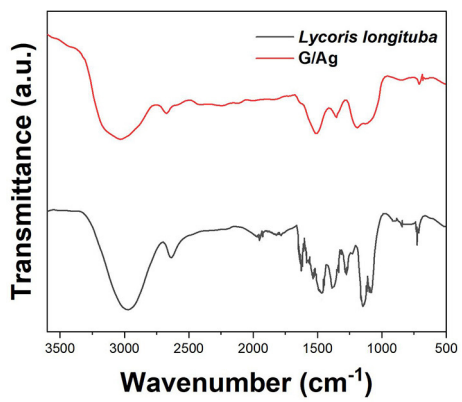

FIGURE 2 | FTIR spectrum of *Lycoris longituba* leaf extract and G/Ag.

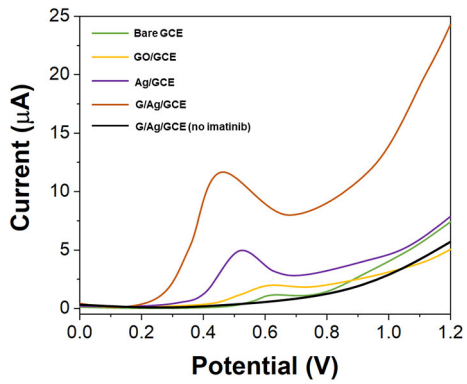

FIGURE 4 | DPV curves of the bare GCE, GO/GCE, Ag/GCE, and G/Ag/GCE toward 10 μM imatinib.

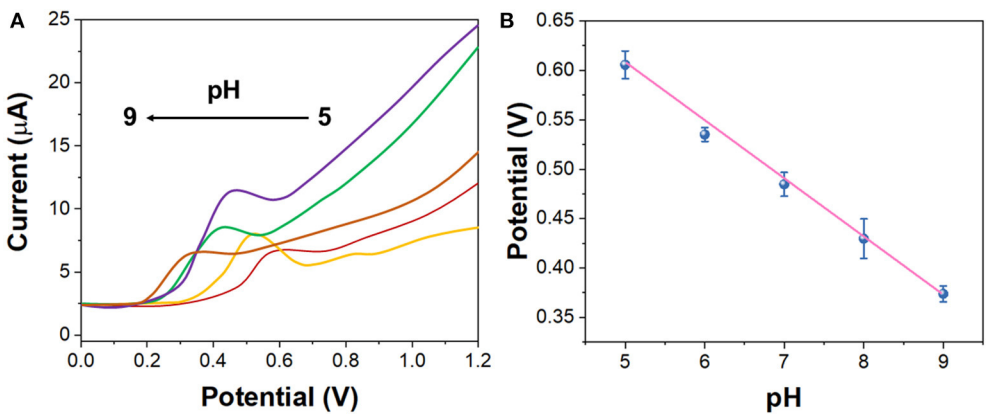

FIGURE 3 | (A) DPV curves of the G/Ag/GCE in 10 μM imatinib solution in the pH range between 4.0 and 8.0. **(B)** Plots of oxidation potential of imatinib vs. pH value.

number of electron and proton were participated in the reaction. In addition, the maximum oxidation response for imatinib was observed at pH = 7.0. Therefore, pH = 7.0 was selected as the optimal condition.

Figure 4 shows the DPV curves of 10 μM imatinib using bare GCE, GO/GCE, Ag/GCE, and G/Ag/GCE. It can be seen that the GCE only exhibited a very small oxidation peak with a current response of 1.34 μA. The modification of GO on the

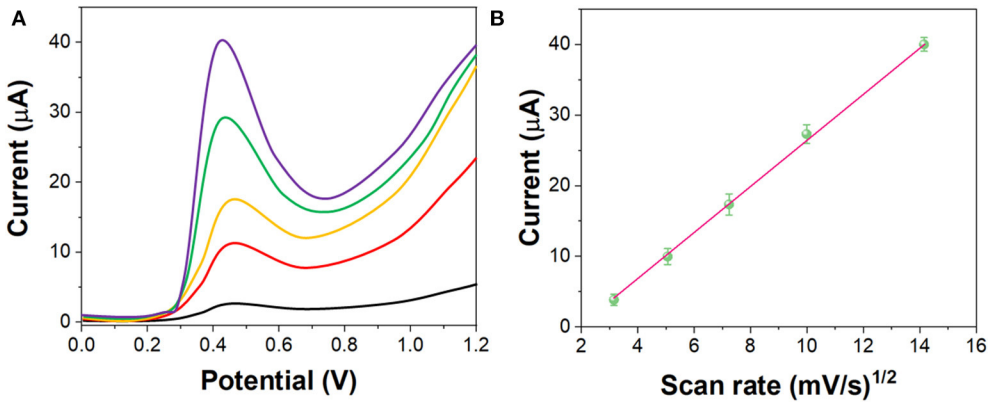

FIGURE 5 | (A) LSV curves of the G/Ag/GCE in 10 μM imatinib solution in the scan rate between 10 and 200 mV/s. **(B)** Plots of $v^{1/2}$ vs. current response.

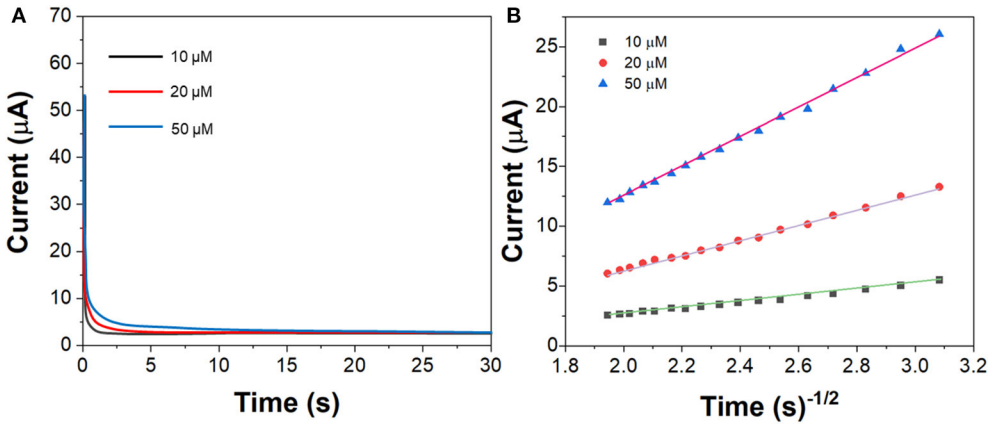

FIGURE 6 | (A) Chronoamperograms of the G/Ag/GCE in imatinib solution in the concentration of 10, 20, and 50 μM. **(B)** Plots of $t^{-1/2}$ vs. current response.

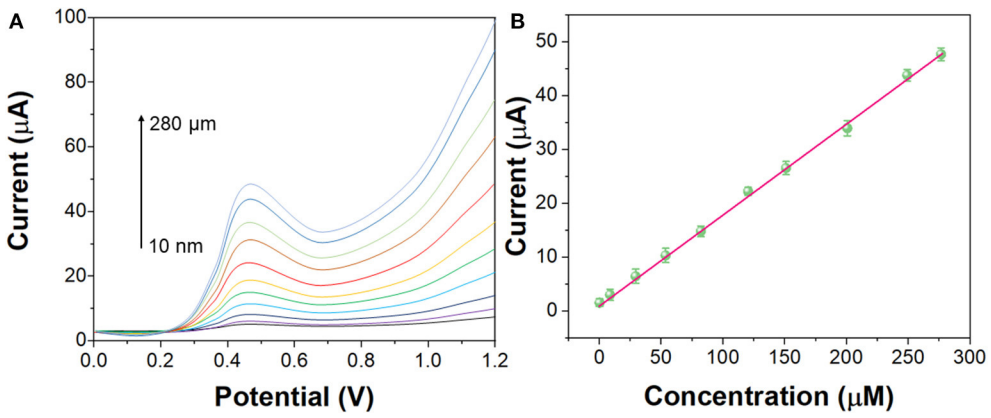

FIGURE 7 | (A) DPV curves of the G/Ag/GCE in imatinib solution in the concentration from 10 nM to 280 μM. **(B)** Linear calibration plot of G/Ag/GCE toward concentration of imatinib.

GCE showed no clear enhancement. In contrast, the modification of Ag nanopartciles on the GCE surface showed an excellent performance toward imatinib oxidation. An enhanced oxidation peak was observed with 4.52 μA response, suggesting the good electrical conductivity of Ag nanoparticles can enhance the sensing performance. In addition, the G/Ag/GCE showed an even higher response toward imatinib with a much lower oxidation potential, suggesting the combination of Ag and reduced GO can trigger the electrocatalytic reaction with imatinib. The electrocatalytic activity of the Ag nanoaprtciles was observed when the corporation with carbon based materials (Asadian et al., 2017; Liu et al., 2017; Majidi and Ghaderi, 2017; Kumar and Goyal, 2018).

Figure 5 shows the LSV curves of G/Ag/GCE toward 10 μM imatinib with different scan rate (from 10 to 200 mV/s). It can be seen that, the electrochemical oxidation current of the imatinib had a liner relationship with the $v^{1/2}$ while the oxidation potential shifted positively along with the increase of the scan rate, indicating the electrochemical behavior of the imatinib obeyed the diffusion-controlled process (Ivanishchev et al., 2016).

Figure 6A shows the chronoamperograms of G/Ag/GCE toward imatinib with 10, 20, and 50 μM. **Figure 6B** shows the corresponded cottrell plots. The diffusion coefficient was calculated to be $\sim 1.94 \times 10^{-5}$ cm^2/s.

As shown in **Figure 7**, under the optimal experimental conditions, the DPV curves of G/Ag/GCE for different concentrations of imatinib were recorded. G/Ag/GCE has a linear relationship with the concentration of imatinib, with a linear range of 10 nM−280 μM and a detection limit of 1.1 nM (S/N = 3). As shown in **Table 1**, compared with other methods, this method has a lower detection limit and a wider linear range. Although there are some detection methods that work better than our proposed sensors, such as LC/MS/MS and LC/TMS, these methods require large instruments and cannot achieve rapid detection.

In order to discuss the selectivity of G/Ag/GCE, 13 common ions that may interfere with the actual detection of imatinib were investigated in this experiment, as shown in **Figure 8**. The results show that when the concentration of sodium ion, potassium ion, copper ion, manganese ion, cobalt ion, magnesium ion, mercury ion, zinc ion, lead ion, nickel ion, barium ion, aluminum ion and chromium ion is 10 times higher than that of imatinib, there is no obvious interference to the actual detection of imatinib. Therefore, the proposed sensor exhibited an excellent anti-interference property.

The proposed sensor has been then used for determining the content of imatinib in serum samples. Standard addition of imatinib was used. **Table 2** shows the performance of the sensor for real sample analysis. It can be seen that excellent recovery performance was observed for each test, indicating the proposed sensor can be applied for real sample sensing.

TABLE 1 | Electrochemical imatinib sensor performance comparison.

Method	Linear detection range	Detection limit	Reference
SWV	19 nM−1.9 μM	5.55 nM	Chen et al., 2014
MS	0.1 nM−1 μM	–	Friedecký et al., 2015
DPV	10 nM−200 μM	7.39 nM	Hatamluyi and Es'haghi, 2017
DPV	30 nM−0.25 μM	6.3 nM	Brycht et al., 2016
LC/MS/MS	100 nM−7.091 μM	0.1 μM	Andriamanana et al., 2013
Liquid chromatography-tandem mass spectrometry	20 nM−2.052 μM	–	Yang et al., 2013
DPV	10 nM-280 μM	1.1 nM	This work

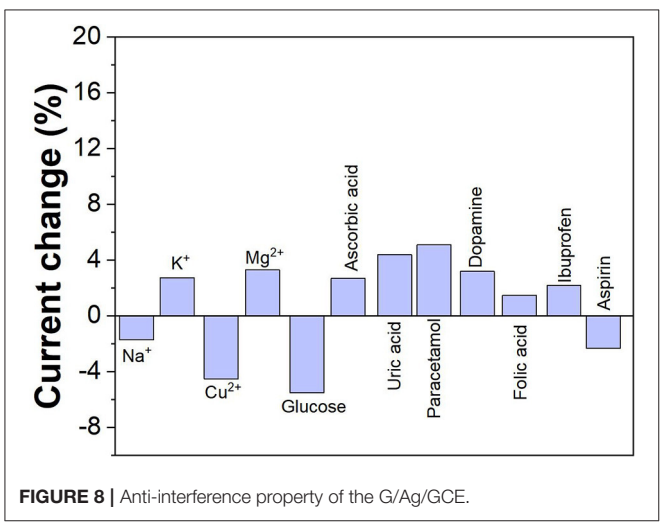

FIGURE 8 | Anti-interference property of the G/Ag/GCE.

CONCLUSIONS

The stable Ag nanoparticles were synthesized with the reduction of GO using leaf extracts of *Lycoris longituba* under hydrothermal condition. TEM, XRD and FTIR were used for characterizations. Based on the enhancement effect of imatinib

TABLE 2 | Electrochemical determination of imatinib content in serum samples using G/Ag/GCE.

Sample	Detected (nM)	Added (nM)	Detected (nM)	Recovery (%)
1	0	10.00	9.77	97.70
2	0	20.00	20.47	102.35
3	0	50.00	50.44	100.88
4	0	100.00	99.36	99.36

on the electrochemical oxidation signal, an electrochemical sensor was constructed using G/Ag nanocomposite.Under the optimal experimental conditions, a linear range of imatinib detection was obtained between 10 nM and 280 μM with a limit of detection of 1.1 nM. The proposed G/Ag/GCE showed an excellent anti-interference property. In addition, it can be applied to the detection of imatinib in real serum sample.

DATA AVAILABILITY STATEMENT

The original contributions presented in the study are included in the article/supplementary material, further inquiries can be directed to the corresponding author/s.

AUTHOR CONTRIBUTIONS

ZW, YW, and JL conceived of the study. YW and ZW supervised the development program, collected materials characterization. ML, CZ, and HZ received and curated samples and analytical records. HZ, ZW, and YW wrote the manuscript. All authors read and approved of the manuscript.

FUNDING

This work was supported by Science and Technology Key Project of Shandong Province, No. 2014GSF18029.

REFERENCES

Ahmed, O. S., Malý, M., Ladner, Y., Philibert, L., Dubský, P., and Perrin, C. (2019). Influence of salt and acetonitrile on the capillary zone electrophoresis analysis of imatinib in plasma samples. *Electrophoresis* 40, 2810–2819. doi: 10.1002/elps.201900188

Alam, A. U., Clyne, D., Jin, H., Hu, N.-X., and Deen, M. J. (2020). Fully integrated, simple, and low-cost electrochemical sensor array for in situ water quality monitoring. *ACS Sens.* 5, 412–422. doi: 10.1021/acssensors.9b02095

Andriamanana, I., Gana, I., Duretz, B., and Hulin, A. (2013). Simultaneous analysis of anticancer agents bortezomib, imatinib, nilotinib, dasatinib, erlotinib, lapatinib, sorafenib, sunitinib and vandetanib in human plasma using LC/MS/MS. *J. Chromatogr. B* 926, 83–91. doi: 10.1016/j.jchromb.2013.01.037

Asadian, E., Shahrokhian, S., Zad, A. I., and Ghorbani-Bidkorbeh, F. (2017). Glassy carbon electrode modified with 3D graphene–carbon nanotube network for sensitive electrochemical determination of methotrexate. *Sens. Actuators B Chem.* 239, 617–627. doi: 10.1016/j.snb.2016.08.064

Brycht, M., Kaczmarska, K., Uslu, B., Ozkan, S. A., and Skrzypek, S. (2016). Sensitive determination of anticancer drug imatinib in spiked human urine samples by differential pulse voltammetry on anodically pretreated boron-doped diamond electrode. *Diam. Relat. Mater.* 68, 13–22. doi: 10.1016/j.diamond.2016.05.007

Buclin, T., Thoma, Y., Widmer, N., André, P., Guidi, M., Csajka, C., et al. (2020). The steps to therapeutic drug monitoring: a structured approach illustrated with imatinib. *Front. Pharmacol.* 11:177. doi: 10.3389/fphar.2020.00177

Cahill, K. N., Katz, H. R., Cui, J., Lai, J., Kazani, S., Crosby-Thompson, A., et al. (2017). KIT inhibition by imatinib in patients with severe refractory asthma. *N. Engl. J. Med.* 376, 1911–1920. doi: 10.1056/NEJMoa1613125

Cao, Y., Wang, L., Shen, C., Wang, C., Hu, X., and Wang, G. (2019). An electrochemical sensor on the hierarchically porous Cu-BTC MOF platform for glyphosate determination. *Sens. Actuators B Chem.* 283, 487–494. doi: 10.1016/j.snb.2018.12.064

Chen, H., Wang, X., Chopra, S., Adams, E., and Van Schepdael, A. (2014). Development and validation of an indirect pulsed electrochemical detection method for monitoring the inhibition of Abl1 tyrosine kinase. *J. Pharm. Biomed. Anal.* 90, 52–57. doi: 10.1016/j.jpba.2013.11.022

Friedecký, D., Mičová, K., Faber, E., Hrdá, M., Široká, J., and Adam, T. (2015). Detailed study of imatinib metabolization using high-resolution mass spectrometry. *J. Chromatogr. A* 1409, 173–181. doi: 10.1016/j.chroma.2015.07.033

Fu, L., Zheng, Y., Zhang, P., Zhang, H., Wu, M., Zhang, H., et al. (2019). An electrochemical method for plant species determination and classification based on fingerprinting petal tissue. *Bioelectrochemistry* 129, 199–205. doi: 10.1016/j.bioelechem.2019.06.001

Fu, L., Zheng, Y., Zhang, P., Zhang, H., Xu, Y., Zhou, J., et al. (2020). Development of an electrochemical biosensor for phylogenetic analysis of Amaryllidaceae based on the enhanced electrochemical fingerprint recorded from plant tissue. *Biosens. Bioelectron.* 159:112212. doi: 10.1016/j.bios.2020.112212

Grante, I., Actins, A., and Orola, L. (2014). Protonation effects on the UV/Vis absorption spectra of imatinib: a theoretical and experimental study. *Spectrochim. Acta. Mol. Biomol. Spectrosc.* 129, 326–332. doi: 10.1016/j.saa.2014.03.059

Hatamluyi, B., and Es'haghi, Z. (2017). A layer-by-layer sensing architecture based on dendrimer and ionic liquid supported reduced graphene oxide for simultaneous hollow-fiber solid phase microextraction and electrochemical determination of anti-cancer drug imatinib in biological samples. *J. Electroanal. Chem.* 801, 439–449. doi: 10.1016/j.jelechem.2017.08.032

Hochhaus, A., Larson, R. A., Guilhot, F., Radich, J. P., Branford, S., Hughes, T. P., et al. (2017). Long-term outcomes of imatinib treatment for chronic myeloid leukemia. *N. Engl. J. Med.* 376, 917–927. doi: 10.1056/NEJMoa1609324

Ivanishchev, A. V., Churikov, A. V., Ivanishcheva, I. A., and Ushakov, A. V. (2016). Lithium diffusion in Li 3 V 2 (PO 4) 3-based electrodes: a joint analysis of electrochemical impedance, cyclic voltammetry, pulse chronoamperometry, and chronopotentiometry data. *Ionics* 22, 483–501. doi: 10.1007/s11581-015-1568-y

Jadoon, T., Mahmood, T., and Ayub, K. (2020). Silver-graphene quantum dots based electrochemical sensor for trinitrotoluene and p-nitrophenol. *J. Mol. Liq.* 306:112878. doi: 10.1016/j.molliq.2020.112878

Karimi-Maleh, H., Alizadeh, M., Orooji, Y., Karimi, F., Baghayeri, M., Rouhi, J., et al. (2021a). Guanine-based DNA biosensor amplified with Pt/SWCNTs nanocomposite as analytical tool for nanomolar determination of daunorubicin as an anticancer drug: a docking/experimental investigation. *Ind. Eng. Chem. Res.* 60, 816–823. doi: 10.1021/acs.iecr.0c04698

Karimi-Maleh, H., Ayati, A., Davoodi, R., Tanhaei, B., Karimi, F., Malekmohammadi, S., et al. (2021b). Recent advances in using of chitosan-based adsorbents for removal of pharmaceutical contaminants: a review. *J. Clean. Prod.* 291:125880. doi: 10.1016/j.jclepro.2021.125880

Karimi-Maleh, H., Orooji, Y., Ayati, A., Qanbari, S., Tanhaei, B., Karimi, F., et al. (2020). Recent advances in removal techniques of Cr(VI) toxic ion from aqueous solution: a comprehensive review. *J. Mol. Liq.* 329:115062. doi: 10.1016/j.molliq.2020.115062

Karthik, R., Sasikumar, R., Chen, S.-M., Vinoth Kumar, J., Elangovan, A., Muthuraj, V., et al. (2017). A highly sensitive and selective electrochemical determination of non-steroidal prostate anti-cancer drug nilutamide based on f-MWCNT in tablet and human blood serum sample. *J. Colloid Interface Sci.* 487, 289–296. doi: 10.1016/j.jcis.2016.10.047

Keerthi, M., Akilarasan, M., Chen, S.-M., Kogularasu, S., Govindasamy, M., Mani, V., et al. (2018). One-pot biosynthesis of reduced graphene oxide/prussian blue microcubes composite and its sensitive detection of prophylactic drug dimetridazole. *J. Electrochem. Soc.* 165:B27. doi: 10.1149/2.0591802jes

Khanam, P. N., and Hasan, A. (2019). Biosynthesis and characterization of graphene by using non-toxic reducing agent from allium cepa extract: anti-bacterial properties. *Int. J. Biol. Macromol.* 126, 151–158. doi: 10.1016/j.ijbiomac.2018.12.213

Kumar, N., and Goyal, R. N. (2018). Silver nanoparticles decorated graphene nanoribbon modified pyrolytic graphite sensor for determination of histamine. *Sens. Actuators Chem.* 268, 383–391. doi: 10.1016/j.snb.2018.04.136

Kumar, S., Bukkitgar, S. D., Singh, S., Singh, V., Reddy, K. R., Shetti, N. P., et al. (2019). Electrochemical sensors and biosensors based on graphene functionalized with metal oxide nanostructures for healthcare applications. *Chem. Select*. 4, 5322–5337. doi: 10.1002/slct.201803871

Li, J., Huang, Y., Huang, L., Ye, L., Zhou, Z., Xiang, G., et al. (2012). Determination of imatinib mesylate and related compounds by field amplified sample stacking with large volume sample injection capillary electrophoresis. *J. Pharm. Biomed. Anal.* 70, 26–31. doi: 10.1016/j.jpba.2012.05.010

Liu, S., Lai, G., Zhang, H., and Yu, A. (2017). Amperometric aptasensing of chloramphenicol at a glassy carbon electrode modified with a nanocomposite consisting of graphene and silver nanoparticles. *Microchim. Acta* 184, 1445–1451. doi: 10.1007/s00604-017-2138-y

Liu, Y., Liang, Y., Yang, R., Li, J., and Qu, L. (2019). A highly sensitive and selective electrochemical sensor based on polydopamine functionalized graphene and molecularly imprinted polymer for the 2, 4-dichlorophenol recognition and detection. *Talanta* 195, 691–698. doi: 10.1016/j.talanta.2018.11.052

Liu, Y., Wei, M., Hu, Y., Zhu, L., and Du, J. (2018). An electrochemical sensor based on a molecularly imprinted polymer for determination of anticancer drug Mitoxantrone. *Sens. Actuators B Chem.* 255, 544–551. doi: 10.1016/j.snb.2017.08.023

Mahmoudi-Moghaddam, H., Tajik, S., and Beitollahi, H. (2019). Highly sensitive electrochemical sensor based on La3+-doped Co3O4 nanocubes for determination of sudan I content in food samples. *Food Chem.* 286, 191–196. doi: 10.1016/j.foodchem.2019.01.143

Majidi, M. R., and Ghaderi, S. (2017). Facile fabrication and characterization of silver nanodendrimers supported by graphene nanosheets: a sensor for sensitive electrochemical determination of Imidacloprid. *J. Electroanal. Chem.* 792, 46–53. doi: 10.1016/j.jelechem.2017.03.028

Muti, M., and Muti, M. (2018). Electrochemical monitoring of the interaction between anticancer drug and DNA in the presence of antioxidant. *Talanta* 178, 1033–1039. doi: 10.1016/j.talanta.2017.08.089

Nandgaonkar, A. G., Wang, Q., Fu, K., Krause, W. E., Wei, Q., Gorga, R., et al. (2014). A one-pot biosynthesis of reduced graphene oxide (RGO)/bacterial cellulose (BC) nanocomposites. *Green Chem.* 16, 3195–3201. doi: 10.1039/C4GC00264D

Ranjana, S., and Mendhulkar, V. D. (2015). FTIR studies and spectrophotometric analysis of natural antioxidants, polyphenols and flavonoids in *Abutilon indicum* (Linn) sweet leaf extract. *J. Chem. Pharm. Res.* 7, 205–211.

Roth, O., Spreux-Varoquaux, O., Bouchet, S., Rousselot, P., Castaigne, S., Rigaudeau, S., et al. (2010). Imatinib assay by HPLC with photodiode-array UV detection in plasma from patients with chronic myeloid leukemia: comparison with LC-MS/MS. *Clin. Chim. Acta* 411, 140–146. doi: 10.1016/j.cca.2009.10.007

Serrano, C., Mariño-Enríquez, A., Tao, D. L., Ketzer, J., Eilers, G., Zhu, M., et al. (2019). Complementary activity of tyrosine kinase inhibitors against secondary kit mutations in imatinib-resistant gastrointestinal stromal tumours. *Br. J. Cancer* 120, 612–620. doi: 10.1038/s41416-019-0389-6

Song, X., and Shi, X. (2019). Biosynthesis of Ag/reduced graphene oxide nanocomposites using Shewanella oneidensis MR-1 and their antibacterial and catalytic applications. *Appl. Surf. Sci.* 491, 682–689. doi: 10.1016/j.apsusc.2019.06.154

Wang, M. Y., Shen, T., Wang, M., Zhang, D., and Chen, J. (2013). One-pot green synthesis of Ag nanoparticles-decorated reduced graphene oxide for efficient nonenzymatic H2O2 biosensor. *Mater. Lett.* 107, 311–314. doi: 10.1016/j.matlet.2013.06.031

Waterhouse, G. I., Bowmaker, G. A., and Metson, J. B. (2001). The thermal decomposition of silver (I, III) oxide: a combined XRD, FT-IR and Raman spectroscopic study. *Phys. Chem. Chem. Phys.* 3, 3838–3845. doi: 10.1039/b103226g

Weng, X., Lin, Z., Xiao, X., Li, C., and Chen, Z. (2018). One-step biosynthesis of hybrid reduced graphene oxide/iron-based nanoparticles by eucalyptus extract and its removal of dye. *J. Clean. Prod.* 203, 22–29. doi: 10.1016/j.jclepro.2018.08.158

Yang, J. S., Cho, E. G., Huh, W., Ko, J.-W., Jung, J. A., and Lee, S.-Y. (2013). Rapid determination of imatinib in human plasma by liquid chromatography-tandem mass spectrometry: application to a pharmacokinetic study. *Bull. Korean Chem. Soc.* 34, 2425–2430. doi: 10.5012/bkcs.2013.34.8.2425

Zahed, F. M., Hatamluyi, B., Lorestani, F., and Es'haghi, Z. (2018). Silver nanoparticles decorated polyaniline nanocomposite based electrochemical sensor for the determination of anticancer drug 5-fluorouracil. *J. Pharm. Biomed. Anal.* 161, 12–19. doi: 10.1016/j.jpba.2018.08.004

Zhou, J., Zheng, Y., Zhang, J., Karimi-Maleh, H., Xu, Y., Zhou, Q., et al. (2020). Characterization of the electrochemical profiles of lycoris seeds for species identification and infrageneric relationships. *Anal. Lett.* 53, 2517–2528. doi: 10.1080/00032719.2020.1746327

Conflict of Interest: The authors declare that the research was conducted in the absence of any commercial or financial relationships that could be construed as a potential conflict of interest.

frontiers in Chemistry

ORIGINAL RESEARCH
published: 14 May 2021
doi: 10.3389/fchem.2021.680593

A Novel Graphene-Based Nanomaterial Modified Electrochemical Sensor for the Detection of Cardiac Troponin I

Jing Li[1], Shenwei Zhang[1], Li Zhang[2], Yu Zhang[1], Hua Zhang[1], Chuanxi Zhang[1], Xuexi Xuan[1], Mingjie Wang[1], Jinying Zhang[2] and Yiqiang Yuan[3]**

[1]Department of Cardiology, The Seventh People's Hospital of Zhengzhou, Zhengzhou, China, [2]Department of Cardiology, The First Affiliated Hospital of Zhengzhou University, Zhengzhou, China, [3]Department of Cardiology, Chest Hospital of Henan Provincial, Zhengzhou, China

Acute myocardial infarction has a high clinical mortality rate. The initial exclusion or diagnosis is important for the timely treatment of patients with acute myocardial infarction. As a marker, cardiac troponin I (cTnI) has a high specificity, high sensitivity to myocardial injury and a long diagnostic window. Therefore, its diagnostic value is better than previous markers of myocardial injury. In this work, we propose a novel aptamer electrochemical sensor. This sensor consists of silver nanoparticles/MoS_2/reduced graphene oxide. The combination of these three materials can provide a synergistic effect for the stable immobilization of aptamer. Our proposed aptamer electrochemical sensor can detect cTnI with high sensitivity. After optimizing the parameters, the sensor can provide linear detection of cTnI in the range of 0.3 pg/ml to 0.2 ng/ml. In addition, the sensor is resistant to multiple interferents including urea, glucose, myoglobin, dopamine and hemoglobin.

Keywords: aptamer electrochemical sensor, reduced graphene oxide, troponin I, mos2, glassy carbon electrode

OPEN ACCESS

Edited by:
Li Fu,
Hangzhou Dianzi University, China

Reviewed by:
Hassan Karimi-maleh,
University of Electronic Science and Technology of China, China
Yuhong Zheng,
Jiangsu Province and Chinese Academy of Sciences, China

****Correspondence:***
Jinying Zhang
Jinyingzhang2021@163.com
Yiqiang Yuan
yqyuan@sutcm.net

Specialty section:
This article was submitted to Electrochemistry, a section of the journal Frontiers in Chemistry

Received: *15 March 2021*
Accepted: *26 April 2021*
Published: *14 May 2021*

Citation:
Li J, Zhang S, Zhang L, Zhang Y, Zhang H, Zhang C, Xuan X, Wang M, Zhang J and Yuan Y (2021) A Novel Graphene-Based Nanomaterial Modified Electrochemical Sensor for the Detection of Cardiac Troponin I. Front. Chem. 9:680593. doi: 10.3389/fchem.2021.680593

INTRODUCTION

Troponin is a regulatory heteropeptide protein found in myogenic fiber filaments that plays a pivotal role in the interaction between actin and myosin. It controls contraction and relaxation of skeletal and cardiac muscles. Troponin is a complex that includes three subunits: ion-binding troponin (cTnC), troponin that inhibits actin-myosin interaction (cTnI) and tropomyosin (cTnT), which is used to bind the myosin complex to promyosin and promote myocardial contraction (Fan et al., 2018; Miao et al., 2019; Phonklam et al., 2020). It has been demonstrated that cTnI is a specific biomarker for myocardial injury in dogs, cats, horses, pigs, goats, mice and cattle. Damage to myocardial cell integrity is followed by partial release of cTnI into the blood, and elevated cardiac troponin concentrations in peripheral blood indicate myocardial cell damage (Palladino et al., 2018; Karimi-Maleh et al., 2020a; Çimen et al., 2020). Since myocardial infarction is one of the most important factors leading to myocardial cell destruction, monitoring of cTnI blood concentrations is particularly important for the early detection of myocardial infarction (Ye et al., 2018; Lee et al., 2019; Sun et al., 2019a; Karimi-Maleh et al., 2020b, 2021). There is evidence that even small elevations in cTnI may be associated with poor prognosis. However, as with most other current assays, their most significant shortcoming lies within the first few hours of acute myocardial infarction onset. Current cTnI assays are not effective in detecting elevated blood concentrations and are not effective in

monitoring changes in lower concentrations of cTnI. Therefore, the development and application of next-generation cTnI assays is imminent (Negahdary et al., 2017; Zhang et al., 2018; Fu et al., 2019b; Sun et al., 2019b; Zhou et al., 2020).

Radioimmunoassay is a method by which an isotope-labeled antigen is added to an unlabeled antigen to cause a competitive inhibition reaction with the antibody. The radioimmunoassay is equal to the advantages due to its good utility and specificity, as well as its high sensitivity. However, the method has disadvantages such as the existence of radioactive contamination and short half-life of isotopes, which to a certain extent limit the development and application of radioimmunoassay (Qiao et al., 2018; Sarangadharan et al., 2018; Fu et al., 2019a; Wang et al., 2019; Mokhtari et al., 2020; Xu et al., 2020). Fluorescent immunoassay is mainly used for the diagnosis of infectious diseases due to its high sensitivity, and it is one of the oldest labeled immunoassays. However, the detection limit of fluorescence immunoassay is not low enough. Moreover, it is difficult to store fluorescent samples for a long time. Electrochemical immunosensor is an application that combines electrochemiluminescence measurement with immunosensor. It combines the advantages of high sensitivity of electrochemiluminescence and high selectivity of immunoassay, which has attracted the attention of many researchers (Dhawan et al., 2018; Regan et al., 2018; Karimi-Maleh et al., 2020c; Wang et al., 2020). The unique physicochemical properties of nanomaterials make it a promising application in the development of high-performance electrochemical and electrochemiluminescent sensors.

Two-dimensional nano has been widely studied for its high specific surface area and compatibility with miniaturized devices (Khodadadi et al., 2019; Tahernejad-Javazmi et al., 2019). Among them, MoS_2, in which Mo atomic layers are arranged in a hexagonal shape between S atomic layers, has an ultrathin planar structure. It is sensitive to the surrounding environment and becomes a suitable base material for building aptamer sensors (Cai et al., 2018; Chekin et al., 2018). However, MoS_2 has low electrical conductivity and Van Der Waals between the layers tend to agglomerate it. Reduced graphene (rGO) with active edge sites and excellent electrical properties can effectively improve the electrochemical activity of MoS_2. The composite of other nanomaterials in rGO can reduce the layer-layer interaction force, so the performance of rGO can be further ensured (Fathil et al., 2017; Lopa et al., 2019). Among them, silver nanomaterial materials are often used in the design of electrochemical sensors due to their cheap price and good electrocatalytic properties (Zhou et al., 2018; Yan et al., 2019).

This work synthesized AgNPs/MoS_2/rGO nanocomposites. By combining the excellent properties of the composite (large surface area and good electrical conductivity) with the aptamer (high affinity and specificity), a label-free electrochemical aptamer sensor was developed for the sensitive and selective detection of cTnI.

MATERIALS AND METHODS

cTnI and DNA oligonucleotides were obtained from Yeyuan Biotech. Urea, thrombin, myoglobin, horseradish peroxidase, L-cysteine, hemoglobin, and prostate-specific antigen were ordered from Alading Co. Ltd. Graphene oxide (GO) powder was purchased from Xianfeng Nano Tech Co. Ltd. All other reagents are analytically pure and can be used without additional purification. 0.1 M Tris-HCl buffer solution has been used for dissolving amino-modified cTnI aptamer (AcTnl).

Sequence of the AcTnl is: 5′-NH_2-C_6H_{12}-CGTGCAGTAC GCCAACCTTTCTCATGCGCGCTGCCCCTCTTA-3′.

All electrochemical tests, including cyclic voltammetry (CV), differential pulse voltammetry (DPV), and electrochemical impedance spectroscopy (EIS) were performed using the CHI660 electrochemical analyzer/workstation with three-electrode system. SEM image has been recorded using a ZEISS MERLIN.

Synthesis of AgNPs/MoS_2/rGO nanocomposite: 50 mg of $AgNO_3$ was dissolved in 20 ml of ethanol and 100 mg of octadecylamine was added with vigorous stirring. After complete dissolution, 50 mg of glucose and 60 mg of glycine were added and sonicated. The solution was transferred to a hydrothermal kettle and heated at 120°C for overnight. Silver nanoparticles (AgNPs) were obtained after filtration. MoS_2/rGO was prepared by adding 10 mg $Na_2MoO_4.2H_2O$ and 20 mg L-cysteine into 20 ml of GO dispersion (0.5 mg/ml, DMF). The mixture was then transferred into a hydrothermal kettle and heated at 100°C for 5 h. The MoS_2/rGO was collected after the filtration. The AgNPs/MoS_2/rGO nanocomposite was prepared by adding AgNPs into MoS_2/rGO composite dispersion after 1 h sonication.

Electrode fabrication: A glassy carbon electrode (GCE) has been used for sensor fabrication. Specifically, a certain amount of AgNPs/MoS_2/rGO nanocomposite was drop casted on a GCE and dried naturally. Then, a certain amount of AcTnl was drop casted on the AgNPs/MoS_2/rGO/GCE. After drying, the AcTnl/AgNPs/MoS_2/rGO was incubated in the cTnl solution with different concentration for 1 h before electrochemical signal recording.

RESULTS AND DISCUSSION

Figure 1 demonstrates the preparation and sensing strategy of this label-free electrochemical aptamer sensor. AgNPs/MoS_2/rGO immobilized with GCE can immobilize the AcTnl aptamer on the electrode surface via Ag-N bond. In this process, the electrochemical signal of $[Fe(CN)_6]^{3-/4-}$ decreases because the electron transfer is hindered by the nucleobases. When AcTnl/AgNPs/MoS_2/rGO is immersed in the cTnI solution, the electrochemical signal is further reduced due to the formation of AcTnI-cTnI complexes on the electrode surface that further hinder electron transfer. By calculating the relationship between peak current and cTnI concentration, the detection of cTnI concentration can be achieved.

Figure 2 shows the SEM images of AgNPs, MoS_2/rGO, and AgNPs/MoS_2/rGO. The structure of silver nanoflowers can be clearly observed in **Figure 2A**. The SEM images of MoS_2/rGO show the typical wrinkled and folded structure of graphene and the layer-like structure of MoS_2/rGO. The tight contact between

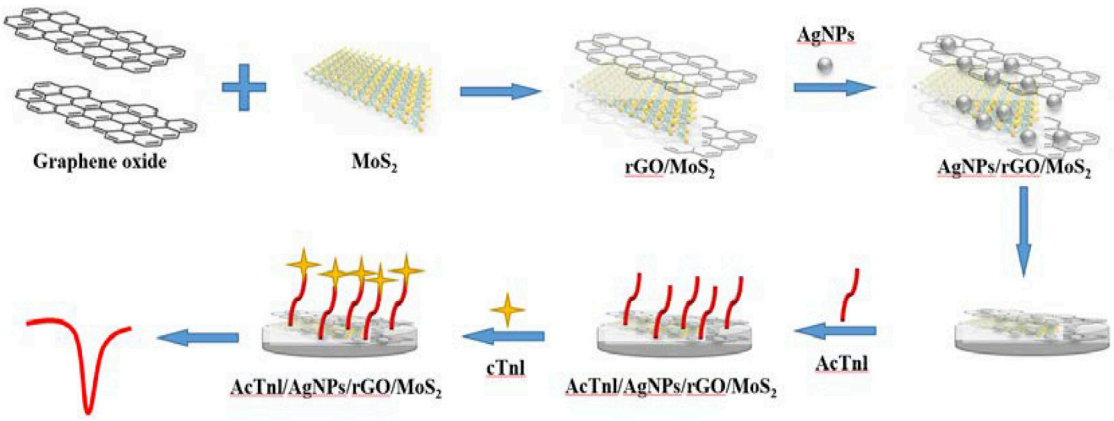

FIGURE 1 | Schematic diagram for the preparation of the AcTnI/AgNPs/MoS_2/rGO sensor for cTnI detection.

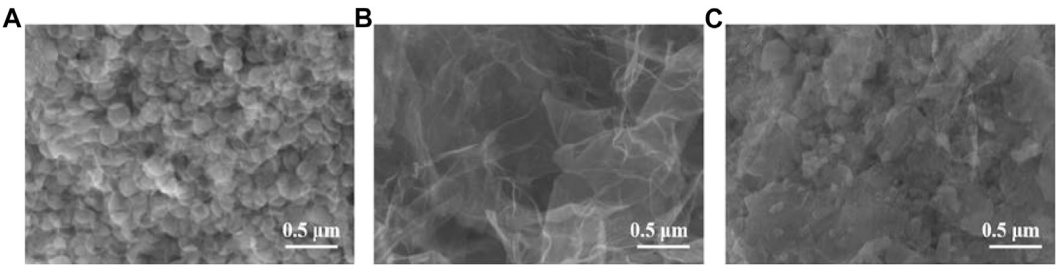

FIGURE 2 | SEM images of **(A)** AgNPs **(B)** MoS_2/rGO, and **(C)** AgNPs/MoS_2/rGO.

MoS_2 and rGO is favorable for electron transfer. The SEM images of AgNPs/MoS_2/rGO nanocomposites clearly observe that AgNPs are wrapped by MoS_2/rGO composites.

We tested the electrochemical behavior of the electrode surface during sensor assembly using a 5.0 mM $[Fe(CN)_6]^{3-/4-}$ solution containing 0.1 M KCl (**Figure 3**). The redox peak current of the modified GCE was significantly increased due to the excellent conductivity and electron transfer of rGO. After the modification of GCE with MoS_2/rGO and AgNPs/MoS_2/rGO, the currents increased significantly in turn, which was caused by the large specific surface area of MoS_2 and the excellent electrochemical properties of AgNPs.

The electrochemical properties of the sensor was further investigated by EIS. In EIS, semicircular and straight regions indicate electron transfer-limited processes and mass transfer control processes (Demirbakan and Kemal Sezgintürk, 2020; Lee et al., 2020), respectively. Considering the variation of the electron transfer resistance (R_{ct}), the EIS method can provide important information to demonstrate the interaction between the aptamer and the target protein. As shown in **Figure 4**, bare GCE presents a small semicircle with an R_{ct} value of 266 Ω. Due to the excellent properties and synergistic effects of rGO, MoS_2 and AgNPs, the R_{ct} value decreases to 91 Ω after AgNPs/MoS_2/rGO modification, indicating that the electron transfer effect is enhanced. This is consistent with the CV results of GCE and AgNPs/MoS_2/rGO/GCE. While the presence of AcTnI leads to an increase in the spatial site blocking effect and hinders electron transfer, the R_{ct} increases sharply to occur at 3.31 kΩ, indicating the binding of AcTnI and AgNWs on the electrode surface. With the binding of the target protein on the AcTnI/AgNPs/MoS_2/rGO/GCE surface, a continued increase in R_{ct} to 5.26 kΩ can be observed, indicating a successful binding with the target protein to its aptamer, which hinders the electron transfer.

In order to improve the sensitivity of detecting cTnI, different parameters were optimized. **Figure 5A** shows the aptamer electrodes assembled with different concentrations of AgNPs in the MoS_2/rGO dispersion. Although AgNPs have excellent electrochemical properties, when AgNPs exceed a certain concentration it may cause a high stacking density, resulting in a lower detection efficiency of the sensor. Therefore, we chose to add 250 μLof AgNPs into the MoS_2/rGO dispersion.

The amount of modification of AgNPs/MoS_2/rGO is an important factor affecting the immobilization of AcTnI. **Figure 5B** shows the electrochemical response of the proposed aptamer sensor AgNPs/MoS_2/rGO at different modification amounts. As the concentration of AgNPs/MoS_2/rGO increases, the electron transfer resistance of the interface may increase,

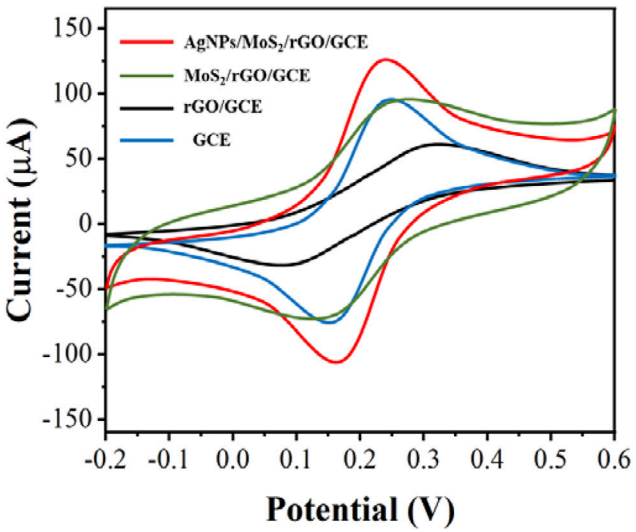

FIGURE 3 | CV of GCE, rGO/GCE, MoS_2/rGO/GCE and AgNPs/MoS_2/rGO/GCE in 5.0 mM $[Fe(CN)_6]^{3-/4-}$. Scan rate: 50 mV/s.

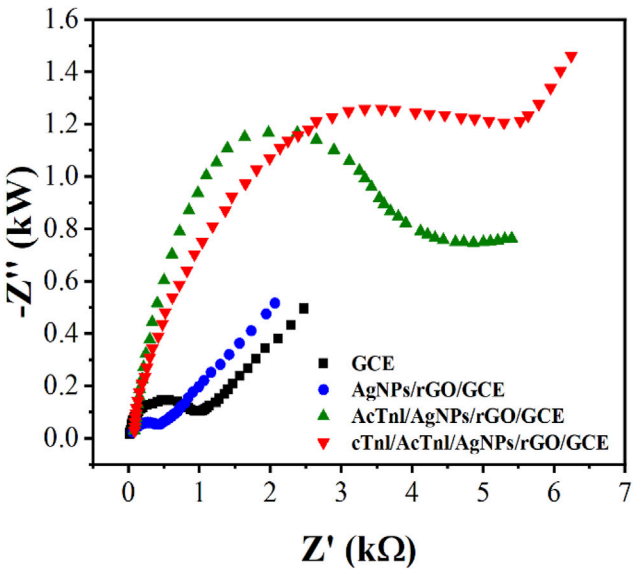

FIGURE 4 | EIS of GCE, rGO/GCE, MoS_2/rGO/GCE and AgNps/MoS_2/rGO/GCE in 5.0 mM $[Fe(CN)_6]^{3-/4-}$.

while there may be some interference with the detection of cTnI. Therefore, 5 μL of AgNPs/MoS_2/rGO dispersion was obtained as the optimal condition.

The concentration of AcTnI affects the charge transfer efficiency of the electrode interface for detecting cTnI. **Figure 6A** shows the effect of different AcTnI concentrations on the DPV signal of AgNPs/MoS_2/rGO. When the concentration reaches 3 μM, the DPV response is significantly reduced, indicating that the surface active site of the sensor may be fully occupied. Considering the size of the aptamer itself, the tightly packed surface prevents the aptamer from specifically binding cTnI. because we chose 3 μM AcTnI as the optimal concentration for the aptamer sensor.

The incubation time of cTnI is also another important factor affecting cTnI detection. As shown in **Figure 6B**, the electrochemical signal did not change significantly after the incubation time of AcTnI reached 30 min. This indicates that the bioaffinity between AcTnI on the electrode surface and the cTnI target saturated. On the other hand, the current response stabilizes due to the spatial potential resistance effect, leading to a decrease in sensitivity to the target. Therefore, we chose 30 min as the optimal incubation time.

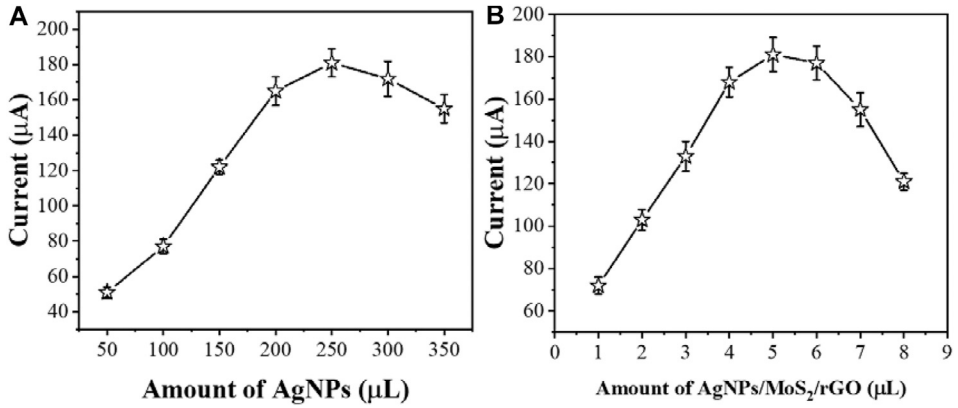

FIGURE 5 | The effect of **(A)** amount of AgNPs and **(B)** AgNPs/MoS_2/rGO composite for sensing performance ($n \geq 3$).

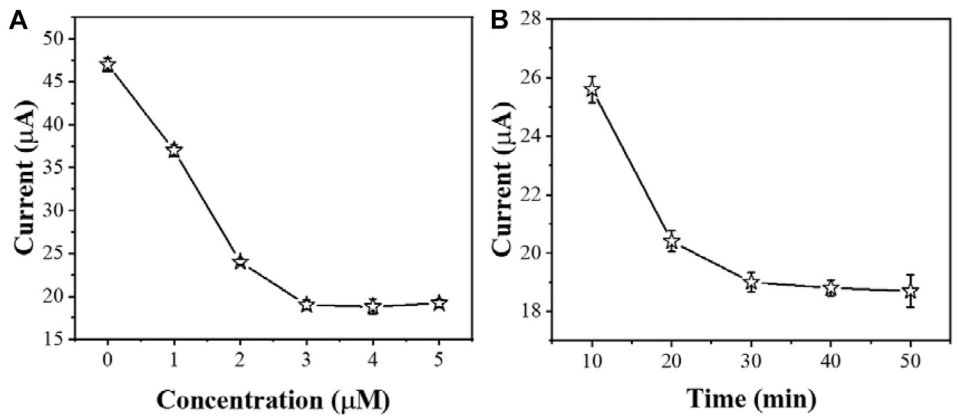

FIGURE 6 | The effect of **(A)** amount of AcTnI and **(B)** incubation time for sensing performance ($n \geq 3$).

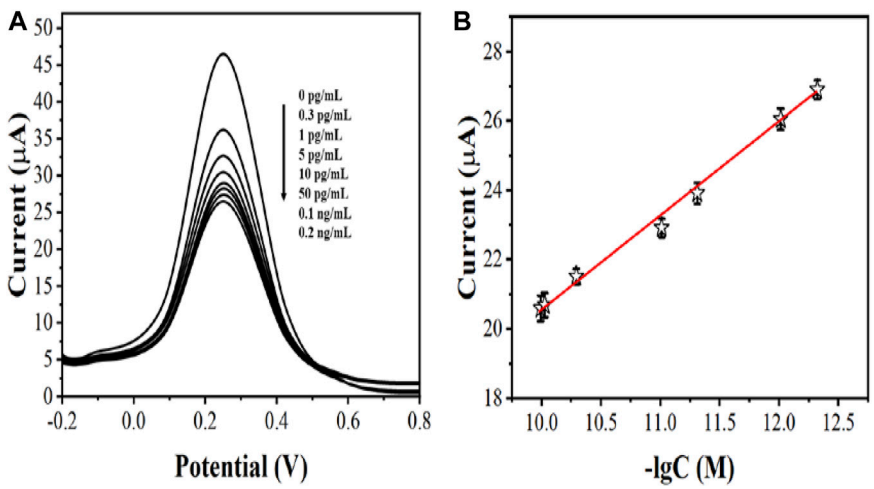

FIGURE 7 | (A) DPV curves of AcTnI/AgNPs/MoS_2/rGO/GCE toward 0 pg/ml, 0.3 pg/ml, 1 pg/ml, 5 pg/ml, 10 pg/ml, 50 pg/ml, 0.1 ng/ml, and 0.2 ng/ml **(B)** Linear relationship between current and logarithm of the cTnI concentrations ($n \geq 3$).

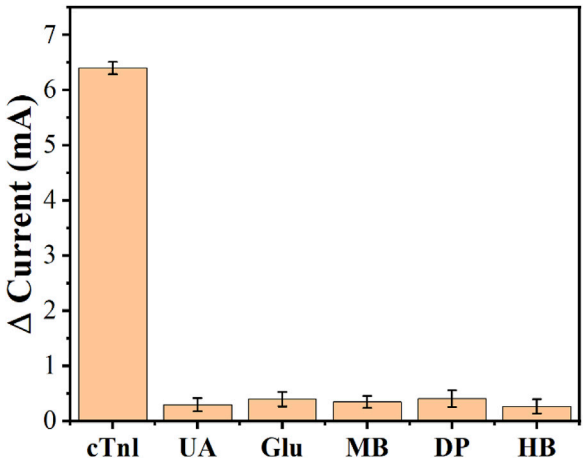

FIGURE 8 | Anti-interference performance of the AcTnI/AgNPs/MoS_2/rGO/GCE toward UA, Glu, MB, DP, and HB.

After optimizing the parameters, we immersed AcTnI/AgNPs/MoS_2/rGO/GCE in different concentrations of cTnI solutions. Then, we detected the electrochemical signal by DPV in a 5 mM $[Fe(CN)_6]^{3-/4-}$ solution containing 0.5 M KCl (**Figure 7A**). We recorded the linear relationship between the peak value of DPV and the negative logarithm of the concentration of the cTnI standard solution to establish a standard working curve (**Figure 7B**). It can be seen that the DPV signal correlates well with the negative logarithm of the cTnI concentration in the range of 0.3 pg/mL–0.2 ng/ml with the linear equation: Ip (μA) = −2.73 logc (g/ml) −6.41 (R^2 = 0.9947) and the limit of detection limit was 0.27 pg/ml.

To examine the performance of the aptamer sensor, we tested the reproducibility, stability and specificity of AcTnI/AgNPs/MoS_2/rGO/GCE. The RSD of 1.72% was recorded by checking 5 parallel measurements on the same sensor, indicating that the electrochemical aptamer sensor for cTnI detection has good reproducibility. The stability of the prepared aptamer sensor was further evaluated by measuring the DPV current of the modified electrode after one month. The electrochemical signal before and after storage changed slightly with a 5.2% decrease in the peak DPV, demonstrating the good stability of the proposed electrochemical aptamer sensor for cTnI detection.

To determine the selectivity of the developed aptamer sensor, a series of proteins were used for comparison, such as: urea (UA), glucose (Glu), myoglobin (MB), dopamine (DP), and hemoglobin (HB). Among them, the concentration of cTnI was 50 pg/ml and the concentration of other infectants was 0.2 ng/ml due to the excellent specific discrimination between cTnI and AcTnI, the aptamer sensor for interferers showed negligible change in current response compared to cTnI, and the results are shown in **Figure 8**. The proposed aptamer sensor has good selectivity and specific anti-interference ability.

CONCLUSION

In summary, an aptamer electrochemical sensor was constructed using AgNPs/MoS_2/rGO nanocomposite. By combining the excellent properties of the composite (large surface area and good electrical conductivity) with the aptamer (high affinity and specificity), a label-free electrochemical aptamer sensor was developed for the sensitive and selective detection of cTnI. After the optimizations, the proposed aptamer sensor can linear detect cTnl between 0.3 pg/mL–0.2 ng/ml with a low limit of detection of 0.27 pg/ml. In addition, the proposed aptamer sensor has good selectivity and specific anti-interference ability.

DATA AVAILABILITY STATEMENT

The original contributions presented in the study are included in the article/Supplementary Material, further inquiries can be directed to the corresponding authors.

AUTHOR CONTRIBUTIONS

JL and SZ conceived of the study. JZ and YY supervised the development program, LZ, JL, and HZ conducted the materials characterization. YZ, CZ, and XX received and curated samples and analytical records. SZ, MW, and JZ wrote the manuscript. All authors read and approved of the manuscript.

FUNDING

This work was funded by Science and Technology Research Plan Joint Construction Project of Henan Province (LHGJ20191112).

REFERENCES

Cai, Y., Kang, K., Li, Q., Wang, Y., and He, X. (2018). Rapid and Sensitive Detection of Cardiac Troponin I for Point-Of-Care Tests Based on Red Fluorescent Microspheres. *Molecules* 23, 1102. doi:10.3390/molecules23051102

Chekin, F., Vasilescu, A., Jijie, R., Singh, S. K., Kurungot, S., Iancu, M., et al. (2018). Sensitive Electrochemical Detection of Cardiac Troponin I in Serum and Saliva by Nitrogen-Doped Porous Reduced Graphene Oxide Electrode. *Sensors Actuators B: Chem.* 262, 180–187. doi:10.1016/j.snb.2018.01.215

Çimen, D., Bereli, N., Günaydın, S., and Denizli, A. (2020). Detection of Cardiac Troponin-I by Optic Biosensors with Immobilized Anti-cardiac Troponin-I Monoclonal Antibody. *Talanta* 219, 121259. doi:10.1016/j.talanta.2020.121259

Demirbakan, B., and Kemal Sezgintürk, M. (2020). A Novel Ultrasensitive Immunosensor Based on Disposable Graphite Paper Electrodes for Troponin T Detection in Cardiovascular Disease. *Talanta* 213, 120779. doi:10.1016/j.talanta.2020.120779

Dhawan, S., Sadanandan, S., Haridas, V., Voelcker, N. H., and Prieto-Simón, B. (2018). Novel Peptidylated Surfaces for Interference-free Electrochemical Detection of Cardiac Troponin I. *Biosens. Bioelectron.* 99, 486–492. doi:10.1016/j.bios.2017.08.024

Fan, D., Bao, C., Khan, M. S., Wang, C., Zhang, Y., Liu, Q., et al. (2018). A Novel Label-free Photoelectrochemical Sensor Based on N,S-GQDs and CdS Co-sensitized Hierarchical Zn2SnO4 Cube for Detection of Cardiac Troponin I. *Biosens. Bioelectron.* 106, 14–20. doi:10.1016/j.bios.2018.01.050

Fathil, M. F. M., Md Arshad, M. K., Ruslinda, A. R., Gopinath, S. C. B., Nuzaihan M.N., M., Adzhri, R., et al. (2017). Substrate-gate Coupling in ZnO-FET Biosensor for Cardiac Troponin I Detection. *Sensors Actuators B: Chem.* 242, 1142–1154. doi:10.1016/j.snb.2016.09.131

Fu, L., Wu, M., Zheng, Y., Zhang, P., Ye, C., Zhang, H., et al. (2019a). Lycoris Species Identification and Infrageneric Relationship Investigation via Graphene Enhanced Electrochemical Fingerprinting of Pollen. *Sensors Actuators B: Chem.* 298, 126836. doi:10.1016/j.snb.2019.126836

Fu, L., Zheng, Y., Zhang, P., Zhang, H., Wu, M., Zhang, H., et al. (2019b). An Electrochemical Method for Plant Species Determination and Classification Based on Fingerprinting Petal Tissue. *Bioelectrochemistry* 129, 199–205. doi:10.1016/j.bioelechem.2019.06.001

Karimi-Maleh, H., Alizadeh, M., Orooji, Y., Karimi, F., Baghayeri, M., Rouhi, J., et al. (2021). Guanine-Based DNA Biosensor Amplified with Pt/SWCNTs Nanocomposite as Analytical Tool for Nanomolar Determination of Daunorubicin as an Anticancer Drug: A Docking/Experimental Investigation. *Ind. Eng. Chem. Res.* 60, 816–823. doi:10.1021/acs.iecr.0c04698

Karimi-Maleh, H., Ayati, A., Ghanbari, S., Orooji, Y., Tanhaei, B., Karimi, F., et al. (2021c). Recent Advances in Removal Techniques of Cr(VI) Toxic Ion from Aqueous Solution: A Comprehensive Review. *J. Mol. Liquids* 329, 115062. doi:10.1016/j.molliq.2020.115062

Karimi-Maleh, H., Karimi, F., Malekmohammadi, S., Zakariae, N., Esmaeili, R., Rostamnia, S., et al. (2020a). An Amplified Voltammetric Sensor Based on Platinum Nanoparticle/polyoxometalate/two-Dimensional Hexagonal Boron Nitride Nanosheets Composite and Ionic Liquid for Determination of N-Hydroxysuccinimide in Water Samples. *J. Mol. Liquids* 310, 113185. doi:10.1016/j.molliq.2020.113185

Karimi-Maleh, H., Kumar, B. G., Rajendran, S., Qin, J., Vadivel, S., Durgalakshmi, D., et al. (2020b). Tuning of Metal Oxides Photocatalytic Performance Using Ag Nanoparticles Integration. *J. Mol. Liquids* 314, 113588. doi:10.1016/j.molliq.2020.113588

Khodadadi, A., Faghih-Mirzaei, E., Karimi-Maleh, H., Abbaspourrad, A., Agarwal, S., and Gupta, V. K. (2019). A New Epirubicin Biosensor Based on Amplifying DNA Interactions with Polypyrrole and Nitrogen-Doped Reduced Graphene: Experimental and Docking Theoretical Investigations. *Sensors actuators b: Chem.* 284, 568–574. doi:10.1016/j.snb.2018.12.164

Lee, K. W., Kim, K. R., Chun, H. J., Jeong, K. Y., Hong, D.-K., Lee, K.-N., et al. (2020). Time-resolved Fluorescence Resonance Energy Transfer-Based Lateral Flow Immunoassay Using a Raspberry-type Europium Particle and a Single Membrane for the Detection of Cardiac Troponin I. *Biosens. Bioelectron.* 163, 112284. doi:10.1016/j.bios.2020.112284

Lee, T., Ahn, J.-H., Choi, J., Lee, Y., Kim, J.-M., Park, C., et al. (2019). Development of the Troponin Detection System Based on the Nanostructure. *Micromachines* 10, 203. doi:10.3390/mi10030203

Lopa, N. S., Rahman, M. M., Ahmed, F., Ryu, T., Sutradhar, S. C., Lei, J., et al. (2019). Simple, Low-Cost, Sensitive and Label-free Aptasensor for the Detection of Cardiac Troponin I Based on a Gold Nanoparticles Modified Titanium Foil. *Biosens. Bioelectron.* 126, 381–388. doi:10.1016/j.bios.2018.11.012

Miao, L., Jiao, L., Tang, Q., Li, H., Zhang, L., and Wei, Q. (2019). A Nanozyme-Linked Immunosorbent Assay for Dual-Modal Colorimetric and Ratiometric Fluorescent Detection of Cardiac Troponin I. *Sensors Actuators B: Chem.* 288, 60–64. doi:10.1016/j.snb.2019.02.111

Mokhtari, Z., Khajehsharifi, H., Hashemnia, S., Solati, Z., Azimpanah, R., and Shahrokhian, S. (2020). Evaluation of Molecular Imprinted Polymerized Methylene Blue/aptamer as a Novel Hybrid Receptor for Cardiac Troponin I (cTnI) Detection at Glassy Carbon Electrodes Modified with New Biosynthesized ZnONPs. *Sensors Actuators B: Chem.* 320, 128316. doi:10.1016/j.snb.2020.128316

Negahdary, M., Behjati-Ardakani, M., Sattarahmady, N., Yadegari, H., and Heli, H. (2017). Electrochemical Aptasensing of Human Cardiac Troponin I Based on an Array of Gold Nanodumbbells-Applied to Early Detection of Myocardial Infarction. *Sensors Actuators B: Chem.* 252, 62–71. doi:10.1016/j.snb.2017.05.149

Palladino, P., Minunni, M., and Scarano, S. (2018). Cardiac Troponin T Capture and Detection in Real-Time via Epitope-Imprinted Polymer and Optical Biosensing. *Biosens. Bioelectron.* 106, 93–98. doi:10.1016/j.bios.2018.01.068

Phonklam, K., Wannapob, R., Sriwimol, W., Thavarungkul, P., and Phairatana, T. (2020). A Novel Molecularly Imprinted Polymer PMB/MWCNTs Sensor for Highly-Sensitive Cardiac Troponin T Detection. *Sensors Actuators B: Chem.* 308, 127630. doi:10.1016/j.snb.2019.127630

Qiao, X., Li, K., Xu, J., Cheng, N., Sheng, Q., Cao, W., et al. (2018). Novel Electrochemical Sensing Platform for Ultrasensitive Detection of Cardiac Troponin I Based on Aptamer-MoS2 Nanoconjugates. *Biosens. Bioelectron.* 113, 142–147. doi:10.1016/j.bios.2018.05.003

Regan, B., O'Kennedy, R., and Collins, D. (2018). Point-of-Care Compatibility of Ultra-sensitive Detection Techniques for the Cardiac Biomarker Troponin I-Challenges and Potential Value. *Biosensors* 8, 114. doi:10.3390/bios8040114

Sarangadharan, I., Regmi, A., Chen, Y.-W., Hsu, C.-P., Chen, P.-c., Chang, W.-H., et al. (2018). High Sensitivity Cardiac Troponin I Detection in Physiological Environment Using AlGaN/GaN High Electron Mobility Transistor (HEMT) Biosensors. *Biosens. Bioelectron.* 100, 282–289. doi:10.1016/j.bios.2017.09.018

Sun, D., Lin, X., Lu, J., Wei, P., Luo, Z., Lu, X., et al. (2019a). DNA Nanotetrahedron-Assisted Electrochemical Aptasensor for Cardiac Troponin I Detection Based on the Co-catalysis of Hybrid Nanozyme, Natural Enzyme and Artificial DNAzyme. *Biosens. Bioelectron.* 142, 111578. doi:10.1016/j.bios.2019.111578

Sun, D., Luo, Z., Lu, J., Zhang, S., Che, T., Chen, Z., et al. (2019b). Electrochemical Dual-Aptamer-Based Biosensor for Nonenzymatic Detection of Cardiac Troponin I by Nanohybrid Electrocatalysts Labeling Combined with DNA Nanotetrahedron Structure. *Biosens. Bioelectron.* 134, 49–56. doi:10.1016/j.bios.2019.03.049

Tahernejad-Javazmi, F., Shabani-Nooshabadi, M., and Karimi-Maleh, H. (2019). 3D Reduced Graphene oxide/FeNi3-Ionic Liquid Nanocomposite Modified Sensor; an Electrical Synergic Effect for Development of Tert-Butylhydroquinone and Folic Acid Sensor. *Composites B: Eng.* 172, 666–670. doi:10.1016/j.compositesb.2019.05.065

Wang, S., Zhao, Y., Wang, M., Li, H., Saqib, M., Ge, C., et al. (2019). Enhancing Luminol Electrochemiluminescence by Combined Use of Cobalt-Based Metal Organic Frameworks and Silver Nanoparticles and its Application in Ultrasensitive Detection of Cardiac Troponin I. *Anal. Chem.* 91, 3048–3054. doi:10.1021/acs.analchem.8b05443

Wang, Y., Yang, Y., Chen, C., Wang, S., Wang, H., Jing, W., et al. (2020). One-step Digital Immunoassay for Rapid and Sensitive Detection of Cardiac Troponin I. *ACS Sens.* 5, 1126–1131. doi:10.1021/acssensors.0c00064

Xu, Y., Lu, Y., Zhang, P., Wang, Y., Zheng, Y., Fu, L., et al. (2020). Infrageneric Phylogenetics Investigation of Chimonanthus Based on Electroactive Compound Profiles. *Bioelectrochemistry* 133, 107455. doi:10.1016/j.bioelechem.2020.107455

Yan, M., Ye, J., Zhu, Q., Zhu, L., Huang, J., and Yang, X. (2019). Ultrasensitive Immunosensor for Cardiac Troponin I Detection Based on the Electrochemiluminescence of 2D Ru-MOF Nanosheets. *Anal. Chem.* 91, 10156–10163. doi:10.1021/acs.analchem.9b02169

Ye, J., Zhu, L., Yan, M., Zhu, Q., Lu, Q., Huang, J., et al. (2018). Dual-wavelength Ratiometric Electrochemiluminescence Immunosensor for Cardiac Troponin I Detection. *Anal. Chem.* 91, 1524–1531. doi:10.1021/acs.analchem.8b04640

Zhang, T., Ma, N., Ali, A., Wei, Q., Wu, D., and Ren, X. (2018). Electrochemical Ultrasensitive Detection of Cardiac Troponin I Using Covalent Organic Frameworks for Signal Amplification. *Biosens. Bioelectron.* 119, 176–181. doi:10.1016/j.bios.2018.08.020

Zhou, J., Zheng, Y., Zhang, J., Karimi-Maleh, H., Xu, Y., Zhou, Q., et al. (2020). Characterization of the Electrochemical Profiles of Lycoris Seeds for Species Identification and Infrageneric Relationships. *Anal. Lett.* 53, 2517–2528. doi:10.1080/00032719.2020.1746327

Zhou, W., Li, K., Wei, Y., Hao, P., Chi, M., Liu, Y., et al. (2018). Ultrasensitive Label-free Optical Microfiber Coupler Biosensor for Detection of Cardiac Troponin I Based on Interference Turning Point Effect. *Biosens. Bioelectron.* 106, 99–104. doi:10.1016/j.bios.2018.01.061

Conflict of Interest: The authors declare that the research was conducted in the absence of any commercial or financial relationships that could be construed as a potential conflict of interest.

frontiers in Chemistry

ORIGINAL RESEARCH
published: 31 May 2021
doi: 10.3389/fchem.2021.696906

Graphene-Assisted Sensor for Rapid Detection of Antibiotic Resistance in *Escherichia coli*

Chunlei Li[1] *and Feng Sun*[2]*

[1]Department of Gastroenterology, Jiaozhou Central Hospital, Jiaozhou, China, [2]Department of Colorectal and Anal Surgery, The First Affiliated Hospital of Guangzhou University of Traditional Chinese Medicine, Guangzhou, China

In recent years, antibiotic-resistant bacteria caused by antibiotic abuse in the medical industry have become a new environmental pollutant that endangers public health. Therefore, it is necessary to establish a detection method for evaluating drug-resistant bacteria. In this work, we used *Escherichia coli* as a target model and proposed a method to evaluate its drug resistance for three antibiotics. Graphene dispersion was used to co-mix with *E. coli* cells for the purpose of increasing the current signal. This electrochemical-based sensor allows the evaluation of the activity of *E. coli* on the electrode surface. When antibiotics were present, the electrocatalytic reduction signal was diminished because of the reduced activity of *E. coli*. Based on the difference in the electrochemical reduction signal, we can evaluate the antibiotic resistance of different *E. coli* strains.

Keywords: electrochemical sensors, drug-resistant strains, activity determination, antibiotics, electrode modification, catalytic reduction current

OPEN ACCESS

Edited by:
Fatemeh Karimi,
Quchan University of Advanced Technology, Iran

Reviewed by:
Somaye Cheraghi,
Shahid Bahonar University of Kerman, Iran
Vahid Arabali,
Islamic Azad University Sari Branch, Iran

***Correspondence:**
Feng Sun
sunfeng@wcsy-uni.cn

Specialty section:
This article was submitted to Electrochemistry, a section of the journal Frontiers in Chemistry

Received: *18 April 2021*
Accepted: *17 May 2021*
Published: *31 May 2021*

Citation:
Li C and Sun F (2021) Graphene-Assisted Sensor for Rapid Detection of Antibiotic Resistance in Escherichia coli. *Front. Chem. 9:696906. doi: 10.3389/fchem.2021.696906*

INTRODUCTION

Antibiotics are secondary metabolites that can interfere with cell growth and development (Simioni et al., 2017; Wang M. et al., 2019). They are mainly of microbial origin. The biochemist Fleming first discovered penicillin in 1929. Penicillin played an important role in World War II and was very effective in controlling bacterial infections (Alsaiari et al., 2021). However, the harm of antibiotics to the human body should not be underestimated. For example, furacilin enters the human body through food and may cause cancer with long-term consumption (Hu et al., 2010). Similarly, the commonly used sulfonamide antibiotic sulfadimethoxine has tumorigenic effects (Zhuang et al., 2019). According to the classification of chemical structure, antibiotics can be roughly divided into quinolone antibiotics, sulfonamide antibiotics, chloramphenicol antibiotics, aminoglycoside antibiotics, beta-lactam antibiotics and tetracycline antibiotics (Sharaha et al., 2017).

Large amounts of antibiotics are often used in the medical industry, and bacteria can develop resistance under the pressure of antibiotic selection. Antibiotic resistance genes (ARGs) are intrinsic to the development of drug resistance (Osman et al., 2021). Earlier studies have found that resistant bacteria are able to transfer the resistance genes they contain to other bacteria through animal excreta at the genetic level, eventually causing the large-scale presence of resistant bacteria (Hu et al., 2017).

Drug-resistant bacteria (ARB) are some bacteria that are originally sensitive and turn out to be resistant to drugs (Bengtson et al., 2017; Mulat et al., 2019). However, in low concentrations of antibiotics, some bacteria that were previously resistant tend to lose their resistance. This is because sensitive bacteria require fewer nutrients than resistant bacteria and have an advantage when competing with resistant bacteria, which inhibit the growth of resistant bacteria (Mishra et al., 2018; Sun et al., 2020). Therefore, reducing the abuse of antibiotics can reduce the risk of drug resistance. In

general, long-term use of antibiotics tends to lead to the development of bacterial resistance (Gorlenko et al., 2020; Karimi-Maleh et al., 2020; Zhao et al., 2020). Bacterial resistance has become one of the top 10 global health threats, and its contamination is widespread and persistent. ARGs enter the human body through the food chain and cause an imbalance in the normal flora and increase the resistance of pathogenic and conditionally pathogenic bacteria in the body, posing a serious threat to the health of the body and disease control (Wang Y. et al., 2019; Karimi-Maleh et al., 2021a).

The traditional method for detection of bacterial resistance is the microbial inhibition method. Traditional microbial suppression methods are mostly based on bacterial isolation and culture methods, mainly for the detection of bacterial drug resistance phenotypes (Asghar et al., 2017; Zhou et al., 2017; Karimi-Maleh et al., 2021b, 2021c). The commonly used detection methods are mainly paper diffusion method and agar dilution method. The paper diffusion method is to apply a drug-sensitive tablet to M–H agar that has been inoculated with the bacteria to be tested, and then measure the inhibition circle after incubation. The size of the inhibition circle is closely related to the resistance of bacteria, and the strength of bacterial resistance to antibiotics is analyzed according to its size (Sedki et al., 2017). Polymerase chain reaction (PCR) is a molecular biology technique that allows rapid amplification of target genes. Compared with traditional microbial inhibition methods, this technique has the advantages of being less time-consuming and easier to perform, and it can also meet the requirements of simultaneous detection of large quantities of samples (Bagheri et al., 2019; Phung et al., 2020). However, the PCR technique also has some shortcomings, such as easy contamination. Even a very small amount of contamination can still cause false positives (Wu et al., 2020; Zhang X. et al., 2020; Zhi-bin et al., 2021). Moreover, this technique is limited by the design of primers. Quantitative real-time fluorescent PCR (qPCR) is based on normal PCR, where a fluorescent dye or probe is added to the PCR reaction system to reflect the amount of PCR product in real time by changes in fluorescence signal. During the qPCR process, the entire process is monitored in real time, allowing the quantification of the amount of starting template (Waseem et al., 2019). The method is more specific, but expensive and not suitable for analysis of a large number of samples. Therefore, it is necessary to develop a rapid way to evaluate bacterial resistance.

In recent years, there have been recent advances in the electrochemical ultrasensitive detection of bacteria (Farooq et al., 2020; Fu et al., 2020; Khan et al., 2020; Zhang L. et al., 2020). The principle of electrochemical methods for detecting bacterial drug sensitivity is that bacterial respiration relies mainly on electron transfer in the respiratory chain, and the coincidental introduction of redox probes intervenes in the bacterial respiratory chain. The electrochemical changes generated by the respiratory chain activity can be detected rapidly and reliably by electrochemical methods. Ertl et al. (2000, 2003) used potassium ferricyanide as a redox probe. *Escherichia coli* was mixed with a solution of potassium ferricyanide after 15 min of interaction with antibiotics, and the electrical signal was measured by the chronoelectric method. The results were in complete agreement with the conventional paper diffusion method. This method can provide a report in <25 min. However, the IC_{50} values measured by electrochemical method were 100 times higher than the results obtained by standard turbidity method, and the electrodes were found to adsorb antibiotics during the test. Chotinantakul et al. (2014) improved the test protocol based on Ertl et al. The antibiotics were removed by centrifugation of *E. coli* after interaction with bacteria and resuspended in a test solution containing potassium ferricyanide, which gave the results of the drug sensitivity test in 3–6 h.

However, the detection of bacterial resistance using conventional commercial electrodes has the disadvantage of insufficient sensitivity. Therefore, improving the performance of electrodes can be a good way to improve the accuracy of detection. In this work, we modified the conventional glassy carbon electrode (GCE) with surface graphene ink, which can greatly improve the sensing performance of the electrode (Baghayeri, 2017; Zhang M. et al., 2020; Mohanraj et al., 2020; Xu et al., 2020). The modified electrode can detect the electrochemical reduction behavior of *E. coli* more sensitively. Likewise, the differences in the altered electrochemical behavior were amplified due to the influence of different antibiotics after This technique could potentially be applied for the evaluation of resistance for *E. coli*.

MATERIALS AND METHODS

All electrochemical measurements were carried out using a CHI660E working station. A three-electrode system was applied for all measurements. Specifically, a glassy carbon electrode (GCE), a Pt foil and an Ag/AgCl electrode were used as working electrode, counter electrode and reference electrode, respectively. *Escherichia coli* J53 was purchased from Beijing Bio Bo Wei Biotechnology Co., Ltd. Ofloxacin, penicillin and cefepime was purchased from Sinopharm Chemical Reagent Co., Ltd. Graphene dispersion was purchased from Jiangsu XFNANO Materials Tech Co., Ltd. All other reagents used in this work were analytical grade and used without further purification. Phosphate buffer solution (PBS, 0.1 M) was prepared by mixed stock solutions of 0.1 M disodium hydrogen phosphate and sodium dihydrogen phosphate until reach to the desired pH.

Escherichia coli J53 was grown over night in a Luria Bertani (LB) medium (100 ml) at 37°C with shaking. The cells of *E. coli* were collected after centrifugation and washed by PBS. The colony forming units (CFU) were then counted. Then, the *E. coli* was diluted by graphene dispersion to reach a desired CFU by stirring.

Electrode surface modification was conducted by drop coating of desired concentration of graphene-*E. coli* dispersion on the GCE surface and kept in a humid chamber for 1 h before analysis. Then, the electrode was inserted into a PBS and conducted a voltammetric scan. The *E. coli* modified GCE was prepared using a similar method but with out the mixing of graphene dispersion.

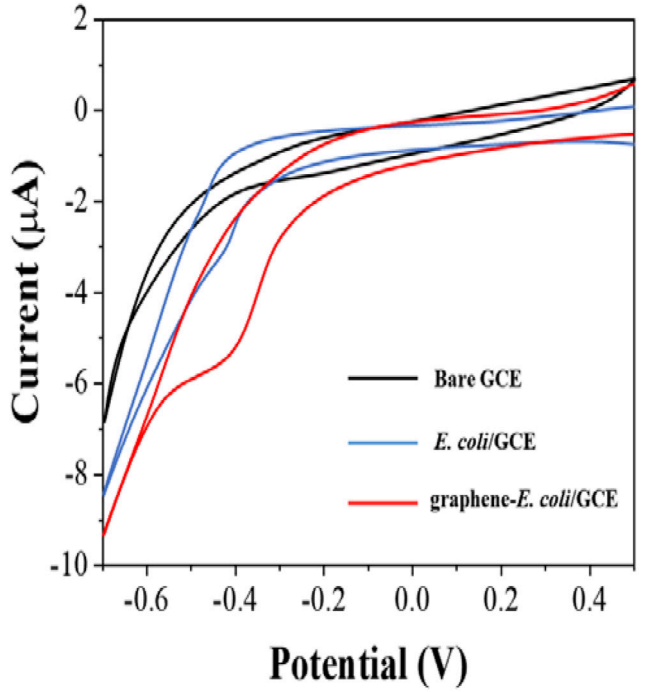

FIGURE 1 | CVs of bare GCE, *E. coli*/GCE and graphene-*E. coli*/GCE in PBS (pH = 7).

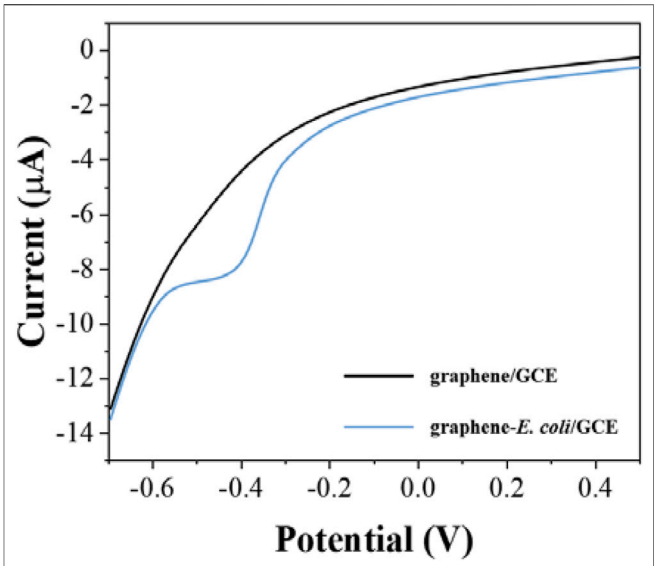

FIGURE 2 | DPV curves of graphene/GCE and graphene-*E. coli*/GCE in PBS (pH = 7).

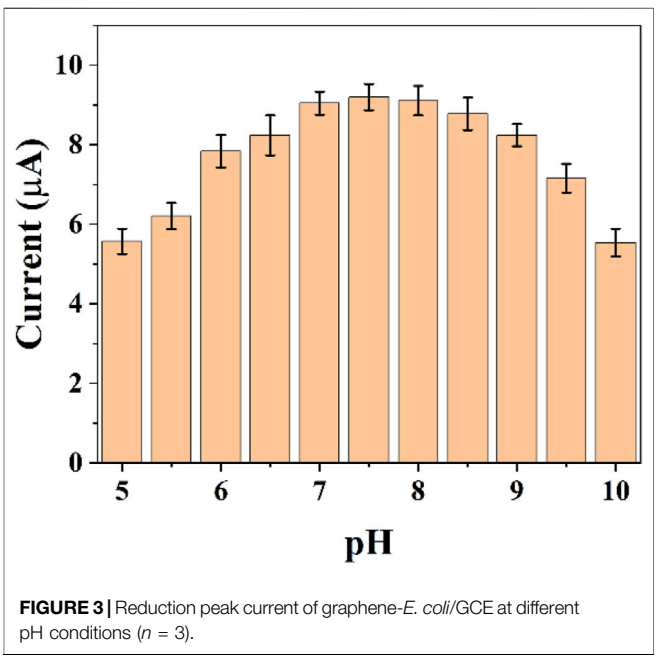

FIGURE 3 | Reduction peak current of graphene-*E. coli*/GCE at different pH conditions (*n* = 3).

For antibiotic resistance tests, 5 μL of ofloxacin, penicillin and cefepime solution was drop coated at graphene-*E. coli* modified GCE. Then, the electrode was kept in a humid chamber. The viability test was carried out at 1 h interval.

RESULTS AND DISCUSSION

Since bacterial cells have their own oxidoreductase system, which has been shown to be involved in electron transfer (Couto et al., 2018), we first investigated the direct electrochemical behavior of *E. coli*. First, we performed cyclic voltammetry (CV) tests only × 10^7 CFU *E coli* with directly coated on the GCE surface (**Figure 1**). Comparing to bare GCE, we could see a clear reduction peak at around −0.4 V, which indicates that the electroactivity of bacterial cells undergoes surface electrode reaction. However, the reduction current of this reduction peak is not particularly pronounced and is only 3.2 μA. In contrast, the intensity of the reduction current of *E. coli* is significantly higher after co-mixing with graphene. There are two reasons for this increase. The first one is that the excellent electrical properties of graphene itself improve the electron transfer rate (Pourmadadi et al., 2019). The second is that the lamellar structure of graphene greatly enhances the electrochemically active area (Gupta et al., 2019). It enables more cells to participate in the electrochemical reaction after wrapping *E. coli*. Therefore, with the assistance of graphene, it became possible to evaluate the antibiotic resistance of *E. coli* cells from its electrochemical behavior.

After determining the electrochemical behavior of *E. coli*, we used the electrochemical reduction peak as a probe for cell viability evaluation. To make the detection more sensitive, we further investigated the electrodes with differential pulse voltammetry (DPV). **Figure 2** shows the DPV curves of graphene/GCE and graphene-*E. coli*/GCE. It can be seen that graphene/GCE shows only a flat curve, but the curve of graphene-*E. coli*/GCE has a clear reduction peak. At the same

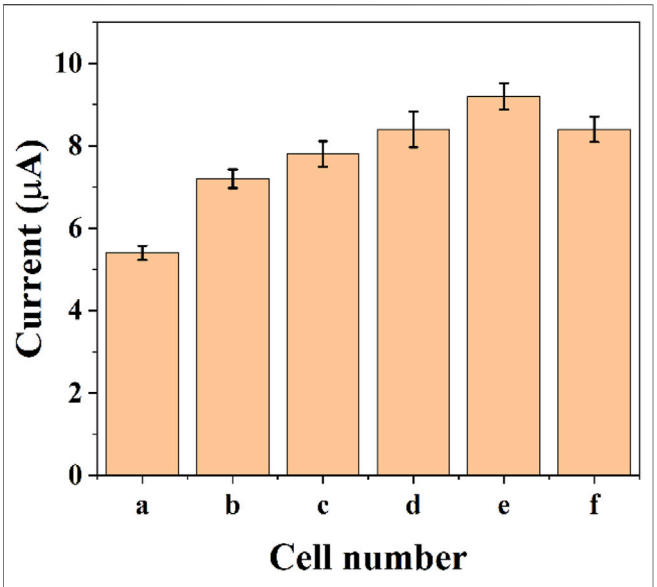

FIGURE 4 | Reduction peak current of graphene-*E. coli*/GCE at PBS with 1×10^5 CFU **(A)**, 5×10^5 CFU **(B)**, 1×10^6 CFU **(C)**, 5×10^6 CFU **(D)**, 1×10^7 CFU **(E)**, and 5×10^7 CFU **(F)** (n = 3).

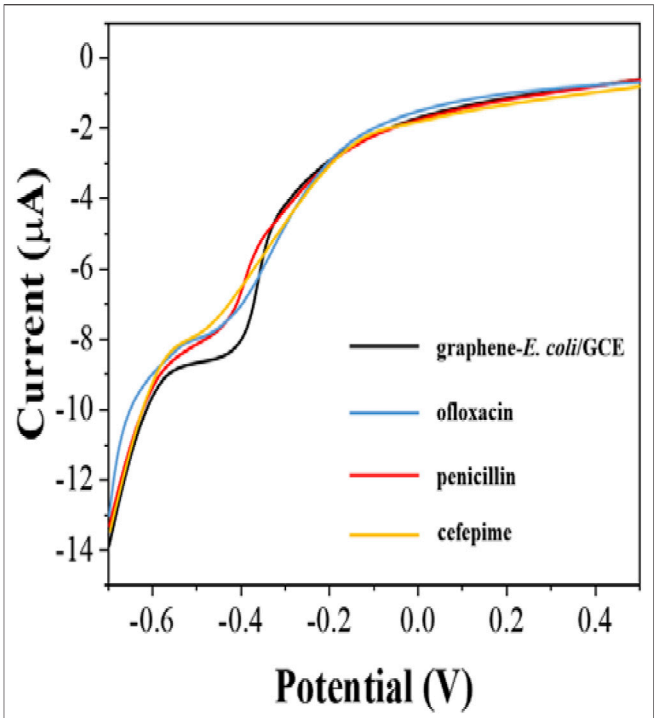

FIGURE 5 | DPV curves of graphene-*E. coli*/GCE before and after addition of ofloxacin, penicillin and cefepime at PBS.

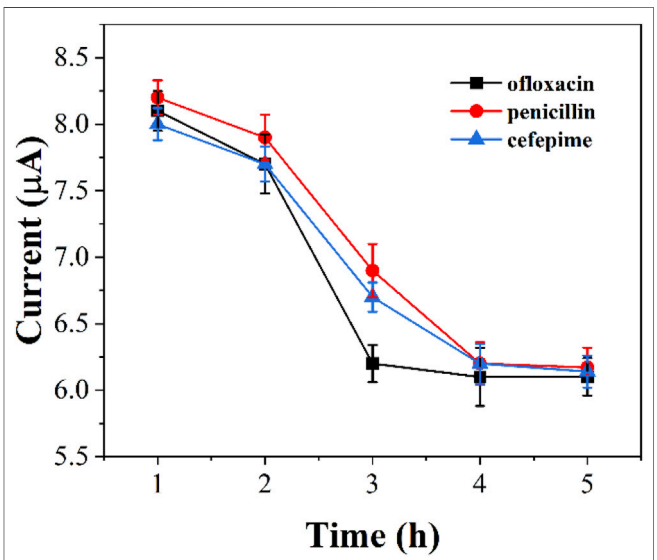

FIGURE 6 | Reduction peak currents of graphene-*E. coli*/GCE at PBS after addition of ofloxacin, penicillin and cefepime (n = 3).

time, the reduction peak on DPV has some shift against CV, which is due to the amplitude added by DPV (Vilas-Boas et al., 2019). We can see that the DPV test has a better signal-to-noise ratio than the CV. This reduction reaction is catalyzed by some macromolecules in *E. coli* cells. The substances involved may be cell surface c-type cytochromes and bacterial outer membrane reductases, dehydrogenases and flavoproteins (Vinod et al., 2002).

The pH of the buffer solution can significant effect on electrochemistry. Electrochemically active substances have different electrochemical behaviors at different pH conditions. In the same time, the activity of *E. coli* is different in different pH environments. Therefore, it is necessary for us to optimize the pH conditions. **Figure 3** shows the difference of reduction currents between pH 5–10. It can be seen that the intensity of the currents gradually increases as the acidic conditions move toward the neutral conditions. The current peaks reached the maximum at 7.5. As the pH environment gradually becomes alkaline, the current value of the reduction peak starts to decrease. We finally chose the optimal pH environment as 7.5.

The reduction current of DPV will also increase due to the increase in the number of cells. **Figure 4** shows the assay with graphene-*E. coli*/GCE for 1×10^5 CFU, 5×10^5 CFU, 1×10^6 CFU, 5×10^6 CFU, 1×10^7 CFU, and 5×10^7 CFU. It can be seen that the reduction current increases as the number of cells increases. This may be due to the fact that more cells are involved in the electrochemical reaction. However, too many cells also lead to a decrease in the current, which is due to the fact that *E. coli* itself does not have a good conductivity. Too many cells form a thicker film, which hinders the transfer of electrons. These results are in accordance with works published recent years regards to the electrochemistry of *E. coli* cells (Setterington and Alocilja, 2011; Dos Santos et al., 2013). To reveal the maximum variability, we chose 1×10^7 CFU as the optimal condition.

Since antibiotics can kill *E. coli*. The inactive *E. coli* is unable to perform effective electrochemical catalytic reaction. Therefore,

the difference in reduction current can be used to detect the number of surviving *E. coli* on the electrode surface. However, *E. coli* possessing antibiotic resistance can survive in the presence of antibiotics and therefore the behavior of electrochemical reduction will receive only a small effect. In this work, we tested the susceptibility of *E. coli* to ofloxacin, penicillin and cefepime. **Figure 5** shows the electrochemical behavior of graphene-*E. coli*/GCE 1 h after the addition of ofloxacin, penicillin and cefepime. It can be seen that there is a corresponding decrease in the reduction current in each curve compared to the electrochemical behavior without the addition of antibiotics. It represents a decrease in the number of cells able to participate in the electrochemically catalyzed reduction due to the destruction of *E. coli* by antibiotics and therefore a decrease in the current.

We monitored the bacterial inhibition of the three antibiotics. **Figure 6** shows the electrochemical reduction currents at different times after the addition of antibiotics to graphene-*E. coli*/GCE. It can be seen that the electrochemical reduction current increases with time, indicating that the antibiotic continues to have an effect on *E. coli.* Ofloxacin after about 3 h The reduction current has no longer changes after 3 h after the addition of ofloxacin. The same was true for penicillin and cefepime, which took about 4 h. We can observe a gradual loss of activity of *E. coli* during this process. However, if *E. coli* has antibiotic resistance, it can maintain the original intensity of the reduction current. Therefore, this technique could potentially be used to identify drug-resistant strains of *E. coli*.

CONCLUSION

In this work, we coated *E. coli* cells with a graphene dispersion, which was then immobilized on the electrode surface. This approach allows the evaluation of the activity of *E. coli* on the electrode surface. The electrocatalytic reduction current is the indicator in this evaluation. The current is proportional to the activity of the cells on the surface of the electrode according to the electrode. The antibiotic has an effect on the cells that result in the decreasing of the electrocatalytic reduction signal. Therefore, this strategy can be used to evaluate the resistance of cells to antibiotics. After optimization of the parameters, we successfully evaluated the resistance of *E. coli* to ofloxacin, penicillin and cefepime.

DATA AVAILABILITY STATEMENT

The original contributions presented in the study are included in the article/Supplementary Material, further inquiries can be directed to the corresponding author.

AUTHOR CONTRIBUTIONS

CL and FS conducted the experiments and analysis. CL and FSwrote the manuscript. All authors read and approved the manuscript.

REFERENCES

Abdullah, A., Asghar, A., Butt, M. S., Shahid, M., and Huang, Q. (2017). Evaluating the Antimicrobial Potential of green Cardamom Essential Oil Focusing on Quorum Sensing Inhibition of Chromobacterium Violaceum. *J. Food Sci. Technol.* 54, 2306–2315. doi:10.1007/s13197-017-2668-7

Alsaiari, N. S., Katubi, K. M. M., Alzahrani, F. M., Siddeeg, S. M., and Tahoon, M. A. (2021). The Application of Nanomaterials for the Electrochemical Detection of Antibiotics: A Review. *Micromachines* 12, 308. doi:10.3390/mi12030308

Baghayeri, M. (2017). Pt Nanoparticles/reduced Graphene Oxide Nanosheets as a Sensing Platform: Application to Determination of Droxidopa in Presence of Phenobarbital. *Sensors Actuators B: Chem.* 240, 255–263. doi:10.1016/j.snb.2016.08.161

Bagheri, S. S., Peighambari, S. M., Soltani, M., and Malekan, M. (2019). RAPD-PCR and Drug Resistance Pattern of *Staphylococcus aureus* Isolates Recovered from Companion and Wild Birds. *Iranj. Vet. Med.* 13, 356–364. 10.22059/IJVM.2019.282080.1004991

Bengtson, H. N., Homolka, S., Niemann, S., Reis, A. J., da Silva, P. E., Gerasimova, Y. V., et al. (2017). Multiplex Detection of Extensively Drug Resistant Tuberculosis Using Binary Deoxyribozyme Sensors. *Biosens. Bioelectron.* 94, 176–183. doi:10.1016/j.bios.2017.02.051

Chotinantakul, K., Suginta, W., and Schulte, A. (2014). Advanced Amperometric Respiration Assay for Antimicrobial Susceptibility Testing. *Anal. Chem.* 86, 10315–10322. doi:10.1021/ac502554s

Couto, R. A. S., Chen, L., Kuss, S., and Compton, R. G. (2018). Detection of *Escherichia coli* Bacteria by Impact Electrochemistry. *Analyst* 143, 4840–4843. doi:10.1039/c8an01675e

Dos Santos, M. B., Agusil, J., Prieto-Simón, B., Sporer, C., Teixeira, V., and Samitier, J. (2013). Highly Sensitive Detection of Pathogen *Escherichia coli* O157: H7 by Electrochemical Impedance Spectroscopy. *Biosens. Bioelectron.* 45, 174–180. doi:10.1016/j.bios.2013.01.009

Ertl, P., Unterladstaetter, B., Bayer, K., and Mikkelsen, S. R. (2000). Ferricyanide Reduction byEscherichiacoli: Kinetics, Mechanism, and Application to the Optimization of Recombinant Fermentations. *Anal. Chem.* 72, 4949–4956. doi:10.1021/ac000358d

Ertl, P., Wagner, M., Corton, E., and Mikkelsen, S. R. (2003). Rapid Identification of Viable *Escherichia coli* Subspecies with an Electrochemical Screen-Printed Biosensor Array. *Biosens. Bioelectron.* 18, 907–916. doi:10.1016/s0956-5663(02)00206-3

Farooq, U., Ullah, M. W., Yang, Q., Aziz, A., Xu, J., Zhou, L., et al. (2020). High-density Phage Particles Immobilization in Surface-Modified Bacterial Cellulose for Ultra-sensitive and Selective Electrochemical Detection of *Staphylococcus aureus*. *Biosens. Bioelectron.* 157, 112163. doi:10.1016/j.bios.2020.112163

Fu, Y., Zhou, X., Duan, X., Liu, C., Huang, J., Zhang, T., et al. (2020). A LAMP-Based Ratiometric Electrochemical Sensing for Ultrasensitive Detection of Group B Streptococci with Improved Stability and Accuracy. *Sensors Actuators B: Chem.* 321, 128502. doi:10.1016/j.snb.2020.128502

Gorlenko, C. L., Kiselev, H. Y., Budanova, E. V., Zamyatnin, A. A., and Ikryannikova, L. N. (2020). Plant Secondary Metabolites in the Battle of Drugs and Drug-Resistant Bacteria: New Heroes or Worse Clones of Antibiotics? *Antibiotics* 9, 170. doi:10.3390/antibiotics9040170

Gupta, A., Bhardwaj, S. K., Sharma, A. L., and Deep, A. (2019). A Graphene Electrode Functionalized with Aminoterephthalic Acid for Impedimetric Immunosensing of *Escherichia coli*. *Microchim. Acta* 186, 1–7. doi:10.1007/s00604-019-3952-1

Hu, C., Kalsi, S., Zeimpekis, I., Sun, K., Ashburn, P., Turner, C., et al. (2017). Ultra-fast Electronic Detection of Antimicrobial Resistance Genes Using Isothermal Amplification and Thin Film Transistor Sensors. *Biosens. Bioelectron.* 96, 281–287. doi:10.1016/j.bios.2017.05.016

Hu, K., Huang, X., Jiang, Y., Fang, W., and Yang, X. (2010). Monoclonal Antibody Based Enzyme-Linked Immunosorbent Assay for the Specific Detection of Ciprofloxacin and Enrofloxacin Residues in Fishery Products. *Aquaculture* 310, 8–12. doi:10.1016/j.aquaculture.2010.08.008

Karimi-Maleh, H., Alizadeh, M., Orooji, Y., Karimi, F., Baghayeri, M., Rouhi, J., et al. (2021a). Guanine-Based DNA Biosensor Amplified with Pt/SWCNTs Nanocomposite as Analytical Tool for Nanomolar Determination of Daunorubicin as an Anticancer Drug: A Docking/Experimental Investigation. *Ind. Eng. Chem. Res.* 60, 816–823. doi:10.1021/acs.iecr.0c04698

Karimi-Maleh, H., Karimi, F., Malekmohammadi, S., Zakariae, N., Esmaeili, R., Rostamnia, S., et al. (2020). An Amplified Voltammetric Sensor Based on Platinum Nanoparticle/polyoxometalate/two-Dimensional Hexagonal boron Nitride Nanosheets Composite and Ionic Liquid for Determination of N-Hydroxysuccinimide in Water Samples. *J. Mol. Liquids* 310, 113185. doi:10.1016/j.molliq.2020.113185

Karimi-Maleh, H., Orooji, Y., Karimi, F., Alizadeh, M., Baghayeri, M., Rouhi, J., et al. (2021b). A Critical Review on the Use of Potentiometric Based Biosensors for Biomarkers Detection. *Biosens. Bioelectron.* 184, 113252. doi:10.1016/j.bios.2021.113252

Karimi-Maleh, H., Yola, M. L., Atar, N., Orooji, Y., Karimi, F., Senthil Kumar, P., et al. (2021c). A Novel Detection Method for Organophosphorus Insecticide Fenamiphos: Molecularly Imprinted Electrochemical Sensor Based on Core-Shell Co3O4@MOF-74 Nanocomposite. *J. Colloid Interf. Sci.* 592, 174–185. doi:10.1016/j.jcis.2021.02.066

Khan, M. Z. H., Hasan, M. R., Hossain, S. I., Ahommed, M. S., and Daizy, M. (2020). Ultrasensitive Detection of Pathogenic Viruses with Electrochemical Biosensor: State of the Art, 166. *Biosens. Bioelectron.* 112431. doi:10.1016/j.bios.2020.112431

Mishra, M., Arukha, A. P., Patel, A. K., Behera, N., Mohanta, T. K., and Yadav, D. (2018). Multi-drug Resistant Coliform: Water Sanitary Standards and Health Hazards. *Front. Pharmacol.* 9, 311. doi:10.3389/fphar.2018.00311

Mohanraj, J., Durgalakshmi, D., Rakkesh, R. A., Balakumar, S., Rajendran, S., and Karimi-Maleh, H. (2020). Facile Synthesis of Paper Based Graphene Electrodes for point of Care Devices: a Double Stranded DNA (dsDNA) Biosensor. *J. Colloid Interf. Sci.* 566, 463–472. doi:10.1016/j.jcis.2020.01.089

Mulat, M., Pandita, A., and Khan, F. (2019). Medicinal Plant Compounds for Combating the Multi-Drug Resistant Pathogenic Bacteria: a Review. *Cpb* 20, 183–196. doi:10.2174/1872210513666190308133429

Osman, K. M., da Silva Pires, Á., Franco, O. L., Saad, A., Hamed, M., Naim, H., et al. (2021). Nile tilapia (*Oreochromis niloticus*) as an Aquatic Vector for Pseudomonas Species of Medical Importance: Antibiotic Resistance Association with Biofilm Formation, Quorum Sensing and Virulence. *Aquaculture* 532, 736068. doi:10.1016/j.aquaculture.2020.736068

Phung, T. T. B., Chu, S. V., Vu, S. T., Pham, H. T., Nguyen, H. M., Nguyen, H. D., et al. (2020). COLD-PCR Method for Early Detection of Antiviral Drug-Resistance Mutations in Treatment-Naive Children with Chronic Hepatitis B. *Diagnostics* 10, 491. doi:10.3390/diagnostics10070491

Pourmadadi, M., Shayeh, J. S., Omidi, M., Yazdian, F., Alebouyeh, M., and Tayebi, L. (2019). A Glassy Carbon Electrode Modified with Reduced Graphene Oxide and Gold Nanoparticles for Electrochemical Aptasensing of Lipopolysaccharides from *Escherichia coli* Bacteria. *Microchim. Acta* 186, 1–8. doi:10.1007/s00604-019-3957-9

Sedki, M., Hassan, R. Y. A., Hefnawy, A., and El-Sherbiny, I. M. (2017). Sensing of Bacterial Cell Viability Using Nanostructured Bioelectrochemical System: rGO-Hyperbranched Chitosan Nanocomposite as a Novel Microbial Sensor Platform. *Sensors Actuators B: Chem.* 252, 191–200. doi:10.1016/j.snb.2017.05.163

Setterington, E. B., and Alocilja, E. C. (2011). Rapid Electrochemical Detection of Polyaniline-Labeled *Escherichia coli* O157:H7. *Biosens. Bioelectron.* 26, 2208–2214. doi:10.1016/j.bios.2010.09.036

Sharaha, U., Rodriguez-Diaz, E., Riesenberg, K., Bigio, I. J., Huleihel, M., and Salman, A. (2017). Using Infrared Spectroscopy and Multivariate Analysis to Detect Antibiotics' ResistantEscherichia coliBacteria. *Anal. Chem.* 89, 8782–8790. doi:10.1021/acs.analchem.7b01025

Simioni, N. B., Silva, T. A., Oliveira, G. G., and Fatibello-Filho, O. (2017). A Nanodiamond-Based Electrochemical Sensor for the Determination of Pyrazinamide Antibiotic. *Sensors Actuators B: Chem.* 250, 315–323. doi:10.1016/j.snb.2017.04.175

Sun, Y., Zhao, C., Niu, J., Ren, J., and Qu, X. (2020). Colorimetric Band-Aids for point-of-care Sensing and Treating Bacterial Infection. *ACS Cent. Sci.* 6, 207–212. doi:10.1021/acscentsci.9b01104

Vilas-Boas, Â., Valderrama, P., Fontes, N., Geraldo, D., and Bento, F. (2019). Evaluation of Total Polyphenol Content of Wines by Means of Voltammetric Techniques: Cyclic Voltammetry vs Differential Pulse Voltammetry. *Food Chem.* 276, 719–725. doi:10.1016/j.foodchem.2018.10.078

Vinod, M. P., Bellur, P., and Becker, D. F. (2002). Electrochemical and Functional Characterization of the Proline Dehydrogenase Domain of the PutA Flavoprotein fromEscherichia Coli†. *Biochemistry* 41, 6525–6532. doi:10.1021/bi025706f

Wang, M., Hu, M., Liu, J., Guo, C., Peng, D., Jia, Q., et al. (2019). Covalent Organic Framework-Based Electrochemical Aptasensors for the Ultrasensitive Detection of Antibiotics. *Biosens. Bioelectron.* 132, 8–16. doi:10.1016/j.bios.2019.02.040

Wang, Y., Dong, W., Odah, K. A., Kong, L., and Ma, H. (2019). Transcriptome Analysis Reveals AI-2 Relevant Genes of Multi-Drug Resistant *Klebsiella pneumoniae* in Response to Eugenol at Sub-MIC. *Front. Microbiol.* 10, 1159. doi:10.3389/fmicb.2019.01159

Waseem, H., Jameel, S., Ali, J., Saleem Ur Rehman, H., Tauseef, I., Farooq, U., et al. (2019). Contributions and Challenges of High Throughput qPCR for Determining Antimicrobial Resistance in the Environment: a Critical Review. *Molecules* 24, 163. doi:10.3390/molecules24010163

Wu, W., Wu, M., Zhou, J., Xu, Y., Li, Z., Yao, Y., et al. (2020). Development of Electrochemical Sensor for Fast Liquor Authentication. *Sens. Mater.* 32, 2941–2948. doi:10.18494/sam.2020.2972

Xu, Y., Lu, Y., Zhang, P., Wang, Y., Zheng, Y., Fu, L., et al. (2020). Infrageneric Phylogenetics Investigation of Chimonanthus Based on Electroactive Compound Profiles. *Bioelectrochemistry* 133, 107455. doi:10.1016/j.bioelechem.2020.107455

Zhang, L., Liang, W., Ran, Q., Liu, F., Chen, D., Xiong, Y., et al. (2020). Ultrasensitive Detection of NDM-1 Resistant Bacteria Based on Signal Amplification with sandwich-type LNA Electrochemical Biochips. *Sensors Actuators B: Chem.* 306, 127556. doi:10.1016/j.snb.2019.127556

Zhang, M., Pan, B., Wang, Y., Du, X., Fu, L., Zheng, Y., et al. (2020). Recording the Electrochemical Profile of Pueraria Leaves for Polyphyly Analysis. *ChemistrySelect* 5, 5035–5040. doi:10.1002/slct.202001100

Zhang, X., Yang, R., Li, Z., Zhang, M., Wang, Q., Xu, Y., et al. (2020). Electroanalytical Study of Infrageneric Relationship of Lagerstroemia Using Glassy Carbon Electrode Recorded Voltammograms. *Rmiq* 19, 281–291. doi:10.24275/rmiq/bio1750

Zhao, L., Liu, Y., Zhang, Z., Wei, J., Xie, S., and Li, X. (2020). Fibrous Testing Papers for Fluorescence Trace Sensing and Photodynamic Destruction of Antibiotic-Resistant Bacteria. *J. Mater. Chem. B* 8, 2709–2718. doi:10.1039/d0tb00002g

Zhi-bin, L., Min, W., Xiao-cui, W., Min, H., He-ping, X., and Qing, Z. (2021). The Value of PCR-Reverse Dot Blot Hybridization in Detecting the Drug Resistance of *Mycobacterium tuberculosis* in Sputum Specimens of Retreatment Smear-Positive Pulmonary Tuberculosis Patients. *Chin. J. Antituberc.* 43, 47. doi:10.17343/sdutfd.534941

Zhou, T., Han, H., Liu, P., Xiong, J., Tian, F., and Li, X. (2017). Microbial Fuels Cell-Based Biosensor for Toxicity Detection: A Review. *Sensors* 17, 2230. doi:10.3390/s17102230

Zhuang, J., Wang, S., Tan, Y., Xiao, R., Chen, J., Wang, X., et al. (2019). Degradation of Sulfadimethoxine by Permanganate in Aquatic Environment: Influence Factors, Intermediate Products and Theoretical Study. *Sci. Total Environ.* 671, 705–713. doi:10.1016/j.scitotenv.2019.03.277

Conflict of Interest: The authors declare that the research was conducted in the absence of any commercial or financial relationships that could be construed as a potential conflict of interest.

frontiers in Chemistry

ORIGINAL RESEARCH
published: 31 May 2021
doi: 10.3389/fchem.2021.689735

A Methylene Blue Assisted Electrochemical Sensor for Determination of Drug Resistance of *Escherichia coli*

Rongshuai Duan[1,2], *Xiao Fang*[1] *and Dongliang Wang*[1,3]*

[1]Department of Food and Drugs, Shandong Institute of Commerce and Technology, Jinan, China, [2]Qilu Medical University, Jinan, China, [3]Dong-E E-Jiao Co. Ltd., Liaocheng, China

Due to the abuse of antibiotics in clinical, animal husbandry, and aquaculture, drug-resistant pathogens are produced, which poses a great threat to human and the public health. At present, a rapid and effective drug sensitivity test method is urgently needed to effectively control the spread of drug-resistant bacteria. Using methylene blue as a redox probe, the electrochemical signals of methylene blue in drug-resistant *Escherichia coli* strains were analyzed by a CV method. Graphene ink has been used for enhancing the electrochemical signal. Compared with the results of the traditional drug sensitivity test, we proposed a rapid electrochemical drug sensitivity test method which can effectively identify the drug sensitivity of *Escherichia coli*. The sensitivity of four *E. coli* isolates to ciprofloxacin, gentamicin, and ampicillin was tested by an electrochemical drug sensitivity test. The respiratory activity value %RA was used as an indicator of bacterial resistance by electrochemical method.

Keywords: graphene, drug resistant, *Escherichia coli*, glassy carbon electrode, methylene blue

OPEN ACCESS

Edited by:
Fatemeh Karimi,
Quchan University of Advanced Technology, Iran

Reviewed by:
Mehdi Baghayeri,
Hakim Sabzevari University, Iran
Hassan Karimi-maleh,
University of Electronic Science and Technology of China, China

***Correspondence:**
Dongliang Wang
dongliangwdl@163.com

Specialty section:
This article was submitted to Electrochemistry, a section of the journal Frontiers in Chemistry

Received: *01 April 2021*
Accepted: *03 May 2021*
Published: *31 May 2021*

Citation:
Duan R, Fang X and Wang D (2021) A Methylene Blue Assisted Electrochemical Sensor for Determination of Drug Resistance of Escherichia coli. *Front. Chem. 9:689735. doi: 10.3389/fchem.2021.689735*

INTRODUCTION

Escherichia coli is a Gram-negative short bacillus, and it is also the most important and the most abundant bacteria in the intestines of human beings and many animals (Jijie et al., 2018; Thakur et al., 2018). For a long time, it was thought that *E. coli* was not pathogenic in general, but some *E. coli* with special serotypes were found to be pathogenic to humans and animals, causing diarrhea, adult pleurisy, and septicemia. Food safety is one of the most important food safety problems (Brosel-Oliu et al., 2018; Zhou et al., 2018). With the abuse of antibiotics in clinic, animal husbandry, and aquaculture, the problem of antibiotic resistance of bacteria in the world is becoming increasingly serious. Foodborne drug-resistant bacteria may transmit drug resistance and drug-resistant genes to humans through food chain, thus causing human infection (Gomez-Cruz et al., 2018; Zhu et al., 2018). As an important mediator of drug-resistant genes, *E. coli* has the characteristics of easily producing drug resistance and a rapid variation of drug resistance. Its resistance spectrum will be further expanded with the change of time, which undoubtedly increases the harm of *E. coli*. In order to control the food safety problems caused by foodborne pathogens from the source, effective drug sensitivity detection methods are of great significance to prevent and control the infection and spread of foodborne drug-resistant bacteria (Hua et al., 2018; Yao et al., 2018; Zeinhom et al., 2018).

In recent years, electrochemical methods have been reported in the ultrasensitive detection of bacteria (Zheng et al., 2019; Karimi-Maleh et al., 2020a, 2021a). The principle of electrochemical

detection of bacterial drug sensitivity is mainly based on the electron transfer of respiratory chain in bacterial energy metabolism (Fu et al., 2019; Xu et al., 2020; Zhang et al., 2020; Zhou et al., 2020; Nodehi et al., 2021a; Nodehi et al., 2021b). The respiration of bacteria involves the directional and orderly transfer of electroactive particles and the redox reaction of cellular substances (Khodadadi et al., 2019; Shamsadin-Azad et al., 2019; Karimi-Maleh et al., 2020b). The electrochemical changes of respiratory chain activity can be detected by electrochemical methods. The respiratory activity of bacteria can be observed by analyzing the electrical signals of redox probes so as to determine the drug sensitivity of bacteria. Ertl et al. (2000) and Ertl et al. (2003) used potassium ferricyanide as redox probe to explore an electrochemical method for the detection of drug sensitivity of *E. coli*. They treated *E. coli* with antibiotics for 20 min and then measured the electrical signals in the solution containing potassium ferricyanide to determine the drug sensitivity of the bacteria. The results were consistent with the traditional paper diffusion method. This method can provide a report within 25 min, but the IC_{50} value of penicillin and chloramphenicol is 100 times higher than that of the standard method. Chotinantakul et al. (2014) improved the experimental scheme. After the interaction between *E. coli* and bacteria, antibiotics were removed by centrifugation and then added to the test solution containing potassium ferricyanide to eliminate the influence of antibiotics on electrochemical test. This method can give the results of drug sensitivity test in 36 h.

With the development of microcomputer processing technology, the size of electrode can be reduced to micron or even nano level, which provides a technical support for the development of portable rapid detection system for drug-resistant bacteria (Naderi Asrami et al., 2020; Baghayeri et al., 2021; Karimi-Maleh et al., 2021b; Karimi-Maleh et al., 2021c). Besant et al. Besant et al. (2015) limited the volume of bacterial solution in a container of 2.75 nL and detected the reduction of azurol by electrochemical method to reflect the bacterial metabolic activity. This rapid electrochemical drug sensitivity test method can report the drug sensitivity of bacteria within 1 h.

Methylene blue (MB) is a dye widely studied in photodynamics. At the same time, due to its electrochemical characteristics, there are also some studies on its application in the field of chemically modified electrodes (Cui et al., 2018; Guo et al., 2018; Yao et al., 2018; Taghdisi et al., 2019). The blue MB can be reduced to colorless l mb by bacterial respiration, and the greater the bacterial count, the shorter the fading time of methylene blue. Due to its redox properties, MB is often used as a redox probe in electrochemical detection (Yu et al., 2019). Graphene has been frequently used for surface modification of electrochemical sensors since its discovery. Its excellent electrical properties can greatly enhance the sensing signal. Based on the theory of electron transfer in the process of energy metabolism of bacteria, the electrochemical characteristics of MB in *E. coli* from food sources *in vivo* were studied by using MB as a redox probe. Graphene ink has been used for electrode surface modification. Combined with traditional drug sensitivity test methods, we constructed a fast, sensitive, portable, and low-cost electrochemical sensor system for a rapid detection of drug resistance of foodborne bacteria.

TABLE 1 | Antibiotic susceptibility test results of E1–E4 toward ciprofloxacin, gentamicin, and ampicillin.

Strain	Antibiotics		
	Ciprofloxacin	Gentamicin	Ampicillin
E1	S	S	R
E2	R	S	R
E3	R	R	R
E4	R	R	S

MATERIALS AND METHODS

Reagents: methylene blue, potassium dihydrogen phosphate, potassium hydrogen phosphate, trisodium citrate, magnesium sulfate, calcium chloride, ammonium sulfate, ammonium chloride, and ammonium formate were purchased from Aladdin Co., Ltd. Graphene ink was purchased from Lowye Tech. Co., Ltd. Tryptone, agar powder, and yeast extract powder were purchased from Tianchen Biological Reagent Co., Ltd. Ciprofloxacin, gentamicin, and ampicillin were purchased from Shanghai Yeyuan Biotech. Co., Ltd. *E. coli* ATCC25922 was purchased from Guangdong Huankai Co., Ltd. All-field *E. coli* (E1–E4) were collected from Qilu Medical University. **Table 1** shows the antibiotic susceptibility test results of E1–E4 toward ciprofloxacin, gentamicin, and ampicillin.

LB broth: weigh 20 g tryptone, 20 g sodium chloride, and 10 g yeast extract, respectively, heat them, and dissolve them in 2,000 ml pure water. After adjusting pH to 7.2, the mixture was poured into conical flasks at 120°C. The mixture was sterilized with high-pressure steam for 15 min and then cooled them for standby.

LB agar: weigh 20 g tryptone, 20 g sodium chloride, 10 g yeast extract, and 30 g agar powder and heat them into 20,00 ml pure water. Adjust the pH to 7.2 and transfer into conical flasks, sterilize with 120°C high-pressure steam for 15 min, and then keep them in a 60°C water bath.

Colony count of *E. coli* ATCC 25922: The LB agar at 60 °C was poured into the culture dish. The agar in each culture dish was about 5 mm high. After the bacterial solution was diluted with 10 times of normal saline, three samples with appropriate dilution were selected, and 100 μL homogenate was added into the plate for coating. At the same time, take 100 μL blank diluent and add two sterile plates as blank control. The plate was inverted and cultured in 37 °C incubator for 24 h, and the colony count was conducted.

Effect of MB on the activity of *E. coli* ATCC25922: The bacterial suspension with 5 ml OD_{600} as 0.6–0.8 (LB broth as blank control) was taken and centrifuged at 4,000 rpm for 15 min. After the supernatant was removed, the cells were redistributed in four different concentrations (0.1, 0.2, 0.3, and 0.4 mM) of MB solution. Under the condition of strictly avoiding light, the plate

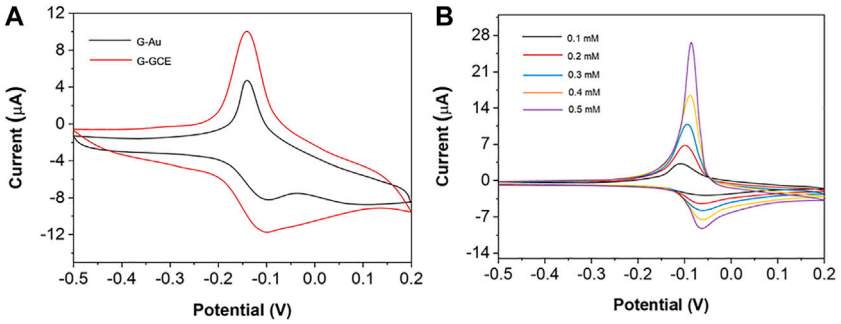

FIGURE 1 | (A) CV of 0.1 mM methylene blue on G–Au and G–GCE. **(B)** CV curve of different concentration of MB.

TABLE 2 | Plate colony count of *E.coli* ATCC 25922 was determined after the interaction of MB.

Concentration of MB (mM)	10^5	10^6	10^7
0	44.32	10.62	7.71
0.1	43.22	8.27	2.23
0.2	41.22	7.32	1.66
0.3	37.20	6.55	0.21
0.4	32.26	3.67	0.00

colony count was carried out after being exposed to 150 rmp at 37°C for 10 min.

Electrochemical drug sensitivity test: The respiratory activity value %RA was used as an indicator of bacterial resistance by electrochemical method. The following equation has been used for calculation:

$$\%RA = \frac{|I0 - I + drug|}{|I0 - I - drug|} \times 100,$$

where %RA is respiratory activity; I_0 is the current value of 0.2 mM MB; and I_{-drug} is the current value in the absence of the antibiotics. I_{+drug} is the current value in the presence of the antibiotics. A higher %RA value reflects a higher respiratory activity of bacteria, suggesting the antibiotics have little effect on bacteria.

RESULTS AND DISCUSSION

In order to obtain the maximum electrical signal, 0.1 mM methylene blue was scanned with graphene ink–modified gold electrode (G-Au) and graphene ink–modified glassy carbon electrode (G-GCE), respectively. It can be seen from **Figure 1A** that the redox electric signal of methylene blue on the G-GCE is significantly greater than that on the G-Au, which may be due to the faster electron conduction velocity of methylene blue on the carbon material than on the G-Au. Therefore, we choose the G-GCE as the working electrode of the follow-up experiment. In order to explore the relationship between MB concentration and electrochemical response signal,

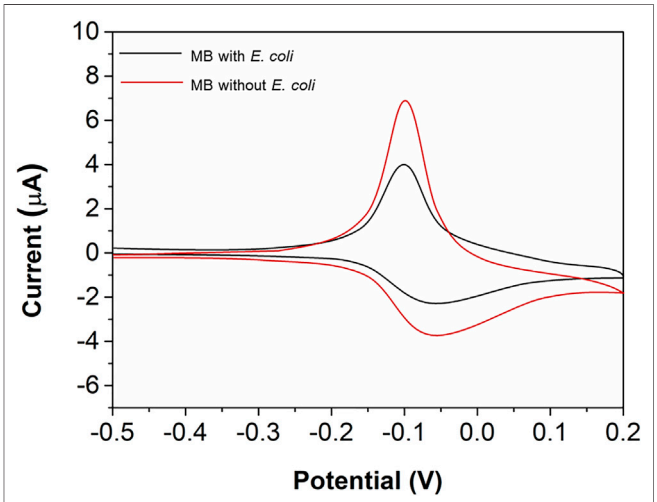

FIGURE 2 | CV curve of MB in the presence and absence of *b*.

CV scanning was performed on 5 different concentrations of MB. As shown in **Figure 1B**, there is a good linear relationship between MB concentration and the peak current of CV, and the current response signal increases with the increase of MB concentration.

As a photosensitizer, MB can damage DNA and protein of *E. coli*. In order to ensure the activity of *E. coli* ATCC25922, the plate colony count of 0.1, 0.2, 0.3, and 0.4 mM MB and 10^8 CFU/mL *E coli* was studied. Results as shown in **Table 2**, the inhibitory effect of MB on *E. coli* ATCC25922 was not particularly obvious when the concentration of MB was 0.1–0.4 mM. However, with the increase of MB concentration, the colony number of 10^5 dilution degree decreased. Therefore, the higher the concentration of MB, the greater the electrochemical signal. Finally, 0.2 mM was used as the working concentration of MB *in vivo* interaction with *E. coli* ATCC25922.

In order to explore the change of electrochemical signal of MB in *E. coli in vivo*, *E. coli* ATCC25922 was mixed with 0.2 mM MB for 7 min, and then the CV was scanned immediately. As shown in **Figure 2**, compared with the blank, *E. coli* ATCC25922 showed a significant decrease in the electrical signal and blue fading in the

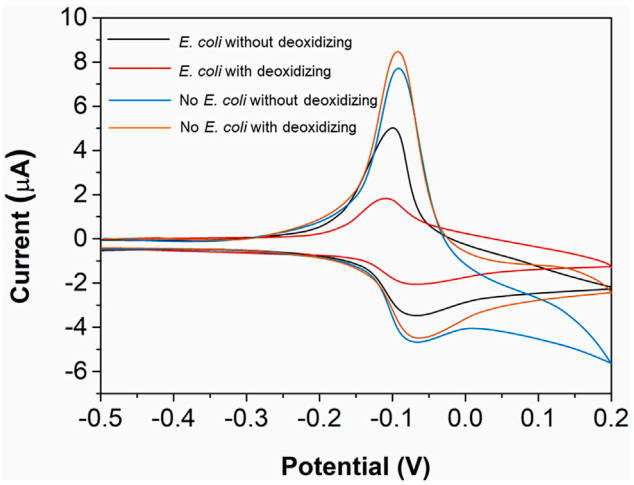

FIGURE 3 | Effect of dissolved oxygen on CV signal of MB in the presence of *E. coli* ATCC25922.

test solution. It was found that the reduction peak current of CV decreased by 35.7%, and the oxidation peak current decreased by 44.6%. This phenomenon is similar to that of Besant et al. (Besant et al., 2015) after mixing *E. coli* and azurol for a period of time. The fading of blue in the test solution is due to the reduction of blue MB to colorless L-MB by aerobic respiration of *E. coli* ATCC25922. The decrease of electrical signal after adding *E. coli* ATCC25922 is due to the fact that MB, as a redox shuttle, mediates the respiratory chain of bacteria and obtains electrons to be reduced during aerobic respiration. This results in a decrease in the concentration of the oxidized MB that can be detected in the solution, resulting in a decrease in the current value.

In order to explore the interaction between oxygen and MB and bacteria, the methylene blue solution with and without bacteria was deoxidized for 7 min, and the CV results are shown in **Figure 3**. In order to explore the interaction between oxygen and MB and bacteria, the MB solution with and without bacteria was deoxidized for 7 min, and the CV results are shown in **Figure 3**. It can be seen from CV that the current is lower than that without adding *E. coli* ATCC25922, no matter whether or not deoxidizing. This is due to the respiration of *E. coli*, which reduces a part of MB in the solution, resulting in the decrease of MB concentration and current. It should be noted that the current decreased more after the addition of *E. coli* with the deoxidization, which indicated that the removal of dissolved oxygen accelerated the reduction of MB by *E. coli*. The CV diagram shows that when the potential is −0.5 V, the current of adding bacteria without deoxidizing is the same as that without adding bacteria, indicating that there is no dissolved oxygen in the solution even though there is no deoxidization after adding bacteria. This is due to the respiration of living *E. coli*, which consumes oxygen in the solution. Therefore, the respiration of *E. coli* still preferentially consumes oxygen and then reduces MB in the presence of oxygen in the solution. The reduction of MB by *E. coli* can be accelerated by removing dissolved oxygen from the solution.

In order to explore the relationship between the action time and the electrical signal, the CV diagram of *E. coli* ATCC25922 mixed with 0.2 mM MB for different time was scanned, and the results are shown in **Figure 4**. The figure represents the reduction of MB by *E. coli* ATCC25922. It can be seen from **Figure 4** that the current remains basically unchanged in the first 0–4 min. Then, the current increased rapidly in 4–8 min and reached a stable level in 8–12 min. This shows that in the first 4 min, the oxygen in the solution has not been completely consumed. The reduction of MB by *E. coli* ATCC25922 is a slow process. At 4–8 min, the effect of oxygen was reduced, and MB was rapidly reduced by bacterial respiration. During the 8–12 min, all MB in the solution was reduced. In the experiment, it can also be observed by naked eyes that the test solution gradually changes from dark blue to colorless.

In order to explore the relationship between different concentrations of *E. coli* ATCC25922 and MB electrical signals, CV of different concentrations of *E. coli* ATCC25922 and 0.2 mM MB were scanned. It can be seen from **Figure 5A** that CV oxidation peak and reduction peak are inversely proportional to the concentration of *E. coli* ATCC25922. The correlation curve between CV reduction peak current and the concentration of *E. coli* ATCC25922 was obtained by linear fitting, and the curve is shown in **Figure 5B**. The regression equation was established as follows: Y = 0.266x-3.566 (R^2 = 0.9956).

In order to explore the appropriate concentration of antibiotics for electrochemical drug sensitivity test, CV was used to study the change of %RA value of 0.25, 0.5, 1, and 2 g/L gentamicin with *E. coli* 25,922 and E3 for 1 h. The results are shown in **Figure 6**. It can be seen from the figure that the %RA value of sensitive strain ATCC25922 is basically kept below 60 within the test range of gentamicin concentration, while the %RA value of drug-resistant strain E3 is about 90 when gentamicin concentration is 0.25 and 0.5 g/L. When the concentration of

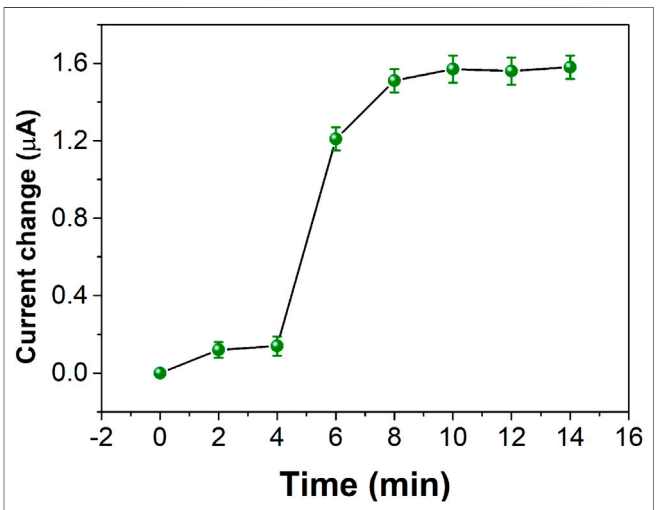

FIGURE 4 | Current overtime for *E. coli* ATCC 25922 interacting with MB for different periods.

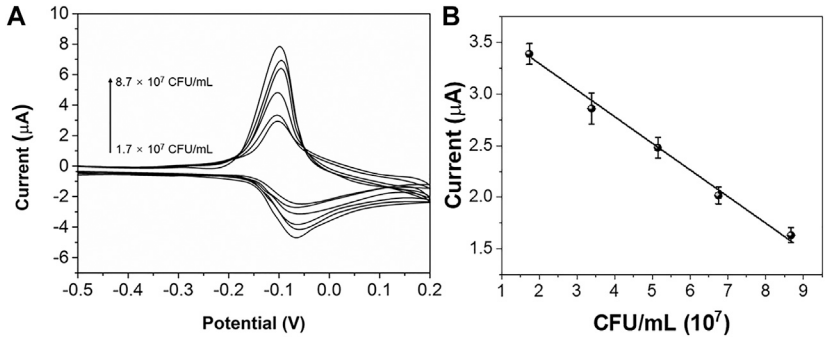

FIGURE 5 | (A) CV curve of MB in the presence of different concentrations of *E. coli* ATCC 25922. **(B)** Plots of peak currents vs. the concentration of *E. coli* ATCC 25922.

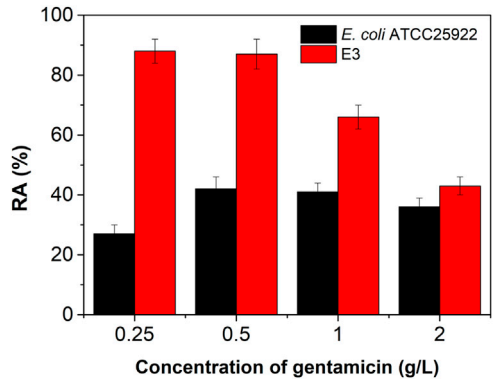

FIGURE 6 | %RA change of *E. coli* ATCC 25922 and E3 toward gentamicin.

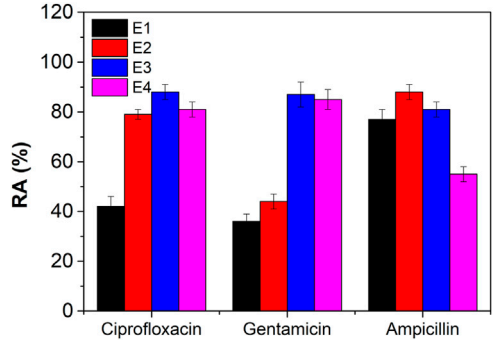

FIGURE 7 | %RA changes of E1–E4 toward ciprofloxacin, gentamicin, and ampicillin.

gentamicin increased, although %RA began to decrease, it was still higher than that of sensitive strain ATCC25922. In order to make the electrochemical method accurately detect the difference between sensitive strains and drug-resistant strains, so as not to inhibit the respiratory activity of drug-resistant strains, 0.5 g/L was selected as the concentration of electrochemical drug sensitivity test.

We used electrochemical techniques to detect ciprofloxacin, gentamicin, and ampicillin in E1–E4. As shown in **Figure 7**, the %RA value of antibiotic resistant bacteria is almost 100. In contrast, the %RA values of bacteria sensitive to antibiotics were less than 75. When the %RA measured by electrochemical method is less than 75, it can be preliminarily determined that the bacteria are sensitive to the antibiotic. When 75<%RA<100 determined by electrochemical method, the antibiotic resistance of bacteria can be preliminarily determined.

CONCLUSION

In this work, CV was used to study the electrochemical characteristics of MB in the presence of *E. coli* ATCC25922. We constructed the correlation curve between the CV peak current and the concentration of *E. coli* ATCC25922. It provides a theoretical basis for electrochemical detection of bacteria. At the same time, we explored the electrochemical detection of foodborne *E. coli* drug sensitivity. The sensitivity of four *E. coli* isolates to three antibiotics was tested by the electrochemical drug sensitivity test. The results showed that bacteria were considered to be resistant to antibiotics when the standard of drug sensitivity was 75<%RA<100.

DATA AVAILABILITY STATEMENT

The original contributions presented in the study are included in the article/Supplementary Material, further inquiries can be directed to the corresponding author.

AUTHOR CONTRIBUTIONS

RD and DW conceived of the study. DW supervised the development program. RD and XF conducted the analysis. RD and DW wrote the manuscript. All authors read and approved of the manuscript.

FUNDING

This work was supported by Research Project of Development Plan of Youth Innovation Team in Colleges and Universities of Shandong Province 2019 (No.2019KJE014) and The Open Project of Shandong Collaborative Innovation Center for Donkey Industry Technology (No.3193308).

REFERENCES

Baghayeri, M., Amiri, A., Fayazi, M., Nodehi, M., and Esmaeelnia, A. (2021). Electrochemical Detection of Bisphenol a on a MWCNTs/CuFe2O4 Nanocomposite Modified Glassy Carbon Electrode. *Mater. Chem. Phys.* 261, 124247. doi:10.1016/j.matchemphys.2021.124247

Besant, J. D., Sargent, E. H., and Kelley, S. O. (2015). Rapid Electrochemical Phenotypic Profiling of Antibiotic-Resistant Bacteria. *Lab. Chip* 15, 2799–2807. doi:10.1039/c5lc00375j

Brosel-Oliu, S., Ferreira, R., Uria, N., Abramova, N., Gargallo, R., Muñoz-Pascual, F.-X., et al. (2018). Novel Impedimetric Aptasensor for Label-free Detection of *Escherichia coli* O157:H7. *Sensors Actuators B: Chem.* 255, 2988–2995. doi:10.1016/j.snb.2017.09.121

Chotinantakul, K., Suginta, W., and Schulte, A. (2014). Advanced Amperometric Respiration Assay for Antimicrobial Susceptibility Testing. *Anal. Chem.* 86, 10315–10322. doi:10.1021/ac502554s

Cui, L., Lu, M., Li, Y., Tang, B., and Zhang, C.-y. (2018). A Reusable Ratiometric Electrochemical Biosensor on the Basis of the Binding of Methylene Blue to DNA with Alternating at Base Sequence for Sensitive Detection of Adenosine. *Biosens. Bioelectron.* 102, 87–93. doi:10.1016/j.bios.2017.11.025

Ertl, P., Unterladstaetter, B., Bayer, K., and Mikkelsen, S. R. (2000). Ferricyanide Reduction byEscherichiacoli: Kinetics, Mechanism, and Application to the Optimization of Recombinant Fermentations. *Anal. Chem.* 72, 4949–4956. doi:10.1021/ac000358d

Ertl, P., Wagner, M., Corton, E., and Mikkelsen, S. R. (2003). Rapid Identification of Viable *Escherichia coli* Subspecies with an Electrochemical Screen-Printed Biosensor Array. *Biosens. Bioelectron.* 18, 907–916. doi:10.1016/s0956-5663(02)00206-3

Fu, L., Xie, K., Wang, A., Lyu, F., Ge, J., Zhang, L., et al. (2019). High Selective Detection of Mercury (II) Ions by Thioether Side Groups on Metal-Organic Frameworks. *Analytica Chim. Acta* 1081, 51–58. doi:10.1016/j.aca.2019.06.055

Gomez-Cruz, J., Nair, S., Manjarrez-Hernandez, A., Gavilanes-Parra, S., Ascanio, G., and Escobedo, C. (2018). Cost-effective Flow-Through Nanohole Array-Based Biosensing Platform for the Label-free Detection of Uropathogenic *E. coli* in Real Time. *Biosens. Bioelectron.* 106, 105–110. doi:10.1016/j.bios.2018.01.055

Guo, J., Yuan, C., Yan, Q., Duan, Q., Li, X., and Yi, G. (2018). An Electrochemical Biosensor for microRNA-196a Detection Based on Cyclic Enzymatic Signal Amplification and Template-free DNA Extension Reaction with the Adsorption of Methylene Blue. *Biosens. Bioelectron.* 105, 103–108. doi:10.1016/j.bios.2018.01.036

Hua, R., Hao, N., Lu, J., Qian, J., Liu, Q., Li, H., et al. (2018). A Sensitive Potentiometric Resolved Ratiometric Photoelectrochemical Aptasensor for *Escherichia coli* Detection Fabricated with Non-metallic Nanomaterials. *Biosens. Bioelectron.* 106, 57–63. doi:10.1016/j.bios.2018.01.053

Jijie, R., Kahlouche, K., Barras, A., Yamakawa, N., Bouckaert, J., Gharbi, T., et al. (2018). Reduced Graphene Oxide/polyethylenimine Based Immunosensor for the Selective and Sensitive Electrochemical Detection of Uropathogenic *Escherichia coli*. *Sensors Actuators B: Chem.* 260, 255–263. doi:10.1016/j.snb.2017.12.169

Karimi-Maleh, H., Alizadeh, M., Orooji, Y., Karimi, F., Baghayeri, M., Rouhi, J., et al. (2021a). Guanine-Based DNA Biosensor Amplified with Pt/SWCNTs Nanocomposite as Analytical Tool for Nanomolar Determination of Daunorubicin as an Anticancer Drug: A Docking/Experimental Investigation. *Ind. Eng. Chem. Res.* 60, 816–823. doi:10.1021/acs.iecr.0c04698

Karimi-Maleh, H., Karimi, F., Malekmohammadi, S., Zakariae, N., Esmaeili, R., Rostamnia, S., et al. (2020a). An Amplified Voltammetric Sensor Based on Platinum Nanoparticle/polyoxometalate/two-Dimensional Hexagonal Boron Nitride Nanosheets Composite and Ionic Liquid for Determination of N-Hydroxysuccinimide in Water Samples. *J. Mol. Liquids* 310, 113185. doi:10.1016/j.molliq.2020.113185

Karimi-Maleh, H., Karimi, F., Orooji, Y., Mansouri, G., Razmjou, A., Aygun, A., et al. (2020b). A New Nickel-Based Co-crystal Complex Electrocatalyst Amplified by NiO Dope Pt Nanostructure Hybrid; a Highly Sensitive Approach for Determination of Cysteamine in the Presence of Serotonin. *Sci. Rep.* 10, 11699. doi:10.1038/s41598-020-68663-2

Karimi-Maleh, H., Orooji, Y., Karimi, F., Alizadeh, M., Baghayeri, M., Rouhi, J., et al. (2021b). A Critical Review on the Use of Potentiometric Based Biosensors for Biomarkers Detection. *Biosens. Bioelectron.* 184, 113252. doi:10.1016/j.bios.2021.113252

Karimi-Maleh, H., Yola, M. L., Atar, N., Orooji, Y., Karimi, F., Senthil Kumar, P., et al. (2021c). A Novel Detection Method for Organophosphorus Insecticide Fenamiphos: Molecularly Imprinted Electrochemical Sensor Based on Core-Shell Co3O4@MOF-74 Nanocomposite. *J. Colloid Interf. Sci.* 592, 174–185. doi:10.1016/j.jcis.2021.02.066

Khodadadi, A., Faghih-Mirzaei, E., Karimi-Maleh, H., Abbaspourrad, A., Agarwal, S., and Gupta, V. K. (2019). A New Epirubicin Biosensor Based on Amplifying DNA Interactions with Polypyrrole and Nitrogen-Doped Reduced Graphene: Experimental and Docking Theoretical Investigations. *Sensors Actuators B: Chem.* 284, 568–574. doi:10.1016/j.snb.2018.12.164

Naderi Asrami, P., Aberoomand Azar, P., Saber Tehrani, M., and Mozaffari, S. A. (2020). Glucose Oxidase/Nano-ZnO/Thin Film Deposit FTO as an Innovative Clinical Transducer: A Sensitive Glucose Biosensor. *Front. Chem.* 8, 503. doi:10.3389/fchem.2020.00503

Nodehi, M., Baghayeri, M., Behazin, R., and Veisi, H. (2021a). Electrochemical Aptasensor of Bisphenol A Constructed Based on 3D Mesoporous Structural SBA-15-Met with a Thin Layer of Gold Nanoparticles. *Microchemical J.* 162, 105825. doi:10.1016/j.microc.2020.105825

Nodehi, M., Baghayeri, M., and Veisi, H. (2021b). Preparation of GO/Fe3O4@PMDA/AuNPs Nanocomposite for Simultaneous Determination of As3+ and Cu2+ by Stripping Voltammetry. *Talanta* 230, 122288. doi:10.1016/j.talanta.2021.122288

Shamsadin-Azad, Z., Taher, M. A., Cheraghi, S., and Karimi-Maleh, H. (2019). A Nanostructure Voltammetric Platform Amplified with Ionic Liquid for Determination of Tert-Butylhydroxyanisole in the Presence Kojic Acid. *Food Measure* 13, 1781–1787. doi:10.1007/s11694-019-00096-6

Taghdisi, S. M., Danesh, N. M., Nameghi, M. A., Ramezani, M., Alibolandi, M., Hassanzadeh-Khayat, M., et al. (2019). A Novel Electrochemical Aptasensor Based on Nontarget-Induced High Accumulation of Methylene Blue on the Surface of Electrode for Sensing of α-synuclein Oligomer. *Biosens. Bioelectron.* 123, 14–18. doi:10.1016/j.bios.2018.09.081

Thakur, B., Zhou, G., Chang, J., Pu, H., Jin, B., Sui, X., et al. (2018). Rapid Detection of Single *E. coli* Bacteria Using a Graphene-Based Field-Effect Transistor Device. *Biosens. Bioelectron.* 110, 16–22. doi:10.1016/j.bios.2018.03.014

Xu, Y., Lu, Y., Zhang, P., Wang, Y., Zheng, Y., Fu, L., et al. (2020). Infrageneric Phylogenetics Investigation of Chimonanthus Based on Electroactive Compound Profiles. *Bioelectrochemistry* 133, 107455. doi:10.1016/j.bioelechem.2020.107455

Yao, L., Wang, L., Huang, F., Cai, G., Xi, X., and Lin, J. (2018). A Microfluidic Impedance Biosensor Based on Immunomagnetic Separation and Urease Catalysis for Continuous-Flow Detection of *E. coli* O157:H7. *Sensors Actuators B: Chem.* 259, 1013–1021. doi:10.1016/j.snb.2017.12.110

Yu, Z., Luan, Y., Li, H., Wang, W., Wang, X., and Zhang, Q. (2019). A Disposable Electrochemical Aptasensor Using Single-Stranded DNA-Methylene Blue Complex as Signal-Amplification Platform for Sensitive Sensing of Bisphenol A. *Sensors Actuators B: Chem.* 284, 73–80. doi:10.1016/j.snb.2018.12.126

Zeinhom, M. M. A., Wang, Y., Song, Y., Zhu, M.-J., Lin, Y., and Du, D. (2018). A Portable Smart-Phone Device for Rapid and Sensitive Detection of *E. coli* O157:H7 in Yoghurt and Egg. *Biosens. Bioelectron.* 99, 479–485. doi:10.1016/j.bios.2017.08.002

Zhang, M., Pan, B., Wang, Y., Du, X., Fu, L., Zheng, Y., et al. (2020). Recording the Electrochemical Profile of Pueraria Leaves for Polyphyly Analysis. *ChemistrySelect* 5, 5035–5040. doi:10.1002/slct.202001100

Zheng, L., Cai, G., Wang, S., Liao, M., Li, Y., and Lin, J. (2019). A Microfluidic Colorimetric Biosensor for Rapid Detection of *Escherichia coli* O157:H7 Using Gold Nanoparticle Aggregation and Smart Phone Imaging. *Biosens. Bioelectron.* 124-125 (125), 143–149. doi:10.1016/j.bios.2018.10.006

Zhou, C., Zou, H., Li, M., Sun, C., Ren, D., and Li, Y. (2018). Fiber Optic Surface Plasmon Resonance Sensor for Detection of *E. coli* O157:H7 Based on Antimicrobial Peptides and AgNPs-rGO. *Biosens. Bioelectron.* 117, 347–353. doi:10.1016/j.bios.2018.06.005

Zhou, J., Zheng, Y., Zhang, J., Karimi-Maleh, H., Xu, Y., Zhou, Q., et al. (2020). Characterization of the Electrochemical Profiles of Lycoris Seeds for Species Identification and Infrageneric Relationships. *Anal. Lett.* 53, 2517–2528. doi:10.1080/00032719.2020.1746327

Zhu, C., Zhao, G., and Dou, W. (2018). Core-shell Red Silica Nanoparticles Based Immunochromatographic Assay for Detection of *Escherichia coli* O157:H7. *Analytica Chim. Acta* 1038, 97–104. doi:10.1016/j.aca.2018.07.003

Conflict of Interest: DW was employed by Dong-E E-Jiao Co. Ltd.

The remaining authors declare that the research was conducted in the absence of any commercial or financial relationships that could be construed as a potential conflict of interest.

frontiers in Chemistry

ORIGINAL RESEARCH
published: 23 June 2021
doi: 10.3389/fchem.2021.709487

Evaluation of Peroxidase in Herbal Medicines Based on an Electrochemical Sensor

Yinzi Yue[1†], Lianlin Su[2†], Min Hao[3], Wenting Li[1], Li Zeng[1] and Shuai Yan[4]**

[1]First Clinical Medical School, Nanjing University of Chinese Medicine, Nanjing, China, [2]School of Pharmacy, Nanjing University of Chinese Medicine, Nanjing, China, [3]School of Pharmacy, Zhejiang Chinese Medicine University, Hangzhou, China, [4]Department of Anorectal, Suzhou TCM Hospital Affiliated to Nanjing University of Chinese Medicine, Suzhou, China

Peroxidases are species-specific. Differences in peroxidase can objectively reflect the genetics among species. The use of peroxidase to assist in species identification is relatively simple and effective. In this work, we proposed a graphene-modified electrode. This electrode can amplify the signal of electrocatalytic reduction of hydrogen peroxide. Since peroxidase can catalyze the reduction of hydrogen peroxide, this signal can be used as an indicator to demonstrate the content of peroxidase in different plant tissues. Twelve herbal medicines were selected for our study. The results show that this electrochemical-based detection technique was comparable to colorimetric method in terms of accuracy.

Keywords: peroxidase activity, herbal medicines, electrochemical evaluation, rapid detection, hydrogen peroxide

OPEN ACCESS

Edited by:
Fatemeh Karimi, Quchan University of Advanced Technology, Iran

Reviewed by:
Somaye Cheraghi, Shahid Bahonar University of Kerman, Iran
Vahid Arabali, Islamic Azad University Sari Branch, Iran

****Correspondence:***
Li Zeng
zengbingli@njucm.edu.cn
Shuai Yan
doctor_shuaiyan@njucm.edu.cn

†These authors have contributed equally to this work

Specialty section:
This article was submitted to Electrochemistry, a section of the journal Frontiers in Chemistry

Received: *14 May 2021*
Accepted: *10 June 2021*
Published: *23 June 2021*

Citation:
Yue Y, Su L, Hao M, Li W, Zeng L and Yan S (2021) Evaluation of Peroxidase in Herbal Medicines Based on an Electrochemical Sensor. Front. Chem. 9:709487. doi: 10.3389/fchem.2021.709487

INTRODUCTION

The phenolics and enzymes in plant tissues are distributed in different locations in the cell. Enzymes cannot come into contact with phenolic substrates, so enzymatic browning does not occur (Paravisini and Peterson, 2019; Kizilgeci et al., 2020; Moon et al., 2020; Özkan, 2020). However, if damage or dehydration leads to the destruction of plant cell structure and changes the regionalized distribution of phenolics and enzymes, the contact between phenolic substances, enzymes and oxygen will cause enzymatic browning (Barpete et al., 2020). The presence of phenolic substrates, enzymes and oxygen is necessary for enzymatic browning to occur. Enzymes that cause enzymatic browning of plant include polyphenol oxidase, peroxidase, catalase, superoxide dismutase (Demir and Işık, 2020), phenylalanine aminotransferase, etc. Among them, peroxidase is the main oxidase that causes enzymatic browning in most plants (Ozbek et al., 2021; Tenish et al., 2021).

Peroxidase is an oxidase that uses hydrogen peroxide as an electron acceptor to catalyze substrates and is widely found in plants, animals, and microorganisms (Chen et al., 2020; Karimi-Maleh et al., 2021a; Lazzarotto et al., 2021). Most peroxidases contain heme cofactors and are mostly heme-binding proteins containing iron ions. There are also some peroxidases in which the iron of heme is replaced by copper, manganese, vanadium or selenium (Dong et al., 2020; Karimi-Maleh et al., 2021c). Therefore, according to the different cofactors, ferric heme peroxidases can be divided into two categories. The third type of structure is the chloride peroxidase and the cytochrome c peroxidase containing two hemoglobins (Fu et al., 2019; Li et al., 2020; Zhou et al., 2020). In addition, depending on the isoelectric point, it can be divided into acid peroxidase, neutral peroxidase and basic peroxidase. According to the binding state, it can be divided into soluble peroxidase, ion-bound peroxidase and covalent-bound peroxidase (Xu et al., 2020; Karimi-Maleh et al., 2021b).

The activity and number of peroxidases vary greatly in different tissues and organs, different growth, development periods, different physiological states and different varieties of plants.

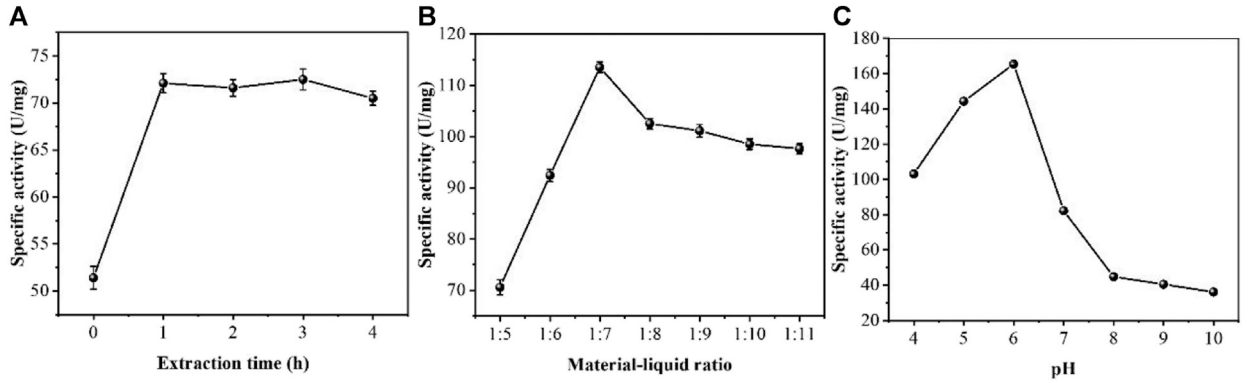

FIGURE 1 | Effect of **(A)** extraction time **(B)** material-liquid ratio and **(C)** pH on enzyme specific activity of *Erycibe obtusifolia*.

Peroxidases can largely reflect the characteristics of plant growth and development, biometabolic status, ability to adapt to the external environment and genetic differences among varieties. The electrophoretic profiles of peroxidases are relatively stable under certain conditions and are as species-specific as morphological trait indicators (Yang et al., 2020; Ying et al., 2020; Zheng et al., 2020). It has been widely used as a genetic marker in plant variety identification, genetic diversity analysis, plant disease resistance analysis, plant growth and development analysis (Karimi-Maleh et al., 2020).

Non-denaturing discontinuous polyacrylamide gel electrophoresis (native PAGE) does not easily denature proteins. It essentially does not disrupt the natural conformation of proteins and the subunit interactions, so it maintains protein biological activity (Rajhans et al., 2020; Almaz et al., 2021). This method is most widely used in the detection of plant peroxidases because it does not denature proteins. Sodium dodecyl-sulfate-gelatin-poly-acrylamide gel electrophoresis (G-PAGE) is an electrophoretic technique established in the early 1980s, which is a kind of electrophoresis that maintains the enzyme biological activity after electrophoresis (Liu et al., 2020). In phycological studies, peroxidases are species-specific. Differences in peroxidases can objectively reflect the genetics among species. The use of peroxidase to assist in species identification is a relatively simple and effective. Studies have shown that peroxidases are involved in the physiological responses of plants to disease, insect, salt, and drought resistance as well as resistance to biotic stresses (Jamali et al., 2014; Baghizadeh et al., 2015; Karaman, 2021; Karaman et al., 2021).

Recently, an electrochemical-based detection technique has been developed for the study of peroxidase activity in plants (Fu et al., 2021). Since peroxidase can catalyze hydrogen peroxide accordingly, differences in catalytic activity can be used to reflect differences in peroxidase content in plant tissues. This method can potentially be used for the determination of plant sex. Electrochemical detection is a low-cost and university-based analytical technique that is particularly suitable for rapid detection. Therefore, this technology has a bright future in plant detection. There is a very large market for herbal medicine in Asia. Authentication of herbal medicines has been a problem in this market. Based on the above information, the identification of herbal medicines by using the difference of peroxidase is a direction worth exploring.

In this work, twelve herbs were selected for electrochemical testing. The peroxidases in the herbs were first extracted. Graphene-modified electrodes were subsequently used to detect these extracts in the presence of hydrogen peroxide. The results revealed a large variation of peroxidase in different herbs. This technique can potentially be used for the identification of herbal species as well as the control of herbal quality.

EXPERIMENTS

Materials

Ratan of *Erycibe obtusifolia*, leaf of *Panax ginseng* C. A. Mey, leaf of *Murraya exotica* L., rhizome of *Zingiber officinale* Rosc, seed of *Cassia obtusifolia* L., rhizome of *Pinellia ternate* (Thunb.) Breit, rhizome of *Imperata cylindrica* Beauv. var.major (Nees) C.E.Hubb, pericarp of *Zanthoxylum bungeanum* Maxim, seed of *Trichosanthes rosthornii* Harms, pericarp of *Benincasa hispida* (Thunb.) Cogn, rhizome of *Semiaquilegia adozoides* (DC.) Makino and seed of *Strychnos nuxvomica* L. were purchased from local pharmacy and identified by Nanjing University of Chinese Medicine. Disodium hydrogen phosphate, sodium dihydrogen phosphate, potassium dihydrogen phosphate, guaiacol, hydrogen peroxide, graphene ink, sulfuric acid, phosphoric acid, anhydrous ethanol, Thomas Brilliant Blue G-250, bovine serum albumin were all analytically grade.

Peroxidase Extraction

Weigh a certain amount of herbs and add PBS at 4°C. The pulping time was 6 0°s, and then extracted for a certain time at 4°C. The filtered filtrate was frozen and centrifuged at 9,000°r/min for 15°min, and the supernatant was collected as the crude enzyme solution.

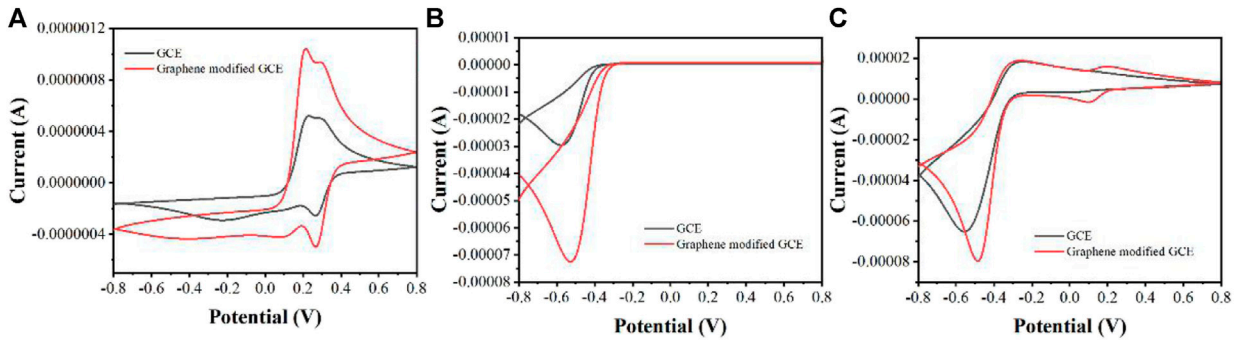

FIGURE 2 | (A) CVs of GCE and graphene modified GCE on *Erycibe obtusifolia* peroxidase extracts in the absence of H_2O_2 **(B)** CVs of GCE and graphene modified GCE toward 1 mM H_2O_2 **(C)** CVs of GCE and graphene modified GCE on *Erycibe obtusifolia* peroxidase extracts in the presence of 1 mM H_2O_2.

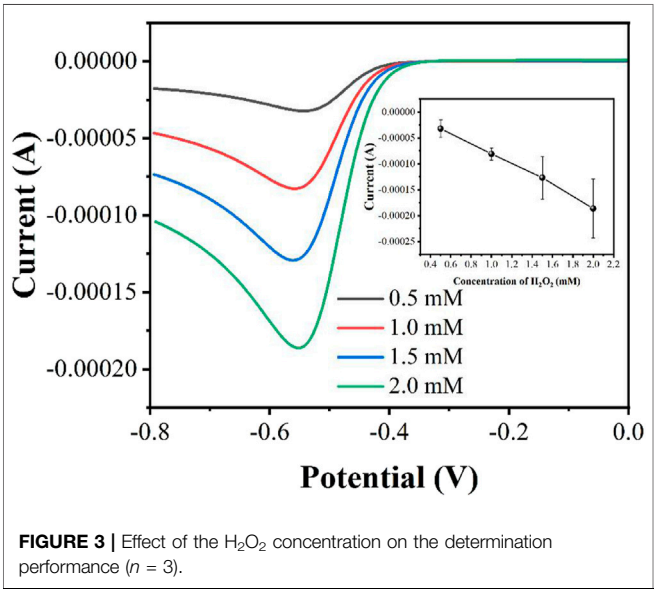

FIGURE 3 | Effect of the H_2O_2 concentration on the determination performance (n = 3).

Enzyme Activity Measurement Based on Colorimetric Assay

Guaiacol was used as the reaction substrate in the colorimetric assay. The reaction system consisted of 2.95 ml of 18 mM guaiacol and 1 mM H_2O_2 (pH 5 PBS). Add 0.05 ml of the enzyme solution, cover the cuvette with a lid and mix rapidly, measure the absorbance value at 470 nm at 30°C, count one time every 10°s, and use 0.01 change in absorbance value per minute as 1 unit of enzyme activity.

Determination of Protein Content

The protein content was determined by the colorimetric method of Bradford's Komas Brilliant Blue G-250. Bovine serum protein was used to make the standard curve. The absorbance value at 595 nm was used as the vertical coordinate for the standard curve. The standard curve was plotted with the standard protein content as the horizontal coordinate, and the protein mass in the sample was calculated by the curve equation. Specific activity is the activity per unit mass of enzyme, expressed as U/mg, specific activity = activity (U)/mass of protein (mg).

Enzyme Activity Measurement Based on Electrochemical Method

All electrochemical measurements were performed using a CHI 820D electrochemical workstation with a three-electrode system. Specifically, a reference electrode (Ag/AgCl), a counter electrode (Pt foil) and a working electrode (glassy carbon electrode, GCE). Graphene ink (0.5 mg/ml) was firstly drop coated on the GCE surface and dried naturally. Then, a linear sweep voltammetry was used for detecting the electrocatalytic of peroxidase toward H_2O_2.

RESULTS AND DISCUSSION

Firstly, we optimized the extraction process of peroxidase. The extraction conditions were optimized using an orthogonal test. The results of the single-factor test were analyzed in an orthogonal test to derive the key factors influencing the peroxidase extraction of *Erycibe obtusifolia*. The effects of different extraction times of 0, 1, 2, 3 and 4 h on the specific activity of *Erycibe obtusifolia* peroxidase were investigated by fixing the material-liquid ratio 1:5 at pH 4. It can be seen from **Figure 1A** that the enzyme specific activity increased with the increase of extraction time and stabilized when the extraction time exceeded 1 h. The reason may be that the enzyme in *Erycibe obtusifolia* tissue was not fully solubilized when the extraction time was less than 1 h. With the increase of time, the enzyme leaching gradually reached the equilibrium, and the enzyme specific activity tended to stabilize. 3 h later, the enzyme specific activity slightly decreased, which might be due to the inactivation of the leached enzyme in the solution environment. **Figure 1B** examines the effect of different stock-to-solution ratios on the specific activity of honeysuckle peroxidase. The peroxidase specific activity increased with the increase of the material-liquid ratio between 1:7 and 1:5. When the material-liquid ratio was less than 1:7, the peroxidase specific activity showed a decreasing

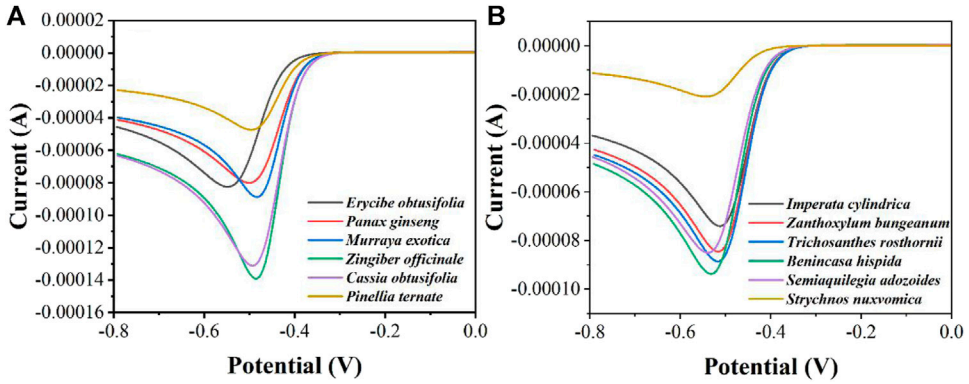

FIGURE 4 | LSV curves of **(A)** *Erycibe obtusifolia, Panax ginseng, Murraya exotica, Zingiber officinale, Cassia obtusifolia, Pinellia ternate* and **(B)** *Imperata cylindrica, Zanthoxylum bungeanum, Trichosanthes rosthornii, Benincasa hispida, Semiaquilegia adozoides*, *Strychnos nuxvomica* in the presence of 1 mM H_2O_2 recorded using a graphene modified GCE.

TABLE 1 | Enzyme activity measurement of *Erycibe obtusifolia*, *Panax ginseng*, *Murraya exotica*, *Zingiber officinale*, *Cassia obtusifolia*, *Pinellia ternate*, *Imperata cylindrica*, *Zanthoxylum bungeanum*, *Trichosanthes rosthornii*, *Benincasa hispida*, *Semiaquilegia adozoides* and *Strychnos nuxvomica* based on colorimetric assay.

Herb	Specific activity (U/mg)	Herb	Specific activity (U/mg)
Erycibe obtusifolia	162	*Panax ginseng*	154
Murraya exotica	174	*Zingiber officinale*	197
Cassia obtusifolia	181	*Pinellia ternate*	72
Imperata cylindrica	149	*Zanthoxylum bungeanum*	169
Trichosanthes rosthornii	152	*Benincasa hispida*	178
Semiaquilegia adozoides	167	*Strychnos nuxvomica*	31

trend with decreasing material-liquid ratio. This may be due to the increase of solids in the extraction system and the relative lack of extraction solution due to the large material-liquid ratio. When the material-liquid ratio was smaller, the enzyme leached from plant tissues was diluted and showed a decrease in enzyme activity. **Figure 1C** examines the effect of different extract pH values on the specific activity of *Erycibe obtusifolia* peroxidase. From **Figure 1C**, it can be seen that the enzyme specific activity showed a trend of increasing and then decreasing between pH 4–9. The buffer pH of six had a better extraction effect. The reason may be that the alkaline and more acidic environment had an effect on the conformation of *Erycibe obtusifolia* peroxidase, which led to a change in the molecular structure of the enzyme causing a partial loss of enzyme activity. On the other hand, it may be that more heteroproteins were leached at pH greater than 6, thus affecting the peroxidase extraction effect.

Figure 2 shows the CV curves of GCE and graphene modified GCE on *Erycibe obtusifolia* peroxidase extracts. In the absence of H_2O_2 (**Figure 2A**), both electrodes have some redox peaks during the anodic scan and cathodic scan. These peaks are due to the oxidation and reduction of some substances possessing electrochemical activity in *Erycibe obtusifolia* extracts, such as flavonoids (Cai et al., 2020), pigments (Pearce et al., 2020), carotenoids (Čižmek and Komorsky-Lovri), etc.

Figure 2B shows the CV curves of the two electrodes in PBS for 1 mM H_2O_2. It can be seen that both electrodes have a reduction of H_2O_2 in the cathodic scan. In contrast, the graphene-modified GCE possesses a very remarkable current signal. Therefore, graphene can significantly increase the current signal due to its excellent electrical properties (Vasseghian et al., 2021).

The same can be observed in the assay of *Erycibe obtusifolia* extracts (**Figure 2C**). It can be seen from the figure that the graphene-modified electrode possesses a very significant current signal. This amplification strategy of the current signal can greatly increase the feasibility of detecting peroxidase by electrochemistry.

The concentration of H_2O_2 affects the performance of electrocatalytic response. In general, the higher the concentration of H_2O_2 will lead a higher reduction current. However, too much H_2O_2 can rapidly deplete the peroxidase enzyme, thus leading to a large variance. **Figure 3** shows the LSV curves in the presence of 0.5, 1, 1.5 and 2 mM H_2O_2. As expected, the reduction current increases with increasing concentration of H_2O_2. However, the reproducibility of the currents becomes worse as the concentration increases. Therefore, we finally chose 1 mM H_2O_2 as the experimental concentration.

In order to distinguish more quickly the differences in peroxidase in different herbal extracts, we measured twelve herbs by LSV (**Figure 4**). It can be seen that *Zingiber officinale* has the highest current and *Strychnos nuxvomica* has the lowest current. According to the data in **Figure 3**, the order of peroxidase activity of the twelve herbs was *Zingiber officinale* > *Cassia obtusifolia* > *Benincasa hispida* > *Murraya exotica*

> *Trichosanthes rosthornii* > *Semiaquilegia adozoides* > *Zanthoxylum bungeanum* > *Erycibe obtusifolia* > *Panax ginseng* > *Imperata cylindrica* > *Pinellia ternate* > *Strychnos nuxvomica*. **Table 1** shows the results of 12 herbs tested by colorimetric assay. Except for *Zanthoxylum bungeanum* and *Semiaquilegia adozoides*, the order of the results is consistent with that of the electrochemical assay. Such results represent that the electrochemical detection techniques we use can be used for the identification and quality control of herbs.

CONCLUSION

Peroxidase can be used as an indicator for the identification of herbs and quality control. An electrochemical-based assay was proposed for the rapid detection of peroxidase in herbal medicines. Graphene was used to modify the electrode to achieve increased signal sensitivity. Peroxidase in herbs can catalyze the electrochemical reduction of H_2O_2, so the electrochemical reduction signal of H_2O_2 can be used as an indicator for the content of peroxidase in the samples. Based on a investigation of 12 herbs, the accuracy of this detection technique is comparable to that of colorimetric method.

DATA AVAILABILITY STATEMENT

The original contributions presented in the study are included in the article/Supplementary Material, further inquiries can be directed to the corresponding authors.

AUTHOR CONTRIBUTIONS

YY and LS conceived of the study. LZ and SY supervised the development program, YY, LS, and MH conducted the materials characterization. MH and WL received and curated samples and analytical records. YY and LS wrote the manuscript. All authors read and approved of the manuscript.

FUNDING

This work was funded by Natural Science Foundation of Nanjing University of Chinese Medicine (XZR2020038), Jiangsu Youth Medical Talents Project (QNRC2016255) and The Fifth Batch of Gusu Health Personnel Training Project in Suzhou (GSWS2020085).

REFERENCES

Almaz, Z., Oztekin, A., Abul, N., Gerni, S., Erel, D., Kocak, S. M., et al. (2021). A New Approach for Affinity-based Purification of Horseradish Peroxidase. *Biotechnol. Appl. Biochem.* 68, 102–113. doi:10.1002/bab.1899

Baghizadeh, A., Karimi-Maleh, H., Khoshnama, Z., Hassankhani, A., and Abbasghorbani, M. (2015). A Voltammetric Sensor for Simultaneous Determination of Vitamin C and Vitamin B6 in Food Samples Using ZrO2 Nanoparticle/Ionic Liquids Carbon Paste Electrode. *Food Anal. Methods* 8, 549–557. doi:10.1007/s12161-014-9926-3

Barpete, S., Gupta, P., Khawar, K. M., Özcan, S., and Kumar, S. (2020). *In Vitro* approaches for Shortening Generation Cycles and Faster Breeding of Low B-N-oxalyl-L-A, B-diaminopropionic Acid Content of Grass Pea (Lathyrus Sativus L.). *Fresenius Environ. Bull.* 29, 2698–2706.

Cai, Y., Huang, W., and Wu, K. (2020). Morphology-controlled Electrochemical Sensing of Erbium- Benzenetricarboxylic Acid Frameworks for Azo Dyes and Flavonoids. *Sensors Actuators B: Chem.* 304, 127370. doi:10.1016/j.snb.2019.127370

Chen, Q., Man, H., Zhu, L., Guo, Z., Wang, X., Tu, J., et al. (2020). Enhanced Plant Antioxidant Capacity and Biodegradation of Phenol by Immobilizing Peroxidase on Amphoteric Nitrogen-Doped Carbon Dots. *Catal. Commun.* 134, 105847. doi:10.1016/j.catcom.2019.105847

Čižmek, L., and Komorsky-Lovrić, Š. (2020). Electrochemistry as a Screening Method in Determination of Carotenoids in Crustacean Samples Used in Everyday Diet. *Food Chem.* 309, 125706.

Demir, Z., and Işık, D. (2020). Using Cover Crops to Improve Soil Quality and Hazelnut Yield. *Fresenius Environ. Bull.* 29, 1974–1987.

Dong, Y., Jing, M., Shen, D., Wang, C., Zhang, M., Liang, D., et al. (2020). The Mirid Bug Apolygus Lucorum Deploys a Glutathione Peroxidase as a Candidate Effector to Enhance Plant Susceptibility. *J. Exp. Bot.* 71, 2701–2712. doi:10.1093/jxb/eraa015

Fu, L., Xie, K., Wang, A., Lyu, F., Ge, J., Zhang, L., et al. (2019). High Selective Detection of Mercury (II) Ions by Thioether Side Groups on Metal-Organic Frameworks. *Analytica Chim. Acta* 1081, 51–58. doi:10.1016/j.aca.2019.06.055

Fu, L., Su, W., Chen, F., Zhao, S., Zhang, H., Karimi-Maleh, H., et al. (2021). Early Sex Determination of Ginkgo Biloba Based on the Differences in the Electrocatalytic Performance of Extracted Peroxidase. *Bioelectrochemistry* 140, 107829. doi:10.1016/j.bioelechem.2021.107829

Jamali, T., Karimi-Maleh, H., and Khalilzadeh, M. A. (2014). A Novel Nanosensor Based on Pt:Co Nanoalloy Ionic Liquid Carbon Paste Electrode for Voltammetric Determination of Vitamin B9 in Food Samples. *LWT - Food Sci. Technology* 57, 679–685. doi:10.1016/j.lwt.2014.01.023

Karaman, C., Karaman, O., Atar, N., and Yola, M. L. (2021). Tailoring of Cobalt Phosphide Anchored Nitrogen and Sulfur Co-doped Three Dimensional Graphene Hybrid: Boosted Electrocatalytic Performance towards Hydrogen Evolution Reaction. *Electrochimica Acta* 380, 138262. doi:10.1016/j.electacta.2021.138262

Karaman, C. (2021). Orange Peel Derived-Nitrogen and Sulfur Co-doped Carbon Dots: a Nano-booster for Enhancing ORR Electrocatalytic Performance of 3D Graphene Networks. *Electroanalysis* 33, 1356–1369. doi:10.1002/elan.202100018

Karimi-Maleh, H., Karimi, F., Malekmohammadi, S., Zakariae, N., Esmaeili, R., Rostamnia, S., et al. (2020). An Amplified Voltammetric Sensor Based on Platinum Nanoparticle/polyoxometalate/two-Dimensional Hexagonal boron Nitride Nanosheets Composite and Ionic Liquid for Determination of N-Hydroxysuccinimide in Water Samples. *J. Mol. Liquids* 310, 113185. doi:10.1016/j.molliq.2020.113185

Karimi-Maleh, H., Alizadeh, M., Orooji, Y., Karimi, F., Baghayeri, M., Rouhi, J., et al. (2021a). Guanine-Based DNA Biosensor Amplified with Pt/SWCNTs Nanocomposite as Analytical Tool for Nanomolar Determination of Daunorubicin as an Anticancer Drug: A Docking/Experimental Investigation. *Ind. Eng. Chem. Res.* 60, 816–823. doi:10.1021/acs.iecr.0c04698

Karimi-Maleh, H., Ayati, A., Davoodi, R., Tanhaei, B., Karimi, F., Malekmohammadi, S., et al. (2021b). Recent Advances in Using of Chitosan-Based Adsorbents for Removal of Pharmaceutical Contaminants: A Review. *J. Clean. Prod.* 291, 125880. doi:10.1016/j.jclepro.2021.125880

Karimi-Maleh, H., Orooji, Y., Karimi, F., Alizadeh, M., Baghayeri, M., Rouhi, J., et al. (2021c). A Critical Review on the Use of Potentiometric Based Biosensors for Biomarkers Detection. *Biosens. Bioelectron.* 184, 113252. doi:10.1016/j.bios.2021.113252

Kizilgeci, F., Mokhtari, N. E. P., and Hossain, A. (2020). Growth and Physiological Traits of Five Bread Wheat (Triticum aestivumL.) Genotypes Are Influenced by Different Levels of Salinity and Drought Stress. *Fresenius Environ. Bull.* 29, 8592–8599.

Lazzarotto, F., Menguer, P. K., Del-Bem, L.-E., Zámocký, M., and Margis-Pinheiro, M. (2021). Ascorbate Peroxidase Neofunctionalization at the Origin of APX-R and APX-L: Evidence from Basal Archaeplastida. *Antioxidants* 10, 597. doi:10.3390/antiox10040597

Li, H., Liu, J.-X., Wang, Y., and Zhuang, J. (2020). The Ascorbate Peroxidase 1 Regulates Ascorbic Acid Metabolism in Fresh-Cut Leaves of tea Plant during Postharvest Storage under Light/dark Conditions. *Plant Sci.* 296, 110500. doi:10.1016/j.plantsci.2020.110500

Liu, R., Zhang, Y., Yao, X., Wu, Q., Wei, M., and Yan, Z. (2020). ε-Viniferin, a Promising Natural Oligostilbene, Ameliorates Hyperglycemia and Hyperlipidemia by Activating AMPK *In Vivo*. *Food Funct.* 11, 10084–10093. doi:10.1039/d0fo01932a

Moon, K. M., Kwon, E.-B., Lee, B., and Kim, C. Y. (2020). Recent Trends in Controlling the Enzymatic browning of Fruit and Vegetable Products. *Molecules* 25, 2754. doi:10.3390/molecules25122754

Ozbek, O., Gokdogan, O., and Baran, M. F. (2021). Investigation on Energy Use Efficiency and Greenhouse Gas Emissions (GHG) of Onion Cultivation. *Fresenius Environ. Bull.* 30, 1125–1133.

Özkan, A. (2020). Effect of Gold Nanoparticle Functionalized Multi-Walled Carbon Nanotubes on the Properties of Na-Bentonite Water Based Drilling Fluid. *Fresenius Environ. Bull.* 29, 143–151.

Paravisini, L., and Peterson, D. G. (2019). Mechanisms Non-enzymatic browning in orange Juice during Storage. *Food Chem.* 289, 320–327. doi:10.1016/j.foodchem.2019.03.049

Pearce, N., Davies, E. S., and Champness, N. R. (2020). Electrochemical and Spectroelectrochemical Investigations of Perylene Peri-Tetracarbonyl Species. *Dyes Pigm.* 183, 108735. doi:10.1016/j.dyepig.2020.108735

Rajhans, G., Sen, S. K., Barik, A., and Raut, S. (2020). Elucidation of Fungal Dye-decolourizing Peroxidase (DyP) and Ligninolytic Enzyme Activities in Decolourization and Mineralization of Azo Dyes. *J. Appl. Microbiol.* 129, 1633–1643. doi:10.1111/jam.14731

Tenish, Z., Minović, J., Jednak, S., and Parežanin, M. (2021). Environmental Degradation and Economic Activites in OECD Countries. *Fresenius Environ. Bull.* 30, 2186–2192.

Le, V. T., Vasseghian, Y., Dragoi, E. N., Moradi, M., and Mousavi Khaneghah, A. (2021). A Review on Graphene-Based Electrochemical Sensor for Mycotoxins Detection. *Food Chem. Toxicol.* 148, 111931. doi:10.1016/j.fct.2020.111931

Xu, Y., Lu, Y., Zhang, P., Wang, Y., Zheng, Y., Fu, L., et al. (2020). Infrageneric Phylogenetics Investigation of Chimonanthus Based on Electroactive Compound Profiles. *Bioelectrochemistry* 133, 107455. doi:10.1016/j.bioelechem.2020.107455

Yang, R., Fan, B., Wang, S. a., Li, L., Li, Y., Li, S., et al. (2020). Electrochemical Voltammogram Recording for Identifying Varieties of Ornamental Plants. *Micromachines* 11, 967. doi:10.3390/mi11110967

Ying, J., Zheng, Y., Zhang, H., and Fu, L. (2020). Room Temperature Biosynthesis of Gold Nanoparticles with Lycoris Aurea Leaf Extract for the Electrochemical Determination of Aspirin. *Rev. Mex. Ing. Quím.* 19, 585–592. doi:10.24275/rmiq/mat741

Zheng, Y., Zhu, J., Fu, L., and Liu, Q. (2020). Phylogenetic Investigation of Yellow Camellias Based on Electrochemical Voltammetric Fingerprints. *Int. J. Electrochem. Sci.* 15, 9622–9630. doi:10.20964/2020.10.54

Zhou, J., Zheng, Y., Zhang, J., Karimi-Maleh, H., Xu, Y., Zhou, Q., et al. (2020). Characterization of the Electrochemical Profiles of Lycoris Seeds for Species Identification and Infrageneric Relationships. *Anal. Lett.* 53, 2517–2528. doi:10.1080/00032719.2020.1746327

Conflict of Interest: The authors declare that the research was conducted in the absence of any commercial or financial relationships that could be construed as a potential conflict of interest.

frontiers in Chemistry

ORIGINAL RESEARCH
published: 25 June 2021
doi: 10.3389/fchem.2021.699368

A New Electrochemical Detection Technique for Organic Matter Content in Ecological Soils

Jinping Liu[1,2], *Tao Yang*[2], *Jiaqi Xu*[1] *and Yankun Sun*[1]*

[1]College of Resources and Environment, Northeast Agricultural University, Harbin, China, [2]Heilongjiang Vocational College of Agricultural Technology, Jiamusi, China

The rapid detection of organic matter in soil is of great interest in agriculture, but the commonly used techniques require laboratory operation. Therefore, the development of a technique that allows rapid detection of soil organic matter in the field is of great interest. In this work, we propose an electrochemical-based approach for the detection of organic matter in soil particles. Since soil particles immobilized directly on the electrode surface can fall off during testing, we introduced graphene to coat the soil particles. The encapsulated soil particles can be stably immobilized on the electrode surface. We have investigated the electrochemical behavior of soil particles. The results show a correspondence between the electrochemical oxidation and reduction of soil particles and the organic matter content in them. We collected soil samples from three sites and constructed an electrochemical modeling, testing framework with stability based on multiple calibrations and random division of the prediction set. We used the equal interval partial least squares (EC-PLS) method for potential optimization to establish the equivalent model set. A joint model for the electrochemical analysis of organic matter in three locations of soil samples was developed for the commonality study.

Keywords: soil organic matter, cyclic voltammetry, graphene, equivalent model set, joint model

OPEN ACCESS

Edited by:
Li Fu,
Hangzhou Dianzi University, China

Reviewed by:
Hongyan Sun,
Shenzhen Institutes of Advanced Technology, China
Xiaopeng Wang,
Suzhou TCM Hospital Affiliated to Nanjing University of Chinese Medicine, China
Yuhong Zheng,
Institute of Botany (CAS), Jiangsu Province and Chinese Academy of Sciences, China

***Correspondence:**
Yankun Sun
sunyankun@neau.edu.cn

Specialty section:
This article was submitted to Electrochemistry, a section of the journal Frontiers in Chemistry

Received: *23 April 2021*
Accepted: *14 June 2021*
Published: *25 June 2021*

Citation:
Liu J, Yang T, Xu J and Sun Y (2021) A New Electrochemical Detection Technique for Organic Matter Content in Ecological Soils. Front. Chem. 9:699368. doi: 10.3389/fchem.2021.699368

INTRODUCTION

Soil organic matter content is one of the most important indicators of soil nutrient supply capacity and fertility. Soil research scholars generally agree that there is a significant positive correlation between soil organic matter content and soil quality. Therefore, the information of soil organic matter content is one of the important value in the evaluation of ecological environment. At present, the determination of soil organic matter content is generally performed in the laboratory by external heating with potassium dichromate and combined spectroscopic/chromatographic analytical techniques such as nuclear magnetic resonance and thermal cracking-mass spectrometry (Yang et al., 2011). These determination methods have the advantage of higher measurement accuracy, however, they require high operator requirements and longer time for detection, while a large amount of reagents are consumed during the monitoring process.

In recent years, near-infrared spectroscopy has rapidly developed into a rapid, nondestructive, multi-component simultaneous analysis technique. However, due to the complex composition of soils, the investigations realized that two factors affect the spectral reflectance properties of soils: the moisture content of the soil and iron-containing oxides. There is a high correlation between the moisture in the soil and the reflectance of the spectrum, and an increase in soil moisture content leads to a decrease in spectral reflectance (Summers et al., 2011). In addition, the presence of iron oxides

causes a decrease in spectral reflectance and there are multiple characteristic absorption summits in the soil spectrum caused by iron oxides (Liu et al., 2018; Babaeian et al., 2019). Furthermore, the ensemble frequency multiplication information of the chemical bonds of hydrogen-containing groups contained in the NIR spectra is very weak, and it is generally necessary to pre-process the spectral data and then build a quantitative calibration model of the spectra by chemometric methods. Due to the presence of objective reasons such as the state of the sample, errors in measurement, and instrument errors, the raw spectra obtained from the instrument often contain some interference information that is not related to the components to be measured. The presence of interfering information can have an impact on subsequent calibration model building such as reduced accuracy or inaccurate prediction. Many studies are currently centered on the development of spectral processing algorithms to reduce the effects of interferences (Cambou et al., 2016; Sharififar et al., 2019). Meanwhile, some scholars have borrowed analytical techniques from other fields for detecting organic matter content in soils. For example, thermogravimetric analysis and differential scanning calorimetry, which are widely used in materials science, have been used for the evaluation of soil organic matter content (Fernández et al., 2012; Siewert and Kučerík, 2015). Wiesheu et al. (Wiesheu et al., 2018) explored the use of isotopic internal standards combined with Raman spectroscopy for the detection of soil organic matter content. These efforts provide very valuable academic implications, but still rely on large instruments in the detection results and require tedious processing of soil samples. In this work, we aim to explore an original detection technique based on solid state electroanalytical chemistry (SSEAC) for the rapid analysis of soil organic matter content in the field.

The application of electrochemical techniques in the field of soil science consists of two main categories: 1) electrochemical remediation of contaminated soils (Muñoz-Morales et al., 2017; Domínguez-Garay et al., 2018), and 2) detection of specific soil contaminants (Zhao and Liu, 2018; Mondal and Subramaniam, 2019). In the second application area, investigations have made a number of breakthroughs using liquid-phase electrochemical analysis techniques that allow specific and highly sensitive detection of pesticide residues and heavy metals in soils. However, it is not reasonable to design techniques for the detection of soil organic matter content using this type of methodology because the soil sample pre-treatment techniques for this type of technique are similar to conventional chemical assays, which rely on laboratory instruments and do not offer superiority. In this work, we propose an alternative approach to evaluate the organic matter content of undigested/dissolved soil samples directly by using the SSEAC technique for rapid detection. Soil particles contain a variety of plant-derived organic matter molecules, some of which are capable of electrochemical oxidation and/or reduction reactions, such as indoles, polyphenols and quinones. In particular, lignin and cross-linked phenolic polymers undergo substitution, addition, coupling and bond cleavage reactions in electrochemical oxidation and reduction. The electrochemical signal of these substances provides an indication that can be used to react to the overall organic matter content of the soil.

EXPERIMENTS

In the study of this paper, soil areas from three locations were collected (A, B, C). Each location was collected 77 soil samples. All soil samples will be used to determine the organic matter content of the soil using conventional and routine chemical methods, but some pretreatment of the soil samples will be required before measurement. At the beginning of the experiment, all the soil samples collected were numbered and recorded separately. The numbered soil samples were placed sequentially on vellum and spread evenly and neatly in a cool, dry and ventilated environment for air-drying. Particular care should be taken not to expose the soil samples to direct sunlight and baking during this process, as this can damage the integrity of the soil sample composition and affect the accuracy of the organic matter measurements. After the air-drying of all soil samples, the visible impurities are removed from the soil samples and the lumpy soil samples are carefully ground so that all soil samples are in a homogeneous fine-grained state. These samples are then passed through a 0.25 mm pore sieve, after which the soil samples are preserved for the subsequent determination of soil organic matter.

All electrochemical measurements were carried out using a CHI 760e working station. Then, the polydopamine functionalized graphene has been used for soil particle encapsulation. Then 2 μL of the dispersion was drop coated on a glassy carbon electrode and used as working electrode. A Pt wire and an Ag/AgCl electrode have been used as counter electrode and reference electrode, respectively.

RESULTS AND DISCUSSION

The underlying technology of SSEAC can be traced back to a series of original works by Scholz's team in the late 1980s and early 1990s (Scholz et al., 1989a, 1989b; Scholz and Lange, 1992). The first analysis of solid particles based on the SSEAC technique was also presented by Scholz's team in 1995 (Scholz et al., 1995). They found a positive correlation between the current intensity of the electrochemical oxygen precipitation reaction and the amount of radiation accumulated on ceramic particles. In the last decade, the Domenech-Carbo team combined metal corrosion and electrochemical redox mechanisms and developed several methods for the analysis of metal particles including electrochemical impedance spectroscopy (Doménech-Carbó et al., 2014), Tafel curves (Doménech-Carbó et al., 2016) and polarization curves (Doménech-Carbó et al., 2012). They also proposed voltammetry of immobilized microparticles (VIMP) for the rapid and effective electrochemical analysis of solid particles. SSEAC analysis is a promising technique for soil analysis due to its low cost and speed, minimal sample requirement, and applicability to both inorganic and organic particles. However, due to technical constraints, a large number of SSEAC assays

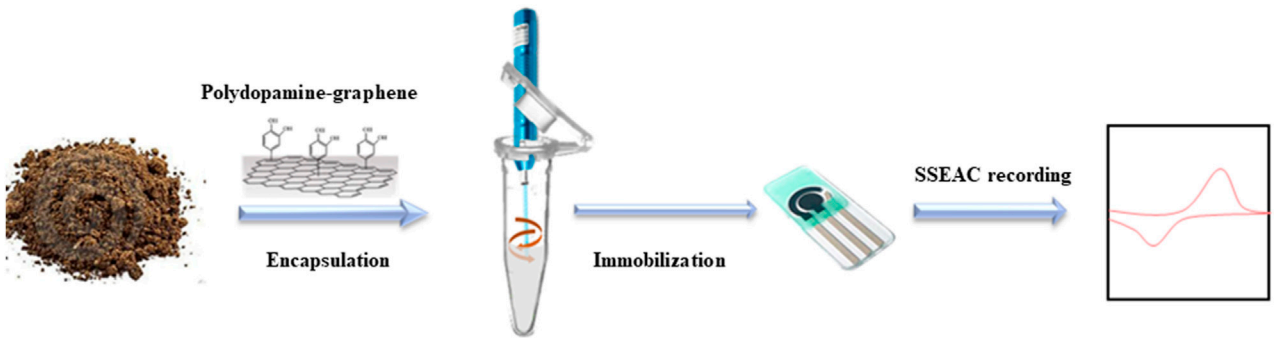

FIGURE 1 | Schematic process of proposed electrochemical method for soil particle encapsulation.

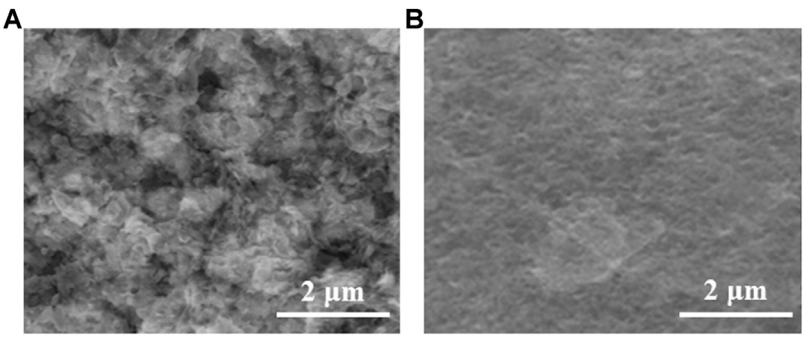

FIGURE 2 | SEM images of **(A)** soil particles and **(B)** polydopamine-graphene encapsulated soil particles on the electrode surface.

based on the VIMP method have a large uncontrollability at both the electrical and sample of the testing process. Therefore, we thought to encapsulate soil particles with polydopamine-modified graphene, which has high specific surface, high electrical conductivity and good immobilization ability. The material was used to adsorb oxidizable organic compounds from the soil particles with high efficiency. The encapsulated soil particles were directly immobilized on the surface of a printed electrode with an integrated three-electrode system for highly sensitive signal acquisition, as shown in **Figure 1**.

This work proposes to perform rapid detection of organic matter content of soil by detecting the reaction of oxidizable organic compounds in soil samples with reactive oxygen species (ROS) generated by *in situ* electrochemistry as an indication. Soil particles were adsorbed and coated with polydopamine-modified graphene and cemented on the electrode surface. This allows for signal acquisition of oxidizable organic compounds in the soil sample. We also investigated the electrochemical response mechanism of soil particles under encapsulation. A reasonable signal acquisition standard was investigated, and the correspondence between the oxidizable organic compounds in soil particles and the overall organic matter content was explored by using the conventional potassium dichromate external heating method and NIR detection method as controls.

Modification of graphene surfaces using polydopamine is often used to improve the dispersion of graphene in the aqueous phase and to achieve efficient modification of other material surfaces with the help of the adhesion of polydopamine. The SEM images in **Figure 2** show the soil particles directly immobilized on the electrode surface and the soil particles after polydopamine-graphene coating. It can be seen that the polydopamine-graphene can coat the soil particles very well from the microscopic point of view, and has good film formation on the electrode surface to achieve stable immobilization. This makes the soil particles not easily detach

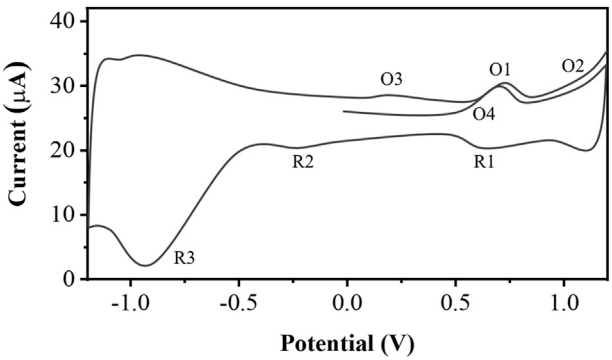

FIGURE 3 | SSEAC spectra of soil particles.

TABLE 1 | Parameters and prediction results of the optimal PLS voltammetric region model for soil SSEAC data.

Location	Region	*F*	SEP^+	SEP_{Ave}	SEP_{SD}	$R_{P,Ave}$	$R_{P,SD}$
A	0.0–1.0 V	9	0.277	0.271	0.022	0.917	0.016
	0.7–1.0 V	6	0.322	0.299	0.021	0.903	0.009
	0.0–1.0 V	9	0.260	0.241	0.014	0.922	0.007
	Whole scan	11	0.247	0.230	0.022	0.919	0.011
B	0.0–1.0 V	13	0.857	0.779	0.057	0.869	0.021
	0.7–1.0 V	17	1.207	1.035	0.124	0.801	0.043
	0.0–1.0 V	17	0.754	0.576	0.155	0.933	0.033
	Whole scan	26	0.611	0.471	0.151	0.951	0.031
C	0.0–1.0 V	20	0.365	0.318	0.041	0.814	0.022
	0.7–1.0 V	29	0.418	0.366	0.061	0.851	0.041
	0.0–1.0 V	17	0.221	0.201	0.020	0.923	0.007
	Whole scan	26	0.209	0.191	0.022	0.955	0.009

from the electrode during the electrochemical detection process and improves the accuracy of the detection.

The cyclic voltammogram of the soil particles after half-derivative convolution is shown in **Figure 3**. There are multiple oxidation peaks (O1, O3, O4) in the range of +0.2 to +0.8 V at the anode. From +1.0 V onwards there is a significant current rise due to oxygen precipitation. During the negative sweep, there is a clear reduction peak at +0.60 V (R1), followed by a series of weak overlapping reduction peaks between +0.2 and 0.6 V (R2). A distinct reduction peak occurs near about −1.0 V due to hydrogen precipitation. These oxidation and reduction peaks are signals due to the electrochemical oxidation or reduction of organic matter in the soil. These observed processes may be due to the superposition of signals from a considerable number of compounds. Nevertheless, if the electrochemical redox fingerprints of lignin and different organic compounds are compared, it is shown that the O1 process is probably the oxidation of the catechol moiety to the corresponding o-quinones. O2 is the oxidation of monophenolic moiety and/or methoxyphenol (Milczarek, 2009; Admassie et al., 2014). R1 is the reduction process of some of the substances in O1 in the cathodic scan, while the R2 process is mainly attributed to the reduction of organic compounds with a quinone structure. During the second anodic scan, the peaks of O1 and O2 were reduced. A series of additional oxidation signals (O3) between −0.1 and +0.2 V appeared, suggesting the generation of new reactive oxygen clusters during the electrochemical process.

We tried to divide the collected soil samples into sample sets, of which 30 samples were the test set and 47 samples were the modeling set. In the modeling set, we divided 23 of the samples into calibration set and 24 samples into prediction set in order to avoid distortion of model evaluation as well as to get stable prediction. In order to better analyze the models built by the EC-PLS method, we selected the first anode scan 0.0–1.0 V and cathode scan 0.7 to −1.0 V, the second anode scan 0.0–1.0 V and the full voltammetric region to build the PLS models, respectively. **Table 1** shows a summary of the optimal PLS model results for different voltammetric regions, from which it can be seen that the best modeling results were obtained for the full voltammetric region, followed by very close modeling results under the anodic scan, indicating that the SSEAC information of oxidizable compounds in the soil can correspond better to the amount of organic matter content in the soil.

From **Table 1**, it can be seen that the three locations of soil samples are best modeled in the whole scan range. However, the number of potentials in the whole scan range in the full CV scan is very high and therefore the model is very complex. The modeling effect of 0–1 V is very close to the whole scan range, which indicates that the information potential of the soil is mainly in this potential window. Therefore, we modeled 0–1 V has been selected for EC-PLS model establishment for three locations of soil samples. **Table 2** shows the parameters and prediction effects of the optimal EC-PLS models for three locations of soils.

From **Table 2**, the optimal EC-PLS model for the soil samples at location A has a starting potential *I*, number of potentials *N*, and number of potential intervals *G* of 0.204 V, 47, and 10, respectively, with corresponding SEP^+ and $R_{P,Ave}$ were 0.248 wt% and 0.922, respectively. The optimal EC-PLS models for the soil samples from location B corresponded to a starting potential *I*, number of potentials *N*, and number of potential intervals *G* of 0.306 V, 33, and 3, respectively. The corresponding SEP^+ and $R_{P,Ave}$ were 0.551 wt% and 0.941, respectively. The optimal EC-PLS model for the soil samples at location C had starting potentials *I*, number of potentials *N* and number of potential intervals *G* of 0.267 V, 31 and 9, respectively. Because different soils contain different components with different information potential intervals (Rasmussen et al., 2018; Liang et al., 2019), the electrochemical voltammogram analysis model differs for different types of soil organic matter.

In order to examine the effect of different information potentials on the model prediction, we fix one of the parameters while varying the remaining parameters and filter the locally optimal models based on the minimum SEP^+ values. In this case, by fixing the potential *I* and varying the remaining parameters, the locally optimal model corresponding to each starting potential *I* is filtered according to the minimum SEP^+ value. Similarly, by fixing the number of potentials *N* and varying the remaining parameters, the local optimum model corresponding to each number of potentials *N* and the corresponding combination of the remaining parameters can be filtered. The EC-PLS local optimum models corresponding to the starting potentials and

TABLE 2 | The parameters and prediction effects of the optimal EC-PLS models for three locations of soils.

Location	Potential (V)	*G*	*N*	*F*	SEP^+	SEP_{Ave}	SEP_{50}	$R_{p,Ave}$	$R_{P,SD}$
A	0.204	47	10	4	0.248	0.233	0.015	0.922	0.006
B	0.306	33	3	11	0.551	0.502	0.044	0.941	0.006
C	0.267	31	9	17	0.206	0.191	0.013	0.950	0.005

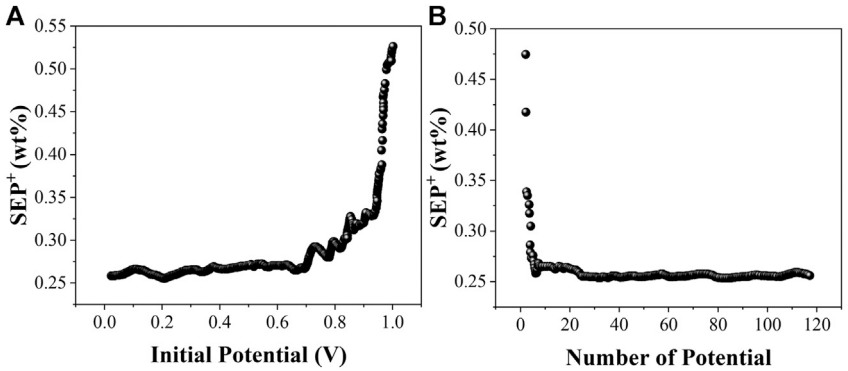

FIGURE 4 | The optimal SEP^+ corresponding to the starting potential *I* and the number of potentials *N* of the soil EC-PLS model for A location.

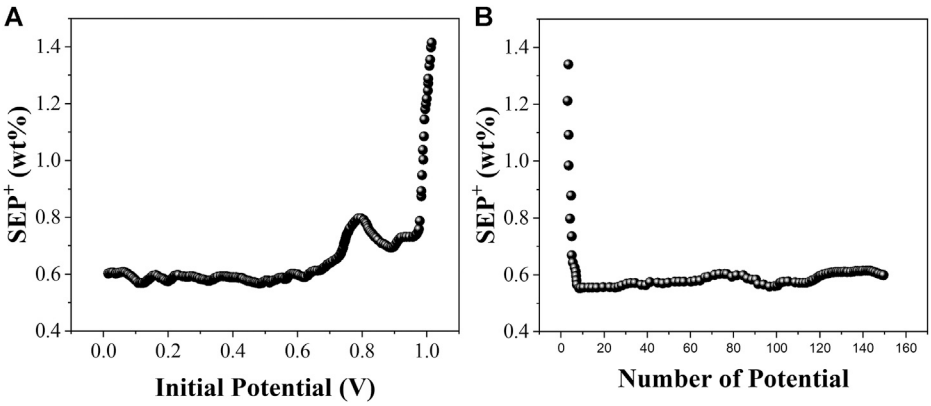

FIGURE 5 | The optimal SEP^+ corresponding to the starting potential *I* and the number of potentials *N* of the soil EC-PLS model for B location.

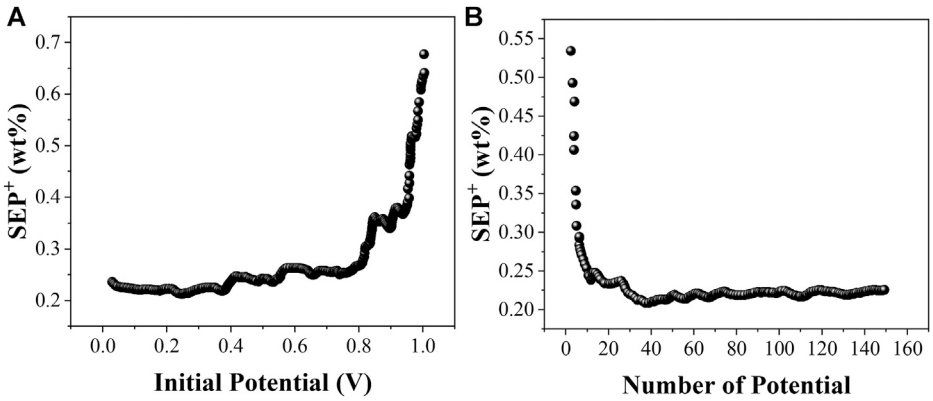

FIGURE 6 | The optimal SEP^+ corresponding to the starting potential *I* and the number of potentials *N* of the soil EC-PLS model for C location.

the number of potentials for the electrochemical analysis models of organic matter from soils at sites A, B and C are shown in **Figure 4**, **Figure 5** and **Figure 6**, respectively.

The EC-PLS local optimum model for the organic matter of site A has a starting potential *I* and a number of potentials *N* of 0.204 V and 47, respectively, and the EC-PLS local optimum

model for the organic matter of site B has a potential wavelength *I* and a number of potentials *N* of 0.306 V and 33, respectively, as seen in **Figure 4**. Based on the previous conclusions, we know that the EC-PLS model for soils with a smaller number of potentials has a much lower model complexity, which helps to improve the model prediction. Moreover, the EC-PLS wavelength models of soils at all three sites are better than the PLS wavelength models of the whole scan range.

CONCLUSION

The detection of organic matter in the soil allows us to accurately grasp the dynamics of soil fertility, which is important for improving the utilization of agricultural resources and the modern management of agriculture. In this work, we propose an alternative approach to evaluate the organic matter content of undigested/dissolved soil samples directly by using the SSEAC technique for rapid detection. Soil particles contain a variety of plant-derived organic matter molecules, some of which are capable of electrochemical oxidation and/or reduction reactions, such as indoles, polyphenols and quinones. The encapsulated soil particles were directly immobilized on the surface of a printed electrode with an integrated three-electrode system for highly sensitive signal acquisition. Analytical models were developed for the analysis of soil organic matter content at each of the three sites based on different modeling approaches.

DATA AVAILABILITY STATEMENT

The original contributions presented in the study are included in the article/supplementary material, further inquiries can be directed to the corresponding author.

AUTHOR CONTRIBUTIONS

JL and YS conceived of the study. YS supervised the development program. JL and TY collected materials characterization. JL, TY and JX received and curated samples and analytical records. JL and YS wrote the manuscript. All authors read and approved of the manuscript.

REFERENCES

Admassie, S., Nilsson, T. Y., and Inganäs, O. (2014). Charge Storage Properties of Biopolymer Electrodes with (Sub)tropical Lignins. *Phys. Chem. Chem. Phys.* 16, 24681–24684. doi:10.1039/c4cp03777d

Babaeian, E., Sadeghi, M., Jones, S. B., Montzka, C., Vereecken, H., and Tuller, M. (2019). Ground, Proximal, and Satellite Remote Sensing of Soil Moisture. *Rev. Geophys.* 57, 530–616. doi:10.1029/2018rg000618

Cambou, A., Cardinael, R., Kouakoua, E., Villeneuve, M., Durand, C., and Barthès, B. G. (2016). Prediction of Soil Organic Carbon Stock Using Visible and Near Infrared Reflectance Spectroscopy (VNIRS) in the Field. *Geoderma* 261, 151–159. doi:10.1016/j.geoderma.2015.07.007

Doménech-Carbó, A., Doménech-Carbó, M. T., Redondo-Marugán, J., Osete-Cortina, L., and Vivancos-Ramón, M. V. (2016). Electrochemical Characterization of Corrosion Products in Leaded Bronze Sculptures Considering Ohmic Drop Effects on Tafel Analysis. *Electroanalysis* 28, 833–845. doi:10.1002/elan.201500613

Doménech-Carbó, A., Doménech-Carbó, M. T., Peiró-Ronda, M. A., Martínez-Lázaro, I., and Barrio-Martín, J. (2012). Application of the Voltammetry of Microparticles for Dating Archaeological lead Using Polarization Curves and Electrochemical Impedance Spectroscopy. *J. Solid State. Electrochem.* 16, 2349–2356. doi:10.1007/s10008-012-1668-9

Doménech-Carbó, A., Lastras, M., Rodríguez, F., Cano, E., Piquero-Cilla, J., and Osete-Cortina, L. (2014). Monitoring Stabilizing Procedures of Archaeological Iron Using Electrochemical Impedance Spectroscopy. *J. Solid State. Electrochem.* 18, 399–409. doi:10.1007/s10008-013-2232-y

Domínguez-Garay, A., Quejigo, J. R., Dörfler, U., Schroll, R., and Esteve-Núñez, A. (2018). Bioelectroventing: an Electrochemical-assisted Bioremediation Strategy for Cleaning-up Atrazine-polluted Soils. *Microb. Biotechnol.* 11, 50–62. doi:10.1111/1751-7915.12687

Fernández, J. M., Peltre, C., Craine, J. M., and Plante, A. F. (2012). Improved Characterization of Soil Organic Matter by thermal Analysis Using CO2/H2O Evolved Gas Analysis. *Environ. Sci. Technol.* 46, 8921–8927. doi:10.1021/es301375d

Liang, C., Amelung, W., Lehmann, J., and Kästner, M. (2019). Quantitative Assessment of Microbial Necromass Contribution to Soil Organic Matter. *Glob. Change Biol.* 25, 3578–3590. doi:10.1111/gcb.14781

Liu, Y., Xie, X., Wang, M., Zhao, Q., and Pan, X. (2018). Removing the Effects of Iron Oxides from Vis-NIR Spectra for Soil Organic Matter Prediction. *Soil Sci. Soc. Am. J.* 82, 87–95. doi:10.2136/sssaj2017.07.0235

Milczarek, G. (2009). Preparation, Characterization and Electrocatalytic Properties of an Iodine|lignin-Modified Gold Electrode. *Electrochimica. Acta* 54, 3199–3205. doi:10.1016/j.electacta.2008.11.050

Mondal, S., and Subramaniam, C. (2019). Point-of-Care, Cable-Type Electrochemical Zn2+ Sensor with Ultrahigh Sensitivity and Wide Detection Range for Soil and Sweat Analysis. *ACS Sust. Chem. Eng.* 7, 14569–14579. doi:10.1021/acssuschemeng.9b02173

Muñoz-Morales, M., Braojos, M., Sáez, C., Cañizares, P., and Rodrigo, M. A. (2017). Remediation of Soils Polluted with Lindane Using Surfactant-Aided Soil Washing and Electrochemical Oxidation. *J. Hazard. Mater.* 339, 232–238. doi:10.1016/j.jhazmat.2017.06.021

Rasmussen, C., Heckman, K., Wieder, W. R., Keiluweit, M., Lawrence, C. R., Berhe, A. A., et al. (2018). Beyond clay: towards an Improved Set of Variables for Predicting Soil Organic Matter Content. *Biogeochemistry* 137, 297–306. doi:10.1007/s10533-018-0424-3

Scholz, F., and Lange, B. (1992). Abrasive Stripping Voltammetry - an Electrochemical Solid State Spectroscopy of Wide Applicability. *Trac. Trends Anal. Chem.* 11, 359–367. doi:10.1016/0165-9936(92)80025-2

Scholz, F., Nitschke, L., and Henrion, G. (1989a). A New Procedure for Fast Electrochemical Analysis of Solid Materials. *Naturwissenschaften* 76, 71–72. doi:10.1007/bf00396709

Scholz, F., Nitschke, L., Henrion, G., and Damaschun, F. (1989b). A Technique to Study the Electrochemistry of Minerals. *Naturwissenschaften* 76, 167–168. doi:10.1007/bf00366398

Scholz, F., Schröder, U., Meyer, S., Brainina, K. Z., Zakhachuk, N. F., Sobolev, N. V., et al. (1995). The Electrochemical Response of Radiation Defects of Non-conducting Materials An Electrochemical Access to Age Determinations. *J. Electroanalytical Chem.* 385, 139–142. doi:10.1016/0022-0728(94)03840-y

Sharififar, A., Singh, K., Jones, E., Ginting, F. I., and Minasny, B. (2019). Evaluating a Low-cost Portable NIR Spectrometer for the Prediction of Soil Organic and Total Carbon Using Different Calibration Models. *Soil Use Manage* 35, 607–616. doi:10.1111/sum.12537

Siewert, C., and Kučerík, J. (2015). Practical Applications of Thermogravimetry in Soil Science. *J. Therm. Anal. Calorim.* 120, 471–480. doi:10.1007/s10973-014-4256-7

Summers, D., Lewis, M., Ostendorf, B., and Chittleborough, D. (2011). Visible Near-Infrared Reflectance Spectroscopy as a Predictive Indicator of Soil Properties. *Ecol. Indicators* 11, 123–131. doi:10.1016/j.ecolind.2009.05.001

Wiesheu, A. C., Brejcha, R., Mueller, C. W., Kögel-Knabner, I., Elsner, M., Niessner, R., et al. (2018). Stable-isotope Raman Microspectroscopy for the

Analysis of Soil Organic Matter. *Anal. Bioanal. Chem.* 410, 923–931. doi:10.1007/s00216-017-0543-z

Yang, X., Ma, F., Yu, H., Zhang, X., and Chen, S. (2011). Effects of Biopretreatment of Corn stover with white-rot Fungus on Low-Temperature Pyrolysis Products. *Bioresour. Techn.* 102, 3498–3503. doi:10.1016/j.biortech.2010.11.021

Zhao, G., and Liu, G. (2018). A Portable Electrochemical System for the On-Site Detection of Heavy Metals in farmland Soil Based on Electrochemical Sensors. *IEEE Sensors J.* 18, 5645–5655. doi:10.1109/jsen.2018.2845306

Conflict of Interest: The authors declare that the research was conducted in the absence of any commercial or financial relationships that could be construed as a potential conflict of interest.

frontiers in Chemistry

ORIGINAL RESEARCH
published: 19 July 2021
doi: 10.3389/fchem.2021.721008

Label-free Electrochemical Impedance Spectroscopy Aptasensor for Ultrasensitive Detection of Lung Cancer Biomarker Carcinoembryonic Antigen

Yawei Wang[1], *Lei Chen*[2], *Tiantian Xuan*[1], *Jian Wang*[1] *and Xiuwen Wang*[1]*

[1]*Department of Medical Oncology, Qilu Hospital, Shandong University, Jinan, China,* [2]*Shandong Academy of Pharmaceutical Sciences, Jinan, China*

In this work, an integrated electrode system consisting of a graphene working electrode, a carbon counter electrode and an Ag/AgCl reference electrode was fabricated on an FR-4 glass fiber plate by a polyethylene self-adhesive mask stencil method combined with a manual screen printing technique. The integrated graphene electrode was used as the base electrode, and AuNPs were deposited on the working electrode surface by cyclic voltammetry. Then, the carcinoembryonic antigen aptamer was immobilized using the sulfhydryl self-assembly technique. The sensor uses $[Fe(CN)_6]^{3-/4-}$ as a redox probe for label free detection of carcinoembryonic antigen based on the impedance change caused by the difference in electron transfer rate before and after the binding of carcinoembryonic antigen aptamer and the target carcinoembryonic antigen. The results showed a good linear relationship when the CEA concentration is in the range of 0.2–15.0 ng/ml. The detection limit was calculated to be 0.085 ng/ml (S/N = 3).

Keywords: screen-printed carbon electrode, aptamer, carcinoembryonic antigen, EIS aptamer sensor, graphene nano-sheet

OPEN ACCESS

Edited by:
Fatemeh Karimi,
Quchan University of Advanced Technology, Iran

Reviewed by:
Somaye Cheraghi,
Shahid Bahonar University of Kerman, Iran
Vahid Arabali,
Islamic Azad University Sari Branch, Iran

***Correspondence:**
Xiuwen Wang
xiuwenwang@vtcuni.com

Specialty section:
This article was submitted to Electrochemistry, a section of the journal Frontiers in Chemistry

Received: *05 June 2021*
Accepted: *07 July 2021*
Published: *19 July 2021*

Citation:
Wang Y, Chen L, Xuan T, Wang J and Wang X (2021) Label-free Electrochemical Impedance Spectroscopy Aptasensor for Ultrasensitive Detection of Lung Cancer Biomarker Carcinoembryonic Antigen. Front. Chem. 9:721008. doi: 10.3389/fchem.2021.721008

INTRODUCTION

In the early 1990s, scientists used *in vitro* screening techniques to isolate RNA and DNA molecules that specifically bind proteins, and these screened single-stranded oligonucleotides were called aptamers (Macugen Diabetic Retinopathy Study Group, 2005; Ostroff et al., 2010). Oligonucleotides are short single-stranded nucleic acid molecules that bind selectively and with high affinity to proteins or other target molecules. Aptamers have many characteristics that antibodies do not have and are often used as recognition elements for aptamer sensors (Pavlov et al., 2004; Zayats et al., 2006).

Aptamers are easy to synthesize and easy to modify compared to other specific recognition elements. In immunoassays, antibodies need to be obtained from animals and live cells. In contrast, nucleic acid aptamers are usually screened *in vitro* using the SELEX technique (Sampson, 2003; Darmostuk et al., 2015). In general, modification of antibodies leads to their inactivation. In contrast, modification of the aptamer does not affect either the activity or the binding of the aptamer to the target molecule (Zhang et al., 2018; Farzadfard et al., 2020). Unlike antibodies, which usually bind only to their corresponding antigens, aptamers can recognize different targets such as proteins Liu et al. (2020), peptides He et al. (2021), amino acids Idili et al. (2019), antibiotics Lin et al. (2018), small

molecules Nakatsuka et al. (2018), viruses Chen et al. (2020), and even metal ions (Zhang Y. et al., 2020). The affinity of the aptamer for the target is far stronger than the binding force between the antibody and the antigen. In addition, aptamers are more stable than antibodies, which can be stored for longer periods of time at room temperature. Aptamers can regain their activity under appropriate conditions after denaturation (Belleperche and DeRosa, 2018). This feature of aptamers allows the lifespan of aptamer sensors to be extended.

Electrochemical aptasensor integrate the disciplines of biology, chemistry, physics, electronics and medicine (Karimi-Maleh et al., 2020; Kir, 2020; Ozbek et al., 2021). These disciplines support and permeate each other, which has led to the gradual development of electrochemical aptasensor (Zheng et al., 2018; Fu et al., 2019a; Zhang M. et al., 2020; Kizilgeci et al., 2020; Özkan, 2020; Karimi-Maleh et al., 2021b). Electrochemical aptamer sensor has the following advantages: fast analysis, simple operation method, good selectivity and high sensitivity. It is an analytical detection device constructed by combining an aptamer as a molecular recognition substance with electrochemical sensing (Fu et al., 2018, 2019b; Xu et al., 2020; Zheng et al., 2020). Therefore, electrochemical aptamer sensor has gradually become a research hotspot.

Currently, cancer remains the most feared disease in the world. In the early twenty-first century, prostate, lung, breast and colon cancers topped the list of deaths in the United States and Canada. In most developing countries, cancer was identified as the second leading cause of death. This led to the use of tumor markers Li et al. (2020a), Duan et al. (2021), Li et al. (2021), Wang et al. (2021), which are chemical-based substances that reflect the presence of tumors. They are not found in normal adult tissues but only in embryonic tissues Karimi-Maleh et al. (2021c), Karaman (2021), Karaman et al. (2021), or are present in tumor tissues at levels that greatly exceed those found in normal tissues (Li et al., 2020b; Vajhadin et al., 2020). Their presence or quantitative changes can reveal the nature of tumors, lend to the understanding of tumor histogenesis, cell differentiation and cell function, which can provide assistance in tumor diagnosis, classification and treatment guidance. Early diagnosis of cancer is crucial to successfully save patients' lives. Therefore, sensitive and specific methods are needed to detect them. Disease detection is achieved by measuring the levels of biomarkers in blood, urine, and other body fluids. Carcinoembryonic antigen (CEA), an acidic glycoprotein with a relative molecular mass of 180 kDa, is of great importance for the development and monitoring of lung cancer (Yang et al., 2018; Song et al., 2020). Usually, the CEA content in biological samples is very low, and the threshold value of CEA in human serum is 5.0 ng/ml. When the CEA content in serum is greater than 5.0 ng/ml, it may be a precursor of lung cancer (Gu et al., 2018; Jozghorbani et al., 2021). Therefore, the detection of CEA is particularly important. So far, fluorescence analysis Qiu et al. (2017), radioimmunoassay Abu-Bakr El-Bayoumy et al. (2018), enzyme-linked immunoassay Wu et al. (2021), electrochemiluminescence Yang et al. (2020) and other methods have been used for CEA detection. Among these methods, electrochemical methods have attracted the interest of scientists due to the advantages of low cost and easy portability.

Graphene, a two-dimensional carbon material with high electron density, dielectric properties and catalytic effects, which make it widely used in biosensors (Mohanraj et al., 2020; Özcan et al., 2020). Most electrochemical aptamer sensors require labeling of the aptamer, which is a complicated process for labeling during experiments and may affect the specific binding of the aptamer to the target (Yang et al., 2017; Alavi-Tabari et al., 2018; Butmee et al., 2020; Naderi Asrami et al., 2020; Karimi-Maleh et al., 2021a). In recent years, label free aptamer sensors have attracted the interest of scientists because of their label-free, simple operation, fast detection speed and low cost (Rizwan et al., 2018). The main detection techniques used for label free aptamer sensors are electrochemical impedance spectroscopy (EIS) and square wave voltammetry coulometry. EIS has been widely developed and applied in the field of analytical chemistry for its high sensitivity (Singh et al., 2021).

In this work, an integrated thick film graphene electrode system consisting of a graphene working electrode, a large area carbon counter electrode and an Ag/AgCl reference electrode was fabricated by a polyethylene self-adhesive mask template method combined with screen printing technique. The integrated graphene electrode was used as the base electrode, and Au nanoparticle was deposited on the surface of the graphene working electrode by cyclic voltammetry. The CEA aptamer was immobilized by the sulfhydryl self-assembly technique, and $[Fe(CN)_6]^{3-/4-}$ was used as the probe. The EIS electrochemical aptamer sensor for label free detection of CEA was constructed based on the change of mass transfer resistance at the electrode before and after the binding of $[Fe(CN)_6]^{3-/4-}$ to the CEA.

MATERIALS AND METHODS

Materials

All reagents were analytical grade and used without further purification. Carcinoembryonic antigen aptamer (CEA-aptamer) was purchased from Bioengineering Co.,Ltd. The sequence of the thiol-labeled CEA aptamer is: 5′-SH-ATACCAGCTTATTCAATT-3'. The carcinoembryonic antigen (CEA) was purchased from Shanghai Leadwave Biotechnology Co. 6-Methoxyl-1-hexanol (MCH) purchased from Sigma. Chloroauric acid ($HAuCl_4H_2O$), potassium ferricyanide ($K_4[Fe(CN)_6]\cdot 3H_2O$, potassium ferricyanide ($K_3[Fe(CN)_6]$), dipotassium hydrogen phosphate (K_2HPO_4), potassium dihydrogen phosphate (KH_2PO_4) were purchased from Sinopharm Group Chemical Reagent Beijing Co.,Ltd. Graphene ink (Sheet diameter: 1–5 μm, Content: 5.0wt%, Solvent: NMP) was purchased from Nanjing XFNANO Materials Tech Co.,Ltd. Conductive silver adhesive purchased from Shanghai Baoyin Electronic Materials Co.,Ltd. FR-4 glass fiber board was purchased from Xi'an Xidian Electric Material Co.,Ltd. 5 mM $K_3[Fe(CN)_6]$–5 mM $K_4[Fe(CN)_6]$–0.1 M PBS (pH 7.0)–1.0 M KC1 was used as the impedance detection solution.

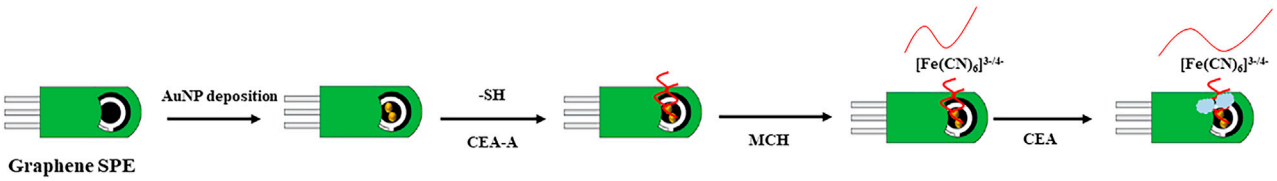

FIGURE 1 | Preparation process of the aptamer sensor and the principle of detecting CEA.

Integrated Graphene Electrode Fabrication

Take the appropriate amount of conductive graphene ink and add it to the Petri dish, scrape it well with a scraper to get a uniform sticky conductive paste. The polyethylene self-adhesive presenter board is pasted onto a cleanly treated FR-4 glass fiberboard substrate (the fiberboard was washed with ethanol and distilled water and dried at room temperature). An integrated three-electrode system containing a graphene working electrode, a carbon counter electrode and a carbon reference electrode was obtained by screen printing technique. Then 1 layer of silver paste was evenly coated at the reference electrode and the prepared integrated electrode was dried in an oven at 70°C. An appropriate amount of 0.1 M $FeCl_3$ solution was dropped on the silver surface, and the silver was oxidized to $FeCl_3$. After 1 h, the $FeCl_3$ solution was removed by rinsing with distilled water and air-dried to obtain the Ag/AgCl reference electrode. Finally, all areas except the working electrode, counter electrode, reference electrode and wire connection points were insulated with insulating tape.

Preparation of Aptamer Sensors

The preparation process of the aptamer sensor and the principle of detecting CEA was shown in **Figure 1**. Firstly, the graphene SPE need to be activated. The SPE electrode was placed in 0.1 M PBS for CV scan. The scanning potential interval is between −0.5 and 1.5 V until a stable electrochemical signal was obtained. The treated SPE was placed in 1 mM $HAuCl_4$ solution and electrodeposited by CV. CV scan was performed at a potential of −1.5–1 V to obtain Au nanoparticle modified SPE (Au/SPCE). The Au/SPE was washed with water and dried at room temperature, then 5 μL of 1 μM CEA-aptamer solution was pipetted onto the Au/SPE surface and incubated for 15 h. The working electrode was then washed with PBS buffer solution to remove the unbound aptamer to obtain CEA-A/Au/SPE. To prevent non-specific adsorption on the electrode surface, 5 μL of 20.0 nM MCH solution was coated to the electrode surface for 10 min to close the blank sites on the electrode surface. Then, the electrode surface was thoroughly washed with PBS buffer solution to remove the excess MCH solution. The aptamer sensor M/CEA-A/Au/SPE was obtained.

Electrochemical Detection

C/M/CEA-A/Au/SPE was obtained by applying 10 μL of CEA solution coated on the surface of the assembled aptamer sensor and incubating it at 37°C for 1 h. The aptamer sensor was then washed with 0.01 M $[Fe(CN)_6]$ pH 7.4 PBS solution to remove the CEA adsorbed on the electrode surface. The aptamer sensor was placed in 15 ml of 5 mM $[Fe(CN)_6]^{3-/4-}$–0.1 M PBS (pH 7.0)–0.1 M KC1 detection solution. The EIS was used for the detection. The frequency range and amplitude was 100 KHz~0.1 Hz and 5.0 mV, respectively. The impedance theoretical value was fitted with the Randles equivalent circuit to analyze the detection signal for quantitative detection of CEA.

RESULTS AND DISCUSSION

The surface morphology of SPE and Au/SPE was characterized using scanning electron microscopy, and the results are shown in **Figure 2**. **Figure 2A** shows the SPE surface is relatively flat with a flaky distribution, which is consistent with the surface morphology of graphene (Kong et al., 2014). When AuNPs were electrodeposited on the graphene electrode surface, a large number of uniform particles appeared on the electrode surface (**Figure 2B**), indicating that AuNPs were successfully deposited on the SPE surface.

Figure 3 shows the EIS of the SPE and Au/SPE with different CV cycles. It can be seen that the electron transfer resistance of $[Fe(CN)_6]^{3-/4-}$ on the SPE surface is relatively large. After the electrodeposition of AuNPs on the SPE surface, the electron transfer resistance of Au/SPE surface gradually decreases when the number of deposited cycle increases from 2 to 5, which indicates that the diffusion of $[Fe(CN)_6]^{3-/4-}$ in Au/SPE was accelerated. This is because AuNPs has high electron density and excellent dielectric properties, which promote electron transfer and increase the reversibility of redox substances on the electrode surface (Chan et al., 2016). When the number of deposition circles continues to increase, the electron transfer impedance of $[Fe(CN)_6]^{3-/4-}$ on the Au/SPE surface almost no longer changes, indicating that the amount of AuNPs deposited on the SPE surface almost reaches saturation.

We then characterized the assembly process of the aptamer sensor using EIS, as shown in **Figure 4** $[Fe(CN)_6]^{3-/4-}$ has a high electron transfer resistance at the SPE surface. When AuNPs were electrodeposited on the SPE surface, the electron transfer resistance decreased. This is because the AuNPs has excellent electrochemical properties, which accelerates the electron transfer rate of $[Fe(CN)_6]^{3-/4-}$ on the electrode surface. When CEA-A was immobilized on the electrode surface by the sulfhydryl self-assembly technique, the electron transfer of $[Fe(CN)_6]^{3-/4-}$ at the electrode surface was hindered. This is due to the fact that the aptamer is a negatively charged phosphate backbone, and $[Fe(CN)_6]^{3-/4-}$ mutually repel each other and hinder electron transfer (Yan et al., 2014). The impedance value further increases after using the sealer MCH to close the blank sites on the

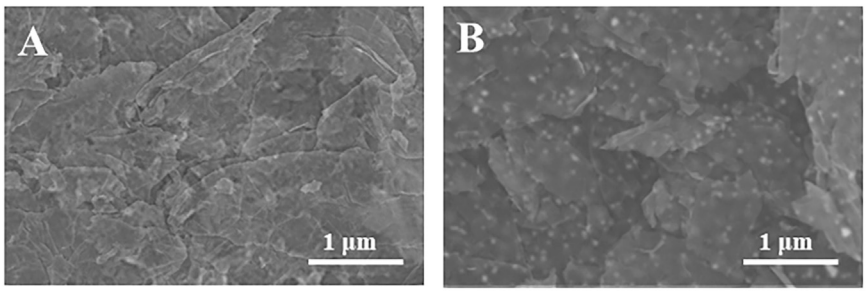

FIGURE 2 | SEM images of SPE and Au/SPE.

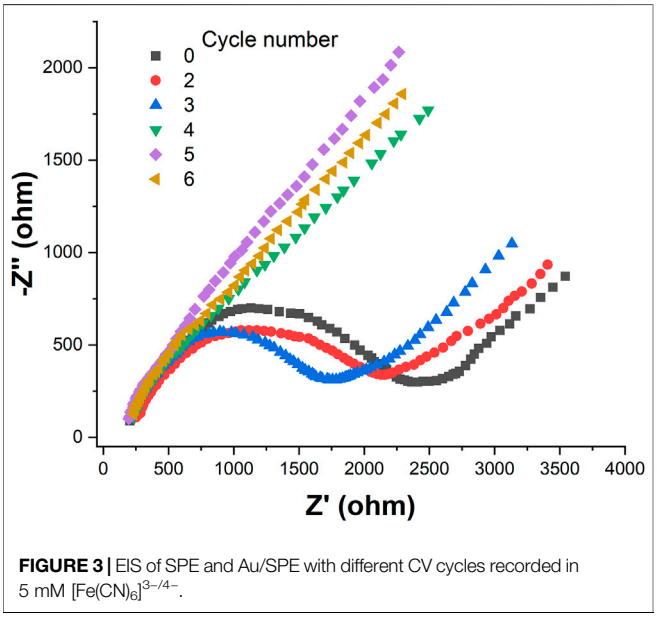

FIGURE 3 | EIS of SPE and Au/SPE with different CV cycles recorded in 5 mM $[Fe(CN)_6]^{3-/4-}$.

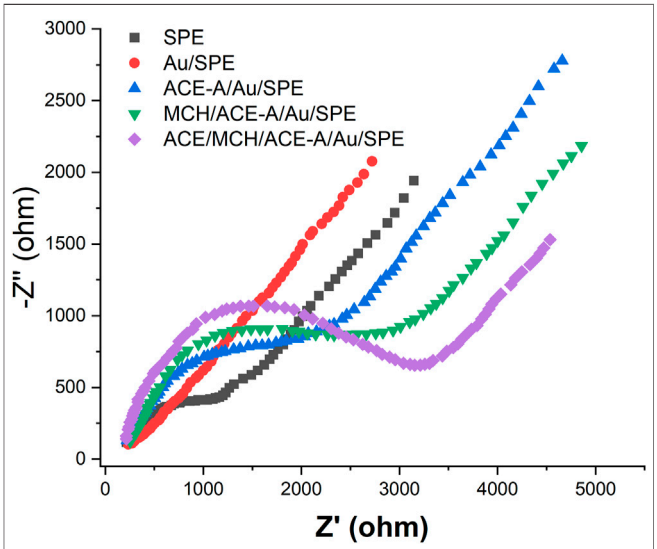

FIGURE 4 | EIS plots of aptamer senor during the fabrication recorded in 5 mM $[Fe(CN)_6]^{3-/4-}$.

electrode surface that are not occupied by the aptamer. When l ng/mL CEA was incubated on the electrode, the impedance value continued to increase because the binding of the target CEA to the aptamer increased the spatial site resistance on the electrode surface and slowed down the electron transfer rate (Huang et al., 2012).

Also, we have characterized the whole assembly process using CV (**Figure 5**). It can be seen from **Figure 5** that $[Fe(CN)_6]^{3-/4-}$ has good reversibility on the SPE. When AuNPs were electrodeposited on the SPE surface, the reversibility of $[Fe(CN)_6]^{3-/4-}$ on Au/SPE was further enhanced and the peak potential difference was significantly reduced. When the CEA-A with sulfhydryl groups self-assembled on the Au/SPE surface through Au-S bonds, the aptamer carrying a negatively charged phosphate backbone would repel the negatively charged $[Fe(CN)_6]^{3-/4-}$ and affect the electron transfer on the electrode surface, making the peak current smaller. Closure of the blank sites on the electrode surface not occupied by the aptamer with MCH formed a dense film on the electrode surface, which made the peak current further smaller. When 1 ng/ml of CEA was

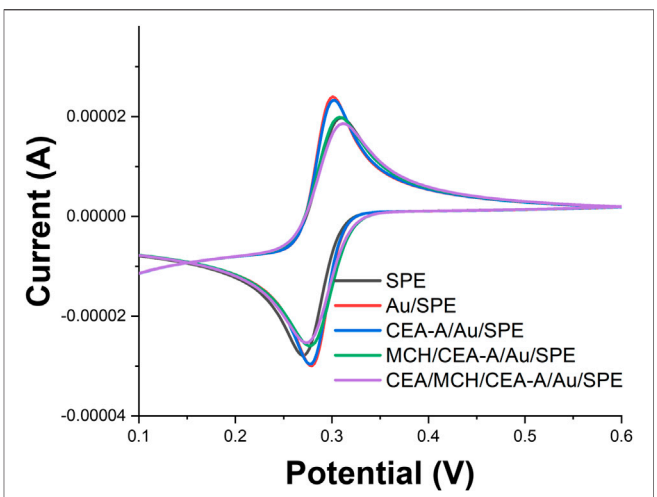

FIGURE 5 | CV profiles of aptamer senor during the fabrication recorded in 5 mM $[Fe(CN)_6]^{3-/4-}$.

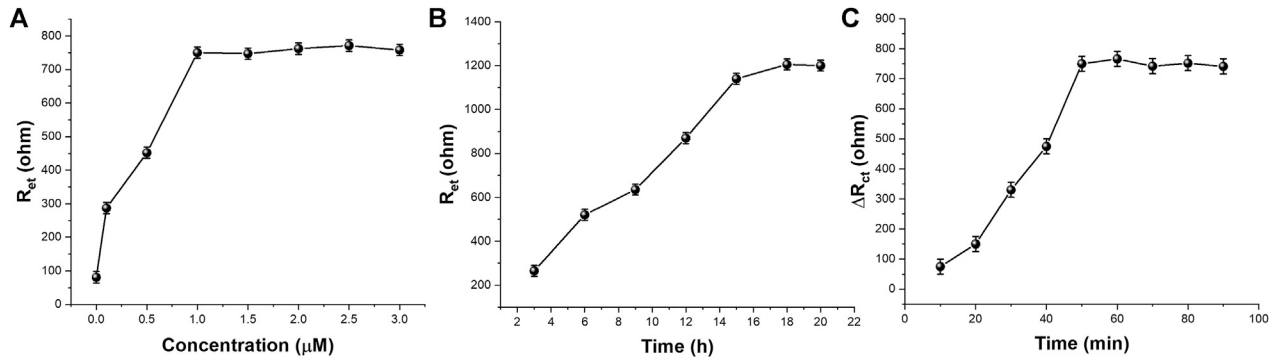

FIGURE 6 | The effect of **(A)** CEA-A concentration **(B)** immobilization time and **(C)** incubation time on the aptasensor performance (n = 3).

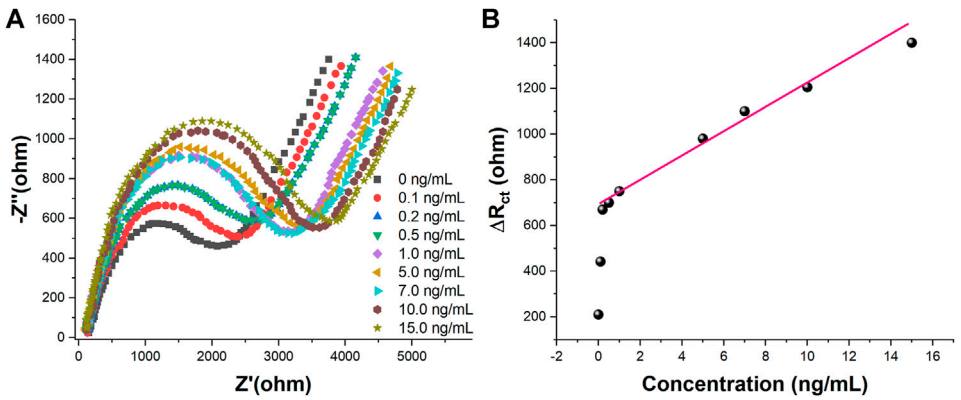

FIGURE 7 | (A) EIS in 5 mM $[Fe(CN)_6]^{3-/4-}$0.1 M PBS (pH 7.0)–1 M KCl of the proposed aptasensor towards 0, 0.1, 0.2, 0.5, 1.0, 5.0, 7.0, 10.0, and 15.0 ng/ml of CEA (B)Plots of R_{ct} vs. CEA concentration.

added, the electron transfer of $[Fe(CN)_6]^{3-/4-}$ was hindered, and the peak potential difference increased and the peak current decreased. After the addition of 10 ng/ml of CEA, the peak current continued to decrease.

The concentration of CEA-A immobilized on the surface of the electrode is an important factor affecting the performance of the sensor, so the CEA-A concentration was optimized. The relationship between the aptamer concentration of carcinoembryonic antigen and the electron transfer resistance (R_{et}) is shown in **Figure 6A**. When the aptamer concentration increased from 0.1 to 1 μM, the Ret of $[Fe(CN)_6]^{3-/4-}$ on the sensor surface also increased gradually. When the aptamer concentration continued to increase to 30 μM, the impedance value reached a plateau and almost stopped changing. This indicates that the amount of CEA-A immobilized on the sensor surface has reached saturation. Therefore, the concentration of carcinoembryonic antigen aptamer was chosen to be 1 μM in subsequent experiments.

The immobilization time of the aptamer is an important factor that affects the performance of the aptamer sensor, therefore, the immobilization time of the aptamer was optimized. **Figure 6B** shows the relationship between the change of $[Fe(CN)_6]^{3-/4-}$ in the sensor surface heart after different times of immobilization of the CEA aptamer on the electrode surface for 1 μM. As can be seen from the figure, the R_{et} of the sensor gradually increases when the immobilization time of the CEA aptamer increases from 3 to 15 h. When the immobilization time increases from 15 to 21 h, the impedance value reaches a plateau and basically stops changing, indicating that the amount of aptamer immobilization has basically reached the saturation state. Therefore, the selected aptamer immobilization time was 15 h.

The binding time between the aptamer sensor and the target CEA is also an important factor affecting the performance of the sensor, so the binding time between the sensor and CEA was investigated in this experiment. The aptamer sensor was incubated with 10 μL of 0.5 ng/ml CEA at 37°C for different times, and the experimental results were shown in **Figure 6C**. It can be seen that when the incubation time was varied between 10–60 min, a significant increase in the electron transfer resistance occurred with the increase of time. When the incubation time was between 60–70 min, there was a small decrease in R_{ct}. When incubation time excess 70 min, R_{ct} tended to be stable. This indicates that 70 min is a more reasonable time for specific binding of the aptamer to the target.

Under the optimized experimental conditions, different concentrations of CEA were measured in 5.0 mM $[Fe(CN)_6]^{3-/4-}$0.1 M PBS (pH 7.0)−1 M KCl using the proposed aptamer sensor. The experimental results were shown in **Figure 7**. **Figure 7A** shows the EIS plots of the aptamer sensor combined with different concentrations of CEA. It can be seen from **Figure 7A** that the impedance value of the aptamer sensor in the blank solution is the smallest, and the impedance value increases gradually when different concentrations of the target CEA were added. This is because CEA binds to the aptamer immobilized on the aptamer sensor, resulting in an increasing electron transfer resistance of $[Fe(CN)_6]^{3-/4-}$.**Figure 7B** shows the variation of electron transfer resistance with CEA concentration. It can be seen from the figure that there is a good linear relationship between the electrochemical aptamer sensor and CEA when the CEA concentration is in the range of 0.2–15.0 ng/ml. The detection limit is 0.085 ng/ml (S/N = 3). The selectivity study was carried out to compare the sensor's selectivity performance of 10 ng/ml of CEA against DHEA, AFP, Leptin, AA, BSA and UA. The results demonstrated high selectivity with standard deviation less than 10%.

CONCLUSION

Graphene ink was used to prepare SPE. a simple and fast unlabeled impedance-based electrochemical aptamer sensor for CEA detection was constructed by electrochemical deposition of AuNPs on the surface of SPE working electrode using cyclic voltammetry. CEA-A was immobilized on the electrode surface by the sulfhydryl self-assembly technique. After optimizations, the sensor can linear detection of CEA in the range of 0.2–15.0 ng/ml. The detection limit is 0.085 ng/ml (S/N = 3).

DATA AVAILABILITY STATEMENT

The original contributions presented in the study are included in the article/supplementary material, further inquiries can be directed to the corresponding author.

AUTHOR CONTRIBUTIONS

Author Contributions YW and XW conceived of the study. JW and SW supervised the development program, YW, LC and TX conducted the materials characterization. YW and TX received and curated samples and analytical records. YW and LC wrote the manuscript. All authors read and approved of the manuscript.

FUNDING

This work was funded by Science and Technology Development Program of Technology of Shandong Province (2014GGH218018).

REFERENCES

Abu-Bakr El-Bayoumy, A. S., Hessien Keshta, A. T., Sallam, K. M., Ebeid, N. H., Elsheikh, H. M., and Bayoumy, B. E.-S. (2018). Extraction, Purification of Prostate-specific Antigen (PSA), and Establishment of Radioimmunoassay System as a Diagnostic Tool for Prostate Disorders. *J. Immunoassay Immunochem.* 39, 12–29. doi:10.1080/15321819.2017.1392320

Alavi-Tabari, S. A. R., Khalilzadeh, M. A., and Karimi-Maleh, H. (2018). Simultaneous Determination of Doxorubicin and Dasatinib as Two Breast Anticancer Drugs Uses an Amplified Sensor With Ionic Liquid and ZnO Nanoparticle. *J. Electroanal. Chem.* 811, 84–88. doi:10.1016/j.jelechem.2018.01.034

Belleperche, M., and DeRosa, M. (2018). pH-Control in Aptamer-Based Diagnostics, Therapeutics, and Analytical Applications. *Pharmaceuticals* 11, 80. doi:10.3390/ph11030080

Butmee, P., Tumcharern, G., Thouand, G., Kalcher, K., and Samphao, A. (2020). An Ultrasensitive Immunosensor Based on Manganese Dioxide-Graphene Nanoplatelets and Core Shell Fe3O4@Au Nanoparticles for Label-Free Detection of Carcinoembryonic Antigen. *Bioelectrochemistry* 132, 107452. doi:10.1016/j.bioelechem.2019.107452

Chan, K. F., Lim, H. N., Shams, N., Jayabal, S., Pandikumar, A., and Huang, N. M. (2016). Fabrication of Graphene/gold-Modified Screen-Printed Electrode for Detection of Carcinoembryonic Antigen. *Mater. Sci. Eng. C* 58, 666–674. doi:10.1016/j.msec.2015.09.010

Chen, Z., Wu, Q., Chen, J., Ni, X., and Dai, J. (2020). A DNA Aptamer Based Method for Detection of SARS-CoV-2 Nucleocapsid Protein. *Virol. Sin.* 35, 351–354. doi:10.1007/s12250-020-00236-z

Darmostuk, M., Rimpelova, S., Gbelcova, H., and Ruml, T. (2015). Current Approaches in SELEX: An Update to Aptamer Selection Technology. *Biotechnol. Adv.* 33, 1141–1161. doi:10.1016/j.biotechadv.2015.02.008

Duan, R., Fang, X., and Wang, D. (2021). A Methylene Blue Assisted Electrochemical Sensor for Determination of Drug Resistance of *Escherichia coli*. *Front. Chem.* 9, 361. doi:10.3389/fchem.2021.689735

Farzadfard, A., Shayeh, J. S., Habibi-Rezaei, M., and Omidi, M. (2020). Modification of Reduced graphene/Au-Aptamer to Develop an Electrochemical Based Aptasensor for Measurement of Glycated Albumin. *Talanta* 211, 120722. doi:10.1016/j.talanta.2020.120722

Fu, L., Xie, K., Zheng, Y., Zhang, L., and Su, W. (2018). Graphene Ink Film Based Electrochemical Detector for Paracetamol Analysis. *Electronics* 7, 15. doi:10.3390/electronics7020015

Fu, L., Wu, M., Zheng, Y., Zhang, P., Ye, C., Zhang, H., et al. (2019a). Lycoris Species Identification and Infrageneric Relationship Investigation Via Graphene Enhanced Electrochemical Fingerprinting of Pollen. *Sens. Actuators B: Chem.* 298, 126836. doi:10.1016/j.snb.2019.126836

Fu, L., Xie, K., Wang, A., Lyu, F., Ge, J., Zhang, L., et al. (2019b). High Selective Detection of Mercury (II) Ions by Thioether Side Groups on Metal-Organic Frameworks. *Analytica Chim. Acta* 1081, 51–58. doi:10.1016/j.aca.2019.06.055

Gu, X., She, Z., Ma, T., Tian, S., and Kraatz, H.-B. (2018). Electrochemical Detection of Carcinoembryonic Antigen. *Biosens. Bioelectron.* 102, 610–616. doi:10.1016/j.bios.2017.12.014

He, Y., Zhou, L., Deng, L., Feng, Z., Cao, Z., and Yin, Y. (2021). An Electrochemical Impedimetric Sensing Platform Based on a Peptide Aptamer Identified by High-Throughput Molecular Docking for Sensitive L-Arginine Detection. *Bioelectrochemistry* 137, 107634. doi:10.1016/j.bioelechem.2020.107634

Huang, K.-J., Wu, Z.-W., Wu, Y.-Y., and Liu, Y.-M. (2012). Electrochemical Immunoassay of Carcinoembryonic Antigen Based on TiO2-Graphene/Thionine/Gold Nanoparticles Composite. *Can. J. Chem.* 90, 608–615. doi:10.1139/v2012-040

Idili, A., Gerson, J., Parolo, C., Kippin, T., and Plaxco, K. W. (2019). An Electrochemical Aptamer-Based Sensor for the Rapid and Convenient Measurement of L-Tryptophan. *Anal. Bioanal. Chem.* 411, 4629–4635. doi:10.1007/s00216-019-01645-0

Jozghorbani, M., Fathi, M., Kazemi, S. H., and Alinejadian, N. (2021). Determination of Carcinoembryonic Antigen as a Tumor Marker Using a Novel Graphene-Based Label-free Electrochemical Immunosensor. *Anal. Biochem.* 613, 114017. doi:10.1016/j.ab.2020.114017

Karaman, C., Karaman, O., Atar, N., and Yola, M. L. (2021). Electrochemical Immunosensor Development Based on Core-Shell High-Crystalline Graphitic Carbon Nitride@ Carbon Dots and Cd 0.5 Zn 0.5 S/d-Ti 3 C 2 T X MXene Composite for Heart-type Fatty Acid–Binding Protein Detection. *Microchim. Acta* 188, 1–15. doi:10.1007/s00604-021-04838-6

Karaman, C. (2021). Orange Peel Derived-Nitrogen and Sulfur Co-doped Carbon Dots: a Nano-booster for Enhancing ORR Electrocatalytic Performance of 3D Graphene Networks. *Electroanalysis* 33, 1356–1369. doi:10.1002/elan.202100018

Karimi-Maleh, H., Kumar, B. G., Rajendran, S., Qin, J., Vadivel, S., Durgalakshmi, D., et al. (2020). Tuning of Metal Oxides Photocatalytic Performance Using Ag Nanoparticles Integration. *J. Mol. Liquids* 314, 113588. doi:10.1016/j.molliq.2020.113588

Karimi-Maleh, H., Alizadeh, M., Orooji, Y., Karimi, F., Baghayeri, M., Rouhi, J., et al. (2021a). Guanine-based DNA Biosensor Amplified with Pt/SWCNTs Nanocomposite as Analytical Tool for Nanomolar Determination of Daunorubicin as an Anticancer Drug: a Docking/experimental Investigation. *Ind. Eng. Chem. Res.* 60, 816–823. doi:10.1021/acs.iecr.0c04698

Karimi-Maleh, H., Orooji, Y., Karimi, F., Alizadeh, M., Baghayeri, M., Rouhi, J., et al. (2021b). A Critical Review on the Use of Potentiometric Based Biosensors for Biomarkers Detection. *Biosens. Bioelectron.*, 184, 113252. doi:10.1016/j.bios.2021.113252

Karimi-Maleh, H., Yola, M. L., Atar, N., Orooji, Y., Karimi, F., Senthil Kumar, P., et al. (2021c). A Novel Detection Method for Organophosphorus Insecticide Fenamiphos: Molecularly Imprinted Electrochemical Sensor Based on Core-Shell Co3O4@MOF-74 Nanocomposite. *J. Colloid Interf. Sci.* 592, 174–185. doi:10.1016/j.jcis.2021.02.066

Kir, H. (2020). Yield and Quality Traits of Some Silage maize Cultivars. *Fresenius Environ. Bull.* 20, 2843–2849.

Kizilgeci, F., Mokhtari, N. E. P., and Hossain, A. (2020). Growth and Physiological Traits of Five Bread Wheat (Triticum aestivumL.) Genotypes Are Influenced by Different Levels of Salinity and Drought Stress. *Fresenius Environ. Bull.* 29, 8592–8599.

Kong, F.-Y., Gu, S.-X., Li, W.-W., Chen, T.-T., Xu, Q., and Wang, W. (2014). A Paper Disk Equipped with graphene/polyaniline/Au Nanoparticles/glucose Oxidase Biocomposite Modified Screen-Printed Electrode: Toward Whole Blood Glucose Determination. *Biosens. Bioelectron.* 56, 77–82. doi:10.1016/j.bios.2013.12.067

Li, W., Yang, Y., Ma, C., Song, Y., Qiao, X., and Hong, C. (2020a). A sandwich-type Electrochemical Immunosensor for Ultrasensitive Detection of Multiple Tumor Markers Using an Electrical Signal Difference Strategy. *Talanta* 219, 121322. doi:10.1016/j.talanta.2020.121322

Li, W., Yang, Y., Ma, C., Song, Y., Qiao, X., and Hong, C. (2020b). Electrochemical Sensor for a Photoassisted Heterogeneous Fenton Self-Oxidation Signal Amplification Strategy. *Sens. Actuators B: Chem.* 324, 128772. doi:10.1016/j.snb.2020.128772

Li, J., Zhang, S., Zhang, L., Zhang, Y., Zhang, H., Zhang, C., et al. (2021). A Novel Graphene-Based Nanomaterial Modified Electrochemical Sensor for the Detection of Cardiac Troponin I. *Front. Chem.* 9, 339. doi:10.3389/fchem.2021.680593

Lin, B., Yu, Y., Cao, Y., Guo, M., Zhu, D., Dai, J., et al. (2018). Point-of-care Testing for Streptomycin Based on Aptamer Recognizing and Digital Image Colorimetry by Smartphone. *Biosens. Bioelectron.* 100, 482–489. doi:10.1016/j.bios.2017.09.028

Liu, M., Wang, J., Chang, Y., Zhang, Q., Chang, D., Hui, C. Y., et al. (2020). *In Vitro* selection of a DNA Aptamer Targeting Degraded Protein Fragments for Biosensing. *Angew. Chem. Int. Ed.* 59, 7706–7710. doi:10.1002/anie.202000025

Macugen Diabetic Retinopathy Study Group (2005). A Phase II Randomized Double-Masked Trial of Pegaptanib, an Anti–vascular Endothelial Growth Factor Aptamer, for Diabetic Macular Edema. *Ophthalmology* 112, 1747–1757. doi:10.1016/j.ophtha.2005.06.007

Mohanraj, J., Durgalakshmi, D., Rakkesh, R. A., Balakumar, S., Rajendran, S., and Karimi-Maleh, H. (2020). Facile Synthesis of Paper Based Graphene Electrodes for point of Care Devices: a Double Stranded DNA (dsDNA) Biosensor. *J. Colloid Interf. Sci.* 566, 463–472. doi:10.1016/j.jcis.2020.01.089

Naderi Asrami, P., Aberoomand Azar, P., Saber Tehrani, M., and Mozaffari, S. A. (2020). Glucose Oxidase/nano-ZnO/thin Film deposit FTO as an Innovative Clinical Transducer: a Sensitive Glucose Biosensor. *Front. Chem.* 8, 503. doi:10.3389/fchem.2020.00503

Nakatsuka, N., Cao, H. H., Deshayes, S., Melkonian, A. L., Kasko, A. M., Weiss, P. S., et al. (2018). Aptamer Recognition of Multiplexed Small-Molecule-Functionalized Substrates. *ACS Appl. Mater. Inter.* 10, 23490–23500. doi:10.1021/acsami.8b02837

Ostroff, R. M., Bigbee, W. L., Franklin, W., Gold, L., Mehan, M., Miller, Y. E., et al. (2010). Unlocking Biomarker Discovery: Large Scale Application of Aptamer Proteomic Technology for Early Detection of Lung Cancer. *PLoS One* 5, e15003. doi:10.1371/journal.pone.0015003

Ozbek, O., Gokdogan, O., and Baran, M. F. (2021). Investigation on Energy Use Efficiency and Greenhouse Gas Emissions (GHG) of Onion Cultivation. *Fresenius Environ. Bull.* 30, 1125–1133.

Özcan, N., Karaman, C., Atar, N., Karaman, O., and Yola, M. L. (2020). A Novel Molecularly Imprinting Biosensor Including Graphene Quantum Dots/multi-Walled Carbon Nanotubes Composite for Interleukin-6 Detection and Electrochemical Biosensor Validation. *ECS J. Solid State. Sci. Technol.* 9, 121010. doi:10.1149/2162-8777/abd149

Özkan, A. (2020). Effect of Gold Nanoparticle Functionalized Multi-Walled Carbon Nanotubes on the Properties of Na-Bentonite Water Based Drilling Fluid. *Fresenius Environ. Bull.* 29, 143–151.

Pavlov, V., Xiao, Y., Shlyahovsky, B., and Willner, I. (2004). Aptamer-functionalized Au Nanoparticles for the Amplified Optical Detection of Thrombin. *J. Am. Chem. Soc.* 126, 11768–11769. doi:10.1021/ja046970u

Qiu, Z., Shu, J., and Tang, D. (2017). Bioresponsive Release System for Visual Fluorescence Detection of Carcinoembryonic Antigen from Mesoporous Silica Nanocontainers Mediated Optical Color on Quantum Dot-Enzyme-Impregnated Paper. *Anal. Chem.* 89, 5152–5160. doi:10.1021/acs.analchem.7b00989

Rizwan, M., Elma, S., Lim, S. A., and Ahmed, M. U. (2018). AuNPs/CNOs/SWCNTs/chitosan-nanocomposite Modified Electrochemical Sensor for the Label-free Detection of Carcinoembryonic Antigen. *Biosens. Bioelectron.* 107, 211–217. doi:10.1016/j.bios.2018.02.037

Sampson, T. (2003). Aptamers and SELEX: the Technology. *World Patent Inf.* 25, 123–129. doi:10.1016/s0172-2190(03)00035-8

Singh, P., Katkar, P. K., Patil, U. M., and Bohara, R. A. (2021). A Robust Electrochemical Immunosensor Based on Core-Shell Nanostructured Silica-Coated Silver for Cancer (Carcinoembryonic-Antigen-CEA) Diagnosis. *RSC Adv.* 11, 10130–10143. doi:10.1039/d0ra09015h

Song, Y., Li, W., Ma, C., Sun, Y., Qiao, J., Li, H., et al. (2020). First Use of Inorganic Copper Silicate-Transduced Enzyme-free Electrochemical Immunosensor for Carcinoembryonic Antigen Detection. *Sens. Actuators B: Chem.* 319, 128311. doi:10.1016/j.snb.2020.128311

Vajhadin, F., Ahadian, S., Travas-Sejdic, J., Lee, J., Mazloum-Ardakani, M., Salvador, J., et al. (2020). Electrochemical Cytosensors for Detection of Breast Cancer Cells. *Biosens. Bioelectron.* 151, 111984. doi:10.1016/j.bios.2019.111984

Wang, N., Wang, J., Zhao, X., Chen, H., Xu, H., Bai, L., et al. (2021). Highly Sensitive Electrochemical Immunosensor for the Simultaneous Detection of Multiple Tumor Markers for Signal Amplification. *Talanta* 226, 122133. doi:10.1016/j.talanta.2021.122133

Wu, Z., Lu, J., Fu, Q., Sheng, L., Liu, B., Wang, C., et al. (2021). A Smartphone-Based Enzyme-Linked Immunochromatographic Sensor for Rapid Quantitative Detection of Carcinoembryonic Antigen. *Sens. Actuators B: Chem.* 329, 129163. doi:10.1016/j.snb.2020.129163

Xu, Y., Lu, Y., Zhang, P., Wang, Y., Zheng, Y., Fu, L., et al. (2020). Infrageneric Phylogenetics Investigation of Chimonanthus Based on Electroactive Compound Profiles. *Bioelectrochemistry* 133, 107455. doi:10.1016/j.bioelechem.2020.107455

Yan, J., Yan, M., Ge, L., Ge, S., and Yu, J. (2014). An Origami Electrochemiluminescence Immunosensor Based on Gold/graphene for Specific, Sensitive point-of-care Testing of Carcinoembryonic Antigen. *Sensors Actuators B: Chem.* 193, 247–254. doi:10.1016/j.snb.2013.11.107

Yang, Y., Liu, Q., Liu, Y., Cui, J., Liu, H., Wang, P., et al. (2017). A Novel Label-free Electrochemical Immunosensor Based on Functionalized Nitrogen-Doped Graphene Quantum Dots for Carcinoembryonic Antigen Detection. *Biosens. Bioelectron.* 90, 31–38. doi:10.1016/j.bios.2016.11.029

Yang, G., Lai, Y., Xiao, Z., Tang, C., and Deng, Y. (2018). Ultrasensitive Electrochemical Immunosensor of Carcinoembryonic Antigen Based on Gold-Label Silver-Stain Signal Amplification. *Chin. Chem. Lett.* 29, 1857–1860. doi:10.1016/j.cclet.2018.11.030

Yang, Y., Hu, G.-B., Liang, W.-B., Yao, L.-Y., Huang, W., Zhang, Y.-J., et al. (2020). An AIEgen-Based 2D Ultrathin Metal-Organic Layer as an Electrochemiluminescence Platform for Ultrasensitive Biosensing of Carcinoembryonic Antigen. *Nanoscale* 12, 5932–5941. doi:10.1039/c9nr10712f

Zayats, M., Huang, Y., Gill, R., Ma, C.-a., and Willner, I. (2006). Label-free and Reagentless Aptamer-Based Sensors for Small Molecules. *J. Am. Chem. Soc.* 128, 13666–13667. doi:10.1021/ja0651456

Zhang, L., Chen, C., Fan, X., and Tang, X. (2018). Photomodulating Gene Expression by Using Caged siRNAs with Single-Aptamer Modification. *Chembiochem* 19, 1259–1263. doi:10.1002/cbic.201700623

Zhang, M., Pan, B., Wang, Y., Du, X., Fu, L., Zheng, Y., et al. (2020a). Recording the Electrochemical Profile of Pueraria Leaves for Polyphyly Analysis. *ChemistrySelect* 5, 5035–5040. doi:10.1002/slct.202001100

Zhang, Y., Li, C.-W., Zhou, L., Chen, Z., and Yi, C. (2020b). "Plug and Play" Logic Gate Construction Based on Chemically Triggered Fluorescence Switching of Gold Nanoparticles Conjugated with Cy3-Tagged Aptamer. *Microchim. Acta* 187, 1–11. doi:10.1007/s00604-020-04421-5

Zheng, Y., Zhang, H., and Fu, L. (2018). Preparation Gold Nanoparticles Using Herb Leaf Extract for Electro-Oxidation Determination of Ascorbic Acid. *Inorg. Nano-Metal Chem.* 48, 449–453. doi:10.1080/24701556.2019.1569687

Zheng, Y., Zhu, J., Fu, L., and Liu, Q. (2020). Phylogenetic Investigation of Yellow Camellias Based on Electrochemical Voltammetric Fingerprints. *Int. J. Electrochem. Sci.* 15, 9622–9630. doi:10.20964/2020.10.54

Conflict of Interest: The authors declare that the research was conducted in the absence of any commercial or financial relationships that could be construed as a potential conflict of interest.

frontiers in Chemistry

MINI REVIEW
published: 29 July 2021
doi: 10.3389/fchem.2021.723186

The Impact of Recent Developments in Electrochemical POC Sensor for Blood Sugar Care

Wei Li[1†], *Weixiang Luo*[2†], *Mengyuan Li*[3], *Liyu Chen*[4], *Liyan Chen*[2], *Hua Guan*[5] *and Mengjiao Yu*[6*]

[1]ICU of Shenzhen People's Hospital, 2nd Clinical Medical College of Jinan University, Shenzhen, China, [2]Nursing Department of Shenzhen People's Hospital, 2nd Clinical Medical College of Jinan University, Shenzhen, China, [3]Hepatological Surgery Department of Shenzhen People's Hospital, 2nd Clinical Medical College of Jinan University, Shenzhen, China, [4]Endocrinology Department of Shenzhen People's Hospital, 2nd Clinical Medical College of Jinan University, Shenzhen, China, [5]Respiratory Department of Shenzhen People's Hospital, 2nd Clinical Medical College of Jinan University, Shenzhen, China, [6]Gastroenterology Department of Shenzhen People's Hospital, 2nd Clinical Medical College of Jinan University, Shenzhen, China

Rapid glucose testing is very important in the care of diabetes. Monitoring of blood glucose is the most critical indicator of disease control in diabetic patients. The invention and popularity of electrochemical sensors have made glucose detection fast and inexpensive. The first generation of glucose sensors had limitations in terms of sensitivity and selectivity. In order to overcome these problems, scientists have used a range of new materials to produce new glucose electrochemical sensors with higher sensitivity, selectivity and lower cost. A variety of different electrochemical sensors including enzymatic electrochemical sensors and enzyme-free electrochemical sensors have been extensively investigated. We discussed the development process of electrochemical glucose sensors in this review. We focused on describing the benefits of carbon materials in nanomaterials, specially graphene for sensors. In addition, we discussed the limitations of the sensors and challenges in future research.

Keywords: enzyme-free electrochemical sensor, point of care, blood sugar care, graphene, carbon materials, enzymatic electrochemical sensor

OPEN ACCESS

Edited by:
Li Fu,
Hangzhou Dianzi University, China

Reviewed by:
Hongyan Sun,
Shenzhen Institutes of Advanced Technology, China
Yuhong Zheng,
Jiangsu Province and Chinese Academy of Sciences, China

***Correspondence:**
Mengjiao Yu
yumengjiao@sutcm.net

†These authors have contributed equally to this work

Specialty section:
This article was submitted to Electrochemistry, a section of the journal Frontiers in Chemistry

Received: *10 June 2021*
Accepted: *19 July 2021*
Published: *29 July 2021*

Citation:
Li W, Luo W, Li M, Chen L, Chen L, Guan H and Yu M (2021) The Impact of Recent Developments in Electrochemical POC Sensor for Blood Sugar Care. Front. Chem. 9:723186. doi: 10.3389/fchem.2021.723186

INTRODUCTION

Blood glucose a very important indicator in medical care due to the close relationship between the level of sugar in the blood and many diseases, such as cardiovascular disease, type II diabetes and obesity. Among them, diabetes is an important chronic disease faced by modern people (Klonoff et al., 2018; Zhu et al., 2020). It has a very high number of patients in both developed and developing countries. Since diabetes leads to metabolic disorders, there is a close link between it and many other diseases, such as kidney disease, nerve damage and heart disease (Chen et al., 2017; Pandey et al., 2017). The monitoring of blood glucose is a very important part of the diagnosis and treatment of diabetes. Therefore, how to quickly test blood glucose is a very important topic in medicine (Pleus et al., 2018).

Electrochemical sensors are the most commonly used method in glucose testing and have been successfully commercialized (Long et al., 2018; Karimi-Maleh et al., 2020; Zhang et al., 2020; Zheng et al., 2020). Electrochemical glucose sensors include enzymatic and non-enzymatic sensors. Among them, non-enzymatic electrochemical sensors are based on the direct electrochemical oxidation of glucose on the electrode surface (Hwang et al., 2018; Ding et al., 2019; Li et al., 2019; Karimi-Maleh

et al., 2021). Enzymatic electrochemical sensors are based on the specific reaction between glucose oxidase and glucose to generate a detection signal (Sehit and Altintas, 2020). For both enzymatic and non-enzymatic electrochemical sensors, the use of suitable nanomaterials in the assembly process can improve the sensitivity of the sensor (Batool et al., 2019; Fan et al., 2021).

In this review, we first discussed the differences between enzymatic and non-enzymatic sensors and compare the two technologies. Then, we introduced the current state-of-the-art in carbon nanomaterials, special graphene for glucose sensors with challenges and opportunities.

GENERATIONS OF ELECTROCHEMICAL GLUCOSE SENSORS

The glucose sensor consists of a modified electrode that selectively catalyzes the oxidation of glucose on the electrode surface and a transducer that converts the chemical signal of the reaction into an electrical signal that is displayed by an instrument (Zhang et al., 2021). Various types of glucose sensors can be constructed by applying different modified electrodes. According to the presence of glucose oxidase (GOx) in the modified electrode, glucose sensors can be divided into two categories: GOx sensors and non-enzymatic glucose (NEG) sensors.

GOx sensors are formed by immobilizing GOx on the surface of a modified electrode in combination with an electrochemical device (Baghayeri et al., 2017; Hou et al., 2018; Mano, 2019; German et al., 2020; Suzuki et al., 2020; Lipińska et al., 2021; Wu et al., 2021). The first enzyme-based modified electrode was developed by Clark and Lyons in 1962 (Clark and Lyons, 1962). The first enzyme-based modified electrode was prepared by Updike and Hicks in 1967 as an electrochemical glucose sensor for the quantitative determination of glucose in serum (Updike and Hicks, 1967). Since then, GOx sensors have been extensively studied and different types of GOx sensors have been fabricated (Chen et al., 2013). According to the different electron acceptors, there are three generations of GOx sensors.

The first generation GOx sensor uses oxygen as the electron acceptor. GOx reduces oxygen to hydrogen peroxide in the presence of glucose and determines the glucose concentration by measuring the decrease in oxygen concentration or the increase in hydrogen peroxide concentration during the reaction (Abellán-Llobregat et al., 2017; Campbell et al., 2017; Bagdžiūnas and Palinauskas, 2020). However, the first generation sensors are susceptible to the oxygen concentration in the detection environment and have poor anti-interference property (Okuda-Shimazaki et al., 2020; Walker and Dick, 2021). At a high potential level some coexisting species such as ascorbic acid and uric acids are electroactive, reducing the selectivity and accuracy of the sensors (Choi et al., 2019; Lee et al., 2019). This problem can be minimized by using a permselective membrane, reducing the access of the interferent to the surface of the sensor transducer.

The second-generation GOx sensor uses an electron transfer mediator instead of oxygen as the electron acceptor, which can overcoming the oxygen limitation of the first-generation GOx sensor (Lin et al., 2019; Yadav et al., 2019). The electron mediators are small, soluble redox-active molecules such as ferrocene derivatives, ferricyanides, conductive organic salts and quinones. These molecules can perform rapid and reversible redox reactions. They accelerate the shuttling of electrons between the active site of the enzyme and the electrode surface, increasing the rate of enzymatic reactions (Mahajan et al., 2018). However, the electron mediator can easily diffuse out of the enzyme layer into the substrate solution, which affects the stability of the sensor.

The third generation GOx sensor does not require oxygen molecules or electron transfer mediator molecules as electron acceptors compared with the previous two generations of GOx sensors (Mehmeti et al., 2017; Çakıroğlu and Özacar, 2017; Dahiya et al., 2020). They are made by immobilizing the enzyme directly on the modified electrode, so that the active site of the enzyme is in close proximity to the electrode for direct electron transfer. This can improve the sensitivity and selectivity of the glucose sensor. The materials used to immobilize the enzyme are often organic conductive composite membranes, organic conductive polymer membranes, metallic nanoparticles or non-metallic nanoparticles (Meng et al., 2018; Xie et al., 2018; Ding et al., 2019; Li et al., 2019; Wang et al., 2019; Shahhoseini et al., 2019). However, the electron transfer rate of third generation GOx sensors is still limited. GOx sensors have good selectivity and sensitivity, but there are still some problems, such as the complex immobilization process of enzymes, which is prone to deactivation and denaturation. The amount of enzymes immobilized each time cannot be accurately controlled (Liu et al., 2017; Khalaf et al., 2020). In addition, the use of enzymes is limited by external conditions such as temperature, pH and humidity (Xu et al., 2017; Parashuram et al., 2019). Therefore, the development of enzyme-free glucose (NEG) sensors is particularly important. Moreover, the biosensor performance also depends on the enzymatic layer thickness with high layer thickness resulting in signal dampening or loss.

The modified electrode surface of NEG does not contain GOx. Depending on the electrochemical detection method, NEG electrochemical sensors can be divided into three categories: potentiometric, voltammetric, and current sensors (Yang et al., 2017; Zheng et al., 2018).

NOBEL METAL-MODIFIED GLUCOSE SENSOR

Several metals, especially noble metals, have been studied as a base material for the electrodes of non-enzymatic glucose sensors. As a result, a deeper understanding of the glucose direct oxidation mechanism was achieved, showing that the mechanism depends directly on the metallic catalyst used in the electrode (Zhong et al., 2017; Wang et al., 2019). Moreover, advances in material science led to the development of several metal alloys and hybrid materials, allowing for improved properties when compared to noble metals and metal oxides alone.

Pt metal is one of the earliest and most widely used electrode materials in glucose sensor because of its good catalytic activity for the oxidation of many compounds, especially glucose. However, Cl^- and other interferences in the solution can strongly adsorb on the Pt electrode surface, occupying the active site and reducing the catalytic activity, which seriously hinders the application of Pt in glucose sensors.

Au electrode is very active in the catalytic oxidation of glucose and have good biocompatibility, making them an excellent electrode material. However, the adsorption of Au electrodes to glucose is much less than that of Pt electrodes and is also susceptible to interference by Cl^-, which affects its catalytic activity and stability (Toghill and Compton, 2010).

The catalytic oxidation of glucose by Pd as an electrode has a high activity. In addition, Pd is cheaper than other noble metals. However, Pd nanoparticles are very prone to polymerization and the catalytic activity can only be maintained for a few minutes. In order to improve the stability of Pd, many modification methods have been investigated.

Metallic Ni electrodes have a very high sensitivity up to 36 6 mA mM/cm^2, while Ni electrodes are not interfered with by Cl^- and have good stability. However, many organic small molecules can be oxidized on the Ni electrode surface, resulting in poor selectivity of the metal Ni electrode for glucose and a narrow linear range for glucose detection (Fleischmann et al., 1971). To address these drawbacks of pure Ni electrodes, scientists have investigated the application of nanostructured Ni with high specific surface area and its oxidants in NEG sensors.

Metallic Cu electrodes are easy to prepare and inexpensive, which have been widely studied and used for NEG sensors in recent years. However, the strong adsorption of Cl^- on the surface of Cu electrode interferes with the detection of glucose. In addition, the electrode has a narrow detection range for glucose. Meher et al. (Meher and Rao, 2013) prepared sandwich structured CuO electrodes by homogeneous deposition under the action of microwave. This electrode has a high specific surface area and pore volume, which in turn improves the sensitivity of the sensor. The response time for the detection of glucose was only 0.7 s and the detection limit was 1 μM. Meanwhile, its stability is very good, with a sensitivity loss of only 1.3% after 1 month of use. However, it has a narrow linear range of 0–3 mM.

CARBON MATERIALS-MODIFIED GLUCOSE SENSOR

Carbon materials, including fullerenes, diamond, carbon nanotubes, graphene, and carbon nanofibers, have been widely used as electrode materials for NEG sensors due to their excellent electrical conductivity and electrochemical inertness. Among them, graphene is most widely used.

Graphene is a planar hexagonal lattice material formed by sp^2-hybridized carbon atoms connected by covalent bonds. Its unique electronic structure characteristics and physicochemical properties make it show unique advantages in electrochemical detection and electroanalysis. It can be used to prepare electrochemical sensors for bioanalysis and environmental detection with high sensitivity, good selectivity, fast current response, wide detection range and low detection limit. The high electrical conductivity of graphene and the large number of boundary points, structural defects and functional groups in its structure provide rich sites for adsorption and electrochemical reactions. This can accelerate electron transfer and enable direct electrochemical reaction and biosensing. Meanwhile, compositionally and structurally rich graphene derivatives offer the possibility to further tune their electrochemical properties. Graphene with different structural features, such as graphene nanoblankets, nanosheets, flake crystals, nanofibers, nanoribbons and quantum dots, have been successively applied to electrochemical investigations.

However, single graphene cannot meet all the requirements for electrochemical detection. The curling, agglomeration, stacking between layers and its dispersion in solvent of graphene itself limit its application in electrochemistry. Therefore, it is necessary to further improve the electrochemical properties and enhance the electrochemical effects of graphene by compounding it with other functional nanomaterials such as inorganic and organic components.

There are many electrochemical sensing methods based on graphene nanocomposites, and the most commonly used ones are electrochemical impedance method/cyclic voltammetry and chrono-current method. Among them, electrochemical impedance spectroscopy is a powerful tool to study the nature of electron transfer on the electrode surface. The Nyquist plot of the impedance spectrum consists of two parts: the semicircular part in the high frequency region corresponds to the electron transfer limitation process. The linear part in the low-frequency region corresponds to the diffusion process. The electron transfer impedance is equal to the diameter of the semicircle. The electron transfer impedance can be obtained from the size of the semicircle diameter of different modified electrodes, and thus the modification of the electrode surface and the electrical properties of different electrode modification materials. Cyclic voltammetry is used to compare the differences in peak current and peak potential between electrodes with different material modifications and different test conditions. This is combined with the scan rate, pH, and concentration of the test substance to obtain visual data for electrochemical performance analysis. The relationship between current and time can be characterized by the chrono-current method when different concentrations of the test substance are added continuously to the test electrolyte. It can obtain specific experimental data such as linear detection range, detection limit and sensitivity from the chrono-current curve.

Hossain and Slaughter (2020) proposed a hybrid glucose biosensor with high sensitivity and selectivity using both multi-walled carbon nanotubes (MWCNTs) and graphene. Chemically derived graphene and MWCNTs functionalized with carboxylic groups were synthesized using a one-step solvothermal technique to produce a suspension containing both materials. This suspension was then drop casted on a Au electrode forming a thin film onto which PtNPs were electrochemically deposited. Finally, GOx was immobilised on the nanostructured electrode and coated with Nf.

Noble metal nanoparticles (NPs) have a great specific surface area, considerable electrical conductivity and reactivity. The sufficient number of surface active sites endows them with excellent electroanalytical and electrocatalytic properties. Combining them with enzymes can act as excellent wires or electron channels to accelerate the electron exchange between the electrode and the redox protein/enzyme interface. Also, as a biocompatible material, it can provide a microenvironment similar to its nature for the immobilization of biomolecules such as proteins and enzymes. This maintains their enzymatic and electrochemical activity and allows more free orientation of protein and enzyme molecules. This can reduce the insulating nature of the protein shell or enzyme 3D structure in direct electron transfer. Immobilization of NPs on the surface of the substrate electrode is a very important step in the preparation of composite electrocatalytic systems based on NPs. Graphene can be used as a conductive carrier for the deposition of electrocatalytic NPs.

Niu et al. (Shan et al., 2010) found that the electrocatalytic activity of graphene composite with AuNPs for H_2O_2 and O_2 increased significantly and showed a wide linear response range, high sensitivity and good reproducibility. Li et al. (Zhou et al., 2010) and Ramaprabhu et al. (Baby et al., 2010) further adsorbed GOD on graphene-AuNP composite electrode to prepare glucose biosensor. The results confirmed the effective retention of bioactivity of GOD in graphene-AuNPs composites. Cyclic voltammograms showed a fast and sensitive response to glucose with typical catalytic oxidation and showed good reproducibility, low detection limits and long-term stability. This excellent property can be attributed to the synergistic effect of graphene with AuNPs and the biocompatibility of the composite. In addition, it can be attributed to the fact that AuNPs prevent the restacking of graphene layers, leading to an increased specific surface area and enhanced sensing performance.

PdNPs are efficient catalysts for chemical conversions such as C-C bond formation, hydrogenation, hydrodehydrogenation, carboxylation and oxidation. It shows excellent sensitivity and selectivity for glucose oxidation. Zhang et al. (Lu et al., 2011) prepared an enzyme-free electrochemical biosensor using graphene-PdNP hybrid material modified electrode and used it for glucose detection. Nafion-graphene was first assembled on the electrode and chemisorbed Pd^{2+}, followed by *in situ* formation of PdNPs on the electrode by reduction of Pd^{2+} by hydrazine hydrate. In alkaline medium, this graphene-PdNP hybrid modified electrode has very high electrochemical activity for the electrocatalytic oxidation of glucose. It can quantify the glucose concentration in a wide linear range of 10 μM-5 mM. The experimental results also showed that the sensor has good reproducibility and long-term stability. It exhibited high selectivity without any interference in the presence of other substances. Similarly, Jiang et al. (Zeng et al., 2011) covalently functionalized graphene with chitosan (CS) to improve its biocompatibility and hydrophilicity. They then further modified PdNPs using an *in situ* reduction method. the CS maintained its structure intact on graphene and the PdNPs were densely modified on graphene without agglomeration. A novel glucose biosensor was prepared by covalently immobilizing GOD on the obtained nanocomposite coating-modified glassy carbon electrode. Due to the synergistic effect of PdNPs and graphene, the electrode showed excellent electrocatalytic activity towards H_2O_2 and promoted a high loading of the enzyme.

Graphene compounded with metal oxide/semiconductor NPs has gained widespread attention because of its excellent electrocatalytic, electrochemical sensing and electrochemical energy conversion properties. The large surface area and high electrical conductivity of graphene itself make it an ideal two-dimensional catalyst carrier for loading metal oxide/semiconductor NPs and provides properties such as selective catalysis or sensing.

Mao et al. (2021) investigated the use of reduced graphene oxide (rGO) to increase the sensitivity and selectivity of a zinc oxide (ZnO) nanorod based biosensor. In this case, a polyethylene terephthalate (PET) substrate was used to hydrothermally synthetise the ZnO nanorods. Then, electrodeposited rGO was used to coat the ZnO/PET working electrode and AuNPs were dispersed on the surface leading to the production of ZnO/rGO/Au/PET. Finally, the GOx was physically adsorbed on the surface of the electrode leading to the fabrication of a GOx/Rgo/ZnO/Au/PET glucose biosensor with a sensitivity of 56.32 μA mM/cm^2 and a linear range from 0.1 to 12 mM.

Graphene can be synergistically optimized not only by nanocomposites with inorganic materials, but also by organic materials for modification or functionalization. They provide a novel and efficient platform for immobilizing redox enzymes, achieving direct electrochemistry, and applying to the design and preparation of third-generation electrochemical sensors. Nafion is a perfluorinated sulfonate ionomer cross-linked polymer. Due to the advantages of simple preparation, excellent electrical conductivity, high chemical stability and biocompatibility, it has been widely used as a protective and selective coating material as well as a carrier for enzyme immobilization in biosensors. Moreover, Nafion films are negatively charged and some foreign substances into AA, UA and *p*-vinylaminophen are easily excluded during detection. Chen et al. (2010) modified GCE after immobilization of GOD on graphene/Nafion films and used it as an electrochemiluminescence sensor for glucose detection. It was shown that GOD maintained good bioactivity after immobilization on the composite film. The sensor showed a linear response of 2–100 μM for glucose with a detection limit of 1 μM. Al-Sagur et al. (2017) synthesised a multifunctional conducting polyacrylic acid (PAA) hydrogel (MFH) integrated with reduced graphene oxide (rGO), vinyl substituted polyaniline (VS-PANI), and lutetium phthalocyanine (LuPc2) to create a three dimensional (3D) robust matrix for GOx immobilization and glucose measurement.

CONCLUSION AND FUTURE PERSPECTIVES

Enzymatic-based glucose biosensors seem to correspond to the ideal model for glucose biosensing. However, many challenges such as short operational lifetime, temperature, and pH range, are limiting their performance requiring the use of more advanced

materials and fabrication techniques. Contrary to enzymatic sensors, non-enzymatic glucose sensing presents higher stability, selectivity, less complex manufacturing procedures, and clinical uses.

Compounding graphene with nanomaterials is an effective way to enhance functionality, and these graphene composite based biosensors show excellent sensitivity and selectivity for glucose detection. However, the development of graphene-based materials and devices is still in its infancy, and there is a need to continue to expand the scientific research of these materials and devices in the field of electroanalysis and electrocatalysis in the future. First, novel methods should be developed for the controlled synthesis and processing of graphene. Second, because graphene in composites is highly susceptible to complex interactions with other molecules leading to agglomeration, suitable methods should also be found to control the morphology and size of other functional nanomaterials on the graphene surface. In addition, the physical and chemical properties of the graphene surface, the interactions between chemicals and biomolecules at the interface and graphene should be studied in more depth. For example, the adsorption mechanism of molecules on graphene, the orientation of biomolecules on graphene Yao the interaction between graphene and biomolecules and the mechanism of its effect on the electron transport properties of graphene These studies can provide a deeper understanding of the electrochemical properties of graphene and its composites, which can facilitate the application of graphene in glucose sensors.

AUTHOR CONTRIBUTIONS

WL and LC (4th author) collected published data. LC (5th author) and HG didi the statistic analysis. WL, WXL, and ML wrote the original manuscript. HG and MY proofread the manuscript. All authors read and approved of the manuscript.

REFERENCES

Abellán-Llobregat, A., Jeerapan, I., Bandodkar, A., Vidal, L., Canals, A., Wang, J., et al. (2017). A Stretchable and Screen-Printed Electrochemical Sensor for Glucose Determination in Human Perspiration. *Biosens. Bioelectron.* 91, 885–891. doi:10.1016/j.bios.2017.01.058

Al-Sagur, H., Komathi, S., Khan, M. A., Gurek, A. G., and Hassan, A. (2017). A Novel Glucose Sensor Using Lutetium Phthalocyanine as Redox Mediator in Reduced Graphene Oxide Conducting Polymer Multifunctional Hydrogel. *Biosens. Bioelectron.* 92, 638–645. doi:10.1016/j.bios.2016.10.038

Baby, T. T., Aravind, S. S. J., Arockiadoss, T., Rakhi, R. B., and Ramaprabhu, S. (2010). Metal Decorated Graphene Nanosheets as Immobilization Matrix for Amperometric Glucose Biosensor. *Sensors Actuators B: Chem.* 145, 71–77. doi:10.1016/j.snb.2009.11.022

Bagdžiūnas, G., and Palinauskas, D. (2020). Poly (9H-Carbazole) as a Organic Semiconductor for Enzymatic and Non-enzymatic Glucose Sensors. *Biosensors* 10, 104. doi:10.3390/bios10090104

Baghayeri, M., Veisi, H., and Ghanei-Motlagh, M. (2017). Amperometric Glucose Biosensor Based on Immobilization of Glucose Oxidase on a Magnetic Glassy Carbon Electrode Modified with a Novel Magnetic Nanocomposite. *Sensors Actuators B: Chem.* 249, 321–330. doi:10.1016/j.snb.2017.04.100

Batool, R., Rhouati, A., Nawaz, M. H., Hayat, A., and Marty, J. L. (2019). A Review of the Construction of Nano-Hybrids for Electrochemical Biosensing of Glucose. *Biosensors* 9, 46. doi:10.3390/bios9010046

Çakıroğlu, B., and Özacar, M. (2017). Tannic Acid Modified Electrochemical Biosensor for Glucose Sensing Based on Direct Electrochemistry. *Electroanalysis* 29, 2719–2726. doi:10.1002/elan.201700420

Campbell, A. S., Islam, M. F., and Russell, A. J. (2017). Intramolecular Electron Transfer through Poly-Ferrocenyl Glucose Oxidase Conjugates to Carbon Electrodes: 1. Sensor Sensitivity, Selectivity and Longevity. *Electrochimica Acta* 248, 578–584. doi:10.1016/j.electacta.2017.07.150

Chen, C., Xie, Q., Yang, D., Xiao, H., Fu, Y., Tan, Y., et al. (2013). Recent Advances in Electrochemical Glucose Biosensors: a Review. *RSC Adv.* 3, 4473–4491. doi:10.1039/c2ra22351a

Chen, X., Ye, H., Wang, W., Qiu, B., Lin, Z., and Chen, G. (2010). Electrochemiluminescence Biosensor for Glucose Based on Graphene/nafion/GOD Film Modified Glassy Carbon Electrode. *Electroanalysis* 22, 2347–2352. doi:10.1002/elan.201000095

Chen, Y., Lu, S., Zhang, S., Li, Y., Qu, Z., Chen, Y., et al. (2017). Skin-like Biosensor System via Electrochemical Channels for Noninvasive Blood Glucose Monitoring. *Sci. Adv.* 3, e1701629. doi:10.1126/sciadv.1701629

Choi, Y.-B., Kim, H.-S., Jeon, W.-Y., Lee, B.-H., Shin, U. S., and Kim, H.-H. (2019). The Electrochemical Glucose Sensing Based on the Chitosan-Carbon Nanotube Hybrid. *Biochem. Eng. J.* 144, 227–234. doi:10.1016/j.bej.2018.10.021

Clark, L. C., Jr, and Lyons, C. (1962). Electrode Systems for Continuous Monitoring in Cardiovascular Surgery. *Ann. N. Y. Acad. Sci.* 102, 29–45. doi:10.1111/j.1749-6632.1962.tb13623.x

Dahiya, A. S., Thireau, J., Boudaden, J., Lal, S., Gulzar, U., Zhang, Y., et al. (2020). Review-Energy Autonomous Wearable Sensors for Smart Healthcare: A Review. *J. Electrochem. Soc.* 167, 037516. doi:10.1149/2.0162003jes

Ding, L., Yan, J., Zhao, Z., and Li, D. (2019). Synthesis of NiGa2O4 Nanosheets for Non-enzymatic Glucose Electrochemical Sensor. *Sensors Actuators B: Chem.* 296, 126705. doi:10.1016/j.snb.2019.126705

Fan, B., Wang, Q., Wu, W., Zhou, Q., Li, D., Xu, Z., et al. (2021). Electrochemical Fingerprint Biosensor for Natural Indigo Dye Yielding Plants Analysis. *Biosensors* 11, 155. doi:10.3390/bios11050155

Fleischmann, M., Korinek, K., and Pletcher, D. (1971). The Oxidation of Organic Compounds at a Nickel Anode in Alkaline Solution. *J. Electroanalytical Chem. Interfacial Electrochemistry* 31, 39–49. doi:10.1016/s0022-0728(71)80040-2

German, N., Ramanaviciene, A., and Ramanavicius, A. (2020). Formation and Electrochemical Evaluation of Polyaniline and Polypyrrole Nanocomposites Based on Glucose Oxidase and Gold Nanostructures. *Polymers* 12, 3026. doi:10.3390/polym12123026

Hossain, M. F., and Slaughter, G. (2020). PtNPs Decorated Chemically Derived Graphene and Carbon Nanotubes for Sensitive and Selective Glucose Biosensing. *J. Electroanalytical Chem.* 861, 113990. doi:10.1016/j.jelechem.2020.113990

Hou, C., Zhao, D., Wang, Y., Zhang, S., and Li, S. (2018). Preparation of Magnetic Fe3O4/PPy@ZIF-8 Nanocomposite for Glucose Oxidase Immobilization and Used as Glucose Electrochemical Biosensor. *J. Electroanalytical Chem.* 822, 50–56. doi:10.1016/j.jelechem.2018.04.067

Hwang, D.-W., Lee, S., Seo, M., and Chung, T. D. (2018). Recent Advances in Electrochemical Non-enzymatic Glucose Sensors - A Review. *Analytica Chim. Acta* 1033, 1–34. doi:10.1016/j.aca.2018.05.051

Karimi-Maleh, H., Ayati, A., Davoodi, R., Tanhaei, B., Karimi, F., Malekmohammadi, S., et al. (2021). Recent Advances in Using of Chitosan-Based Adsorbents for Removal of Pharmaceutical Contaminants: A Review. *J. Clean. Prod.* 291, 125880. doi:10.1016/j.jclepro.2021.125880

Karimi-Maleh, H., Kumar, B. G., Rajendran, S., Qin, J., Vadivel, S., Durgalakshmi, D., et al. (2020). Tuning of Metal Oxides Photocatalytic Performance Using Ag Nanoparticles Integration. *J. Mol. Liquids* 314, 113588. doi:10.1016/j.molliq.2020.113588

Khalaf, N., Ahamad, T., Naushad, M., Al-hokbany, N., Al-Saeedi, S. I., Almotairi, S., et al. (2020). Chitosan Polymer Complex Derived Nanocomposite (AgNPs/NSC) for Electrochemical Non-enzymatic Glucose Sensor. *Int. J. Biol. Macromolecules* 146, 763–772. doi:10.1016/j.ijbiomac.2019.11.193

Klonoff, D. C., Parkes, J. L., Kovatchev, B. P., Kerr, D., Bevier, W. C., Brazg, R. L., et al. (2018). Investigation of the Accuracy of 18 Marketed Blood Glucose Monitors. *Dia Care* 41, 1681–1688. doi:10.2337/dc17-1960

Lee, I., Loew, N., Tsugawa, W., Ikebukuro, K., and Sode, K. (2019). Development of a Third-Generation Glucose Sensor Based on the Open Circuit Potential for Continuous Glucose Monitoring. *Biosens. Bioelectron.* 124-125, 216–223. doi:10.1016/j.bios.2018.09.099

Li, Y., Xie, M., Zhang, X., Liu, Q., Lin, D., Xu, C., et al. (2019). Co-MOF Nanosheet Array: a High-Performance Electrochemical Sensor for Non-enzymatic Glucose Detection. *Sensors Actuators B: Chem.* 278, 126–132. doi:10.1016/j.snb.2018.09.076

Lin, M.-J., Wu, C.-C., and Chang, K.-S. (2019). Effect of Poly-L-Lysine Polycation on the Glucose Oxidase/Ferricyanide Composite-Based Second-Generation Blood Glucose Sensors. *Sensors* 19, 1448. doi:10.3390/s19061448

Lipińska, W., Siuzdak, K., Karczewski, J., Dołęga, A., and Grochowska, K. (2021). Electrochemical Glucose Sensor Based on the Glucose Oxidase Entrapped in Chitosan Immobilized onto Laser-Processed Au-Ti Electrode. *Sens. Actuators B Chem.* 330, 129409. doi:10.1016/j.snb.2020.129409

Liu, G.-q., Zhong, H., Li, X.-r., Yang, K., Jia, F.-f., Cheng, Z.-p., et al. (2017). Research on Nonenzymatic Electrochemical Sensor Using HO-BiONO3 Nanocomposites for Glucose Detection. *Sensors Actuators B: Chem.* 242, 484–491. doi:10.1016/j.snb.2016.11.019

Long, W., Xie, Y., Shi, H., Ying, J., Yang, J., Huang, Y., et al. (2018). Preparation of Nitrogen-Doped Hollow Carbon Spheres for Sensitive Catechol Electrochemical Sensing. *Fullerenes, Nanotubes and Carbon Nanostructures* 26, 856–862. doi:10.1080/1536383x.2018.1512973

Lu, L.-M., Li, H.-B., Qu, F., Zhang, X.-B., Shen, G.-L., and Yu, R.-Q. (2011). *In Situ* synthesis of Palladium Nanoparticle-Graphene Nanohybrids and Their Application in Nonenzymatic Glucose Biosensors. *Biosens. Bioelectron.* 26, 3500–3504. doi:10.1016/j.bios.2011.01.033

Mahajan, A., Banik, S., Chowdhury, S. R., Roy, P. S., and Bhattacharya, S. K. (2018). Size Control Synthesis and Amperometric Sensing Activity of Palladium Nanoparticles for Glucose Detection. *Mater. Today Proc.* 5, 2049–2055. doi:10.1016/j.matpr.2017.09.200

Mano, N. (2019). Engineering Glucose Oxidase for Bioelectrochemical Applications. *Bioelectrochemistry* 128, 218–240. doi:10.1016/j.bioelechem.2019.04.015

Mao, Q., Jing, W., Zhou, F., Liu, S., Gao, W., Wei, Z., et al. (2021). Depositing Reduced Graphene Oxide on ZnO Nanorods to Improve the Performance of Enzymatic Glucose Sensors. *Mater. Sci. Semiconductor Process.* 121, 105391. doi:10.1016/j.mssp.2020.105391

Meher, S. K., and Rao, G. R. (2013). Archetypal sandwich-structured CuO for High Performance Non-enzymatic Sensing of Glucose. *Nanoscale* 5, 2089–2099. doi:10.1039/c2nr33264g

Mehmeti, E., Stanković, D. M., Chaiyo, S., Zavasnik, J., Žagar, K., and Kalcher, K. (2017). Wiring of Glucose Oxidase with Graphene Nanoribbons: an Electrochemical Third Generation Glucose Biosensor. *Microchim. Acta* 184, 1127–1134. doi:10.1007/s00604-017-2115-5

Meng, W., Wen, Y., Dai, L., He, Z., and Wang, L. (2018). A Novel Electrochemical Sensor for Glucose Detection Based on Ag@ZIF-67 Nanocomposite. *Sensors Actuators B: Chem.* 260, 852–860. doi:10.1016/j.snb.2018.01.109

Okuda-Shimazaki, J., Yoshida, H., and Sode, K. (2020). FAD Dependent Glucose Dehydrogenases - Discovery and Engineering of Representative Glucose Sensing Enzymes -. *Bioelectrochemistry* 132, 107414. doi:10.1016/j.bioelechem.2019.107414

Pandey, R., Paidi, S. K., Valdez, T. A., Zhang, C., Spegazzini, N., Dasari, R. R., et al. (2017). Noninvasive Monitoring of Blood Glucose with Raman Spectroscopy. *Acc. Chem. Res.* 50, 264–272. doi:10.1021/acs.accounts.6b00472

Parashuram, L., Sreenivasa, S., Akshatha, S., Udayakumar, V., and Sandeep kumar, S. (2019). A Non-enzymatic Electrochemical Sensor Based on ZrO2: Cu(I) Nanosphere Modified Carbon Paste Electrode for Electro-Catalytic Oxidative Detection of Glucose in Raw Citrus Aurantium Var. Sinensis. *Food Chem.* 300, 125178. doi:10.1016/j.foodchem.2019.125178

Pleus, S., Heinemann, L., and Freckmann, G. (2018). Blood Glucose Monitoring Data Should Be Reported in Detail when Studies about Efficacy of Continuous Glucose Monitoring Systems Are Published. *J. Diabetes Sci. Technol.* 12, 1061–1063. doi:10.1177/1932296817753629

Sehit, E., and Altintas, Z. (2020). Significance of Nanomaterials in Electrochemical Glucose Sensors: An Updated Review (2016-2020). *Biosens. Bioelectron.* 159, 112165. doi:10.1016/j.bios.2020.112165

Shahhoseini, L., Mohammadi, R., Ghanbari, B., and Shahrokhian, S. (2019). Ni(II) 1D-Coordination polymer/C60-Modified Glassy Carbon Electrode as a Highly Sensitive Non-enzymatic Glucose Electrochemical Sensor. *Appl. Surf. Sci.* 478, 361–372. doi:10.1016/j.apsusc.2019.01.240

Shan, C., Yang, H., Han, D., Zhang, Q., Ivaska, A., and Niu, L. (2010). Graphene/AuNPs/chitosan Nanocomposites Film for Glucose Biosensing. *Biosens. Bioelectron.* 25, 1070–1074. doi:10.1016/j.bios.2009.09.024

Suzuki, N., Lee, J., Loew, N., Takahashi-Inose, Y., Okuda-Shimazaki, J., Kojima, K., et al. (2020). Engineered Glucose Oxidase Capable of Quasi-Direct Electron Transfer after a Quick-And-Easy Modification with a Mediator. *Int. J. mol. Sci.* 21, 1137. doi:10.3390/ijms21031137

Toghill, K. E., and Compton, R. G. (2010). Electrochemical Non-enzymatic Glucose Sensors: a Perspective and an Evaluation. *Int. J. Electrochem. Sci.* 5, 1246–1301.

Updike, S. J., and Hicks, G. P. (1967). The Enzyme Electrode. *Nature* 214, 986–988. doi:10.1038/214986a0

Walker, N. L., and Dick, J. E. (2021). Oxidase-loaded Hydrogels for Versatile Potentiometric Metabolite Sensing. *Biosens. Bioelectron.* 178, 112997. doi:10.1016/j.bios.2021.112997

Wang, L., Xu, M., Xie, Y., Qian, C., Ma, W., Wang, L., et al. (2019a). Ratiometric Electrochemical Glucose Sensor Based on Electroactive Schiff Base Polymers. *Sensors Actuators B: Chem.* 285, 264–270. doi:10.1016/j.snb.2019.01.061

Wang, Y., Wang, X., Lu, W., Yuan, Q., Zheng, Y., and Yao, B. (2019b). A Thin Film Polyethylene Terephthalate (PET) Electrochemical Sensor for Detection of Glucose in Sweat. *Talanta* 198, 86–92. doi:10.1016/j.talanta.2019.01.104

Wu, M., Zhang, Q., Fang, Y., Deng, C., Zhou, F., Zhang, Y., et al. (2021). Polylysine-modified MXene Nanosheets with Highly Loaded Glucose Oxidase as cascade Nanoreactor for Glucose Decomposition and Electrochemical Sensing. *J. Colloid Interf. Sci.* 586, 20–29. doi:10.1016/j.jcis.2020.10.065

Xie, F., Cao, X., Qu, F., Asiri, A. M., and Sun, X. (2018). Cobalt Nitride Nanowire Array as an Efficient Electrochemical Sensor for Glucose and H2O2 Detection. *Sensors Actuators B: Chem.* 255, 1254–1261. doi:10.1016/j.snb.2017.08.098

Xu, M., Song, Y., Ye, Y., Gong, C., Shen, Y., Wang, L., et al. (2017). A Novel Flexible Electrochemical Glucose Sensor Based on Gold Nanoparticles/polyaniline Arrays/carbon Cloth Electrode. *Sensors Actuators B: Chem.* 252, 1187–1193. doi:10.1016/j.snb.2017.07.147

Yadav, V. D., Krishnan, R. A., Jain, R., and Dandekar, P. (2019). *In-situ* Silver Nanoparticles Formation as a Tool for Non-enzymatic Glucose Sensing: Study with an Enzyme Mimicking Salt. *Colloids Surf. A: Physicochemical Eng. Aspects* 580, 123715. doi:10.1016/j.colsurfa.2019.123715

Yang, H., Wang, Z., Li, C., and Xu, C. (2017). Nanoporous PdCu alloy as an Excellent Electrochemical Sensor for H2O2 and Glucose Detection. *J. Colloid Interf. Sci.* 491, 321–328. doi:10.1016/j.jcis.2016.12.041

Zeng, Q., Cheng, J.-S., Liu, X.-F., Bai, H.-T., and Jiang, J.-H. (2011). Palladium Nanoparticle/chitosan-Grafted Graphene Nanocomposites for Construction of a Glucose Biosensor. *Biosens. Bioelectron.* 26, 3456–3463. doi:10.1016/j.bios.2011.01.024

Zhang, L., Ren, Z., Su, Z., Liu, Y., Yang, T., Cao, M., et al. (2021). Novel Recurrent Altered Genes in Chinese Patients with Anaplastic Thyroid Cancer. *J. Clin. Endocrinol. Metab.* 106, 988–998. doi:10.1210/clinem/dgab014

Zhang, M., Pan, B., Wang, Y., Du, X., Fu, L., Zheng, Y., et al. (2020). Recording the Electrochemical Profile of Pueraria Leaves for Polyphyly Analysis. *ChemistrySelect* 5, 5035–5040. doi:10.1002/slct.202001100

Zheng, W., Wu, H., Jiang, Y., Xu, J., Li, X., Zhang, W., et al. (2018). A Molecularly-Imprinted-Electrochemical-Sensor Modified with Nano-Carbon-Dots with High Sensitivity and Selectivity for Rapid Determination of Glucose. *Anal. Biochem.* 555, 42–49. doi:10.1016/j.ab.2018.06.004

Zheng, Y., Zhu, J., Fu, L., and Liu, Q. (2020). Phylogenetic Investigation of Yellow Camellias Based on Electrochemical Voltammetric Fingerprints. *Int. J. Electrochem. Sci.* 15, 9622–9630. doi:10.20964/2020.10.54

Zhong, S.-L., Zhuang, J., Yang, D.-P., and Tang, D. (2017). Eggshell Membrane-Templated Synthesis of 3D Hierarchical Porous Au Networks for Electrochemical Nonenzymatic Glucose Sensor. *Biosens. Bioelectron.* 96, 26–32. doi:10.1016/j.bios.2017.04.038

Zhou, K., Zhu, Y., Yang, X., and Li, C. (2010). Electrocatalytic Oxidation of Glucose by the Glucose Oxidase Immobilized in Graphene-Au-Nafion Biocomposite. *Electroanalysis* 22, 259–264. doi:10.1002/elan.200900321

Zhu, L., She, Z.-G., Cheng, X., Qin, J.-J., Zhang, X.-J., Cai, J., et al. (2020). Association of Blood Glucose Control and Outcomes in Patients with COVID-19 and Pre-existing Type 2 Diabetes. *Cel Metab.* 31, 1068–1077. doi:10.1016/j.cmet.2020.04.021

Conflict of Interest: The authors declare that the research was conducted in the absence of any commercial or financial relationships that could be construed as a potential conflict of interest.

Publisher's Note: All claims expressed in this article are solely those of the authors and do not necessarily represent those of their affiliated organizations, or those of the publisher, the editors and the reviewers. Any product that may be evaluated in this article, or claim that may be made by its manufacturer, is not guaranteed or endorsed by the publisher.

frontiers in Chemistry

MINI REVIEW
published: 19 August 2021
doi: 10.3389/fchem.2021.733371

Graphene-Assisted Electrochemical Sensor for Detection of Pancreatic Cancer Markers

Zhenglei Xu[1†], Minsi Peng[1†], Zhuliang Zhang[1], Haotian Zeng[1], Ruiyue Shi[1], Xiaoxin Ma[1], Lisheng Wang[1] and Bihong Liao[2]*

[1]Department of Gastroenterology, The Second Clinical Medical College, Shenzhen People's Hospital, Jinan University, Shenzhen, China, [2]Department of Cardiology, Shenzhen People's Hospital, The Second Clinical Medical College of Jinan University, Shenzhen, China

Pancreatic cancer is a highly lethal gastrointestinal malignancy. Most patients are already in the middle to advanced stages of pancreatic cancer at the time of diagnosis and cannot be treated completely. As a single-atom planar two-dimensional crystal, graphene's unusual electronic structure, specific electronic properties and excellent electron transport capacity make it uniquely advantageous in the field of electrochemical sensing. In this mini-review, we summarize the potential application of graphene in pancreatic cancer detection. K-Ras gene, CEA and MicroRNA are important in the early diagnosis of pancreatic cancer.

Keywords: pancreatic cancer, microRNA-21, microRNA-196a, CEA, signal amplification, k-ras gene

OPEN ACCESS

Edited by:
Li Fu,
Hangzhou Dianzi University, China

Reviewed by:
Xiaopeng Wang,
Suzhou TCM Hospital Affiliated to Nanjing University of Chinese Medicine, China
Shuai Yan,
Suzhou TCM Hospital Affiliated to Nanjing University of Chinese Medicine, China

***Correspondence:**
Bihong Liao
xzllsx@hotmail.com

†These authors have contributed equally to this work

Specialty section:
This article was submitted to Electrochemistry, a section of the journal Frontiers in Chemistry

Received: *30 June 2021*
Accepted: *09 August 2021*
Published: *19 August 2021*

Citation:
Xu Z, Peng M, Zhang Z, Zeng H, Shi R, Ma X, Wang L and Liao B (2021) Graphene-Assisted Electrochemical Sensor for Detection of Pancreatic Cancer Markers. Front. Chem. 9:733371. doi: 10.3389/fchem.2021.733371

INTRODUCTION

Pancreatic cancer is a malignant tumor of the gastrointestinal tract with a high mortality rate. Currently, the diagnosis and treatment of pancreatic cancer are difficult (Neoptolemos et al., 2018). Since the clinical symptoms of early stage pancreatic cancer are not obvious, most patients are already in the middle and late stage of pancreatic cancer when they are diagnosed, and the 1-year survival rate is less than 20%. The 5-years survival rate of pancreatic cancer patients is still less than 3% with the most effective treatment methods available. The 5-years survival rate for patients with advanced pancreatic cancer is almost zero (Rawla et al., 2019). Considering the high mortality rate of pancreatic cancer, the diagnosis of pancreatic cancer at an early stage will significantly reduce the mortality rate of pancreatic cancer (Singhi et al., 2019).

A suitable tumor marker should be highly specific, sensitive and easy to detect. However, numerous clinical studies have shown that it is very difficult to find an ideal tumor marker with 100% specificity and sensitivity and whose level correlates with tumor size, stage and prognosis (Lai et al., 2018). In the clinical diagnosis, some tumor markers with high specificity and complementary tumor detection are often selected to improve the detection rate of tumors (Huang et al., 2018b). Electrochemical sensor devices are an important tool for gene structure analysis and detection. It can be used for rapid identification and detection of specific gene sequences by taking advantage of the specific complementary pairing laws between molecules (Shan and Ma, 2017; Li et al., 2021; Yan et al., 2021).

Graphene is a new type of carbon nanomaterial discovered in 2004. With its ideal flat two-dimensional structure, unique electronic, thermal, optical and mechanical properties, it has excellent prospects for high-tech applications in electronics, mechanics, medicine and aerospace. After carbon nanotubes, it is an emerging carbon nanomaterial with great theoretical and application prospects after carbon nanotubes. As a single-atom planar two-dimensional crystal, graphene's unusual electronic structure, specific electronic properties and excellent electron transport capacity make

it uniquely advantageous in the field of high-sensitivity detection (Akbari jonous et al., 2019). Graphene, on the one hand, combines the redox properties of some bioelectrically active molecules and can detect the target molecule by its redox reaction on the electrode surface and the corresponding current signal (Coroş et al., 2019; Wang et al., 2021b). On the other hand, the bipolarity of graphene can be easily monitored in resistive sensors (Krishnan et al., 2019). Graphene is thus expected to allow highly sensitive monitoring, even of individual molecules adsorbed to or leaving the surface of graphene (Thangamuthu et al., 2019).

In this mini-review, we summarize the potential application of graphene in pancreatic cancer detection. K-Ras gene, CEA and MicroRNA are important in the early diagnosis of pancreatic cancer. Therefore, this mini-review was divided into three sections. Each section first described the value of the clinical application of the analyte. Then, we described how the electrochemical sensor can achieve sensitive detection with the assistance of graphene.

Mutant K-Ras Gene Detection

A large number of studies have shown that the mutation rate of K-Ras gene in pancreatic cancer patients can reach more than 90%, and the product of K-Ras gene expression is K-Ras protein with GTPase activity (Jelski and Mroczko, 2019). The K-Ras gene expression product is K-Ras protein, which has GTPase activity. It is activated when it binds to GTP and inactivated when it binds to GDP (Satoh, 2021). K-Ras proteins are mainly located on the cell membrane. PKC phosphorylates K-Ras protein, which weakens its binding to the cell membrane and leads to a change in location (Meng et al., 2020). K-Ras proteins also act as molecular switches and play important roles in many signaling pathways (Wang et al., 2017). The 12 codon of wild-type K-Ras gene is GGT, which can be mutated to GAT, GTT and GCT. The common mutation type is mainly GAT, and the mutation rate can reach more than 52% (Wang et al., 2019). K-Ras gene mutations are a typical genetic point mutation, and mutant K-Ras genes can be detected in the early stages of pancreatic cancer. Therefore, the mutant K-Ras gene can be a landmark gene for early pancreatic cancer diagnosis (Van Sciver et al., 2018). Detection of mutations in the K-Ras gene enables early pancreatic cancer surveillance and screening. DNA electrochemical sensing electrodes are an important tool for gene structure analysis and detection (Park et al., 2017). It enables the rapid identification and detection of specific gene sequences by exploiting the specific complementary pairing pattern between DNA molecules.

Shu et al. (2020) assembled an electrochemical sensor for efficient and ultrasensitive detection of K-Ras gene fragments using exonuclease III-assisted targeting cycling and π-π stacking between graphene and nucleotide bases. Since the sensor utilized fully complementary target DNA, exonuclease III could trigger the target DNA loop, forming a short single-stranded DNA probe. At the same time, they synthesized a novel ferrocene as a probe for providing an electrochemical signal. This sensor showed an excellent K-Ras detection capability and could reach a detection limit of 20.4 fM.

Graphene quantum dots (GQDs) were used for electrochemiluminescence (ECL) detection of K-Ras genes (Zhang et al., 2020). To improve the quantum yield of GQDs, nitrogen (N-GQDs) was doped in GQDs. This can make the ECL efficiency of N-GQDs greatly improved. Deoxyribonucleic acid (DNA) was used as a ligating medium to adjust the distance between GQDs and AuNPs. DNA double-stranded hybridization was reached after 1 h incubation with the target K-Ras DNA. The assay results showed that this GQDs-based composite could be used for quantitative determination of K-Ras.

MicroRNA Detection

Recent studies have found that aberrant expression of microRNA, a highly conserved class of endogenous non-coding RNA molecules of 18–25 nucleotides in length, is also associated with pancreatic cancer (Kanno et al., 2019; Mohammadi et al., 2019). It is widely present in blood and can regulate gene expression at both transcriptional and post-transcriptional levels. When microRNAs with tumor suppressor effects are formed during the process of gene mutation, deletion, promoter methylation and other changes, their expression is down-regulated or loss of function cannot down-regulate oncogenes normally (Moutinho-Ribeiro et al., 2019; Pang et al., 2019). For example, microRNA-15a, microRNA-16 and Let-7a are down-regulated and their target oncogenes (e.g., BCL-2, RAS) were abnormally expressed, leading to malignant tumorigenesis. When microRNAs with oncogenic effects are overexpressed, they downregulate tumor suppressors or involve other unrelated genes in cell differentiation (Si et al., 2020). Overexpression of oncogenic microRNA-17, microRNA-21 and microRNA-210 downregulates tumor suppressors (e.g., TGFBR2), leading to the appearance of malignant tumors (Bartsch et al., 2018). The abnormal expression of microRNA is closely related to the occurrence, development and metastasis of pancreatic cancer, especially miR-21 is overexpressed in the blood of pancreatic cancer patients (Shen et al., 2018). Moreover, miR-21 can be used to distinguish cancerous pancreas from normal pancreas and also as an indicator of pancreatic cancer prognosis.

Kilic et al. (2015) performed the first electrochemical detection of miR-21 in cell lysates using a graphene-modified disposable pencil-graphite electrode (GME). The surface characteristics of GME were analyzed by electrochemical impedance spectroscopy (EIS) and scanning electron microscopy (SEM). The detection limit of the sensor was reduced by 2.77-fold to 2.09 μg/ml (3.12 pM) by the modification of graphene. In addition, the results of this sensor were used to analyze mir-21 in cell lysates of miR-21 positive breast cancer cell line (MCF-7) and miR-21 negative hepatocellular carcinoma cell line (HUH-7).

Shin Low et al. (2020) proposed a smartphone-based biosensing system for the detection of miR-21 in saliva. reduced graphene oxide/gold (rGO/Au) composite modified screen-printed electrodes are the main body of the sensor. miR-21 and ssDNA probes hybridize and the peak current decreases. Under optimal conditions, this sensor can sub ah between 1 pM and 0.1 mM for miR-21 detection. In addition, Zhang et al. (2014) reported a selective and sensitive biosensing prototype based on graphene nanocomposite with functionalized AuNPs for the sensing of miR-21.

CEA Detection

Carcino-embryonic antigen (CEA), which is widely present in digestive system cancers of endodermal origin, is also present in the digestive tract of normal embryos (Jing et al., 2020). CEA is one of the important markers of pancreatic cancer (Yang et al., 2019). The sensitivity of CEA for the diagnosis of pancreatic cancer is 55–78% and the specificity is 25–75% when the reference value is 2.5 ng/ml (Wang et al., 2021a). When the reference value is 5 ng/ml the sensitivity is 35–53% and the specificity is 32–80%. Currently, the main protein tumor marker for clinical detection of pancreatic cancer is CA19-9; however, CA19-9 is a sialic acid Lewis blood group antigen that may remain undetectable in Lewis-negative individuals with advanced pancreatic cancer (Rizwan et al., 2018). Compared with CA19-9, CEA does not have this problem, so CEA was selected as a serum marker for pancreatic cancer. However, as a tumor marker, the expression level of CEA increases in both upper gastrointestinal tumors and pancreatic cancer (Yue et al., 2021), and the level of CEA in some tumors is even higher than that in pancreatic cancer (Hasanzadeh et al., 2017; Karimi-Maleh et al., 2021a; Karimi-Maleh et al., 2021b; Karimi-Maleh et al., 2021c). The sensitivity and specificity of CEA alone for pancreatic cancer screening are insufficient to meet the clinical need for early pancreatic cancer screening (Wang et al., 2018). Therefore, CEA needs to be combined with pancreatic cancer-specific tumor markers (e.g., miR-21) for the diagnosis of early pancreatic cancer (Li et al., 2017).

Han et al. (2011) prepared a CEA electrochemical based on graphene and several other nanomaterials. They first modified chitosan, ferrocene, and nano-TiO_2 (CS-Fc-TiO_2) composite membranes onto GCE. Then, AuNPs and graphene nanohybrids were self-assembled onto the CS-Fc-TiO_2 composite membrane modified electrode. This combination utilizes the strong interaction between AuNPs and carcinoembryonic antibody (anti-CEA) to further immobilize anti-CEA on the modified electrode surface, resulting in a CEA immunosensor. Due to the high surface free energy, strong adsorption affinity, good adaptability and conductivity of AuNPs, they provide more binding sites and a more suitable microenvironment for the immobilization of biomolecules. The synergistic effect of graphene and AuNPs leads to high conductivity and sensitivity, with linear detection range of 0.01–80 ng/ml for CEA and detection limit of 3.4 pg/ml (S/N = 3). The sensor showed excellent selectivity for CEA by detecting some possible interferents. The relative deviations of the results for six plasma samples were less than 10% compared with those of the commonly used clinical ELISA method. The good agreement between the two methods was obtained, and the simplicity and rapidity of the electrochemical assay showed great potential for its clinical application and for the detection of low levels of protein. Liu et al. (2017) constructed an electrochemical immunosensor for the detection of CEA with a three-dimensional structure of reduced graphene oxide-gold nano (3D RGO-Au) as the substrate material and Cu_2SnZnS_4 (CZTS) as the antibody marker material, with a wide linear range of 0.5 pg/ml to 20 ng/ml and a detection limit of 0.16 pg/ml.

Zhou et al. (2015) reported a novel nucleic acid aptamer/graphene oxide (Apt/GO)-based biosensor for CEA determination by capillary electrophoresis-chemiluminescence (CE-CL). After the CEA aptamer conjugated with horseradish peroxidase (HRP) is mixed with GO, the CL is quenched because the HRP-Apt stacked on GO leads to the chemiluminescence resonance energy transfer. In the presence of CEA, HRP-Apt and CEA form an HRP-Apt-CEA complex, resulting in the separation of the complex from GO. The CL catalyzed by the HRP-Apt-CEA complex can then be detected in the absence of any CRET. the CEA content is calculated from the CL intensity, which is linearly related to the CEA concentration from 0.0654 to 6.54 ng/ml, with a detection limit of 4.8 pg/ml.

Huang et al. (2018a) developed an electrochemical nucleic acid aptamer biosensor based on lead ion (Pb^{2+})-dependent DNA enzyme-assisted signal amplification and graphene quantum dot ionic liquid-ion (GQDs-IL-NF) composite membrane for highly sensitive determination of CEA. The CEA-containing nucleic acid aptamer and the hairpin DNA of the DNAzyme chain recognize the target and form a CEA-nucleic acid aptamer complex in the presence of CEA. In the presence of Pb^{2+}, a DNAzyme-assisted signal amplification reaction was performed to produce large amounts of ssDNA. Adsorption of ssDNA onto GQDs-IL-NF-modified GCEs by π-π stacking. As a result, methylene blue-labeled substrate DNA (MB-substrate) is immobilized on the electrode and generates an electrochemical signal. Under optimal conditions, the biosensor shows a linear range of 0.5 fg/ml to 0.5 ng/ml with a detection limit of 0.34 fg/ml.

CONCLUSION

Graphene, a novel material with a monolayer, two-dimensional carbon nanostructure, has a great specific surface area and excellent electronic, chemical, and mechanical properties. It also has excellent biocompatibility, which makes it extremely useful in all bioelectrical analyses. In the detection of pancreatic cancer, graphene-based biosensors can show excellent sensitivity and selectivity for both proteins (cancer markers) and DNA, making it an ideal material for the construction of efficient, fast, and sensitive detection biosensors. However, there are still some factors affecting the application of graphene in biosensors that need further detailed study. These issues include 1) the effect of the oxygen-containing functional group fraction in graphene on its electrochemical properties; 2) how to prepare graphene with high electrical conductivity and good solution dispersion; 3) the effect of heteroatom doping on the electrochemical properties and stability of graphene; 4) the connection mode and interaction between biomolecules and graphene in sensors; 5) the biocompatibility of graphene in different biosensing applications issues. These studies related to graphene-based materials will open new directions in the field of biosensor research.

AUTHOR CONTRIBUTIONS

ZX and BL contributed to conception and design of the review. MP and ZZ collected papers. ZX and HZ organized the files. ZX, HZ, and RS wrote the first draft of the manuscript. XM and LW wrote sections of the manuscript. BL did the proofreading. All authors contributed to manuscript revision, read, and approved the submitted version.

REFERENCES

Akbari jonous, Z., Shayeh, J. S., Yazdian, F., Yadegari, A., Hashemi, M., and Omidi, M. (2019). An Electrochemical Biosensor for Prostate Cancer Biomarker Detection Using Graphene Oxide-Gold Nanostructures. *Eng. Life Sci.* 19, 206–216. doi:10.1002/elsc.201800093

Bartsch, D., Gercke, N., Strauch, K., Wieboldt, R., Matthäi, E., Wagner, V., et al. (2018). The Combination of MiRNA-196b, LCN2, and TIMP1 Is a Potential Set of Circulating Biomarkers for Screening Individuals at Risk for Familial Pancreatic Cancer. *J. Clin Med.* 7, 295. doi:10.3390/jcm7100295

Coroş, M., Pruneanu, S., and Stefan-van Staden, R.-I. (2019). Recent Progress in the Graphene-Based Electrochemical Sensors and Biosensors. *J. Electrochem. Soc.* 167, 037528.

Han, J., Zhuo, Y., Chai, Y.-Q., Mao, L., Yuan, Y.-L., and Yuan, R. (2011). Highly Conducting Gold Nanoparticles-Graphene Nanohybrid Films for Ultrasensitive Detection of Carcinoembryonic Antigen. *Talanta.* 85, 130–135. doi:10.1016/j.talanta.2011.03.036

Hasanzadeh, M., Shadjou, N., Lin, Y., and de la Guardia, M. (2017). Nanomaterials for Use in Immunosensing of Carcinoembryonic Antigen (CEA): Recent Advances. *Trac Trends Anal. Chem.* 86, 185–205. doi:10.1016/j.trac.2016.11.003

Huang, J.-Y., Zhao, L., Lei, W., Wen, W., Wang, Y.-J., Bao, T., et al. (2018a). A High-Sensitivity Electrochemical Aptasensor of Carcinoembryonic Antigen Based on Graphene Quantum Dots-Ionic Liquid-Nafion Nanomatrix and DNAzyme-Assisted Signal Amplification Strategy. *Biosens. Bioelectron.* 99, 28–33. doi:10.1016/j.bios.2017.07.036

Huang, R., He, N., and Li, Z. (2018b). Recent Progresses in DNA Nanostructure-Based Biosensors for Detection of Tumor Markers. *Biosens. Bioelectron.* 109, 27–34. doi:10.1016/j.bios.2018.02.053

Jelski, W., and Mroczko, B. (2019). Biochemical Diagnostics of Pancreatic Cancer - Present and Future. *Clinica Chim. Acta.* 498, 47–51. doi:10.1016/j.cca.2019.08.013

Jing, A., Xu, Q., Feng, W., and Liang, G. (2020). An Electrochemical Immunosensor for Sensitive Detection of the Tumor Marker Carcinoembryonic Antigen (CEA) Based on Three-Dimensional Porous Nanoplatinum/Graphene. *Micromachines.* 11, 660. doi:10.3390/mi11070660

Kanno, A., Masamune, A., Hanada, K., Kikuyama, M., and Kitano, M. (2019). Advances in Early Detection of Pancreatic Cancer. *Diagnostics.* 9, 18. doi:10.3390/diagnostics9010018

Karimi-Maleh, H., Alizadeh, M., Orooji, Y., Karimi, F., Baghayeri, M., Rouhi, J., et al. (2021a). Guanine-Based DNA Biosensor Amplified With Pt/SWCNTs Nanocomposite as Analytical Tool for Nanomolar Determination of Daunorubicin as an Anticancer Drug: A Docking/Experimental Investigation. *Ind. Eng. Chem. Res.* 60, 816–823. doi:10.1021/acs.iecr.0c04698

Karimi-Maleh, H., Ayati, A., Davoodi, R., Tanhaei, B., Karimi, F., Malekmohammadi, S., et al. (2021b). Recent Advances in Using of Chitosan-Based Adsorbents for Removal of Pharmaceutical Contaminants: A Review. *J. Clean. Prod.* 291, 125880. doi:10.1016/j.jclepro.2021.125880

Karimi-Maleh, H., Orooji, Y., Karimi, F., Alizadeh, M., Baghayeri, M., Rouhi, J., et al. (2021c). A Critical Review on the Use of Potentiometric Based Biosensors for Biomarkers Detection. *Biosens. Bioelectron.* 184, 113252. doi:10.1016/j.bios.2021.113252

Kilic, T., Erdem, A., Erac, Y., Seydibeyoglu, M. O., Okur, S., and Ozsoz, M. (2015). Electrochemical Detection of a Cancer Biomarker Mir-21 in Cell Lysates Using Graphene Modified Sensors. *Electroanalysis.* 27, 317–326. doi:10.1002/elan.201400518

Krishnan, S. K., Singh, E., Singh, P., Meyyappan, M., and Nalwa, H. S. (2019). A Review on Graphene-Based Nanocomposites for Electrochemical and Fluorescent Biosensors. *RSC Adv.* 9, 8778–8881. doi:10.1039/c8ra09577a

Lai, Y., Wang, L., Liu, Y., Yang, G., Tang, C., Deng, Y., et al. (2018). Immunosensors Based on Nanomaterials for Detection of Tumor Markers. *J. Biomed. Nanotechnol.* 14, 44–65. doi:10.1166/jbn.2018.2505

Li, W., Luo, W., Li, M., Chen, L., Chen, L., Guan, H., et al. (2021). The Impact of Recent Developments in Electrochemical Poc Sensor for Blood Sugar Care. *Front. Chem.* 9, 610. doi:10.3389/fchem.2021.723186

Li, Y., Chen, Y., Deng, D., Luo, L., He, H., and Wang, Z. (2017). Water-Dispersible Graphene/Amphiphilic Pyrene Derivative Nanocomposite: High AuNPs Loading Capacity for CEA Electrochemical Immunosensing. *Sensors Actuators B: Chem.* 248, 966–972. doi:10.1016/j.snb.2017.02.138

Liu, L., Du, R., Zhang, Y., and Yu, X. (2017). A Novel Sandwich-Type Immunosensor Based on Three-Dimensional Graphene-Au Aerogels and Quaternary Chalcogenide Nanocrystals for the Detection of Carcino Embryonic Antigen. *New J. Chem.* 41, 9008–9013. doi:10.1039/c7nj02253k

Meng, N., Glorieux, C., Zhang, Y., Liang, L., Zeng, P., Lu, W., et al. (2020). Oncogenic K-Ras Induces Mitochondrial OPA3 Expression to Promote Energy Metabolism in Pancreatic Cancer Cells. *Cancers (Basel).* 12, 65. doi:10.3390/cancers12010065

Mohammadi, H., Yammouri, G., and Amine, A. (2019). Current Advances in Electrochemical Genosensors for Detecting microRNA Cancer Markers. *Curr. Opin. Electrochemistry.* 16, 96–105. doi:10.1016/j.coelec.2019.04.030

Moutinho-Ribeiro, P., Macedo, G., and Melo, S. A. (2019). Pancreatic Cancer Diagnosis and Management: Has the Time Come to Prick the Bubble? *Front. Endocrinol.* 9, 779. doi:10.3389/fendo.2018.00779

Neoptolemos, J. P., Kleeff, J., Michl, P., Costello, E., Greenhalf, W., and Palmer, D. H. (2018). Therapeutic Developments in Pancreatic Cancer: Current and Future Perspectives. *Nat. Rev. Gastroenterol. Hepatol.* 15, 333–348. doi:10.1038/s41575-018-0005-x

Pang, Y., Wang, C., Lu, L., Wang, C., Sun, Z., and Xiao, R. (2019). Dual-SERS Biosensor for One-step Detection of microRNAs in Exosome and Residual Plasma of Blood Samples for Diagnosing Pancreatic Cancer. *Biosens. Bioelectron.* 130, 204–213. doi:10.1016/j.bios.2019.01.039

Park, J. K., Paik, W. H., Song, B. J., Ryu, J. K., Kim, M. A., Park, J. M., et al. (2017). Additional K-Ras Mutation Analysis and Plectin-1 Staining Improve the Diagnostic Accuracy of Pancreatic Solid Mass in EUS-Guided fine Needle Aspiration. *Oncotarget.* 8, 64440–64448. doi:10.18632/oncotarget.16135

Rawla, P., Sunkara, T., and Gaduputi, V. (2019). Epidemiology of Pancreatic Cancer: Global Trends, Etiology and Risk Factors. *World J. Oncol.* 10, 10–27. doi:10.14740/wjon1166

Rizwan, M., Elma, S., Lim, S. A., and Ahmed, M. U. (2018). AuNPs/CNOs/SWCNTs/Chitosan-Nanocomposite Modified Electrochemical Sensor for the Label-Free Detection of Carcinoembryonic Antigen. *Biosens. Bioelectron.* 107, 211–217. doi:10.1016/j.bios.2018.02.037

Satoh, K. (2021). Molecular Approaches Using Body Fluid for the Early Detection of Pancreatic Cancer. *Diagnostics.* 11, 375. doi:10.3390/diagnostics11020375

Shan, J., and Ma, Z. (2017). A Review on Amperometric Immunoassays for Tumor Markers Based on the Use of Hybrid Materials Consisting of Conducting Polymers and noble Metal Nanomaterials. *Microchim. Acta.* 184, 969–979. doi:10.1007/s00604-017-2146-y

Shen, Y., Li, Z., Wang, G., and Ma, N. (2018). Photocaged Nanoparticle Sensor for Sensitive MicroRNA Imaging in Living Cancer Cells With Temporal Control. *ACS Sens.* 3, 494–503. doi:10.1021/acssensors.7b00922

Shin Low, S., Pan, Y., Ji, D., Li, Y., Lu, Y., He, Y., et al. (2020). Smartphone-Based Portable Electrochemical Biosensing System for Detection of Circulating microRNA-21 in Saliva as a Proof-Of-Concept. *Sensors Actuators B: Chem.* 308, 127718. doi:10.1016/j.snb.2020.127718

Shu, Q., Liao, F., Hong, N., Cheng, L., Lin, Y., Cui, H., et al. (2020). A Novel DNA Sensor of Homogeneous Electrochemical Signal Amplification Strategy. *Microchemical J.* 156, 104777. doi:10.1016/j.microc.2020.104777

Si, Y., Xu, L., Wang, N., Zheng, J., Yang, R., and Li, J. (2020). Target MicroRNA-Responsive DNA Hydrogel-Based Surface-Enhanced Raman Scattering Sensor Arrays for microRNA-Marked Cancer Screening. *Anal. Chem.* 92, 2649–2655. doi:10.1021/acs.analchem.9b04606

Singhi, A. D., Koay, E. J., Chari, S. T., and Maitra, A. (2019). Early Detection of Pancreatic Cancer: Opportunities and Challenges. *Gastroenterology.* 156, 2024–2040. doi:10.1053/j.gastro.2019.01.259

Thangamuthu, M., Hsieh, K. Y., Kumar, P. V., and Chen, G.-Y. (2019). Graphene- and Graphene Oxide-Based Nanocomposite Platforms for Electrochemical Biosensing Applications. *Int. J. Mol Sci.* 20, 2975. doi:10.3390/ijms20122975

Van Sciver, R., Lee, M., Lee, C., Lafever, A., Svyatova, E., Kanda, K., et al. (2018). A New Strategy to Control and Eradicate "Undruggable" Oncogenic K-RAS-Driven Pancreatic Cancer: Molecular Insights and Core Principles Learned From Developmental and Evolutionary Biology. *Cancers.* 10, 142. doi:10.3390/cancers10050142

Wang, X., Liao, X., Mei, L., Zhang, M., Chen, S., Qiao, X., et al. (2021a). An Immunosensor Using Functionalized Cu2O/Pt NPs as the Signal Probe for

Rapid and Highly Sensitive CEA Detection with Colorimetry and Electrochemistry Dual Modes. *Sensors Actuators B: Chem.* 341, 130032. doi:10.1016/j.snb.2021.130032

Wang, Y., Chen, L., Xuan, T., Wang, J., and Wang, X. (2021b). Label-Free Electrochemical Impedance Spectroscopy Aptasensor for Ultrasensitive Detection of Lung Cancer Biomarker Carcinoembryonic Antigen. *Front. Chem.* 9, 569. doi:10.3389/fchem.2021.721008

Wang, X., Yang, X., Fei, M., Lifeng, Q., and Zhong, Z. (2017). The Diagnostic Value of the K-Ras Mutation Detection of Endoscopic Ultrasound-Guided fine Needle Aspiration Specimen for Pancreatic Carcinoma. *Chinj. Pancreatol.* 17, 307–310.

Wang, Y., Zhao, G., Zhang, Y., Pang, X., Cao, W., Du, B., et al. (2018). Sandwich-Type Electrochemical Immunosensor for CEA Detection Based on Ag/MoS2@ Fe3O4 and an Analogous ELISA Method with Total Internal Reflection Microscopy. *Sensors Actuators B: Chem.* 266, 561–569. doi:10.1016/j.snb.2018.03.178

Wang, Z.-Y., Ding, X.-Q., Zhu, H., Wang, R.-X., Pan, X.-R., and Tong, J.-H. (2019). KRAS Mutant Allele Fraction in Circulating Cell-Free DNA Correlates With Clinical Stage in Pancreatic Cancer Patients. *Front. Oncol.* 9, 1295. doi:10.3389/fonc.2019.01295

Yan, S., Yue, Y., Zeng, L., Su, L., Hao, M., Zhang, W., et al. (2021). Preparation of Graphene Oxide-Embedded Hydrogel as a Novel Sensor Platform for Antioxidant Activity Evaluation of Scutellaria Baicalensis. *Front. Chem.* 9, 220. doi:10.3389/fchem.2021.675346

Yang, Y., Jiang, M., Cao, K., Wu, M., Zhao, C., Li, H., et al. (2019). An Electrochemical Immunosensor for CEA Detection Based on Au-Ag/rGO@ PDA Nanocomposites as Integrated Double Signal Amplification Strategy. *Microchemical J.* 151, 104223. doi:10.1016/j.microc.2019.104223

Yue, Y., Su, L., Hao, M., Li, W., Zeng, L., and Yan, S. (2021). Evaluation of Peroxidase in Herbal Medicines Based on an Electrochemical Sensor. *Front. Chem.* 9, 479. doi:10.3389/fchem.2021.709487

Zhang, B., Wang, J., Ping, L., Zhong, Y., and Li, F. (2020). Preparation of Graphene Composite and its Application in the Detection of Tumor Markers. *Sci. Adv. Mater.* 12, 1312–1322. doi:10.1166/sam.2020.3829

Zhang, X., Wu, D., Liu, Z., Cai, S., Zhao, Y., Chen, M., et al. (2014). An Ultrasensitive Label-Free Electrochemical Biosensor for MicroRNA-21 Detection Based on a 2′-O-Methyl Modified DNAzyme and Duplex-specific Nuclease Assisted Target Recycling. *Chem. Commun.* 50, 12375–12377. doi:10.1039/C4CC05541A

Zhou, Z.-M., Feng, Z., Zhou, J., Fang, B.-Y., Qi, X.-X., Ma, Z.-Y., et al. (2015). Capillary Electrophoresis-Chemiluminescence Detection for Carcino-Embryonic Antigen Based on Aptamer/Graphene Oxide Structure. *Biosens. Bioelectron.* 64, 493–498. doi:10.1016/j.bios.2014.09.050

Conflict of Interest: The authors declare that the research was conducted in the absence of any commercial or financial relationships that could be construed as a potential conflict of interest.

Publisher's Note: All claims expressed in this article are solely those of the authors and do not necessarily represent those of their affiliated organizations, or those of the publisher, the editors and the reviewers. Any product that may be evaluated in this article, or claim that may be made by its manufacturer, is not guaranteed or endorsed by the publisher.

frontiers in Chemistry

MINI REVIEW
published: 25 August 2021
doi: 10.3389/fchem.2021.735668

Recent Development of Graphene Based Electrochemical Sensor for Detecting Hematological Malignancies-Associated Biomarkers: A Mini-Review

Shougang Wei[1], *Xiuju Chen*[2], *Xinyu Zhang*[3] *and Lei Chen*[4]*

[1]Department of Pediatrics, Yidu Central Hospital, Weifang, China, [2]Department of Public Health, Yidu Central Hospital, Weifang, China, [3]Shandong Freda Pharmaceutical Group Co., Ltd, Linshu, China, [4]Key Laboratory of Biopharmaceuticals, Engineering Laboratory of Polysaccharide Drugs, Shandong Academy of Pharmaceutical Sciences, Jinan, China

Hematologic malignancies are a group of malignant diseases of the hematologic system that seriously endanger human health, mainly involving bone marrow, blood and lymphatic tissues. However, among the available treatments for malignant hematologic diseases, low detection rates and high recurrence rates are major problems in the treatment process. The quantitative detection of hematologic malignancies-related biomarkers is the key to refine the pathological typing of the disease to implement targeted therapy and thus improve the prognosis. In recent years, bioelectrochemical methods for tumor cell and blood detection have attracted the attention of an increasing number of scientists. The development of biosensor technology, nanotechnology, probe technology, and lab-on-a-chip technology has greatly facilitated the development of bioelectrochemical studies of cells, especially for blood and cell-based assays and drug resistance differentiation. To improve the sensitivity of detection, graphene is often used in the design of electrochemical sensors. This mini-review provides an overview of the types of hematological malignancies-associated biomarkers and their detection based on graphene assisted electrochemical sensors.

Keywords: hematological malignancies, leukemia, graphene, electrochemical sesnor, DNA biosensors, label-free biosensors

OPEN ACCESS

Edited by:
Li Fu,
Hangzhou Dianzi University, China

Reviewed by:
Yuhong Zheng,
Institute of Botany, Jiangsu Province and Chinese Academy of Sciences, China
Huaiwei Zhang,
Peking University, China

***Correspondence:**
Lei Chen
chen331l@163.com

Specialty section:
This article was submitted to Electrochemistry, a section of the journal Frontiers in Chemistry

Received: *03 July 2021*
Accepted: *13 August 2021*
Published: *25 August 2021*

Citation:
Wei S, Chen X, Zhang X and Chen L (2021) Recent Development of Graphene Based Electrochemical Sensor for Detecting Hematological Malignancies-Associated Biomarkers: A Mini-Review. Front. Chem. 9:735668. doi: 10.3389/fchem.2021.735668

INTRODUCTION

Hematological malignancies are a series of blood disorders characterized by the malignant transformation of normal cells of bone marrow and extramedullary hematopoietic organs into a large number of tumor cells, which can seriously threaten human health (Chen et al., 2019; Gupta et al., 2020). They are heterogeneous diseases, mainly classified as Leukemia, Lymphoma and Multiple myeloma, and include more than 30 different subtypes. These subtypes differ greatly in terms of etiology, clinical manifestations, diagnosis and treatment, and prognosis. Therefore, a refined stratified diagnosis of the disease is needed to implement targeted therapy and thus improve the prognosis (Fracchiolla et al., 2013; Hianik, 2021; Luo et al., 2021; Zhang et al., 2021). Currently, the clinical diagnosis of hematologic tumors relies on imaging, including X-ray, computed tomography, magnetic resonance imaging, endoscopy, and ultrasound. Although clinical imaging

TABLE 1 | Currently used hematologic tumor-related biomarkers.

Hematological malignancies	Subtype	DNA	miRNA	Protein	Cell
Lymphoma	NHL	C-myc, Bcl-, Bcl-6, Bcl-11, P53, P16, B2M, PTPN1, TNFAIP3	miR-21, miR-155	C-myc, Bax, Bcl2, CD3/4/7/8/20/22/45	Ramos
	HL	B2M, PTPN11, TNFAIP3	-	CD30/68/80	R-S
Leukemia	AML	PML/RARα, AML1-ETO, CBFβ-MYH11	miR-181a, miR-15	CD33	HL-60/K562
	ALL	FLT3, PRAME, NPM1, C-KIT, CEBPA	miR-128/181/204/218/221/331	CD10, CD19	CCRF-CEM
	CML	P185BCR/ABL, TEL/AML1, E2A/PBX1, MLL/AF4	miR-217/221/222 miR-17-92	ABL	K562
	CLL	PRAME/BCR/ABL, ASS	miR-15/16/29/181	CD52	CLL
Multiple myeloma	-	KRAS, NRA, BRAF, TRAF3, CYLD, LTB, TP53, ATM, ATR	miR-21/32/93/133 miR-206/221/222, miR-17-92	CD30/38, M protein, CRP, LDH	MM

techniques can "locate and diagnose" tumors, they have low sensitivity and limited ability to differentiate between benign and malignant lesions (Baldo et al., 2016; Hasanzadeh et al., 2017; Karimi-Maleh et al., 2021). However, these methods have certain limitations: for example, high cost, low sensitivity, long detection period, expensive, complicated detection methods, and some detection methods even have radioactive contamination. Compared with these methods, bioelectrochemical methods have the advantages of simplicity, high sensitivity and low cost. It can be easily implemented for quantitative determination and clinical application of blood samples (Miao et al., 2019; Rasheed et al., 2020; Li et al., 2021; Liu et al., 2021).

With the rapid development of modern biomedical technologies such as molecular biology and genomics, people have gained a deeper understanding of the pathogenesis of hematologic tumors and have discovered a variety of tumor biomarkers related to hematologic tumors. Information about the currently used hematologic tumor-related biomarkers is shown in **Table 1**.

The introduction of nanomaterials in electrochemical analysis increases the conductivity and surface area of electrodes, thus improves the catalytic activity. These properties can improve the sensor detection sensitivity, shorten the response time, and realize the real-time monitoring of the detector (Gurudatt et al., 2019; Hrichi et al., 2019). Nanomaterials are modified onto the surface of electrochemical sensors to capture biomolecules and improve the immobilization efficiency and the sensitivity of the sensors. In addition, nanomaterials can be used as markers to label and can maintain the biological activity of biomolecules and their corresponding components.

Graphene, with its unique physical and chemical properties, is widely used in electrochemical analysis and has become a research hotspot for electrochemical sensors. For example, Ji et al. (2014) used graphene as a sensor interface to capture more antibodies and thus amplify the detection signal. The good performance of the sensor is mainly attributed to the high specific surface area of graphene. The strong adsorption property can immobilize more biomolecules. Its good electrical conductivity improves the electron transfer. Hong et al. (2015); Zhang (2016); Xu et al. (2017) constructed a series of electrochemical immunosensors based on sulfur corynes/graphene complexes as immobilization platforms for primary antibodies. All of these sensors showed a wide detection range, low detection limits and good stability. In addition, reduced graphene can also be applied for the preparation of electrochemical sensors (Yang and Zhang, 2014). Haque et al. Ensafi et al. (2016) prepared an N-acryloxysuccinimide activated amphiphilic polymer-coated reduced graphite oxide as a sensing interface for electrochemical immunosensors. In this paper, we discuss the application of bioelectrochemistry in the detection of hematological malignancies from different perspectives of graphene assisted electrochemical and electrogenerated chemiluminescence biosensors.

LABELED BIOSENSORS

A single target is selected for sensing detection, which is a single-target analysis method. Its direct quantification produces a signal with low interference, good selectivity, high sensitivity and fast response, which can detect the target at trace level. Labeled biosensors are used for quantitative detection by monitoring the change in signal when a marker interacts with a target. The commonly used markers include quantum dots, metal ions, ferrocene, methylene blue, sulfur cordial, anthraquinone and enzymes with redox activity.

DNA electrochemical sensors are used to detect targets by hybridization reactions of nucleic acid DNA. Usually, a single-stranded DNA (ssDNA) probe is immobilized on the electrode surface, and the complementary sequence-specific hybridization between the probe and the target further captures the target DNA (tDNA) into a double-stranded structure (dsDNA), which triggers a change in the electrochemical signal for quantitative analysis of tDNA.

Wang X. et al. (2018) proposed a novel and sensitive electro-generated chemiluminescence (ECL) biosensing system for the detection of the p16INK4a gene. A nanofiber composite was synthesized using graphene as the backbone of pyrrole. This composite serves as a carrier for labeling dsDNA. after optimization, this ECL can detect p16INK4a linearly in the

TABLE 2 | Electrochemical sensor for RNA biomarkers in hematological malignancies.

Target	Sensor	Linear range	LOD	References
miRNA-21	Au-RGO/TiPCd^{2+}/Ru$(NH_3)_6^{3+}$	1 aM–10 pM	0.76 aM	Cheng et al. (2015)
miRNA-21	Graphene/GME	-	3.12 pM	Kilic et al. (2015)
miR-155	SS-probe/GO/GNR	2.0 fM–8.0 pM	0.6 fM	Azimzadeh et al. (2016)
miR-155	Amino-graphene	30 pM–1 nM	12.5 pM	Salimi et al. (2019)
miR-122	Graphene-PGE	0.5–7 μg/ml	1.06 pM	Kilic et al. (2016)

range of 0.1 pM–1 nM, and the detection limit can reach 0.05 pM. Mazloum-Ardakani et al. (2018) reported a biosensor with excellent electrical properties for the detection of acute lymphoblastic leukemia. This sensor does not require the involvement of enzymes and only requires the use of a simple one-step synthesis of poly(catechol). By modification with graphene sheets and AuNPs, the electrical conductivity of poly(catechol) can be greatly enhanced. In this sensor, catechols are used as active probes. Under optimal conditions, the logarithm of this sensor is linear for the target DNA concentration in the range of 100.0 μM to 10.0 pM.

Graphene was also used to prepare electrochemical sensors to detect BCR/ABL fusion genes (Wang et al., 2014). Chitosan (CS) was used to prepare a graphene sheet suspension and modified on GCE, electropolymerized to form a PANI layer and then solidly loaded with AuNPs for the capture probe. The probes were double-labeled with 5′-SH and 3′-biotin for hairpin structure. After hybridization with the target DNA, the hairpin structure is forced open and the streptavidin-alkaline phosphatase can covalently bind to the probe via avidin. Then, the catalytically electroactive 1-naphthyl phosphate can be hydrolyzed to 1-naphthol and exhibit a reduction current for detection. Under optimal conditions, the sensor allows linear detection of the BCR/ABL fusion gene in the range of 10–1000 pM with a detection limit of 2.11 pM.

Several miRNAs are also important markers for the detection of hematological malignancies. Nowadays electrochemical techniques often use sandwich method via nucleotide hybridization to achieve miRNA detection. Cheng et al. (2015) prepared AuNPs-graphene modified GCE, assembled DNA1 to capture the target miRNA-21, and further bound DNA2 to form a sandwich structure. They then used Cd^{2+}-modified titanium phosphate nanoparticles as signal probes, along with $Ru(NH_3)_6^{3+}$ as the electron mediator, bound electrostatically to the sandwich structure. This sensor has a detection linear range of 10^{-18} to 10^{-11} M with a low limit of detection of 0.76 aM. The performance of some other sensors composed of graphene for miRNA detection was listed in **Table 2**.

Protein-based markers are based on the principle of specific binding between antigen and antibody to form stable antigen-antibody complexes, which are converted into detectable electrochemical signals for qualitative and quantitative analysis and detection. He et al. (2013) developed a graphene-assisted electrochemical immunoassay platform for the detection of c-Myc. AuNPs were used as a label for the determination of c-Myc. This sensor is based on a sandwich immunoassay strategy where the target c-Myc is captured by an antibody to c-Myc modified on a gold substrate, followed by the addition of another CAb conjugated to the AuNPs label. sensor allows linear detection of c-Myc between 4.3 Pm–43 nM with a detection limit of 1.5 pM.

Cellular biosensors often employ antigenic antibodies as recognition elements for cellular detection. The target is captured by a specific immune reaction with certain groups on the cell surface and converted into a detectable electrochemical signal for qualitative and quantitative analysis. Yang et al. (2013) assembled a cell sensor using carboxymethyl chitosan-functionalized graphene (CMC-G). This sensor exhibited good electrochemical behavior and cell capture ability for HL-60 cells. Wang J. et al. (2018) proposed an electrochemical biosensor assembled by signal amplification strategy using graphene oxide - polyaniline (PANI) as a modified material for the detection of K562 cells. Polystyrene microspheres functionalized with multilayer CdS QDs were used as a biosensor. the modification of GO-PANI composite not only improved the electron transfer rate but also increased the loading rate of tumor cells. This electrochemical sensor can detect a minimum of three K562 cells.

Recently, aptamers are also often used as recognition elements for cellular assays. Aptamers are short, single-stranded oligonucleotides that are usually highly affinity and specific for the target. Aptamers are smaller and more stable than traditional biomolecular ligands such as antibodies, allowing for better selective recognition of target tumor cells. Liu et al. (2016) found that the morphology of AuNPs can affect the catalytic activity of graphene towards peroxidase mimics. They synthesized Au flowers *in situ* on the hemin/RGO surface and solidified the aptamer. Then, they used this composite to prepare an electrochemical sensor for K562 leukemia cancer cells. Zheng et al. (2019) developed an electrochemical sensor for the highly sensitive detection of K562 in tumor cells. They first designed aptamer-DNA concatamer-CdTe QDs probes by DNA hybridization and covalent assembly. Then, they assembled GCE/GO/PANI/GA/Concanavalin A step by step. this electrochemical sensor can reach the detection limit of 60 cells/ml.

LABEL-FREE ELECTROCHEMICAL SENSORS

Label-free electrochemical sensing methods are mostly used for the detection of DNA and CTC markers in blood tumors. These sensors are generally based on chemical methods to bind the

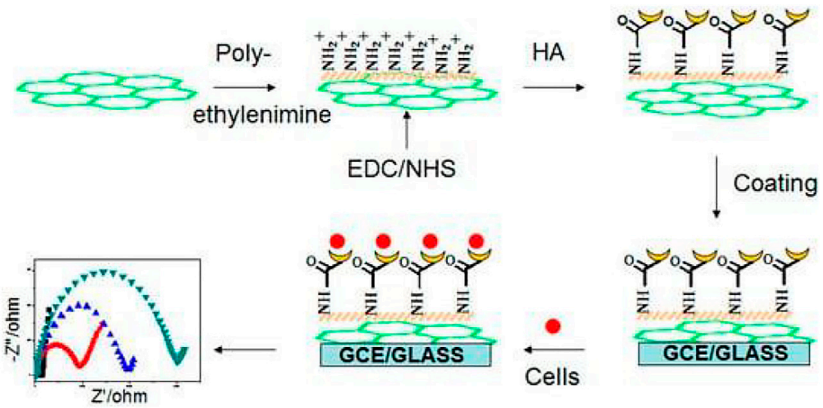

FIGURE 1 | Scheme of hyaluronate-functionalized graphene for label-free HCT-116 detection (Copyright obtained from MDPI.)

target by immobilizing the capture probe on the electrode surface through covalent linkage, including Au-S bonding, amino-carboxy and amino-sulfonic acid groups. In addition, binding is also based on physical methods such as electrostatic adsorption and amino acid functionalized cross-linking.

Jing et al. (2018) prepared an effective hyaluronate-functionalized graphene (HG) by chemical reduction of GO. Using the self-assembly of HG with ethylenediamine and sodium hyaluronate, a label-free electrochemical impedance spectroscopy cell sensor could be assembled. Under optimal conditions, this sensor can provide highly sensitive detection of cancer cells HCT-116. **Figure 1** shows a schematic diagram of this detection strategy.

Shamsipur et al. (2020) exfoliated graphene with gold nanoclusters (Hb@AuNCs) capped with hemoglobin. This graphene has good dispersion due to the fact that Hb@AuNCs can act as stabilizers through non-covalent bonds. This graphene was used to make a highly sensitive electrochemical sensor. Highly sensitive detection of BCR/ABL fusion gene can be performed based on "signal off" and "signal on" strategies". Under optimal conditions, the sensor can detect linearly in the range of 0.1 fM to 10 pM. The detection limit is 0.030 fM.

Zhang et al. (2013) proposed a label-free electrochemical sensor consisting of a combination of GO and polylysine that can be used for the detection of K562 cells. This sensor is a thin film that can immobilize live cells very well. $[Fe(CN)_6]^{3-/4-}$ was used as a detection probe and EIS was used as a technique for the detection. Under optimal conditions, the electron transfer resistance correlates well with the logarithmic value of the K562 cell concentration. The detection range of this sensor was from 100-10^7 cell/mL. The detection limit was 30 cell/mL.

Label-free electrochemical sensors save time and cost by detecting the target material directly without a marker. This can maintain the affinity of the recognition element to the target and thus avoid the interference caused by secondary detection and labeling reagents. However, label-free electrochemical sensors have some drawbacks in practice, such as the possibility of detachment of the recognition element bound to the electrode surface during the experiment and the fluctuation of the EIS, resulting in errors. These problems can lead to relatively poor accuracy in the actual test and limit its practical application.

CONCLUSION

This mini-review presents an introduction to biomarkers and electrochemical detection techniques in hematological malignancies. Among them we focus on the impact of graphene development in the construction of such electrochemical sensors. However, improving the sensitivity, specificity, and practicality of graphene electrochemical biosensing methods in the face of biomarkers present at trace levels in actual clinical samples is still an important current issue. It is clear from the content that the current graphene electrochemical sensor can detect relatively few markers, so more markers can be developed for detection. Graphene-based electrochemical sensors in hematological malignancies biomarker analysis is still focus on the single marker detection. Therefore, selecting multiple types of typical markers for specific tumors for combined detection can make the assay more specific and improve the sensitivity and detection rate of tumor detection. Meanwhile, current electrochemical biosensors are not ideal for the detection of marker molecules in population samples. Effective coupling of sensing design with population sample pre-treatment, integrating target extraction, enrichment and detection, and effectively improving the utility of the sensor will be the focus of future research.

AUTHOR CONTRIBUTIONS

LC supervised the review program, SW, XC and XZ. collected references. SW, XC and LC wrote the draft. L.C. proofread the article.

REFERENCES

Abdul Rasheed, P., Pandey, R. P., Gomez, T., Jabbar, K. A., Prenger, K., Naguib, M., et al. (2020). Nb-based MXenes for Efficient Electrochemical Sensing of Small Biomolecules in the Anodic Potential. *Electrochemistry Commun.* 119, 106811. doi:10.1016/j.elecom.2020.106811

Azimzadeh, M., Rahaie, M., Nasirizadeh, N., Ashtari, K., and Naderi-Manesh, H. (2016). An Electrochemical Nanobiosensor for Plasma miRNA-155, Based on Graphene Oxide and Gold Nanorod, for Early Detection of Breast Cancer. *Biosens. Bioelectron.* 77, 99–106. doi:10.1016/j.bios.2015.09.020

Baldo, S., Buccheri, S., Ballo, A., Camarda, M., La Magna, A., Castagna, M. E., et al. (2016). Carbon Nanotube-Based Sensing Devices for Human Arginase-1 Detection. *Sensing Bio-Sensing Res.* 7, 168–173. doi:10.1016/j.sbsr.2015.11.011

Chen, H., Luo, K., and Li, K. (2019). A Facile Electrochemical Sensor Based on NiO-ZnO/MWCNT-COOH Modified GCE for Simultaneous Quantification of Imatinib and Itraconazole. *J. Electrochem. Soc.* 166, B697–B707. doi:10.1149/2.1071908jes

Cheng, F.-F., He, T.-T., Miao, H.-T., Shi, J.-J., Jiang, L.-P., and Zhu, J.-J. (2015). Electron Transfer Mediated Electrochemical Biosensor for microRNAs Detection Based on Metal Ion Functionalized Titanium Phosphate Nanospheres at Attomole Level. *ACS Appl. Mater. Inter.* 7, 2979–2985. doi:10.1021/am508690x

Ensafi, A. A., Amini, M., Rezaei, B., and Talebi, M. (2016). A Novel Diagnostic Biosensor for Distinguishing Immunoglobulin Mutated and Unmutated Types of Chronic Lymphocytic Leukemia. *Biosens. Bioelectron.* 77, 409–415. doi:10.1016/j.bios.2015.09.063

Fracchiolla, N., Artuso, S., and Cortelezzi, A. (2013). Biosensors in Clinical Practice: Focus on Oncohematology. *Sensors* 13, 6423–6447. doi:10.3390/s130506423

Gupta, V., Braun, T. M., Chowdhury, M., Tewari, M., and Choi, S. W. (2020). A Systematic Review of Machine Learning Techniques in Hematopoietic Stem Cell Transplantation (HSCT). *Sensors* 20, 6100. doi:10.3390/s20216100

Gurudatt, N. G., Chung, S., Kim, J.-M., Kim, M.-H., Jung, D.-K., Han, J.-Y., et al. (2019). Separation Detection of Different Circulating Tumor Cells in the Blood Using an Electrochemical Microfluidic Channel Modified with a Lipid-Bonded Conducting Polymer. *Biosens. Bioelectron.* 146, 111746. doi:10.1016/j.bios.2019.111746

Hasanzadeh, M., Shadjou, N., and de la Guardia, M. (2017). Early Stage Screening of Breast Cancer Using Electrochemical Biomarker Detection. *Trac Trends Anal. Chem.* 91, 67–76. doi:10.1016/j.trac.2017.04.006

He, J.-L., Tian, Y.-F., Cao, Z., Zou, W., and Sun, X. (2013). An Electrochemical Immunosensor Based on Gold Nanoparticle Tags for Picomolar Detection of C-Myc Oncoprotein. *Sensors Actuators B: Chem.* 181, 835–841. doi:10.1016/j.snb.2013.02.063

Hianik, T. (2021). Advances in Electrochemical and Acoustic Aptamer-Based Biosensors and Immunosensors in Diagnostics of Leukemia. *Biosensors* 11, 177. doi:10.3390/bios11060177

Hong, L.-R., Chai, Y.-Q., Zhao, M., Liao, N., Yuan, R., and Zhuo, Y. (2015). Highly Efficient Electrogenerated Chemiluminescence Quenching of PEI Enhanced Ru(bpy) 3 2+ Nanocomposite by Hemin and Au@CeO 2 Nanoparticles. *Biosens. Bioelectron.* 63, 392–398. doi:10.1016/j.bios.2014.07.065

Hrichi, H., Monser, L., and Adhoum, N. (2019). Selective Electrochemical Determination of Etoposide Using a Molecularly Imprinted Overoxidized Polypyrrole Coated Glassy Carbon Electrode. *Int. J. Electrochemistry* 2019, 1–12. doi:10.1155/2019/5394235

Jie, G., Zhang, J., Jie, G., and Wang, L. (2014). A Novel Quantum Dot Nanocluster as Versatile Probe for Electrochemiluminescence and Electrochemical Assays of DNA and Cancer Cells. *Biosens. Bioelectron.* 52, 69–75. doi:10.1016/j.bios.2013.08.006

Jing, A., Zhang, C., Liang, G., Feng, W., Tian, Z., and Jing, C. (2018). Hyaluronate-Functionalized Graphene for Label-free Electrochemical Cytosensing. *Micromachines* 9, 669. doi:10.3390/mi9120669

Karimi-Maleh, H., Orooji, Y., Karimi, F., Alizadeh, M., Baghayeri, M., Rouhi, J., et al. (2021). A Critical Review on the Use of Potentiometric Based Biosensors for Biomarkers Detection. *Biosens. Bioelectron.* 184, 113252. doi:10.1016/j.bios.2021.113252

Kilic, T., Erdem, A., Erac, Y., Seydibeyoglu, M. O., Okur, S., and Ozsoz, M. (2015). Electrochemical Detection of a Cancer Biomarker Mir-21 in Cell Lysates Using Graphene Modified Sensors. *Electroanalysis* 27, 317–326. doi:10.1002/elan.201400518

Kilic, T., Kaplan, M., Demiroglu, S., Erdem, A., and Ozsoz, M. (2016). Label-free Electrochemical Detection of MicroRNA-122 in Real Samples by Graphene Modified Disposable Electrodes. *J. Electrochem. Soc.* 163, B227–B233. doi:10.1149/2.0481606jes

Li, J., Zhang, S., Zhang, L., Zhang, Y., Zhang, H., Zhang, C., et al. (2021). A Novel Graphene-Based Nanomaterial Modified Electrochemical Sensor for the Detection of Cardiac Troponin I. *Front. Chem.* 9, 339. doi:10.3389/fchem.2021.680593

Liu, J., Cui, M., Niu, L., Zhou, H., and Zhang, S. (2016). Enhanced Peroxidase-like Properties of Graphene-Hemin-Composite Decorated with Au Nanoflowers as Electrochemical Aptamer Biosensor for the Detection of K562 Leukemia Cancer Cells. *Chem. Eur. J.* 22, 18001–18008. doi:10.1002/chem.201604354

Liu, J., Yang, T., Xu, J., and Sun, Y. (2021). A New Electrochemical Detection Technique for Organic Matter Content in Ecological Soils. *Front. Chem.* 9, 488. doi:10.3389/fchem.2021.699368

Luo, H., Xia, X., Kim, G. D., Liu, Y., Xue, Z., Zhang, L., et al. (2021). Characterizing Dedifferentiation of Thyroid Cancer by Integrated Analysis. *Sci. Adv.* 7, eabf3657. doi:10.1126/sciadv.abf3657

Mazloum-Ardakani, M., Barazesh, B., Khoshroo, A., Moshtaghiun, M., and Sheikhha, M. H. (2018). A New Composite Consisting of Electrosynthesized Conducting Polymers, Graphene Sheets and Biosynthesized Gold Nanoparticles for Biosensing Acute Lymphoblastic Leukemia. *Bioelectrochemistry* 121, 38–45. doi:10.1016/j.bioelechem.2017.12.010

Miao, G., Xiaoying, W., and Xiaoning, W. (2019). Electrochemical Sensing Detection of Biomarkers in Hematological Malignancies. *Prog. Chem.* 31, 894.

Salimi, A., Kavosi, B., and Navaee, A. (2019). Amine-functionalized Graphene as an Effective Electrochemical Platform toward Easily miRNA Hybridization Detection. *Measurement* 143, 191–198. doi:10.1016/j.measurement.2019.05.008

Shamsipur, M., Samandari, L., Farzin, L., Molaabasi, F., and Mousazadeh, M. H. (2020). Dual-modal Label-free Genosensor Based on Hemoglobin@gold Nanocluster Stabilized Graphene Nanosheets for the Electrochemical Detection of BCR/ABL Fusion Gene. *Talanta* 217, 121093. doi:10.1016/j.talanta.2020.121093

Wang, J., Wang, X., Tang, H., Gao, Z., He, S., Li, J., et al. (2018a). Ultrasensitive Electrochemical Detection of Tumor Cells Based on Multiple Layer CdS Quantum Dots-Functionalized Polystyrene Microspheres and Graphene Oxide - Polyaniline Composite. *Biosens. Bioelectron.* 100, 1–7. doi:10.1016/j.bios.2017.07.077

Wang, L., Hua, E., Liang, M., Ma, C., Liu, Z., Sheng, S., et al. (2014). Graphene Sheets, Polyaniline and AuNPs Based DNA Sensor for Electrochemical Determination of BCR/ABL Fusion Gene with Functional Hairpin Probe. *Biosens. Bioelectron.* 51, 201–207. doi:10.1016/j.bios.2013.07.049

Wang, X., Wang, Y., Shan, Y., Jiang, M., Jin, X., Gong, M., et al. (2018b). A Novel and Sensitive Electrogenerated Chemiluminescence Biosensor for Detection of p16INK4a Gene Based on the Functional Paste-like Nanofibers Composites-Modified Screen-Printed Carbon Electrode. *J. Electroanalytical Chem.* 823, 368–377. doi:10.1016/j.jelechem.2018.06.030

Xu, Y., Xu, Y., Zuo, Z., Zhou, X., Guo, B., Sang, Y., et al. (2017). Triggered Hairpin Switch and *In Situ* Nonlinear Hybridization Chain Reaction Enabling Label-free Electrochemiluminescent Detection of BCR/ABL Fusion Gene. *J. Electroanalytical Chem.* 801, 192–197. doi:10.1016/j.jelechem.2017.07.050

Yang, G., Cao, J., Li, L., Rana, R. K., and Zhu, J.-J. (2013). Carboxymethyl Chitosan-Functionalized Graphene for Label-free Electrochemical Cytosensing. *Carbon* 51, 124–133. doi:10.1016/j.carbon.2012.08.020

Yang, J., and Zhang, W. (2014). Indicator-free Impedimetric Detection of BCR/ABL Fusion Gene Based on Ordered FePt Nanoparticle-Decorated Electrochemically Reduced Graphene Oxide. *J. Solid State. Electrochem.* 18, 2863–2868. doi:10.1007/s10008-014-2551-7

Zhang, D., Zhang, Y., Zheng, L., Zhan, Y., and He, L. (2013). Graphene Oxide/poly-L-Lysine Assembled Layer for Adhesion and Electrochemical Impedance

Detection of Leukemia K562 Cancercells. *Biosens. Bioelectron.* 42, 112–118. doi:10.1016/j.bios.2012.10.057

Zhang, L., Ren, Z., Su, Z., Liu, Y., Yang, T., Cao, M., et al. (2021). Novel Recurrent Altered Genes in Chinese Patients with Anaplastic Thyroid Cancer. *J. Clin. Endocrinol. Metab.* 106, 988–998. doi:10.1210/clinem/dgab014

Zhang, W. (2016). Application of Fe3O4 Nanoparticles Functionalized Carbon Nanotubes for Electrochemical Sensing of DNA Hybridization. *J. Appl. Electrochem.* 46, 559–566. doi:10.1007/s10800-016-0952-2

Zheng, Y., Wang, X., He, S., Gao, Z., Di, Y., Lu, K., et al. (2019). Aptamer-DNA Concatamer-Quantum Dots Based Electrochemical Biosensing Strategy for green and Ultrasensitive Detection of Tumor Cells via Mercury-free Anodic Stripping Voltammetry. *Biosens. Bioelectron.* 126, 261–268. doi:10.1016/j.bios.2018.09.076

Conflict of Interest: Author XZ was employed by the company Shandong Freda Pharmaceutical Group Co., Ltd.

The remaining authors declare that the research was conducted in the absence of any commercial or financial relationships that could be construed as a potential conflict of interest.

Publisher's Note: All claims expressed in this article are solely those of the authors and do not necessarily represent those of their affiliated organizations, or those of the publisher, the editors and the reviewers. Any product that may be evaluated in this article, or claim that may be made by its manufacturer, is not guaranteed or endorsed by the publisher.

frontiers in Chemistry

MINI REVIEW
published: 31 August 2021
doi: 10.3389/fchem.2021.736271

Carbon Material Based Electrochemical Immunosensor for Gastric Cancer Markers Detection

*Zhuliang Zhang†, Minsi Peng†, Defeng Li, Jun Yao, Yingxue Li, Benhua Wu, Lisheng Wang and Zhenglei Xu**

Department of Gastroenterology, Shenzhen People's Hospital, The Second Clinical Medical College, Jinan University, Shenzhen, China

Gastric cancer is one of the most common malignant tumors, and early diagnosis will be of great significance to improve the survival quality and overall treatment outcome evaluation of patients. Nanoelectrochemical immunosensor is an emerging biosensor combining nanotechnology, electrochemical analysis method and immunological technology, which has simple operation, fast analysis speed, high sensitivity, and good selectivity. This mini-review summarized immunoassay techniques, nanotechnology and electrochemical sensing for the early detection of gastric cancer. In particular, we focus on the tension of carbon nanomaterials in this field, including the functionalized preparation of materials, signal enhancement and the construction of novel sensing interfaces. Currently, various tumor markers are being developed, but the more recognized gastric cancer tumor markers are carcinoembryonic antigen (CEA), carbohydrate antigen (CA), CD44V9, miRNAs, and programmed death ligand 1. Among them, the electrochemical immunosensor allows the detection of CEA, CA, and miRNAs. The mini-review focused on the development of using carbon based materials, especially carbon nanotubes and graphene for immunosensor fabrication and gastric cancer markers detection.

Keywords: carbon materials, immunosensor, carbon nanotubes, graphene, gastric cancer, biomarker

OPEN ACCESS

Edited by:
Fatemeh Karimi, Quchan University of Advanced Technology, Iran

Reviewed by:
Somaye Cheraghi, Shahid Bahonar University of Kerman, Iran
Vahid Arabali, Islamic Azad University Sari Branch, Iran

****Correspondence:***
Zhenglei Xu
ZhengleiXu_xzl3@163.com

†These authors have contributed equally to this work

Specialty section:
This article was submitted to Electrochemistry, a section of the journal Frontiers in Chemistry

Received: *05 July 2021*
Accepted: *16 August 2021*
Published: *31 August 2021*

Citation:
Zhang Z, Peng M, Li D, Yao J, Li Y, Wu B, Wang L and Xu Z (2021) Carbon Material Based Electrochemical Immunosensor for Gastric Cancer Markers Detection. Front. Chem. 9:736271. doi: 10.3389/fchem.2021.736271

INTRODUCTION

In recent years, with the increase in the number of gastric cancer patients and their mortality rate, the methods of gastric cancer diagnosis are in urgent need of solution. From the large number of patients who died of gastric cancer, it can be seen that the main reason for the death is the late detection and untimely treatment. In order to better prevention and detection, early gastric cancer detection is crucial. The current methods of early gastric cancer detection include gastroscopy, radioactivity (Archer and Grant, 1991), ultrasound, serum gastric function test, and gastrin 17 combined with pepsinogen serological test. These assays have limitations, such as gastroscopy, ultrasound, and radiological testing can be uncomfortable for patients and are not particularly effective. Biologic tumor markers for gastric cancer is a more common and hot research direction. It can be detected quickly and without negative effects on the patients themselves. Currently, various new tumor markers are being developed, but the more recognized gastric cancer tumor markers are carcinoembryonic antigen (CEA) (Ishigami et al., 2001; Zhang et al., 2021), carbohydrate antigen (CA) (Gaspar et al., 2001), CD44V9 (Mashima et al., 2019), miRNAs (Khandelwal et al., 2019), and programmed death ligand 1 (PD-L1) (Wang et al., 2019).

Biosensors are a multidisciplinary intersection that includes medical, biological, chemical, and electronic technologies (Karimi-Maleh et al., 2021a; Luo et al., 2021). The principle of biosensor analysis and detection is that when the substance to be measured specifically binds to a molecular recognition element (e.g., enzyme or antibody, etc.), the resulting complex is transformed by a converter into a signal that can be output, such as an optical signal or an electrical signal. Electrochemical biosensors are divided into current, potential, capacitance, and conductivity types according to the measurement signal. According to the category of bioactive molecules, they can be divided into enzyme sensors, tissue sensors, immunosensors, DNA sensors, and microbial sensors. Among them, electrochemical biosensors for monitoring specific reactions between antigen→antibodies are called electrochemical immunosensors. There are two key directions in the research of electrochemical immunosensors: 1) designing novel biocompatible biocomponent immobilization interfaces to improve the loading and bioactivity of biocomponents on the sensing interface; 2) employing novel immunoreactive signal amplification techniques to enhance the sensitivity of the sensors. Therefore, there has been a search for good materials for immobilization of bioactive substances and efficient methods for immobilization of biological components.

Nanomaterials have become one of the popular materials for research and application in recent years due to their unique properties in optical, magnetic, electrical, and catalytic properties (Medetalibeyoğlu et al., 2020; Akça et al., 2021; Karimi-Maleh et al., 2021c; Liu et al., 2021). As a modifying material for sensor interfaces and as a solid-loading matrix for biorecognition molecules. Due to their large specific surface area, high surface free energy, good biocompatibility, and rich in surface functional groups, nanomaterials can be used in the construction of biosensing interfaces to effectively increase the specific surface area of electrodes, increase the loading of biomolecules on the electrode surface, accelerate the electron transfer rate, enhance the conductivity of modified electrodes, and accelerate the response of sensors. Carbon is a widely studied and used material in electrochemical sensor preparation. In the macroscopic field, there are three forms of carbon isomers: graphite, diamond, and amorphous carbon. However, the discovery of fullerenes (C60) and carbon nanotubes (CNTs) has led to new forms of carbon materials, and since then, the research on carbon nanomaterials has been booming. In this mini-review, we review the application of carbon nanomaterials, especially CNTs and graphene, in the preparation of electrochemical immunosensors and in the detection of gastric cancer biomarkers.

Carbon Materials Based Electrochemical Biosensors

Carbon nanomaterials play an important role in bioelectrocatalytic reactions due to their high specific surface area and their better biocompatibility (Naderi Asrami et al., 2020; Karaman et al., 2021; Karimi-Maleh et al., 2021b). Their large specific surface area and high surface reactivity lead to enhanced adsorption capacity of the materials, increased active sites on the surface, and improved catalytic efficiency. Compared with conventional sensors, carbon nanomaterials sensors are not only smaller and faster, but also more accurate and reliable. the discovery of CNTs has largely enriched the research of carbon materials and triggered a *trans*-generational material revolution. Britto et al. (1996) first made CNTs into electrodes and used them for the electrocatalytic oxidation of the neurotransmitter dopamine. The preparation method was similar to that of carbon paste electrodes, using bromine imitation as the binder. The CNTs have a good catalytic effect on the electrochemical oxidation of dopamine. Timur et al. (2007) reported the preparation of microbial sensors generated by immobilizing *Pseudomonas aeruginosa* cells on CNTs with osmium polymers as intermediates. By optimizing the amount of CNTs and polymers, the electron migration rate can be increased and can be used for microbial fuel cells and biochemical oxygen demand (BOD) measurements in wastewater.

CNTs have high axial strength and stiffness, so they are often used as reinforcement for composites. Meanwhile, their excellent electrical and thermal conductivity can improve the functionality of composite materials. The use of conducting polymers as sensing electrodes has attracted much attention due to their excellent electrochemical properties. The CNTs/polymer composite materials can be divided into two categories. The first one is to use CNTs as the main body and modify the polymer on the wall of CNTs to increase the solubility of CNTs. Another category is based on polymers as the main body and CNTs as filler materials, mainly for conductive polymer materials, with the aim of improving the conductivity and stability of conductive polymers. Commonly used conductive polymers such as polyaniline (PANI) and polypyrrole (PPy) (Pei et al., 2019; Assari et al., 2020). They have good electrochemical properties to amplify the signal current and eliminate the influence of electrode impurities, and provide a suitable environment for immobilizing biomolecules. Not only the complexation of conductive polymers with CNTs, but also the complexation of noble metals with CNTs has attracted a lot of attention from researchers. Among many noble metals, AuNPs have attracted much attention from researchers due to their ability to maintain the biological activity of adsorbed enzymes and reduce the hindrance of direct electron migration by protein shells.

In addition to CNTs, carbon nanofibers (CNFs) have similar high electrical conductivity, high mechanical strength, large specific surface area, and thermal stability as CNTs. Both of them can be used as good metal nanoparticle catalyst carriers with promising applications in chemical/biological sensing and catalysis. Sheng et al. (2010) introduced porous carbon nanofiber (PCNF)/room temperature ionic liquid (RTIL) membranes, which provide a suitable environment for direct electron migration of ferrous hemoglobin proteins. Hemoglobin (Hb), myoglobin (Mb), and cytochrome C showed a pair of reversible redox peaks on the PCNF/RTIL-modified membranes.

Graphene has received great attention in the field of biosensors in the last decade due to its high specific surface area, fast electron transfer capability and good biocompatibility. Huang et al. (2011)

prepared a sensitive label-free electrochemical immunosensor by modifying carbon ionic liquid electrodes with amino-functionalized graphene and AuNPs complexes. They first applied the amino-modified graphene dropwise on the surface of the carbon paste electrode, and then used electrostatic interaction to adsorb a layer of negatively charged AuNPs on the surface of the GO. A layer of antibodies. The modified electrode is then immersed in bovine serum albumin (BSA) solution to block the active site for non-specific adsorption. By the specific interaction of anti-AFP on AFP, this sensor can detect different concentrations of AFP.

Carcinoembryonic Antigen Detection

CEA, an acidic glycoprotein with human embryonic antigenic properties, was first discovered in 1965. Chen et al. (2012) found that perioperative chemotherapy improved overall survival in patients with normal CEA levels prior to treatment in 2012. Bacac et al. (2016) discovered a novel bispecific antibody to carcinoembryonic antigen T cells for the treatment of CEA-expressing solid tumors currently in phase I clinical trials in 2016.

CNTs are a very useful substrate material. For example, Lv et al. (2018) immobilized bimetallic core-shell rhodium@palladium nanodendrites (Rh@Pd NDs) onto sulfate-based functionalized MWCNTs. This composite can be used as a simple electrochemical immunosensor. Rh@Pd NDs possess a unique dendritic nanostructure that provides an abundance of catalytically active sites. Meanwhile, MWCNTs improve the performance of the sensor due to their excellent electrical conductivity, good solubility, and high surface area. Their proposed electrochemical immunosensor can provide linear detection of CEA within 25 fg/ml-100 ng/ml under optimal conditions. To further improve the immobilization performance, cyclodextrins can be modified on CNTs. Han et al. (2017) prepared a novel sensitive sandwich-type non-enzymatic electrochemical immunosensor using cyclodextrin-modified MWCNTs. Synthesized silver nanoparticles-carbon nanotubes/manganese dioxide (Ag NPs-MWCNTs/MnO_2) were used as a label for Ab2 to achieve duplex amplification of the electrochemical signal. This immunosensor can reach the detection limit of 0.03 pg/ml for CEA. In addition to cyclodextrins, chitosan also has a similar role. Gao et al. (2011) prepared a chitosan-carbon nanotube-gold nanoparticles nanocomposite membrane. This composite membrane was able to exhibit better electrical conductivity, high stability and good biocompatibility due to its three-dimensional structure. Under optimal conditions, this immunosensor can detect CEA in two linear ranges between 0.1–2.0 and 2.0–200.0 ng/ml with a detection limit of 0.04 ng/ml.

Graphene is now replacing carbon nanotubes in the development of many sensors. For example, Jozghorbani et al. (2021) developed a label-free electrochemical immunosensor for the detection of CEA. They modified reduced graphene oxide (rGO) on the surface of a glassy carbon electrode to form an interface for binding antibodies. rGO has carboxyl groups on the surface that can be used to bind to antibodies. This binding between antibody and rGO can be confirmed by CV and EIS characterization. The weakening of the electrochemical signal can be used as a signal of successful antibody modification. This immunosensor allows linear detection of CEA in the concentration range of 0.1–5 ng/ml. The detection limit can reach 0.05 ng/ml. Chen et al. (2018) prepared AuNPs-TiO_2-graphene composites for sandwich immunosensing detection of CEA. in this work, graphene was first modified with dopamine via π-stacking and then immobilized with TiO_2 nanoparticles. After that, AuNPs-TiO_2-graphene composites were synthesized by photoreduction method under UV irradiation. The AuNPs interacted with HRP-Ab2 and covalently attached HRP-Ab2. Under optimal conditions, this sandwich immunosensor could detect CEA linearly in a wide range of 0.005–200 ng/ml, and the detection limit It can reach 3.33 pg/ml.

Carbohydrate Antigen Detection

CA is a tumor cell-associated antigen. CA125, CA19-9, and CA72-4 were considered to have the strongest correlation with gastric cancer. Clinical data from Abbas et al. (Gao et al., 2018) showed that elevated pre-treatment CA199 levels are associated with a higher risk of tumor progression and a worse prognosis in gastric cancer. CA199 can be reduced with the use of anti-angiogenic agents and first-line platinum-based chemotherapy.

The role of carbon material in the CA199 assay is very similar to that of the previous assay for CEA. Kalyani et al. (2021) reported an electrochemical immunosensor based on MWCNT-Fe_3O_4, which was dispersed in chitosan for immobilization of specific antibodies. The detection range of this electrochemical immunosensor was 1.0 pg/ML-100 ng, ml. the detection limit was 0.163 pg/ml. Very similarly, Huang et al. (2017) synthesized a polysulfate-gold composite (AuNPs@PThi). This AuNPs@PThi can act as a sensitive redox probe and is capable of amplifying electrochemical signals. Under optimal conditions, this label-free immunosensor can linearly detect CA199 from 6.5–520 U/ml with detection limits up to 0.26 U/ml.

The function of graphene here also remains as a substrate and is used to improve the performance of the electrodes. As shown in **Figure 1**, the Zn-Co-S/graphene composite can be used to detect CA199 (Su et al., 2021). The Zn-Co-S dot-like nanoparticles grown on graphene can form a conductive network, allowing the direct reduction of H_2O_2 by the active site. This electrochemical immunosensor can detect CA199 linearly between 6.3 and 300 U/ml with a detection limit of 0 U/ml. For practical considerations, electrochemical immunosensors can also be assembled on screen-printed electrodes (SPEs). Mic et al. (2020) modified SPEs with thermally reduced graphene oxide (TRGO). The modified electrodes can interact with CA199-His molecules by adsorption. It was shown that TRGO has a very strong affinity for CA199-His, to the extent that it can be used for quantitative detection.

miRNA Detection

miRNAs are a class of small non-coding single-stranded RNAs about 19–25 nt long that are commonly found in plants and animals. They can inhibit the transcription or translation of target genes by incomplete binding to target mRNAs to perform their biological functions. Since the year 2,000, miRNAs have been

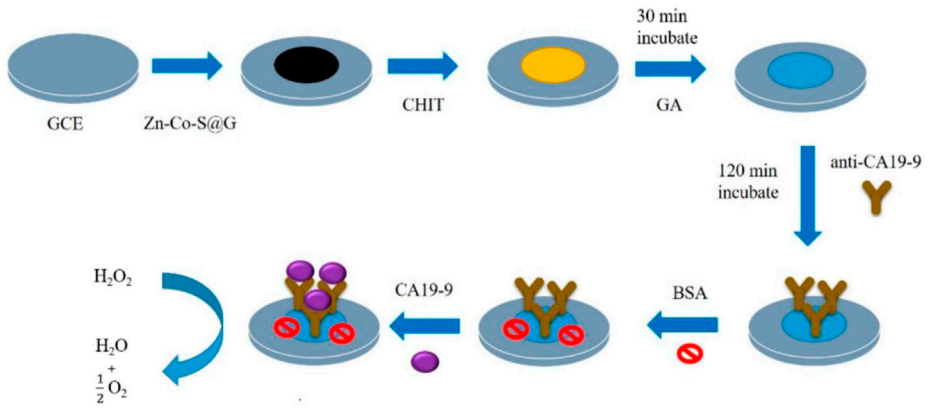

FIGURE 1 | Scheme of fabrication of the Zn-Co-S/graphene electrochemical immunosensor for CA199 detection.

widely studied worldwide and more than two thousand miRNAs have been identified and characterized. miRNAs are widely involved in the development of gastric cancer (Daneshpour et al., 2018; Huang et al., 2019). *H. pylori* (HP) is a class I gastric carcinogen. miR-223, miR-125a, and miR-21 expression was found to be significantly increased in positive gastric cancer specimens, while miR-218 expression was significantly decreased. This suggests that HP infection may promote gastric cancer formation by altering the corresponding miRNAs. Several studies also demonstrated that miR-551b-3p, miR-100-5p, and miR-363-3 were significantly down-regulated in gastric cancer tissues and cells. miR-215 was significantly up-regulated in gastric cancer tissues and cells. miR-429 aberrant expression may be associated with age differences in gastric cancer development. However, there are not many applications of carbon nanomaterials in miRNA detection. Yammouri et al. (2017) compared the detection of miR-125a by carbon black, MWCNT and GO after preparing an electrochemical immunosensor. Surprisingly, the lowest detection limit of microRNA-125a was obtained with the sensor modified with carbon black.

CONCLUSION

Gastric cancer is a malignant tumor originating from the epithelial cells of the gastric mucosa, and it is the second leading cause of cancer death worldwide. The development of new immunoassay techniques that are rapid, sensitive, high-throughput, low-cost, easy for clinical dissemination and field application is crucial for early diagnosis, prognosis monitoring, and treatment of gastric cancer. Carbon nanomaterials have very high specific surface area, electrical conductivity and good mechanical properties, which are ideal materials required in electrochemistry. A large number of theoretical and practical studies have been conducted on the application of carbon nanotubes and graphene in the field of electrochemistry, which fully demonstrate the application prospects of carbon materials as new sensing materials. An ideal tumor marker should have high sensitivity, good specificity, and high accuracy. Although many tumor markers have been continuously discovered, studied and applied, a tumor marker with high sensitivity, and specificity has not been found yet. Immunosensors will become a widely used novel test in the field of medical diagnosis. Various novel signal-enhanced immunosensors can effectively improve the sensitivity and specificity of tumor marker diagnosis and enable the detection of gastric cancer markers.

AUTHOR CONTRIBUTIONS

ZZ, MP, and ZX conceptualized the idea. ZZ, MP, DL, JY, and YL wrote the original draft. BW, LW, and ZX reviewed and edited the paper. ZX supervised the work. ZZ, MP, BW, and LW obtained the resources.

REFERENCES

Akça, A., Karaman, O., and Karaman, C. (2021). Mechanistic Insights into Catalytic Reduction of N2O by CO over Cu-Embedded Graphene: A Density Functional Theory Perspective. *ECS J. Solid State. Sci. Technol.* 10, 041003. doi:10.1149/2162-8777/abf481

Archer, A. G., and Grant, D. C. (1991). Recent Developments in Diagnostic Radiology of Primary and Recurrent Gastric Cancer. *Cancer Treat. Res.* 55, 107–131. doi:10.1007/978-1-4615-3882-0_7

Assari, P., Rafati, A. A., Feizollahi, A., and Joghani, R. A. (2020). Fabrication of a Sensitive Label Free Electrochemical Immunosensor for Detection of Prostate Specific Antigen Using Functionalized Multi-Walled Carbon Nanotubes/polyaniline/AuNPs. *Mater. Sci. Eng. C* 115, 111066. doi:10.1016/j.msec.2020.111066

Bacac, M., Fauti, T., Sam, J., Colombetti, S., Weinzierl, T., Ouaret, D., et al. (2016). A Novel Carcinoembryonic Antigen T-Cell Bispecific Antibody (CEA TCB) for the Treatment of Solid Tumors. *Clin. Cancer Res.* 22, 3286–3297. doi:10.1158/1078-0432.ccr-15-1696

Britto, P. J., Santhanam, K. S. V., and Ajayan, P. M. (1996). Carbon Nanotube Electrode for Oxidation of Dopamine. *Bioelectrochemistry Bioenerg.* 41, 121–125. doi:10.1016/0302-4598(96)05078-7

Chen, S., Chen, Y.-B., Li, Y.-F., Feng, X.-Y., Zhou, Z.-W., and Yuan, X.-H. (2012). Normal Carcinoembryonic Antigen Indicates Benefit from Perioperative Chemotherapy to Gastric Carcinoma Patients. *World J. Gastroenterol.* 18, 3910. doi:10.3748/wjg.v18.i29.3910

Chen, Y., Li, Y., Deng, D., He, H., Yan, X., Wang, Z., et al. (2018). Effective Immobilization of Au Nanoparticles on TiO2 Loaded Graphene for a Novel sandwich-type Immunosensor. *Biosens. Bioelectron.* 102, 301–306. doi:10.1016/j.bios.2017.11.009

Daneshpour, M., Karimi, B., and Omidfar, K. (2018). Simultaneous Detection of Gastric Cancer-Involved miR-106a and Let-7a through a Dual-Signal-Marked Electrochemical Nanobiosensor. *Biosens. Bioelectron.* 109, 197–205. doi:10.1016/j.bios.2018.03.022

Gao, X., Zhang, Y., Wu, Q., Chen, H., Chen, Z., and Lin, X. (2011). One Step Electrochemically Deposited Nanocomposite Film of Chitosan-Carbon Nanotubes-Gold Nanoparticles for Carcinoembryonic Antigen Immunosensor Application. *Talanta* 85, 1980–1985. doi:10.1016/j.talanta.2011.07.012

Gao, Y., Wang, J., Zhou, Y., Sheng, S., Qian, S. Y., and Huo, X. (2018). Evaluation of Serum CEA, CA19-9, CA72-4, CA125 and Ferritin as Diagnostic Markers and Factors of Clinical Parameters for Colorectal Cancer. *Sci. Rep.* 8, 2732–2739. doi:10.1038/s41598-018-21048-y

Gaspar, M. J., Arribas, I., Coca, M. C., and Díez-Alonso, M. (2001). Prognostic Value of Carcinoembryonic Antigen, CA 19-9 and CA 72-4 in Gastric Carcinoma. *Tumor Biol.* 22, 318–322. doi:10.1159/000050633

Han, J., Li, Y., Feng, J., Li, M., Wang, P., Chen, Z., et al. (2017). A Novel Sandwich-Type Immunosensor for Detection of Carcino-Embryonic Antigen Using Silver Hybrid Multiwalled Carbon Nanotubes/manganese Dioxide. *J. Electroanalytical Chem.* 786, 112–119. doi:10.1016/j.jelechem.2017.01.021

Huang, K.-J., Niu, D.-J., Sun, J.-Y., and Zhu, J.-J. (2011). An Electrochemical Amperometric Immunobiosensor for Label-Free Detection of α-fetoprotein Based on Amine-Functionalized Graphene and Gold Nanoparticles Modified Carbon Ionic Liquid Electrode. *J. Electroanalytical Chem.* 656, 72–77. doi:10.1016/j.jelechem.2011.01.007

Huang, R., He, L., Xia, Y., Xu, H., Liu, C., Xie, H., et al. (2019). A Sensitive Aptasensor Based on a Hemin/G-Quadruplex-Assisted Signal Amplification Strategy for Electrochemical Detection of Gastric Cancer Exosomes. *Small* 15, 1900735. doi:10.1002/smll.201900735

Huang, Z., Jiang, Z., Zhao, C., Han, W., Lin, L., Liu, A., et al. (2017). Simple and Effective Label-Free Electrochemical Immunoassay for Carbohydrate Antigen 19-9 Based on Polythionine-Au Composites as Enhanced Sensing Signals for Detecting Different Clinical Samples. *Int. J. Nanomedicine.* 12, 3049–3058. doi:10.2147/ijn.s131805

Ishigami, S., Natsugoe, S., Hokita, S., Che, X., Tokuda, K., Nakajo, A., et al. (2001). Clinical Importance of Preoperative Carcinoembryonic Antigen and Carbohydrate Antigen 19-9 Levels in Gastric Cancer. *J. Clin. Gastroenterol.* 32, 41–44. doi:10.1097/00004836-200101000-00010

Jozghorbani, M., Fathi, M., Kazemi, S. H., and Alinejadian, N. (2021). Determination of Carcinoembryonic Antigen as a Tumor Marker Using a Novel Graphene-Based Label-Free Electrochemical Immunosensor. *Anal. Biochem.* 613, 114017. doi:10.1016/j.ab.2020.114017

Kalyani, T., Sangili, A., Nanda, A., Prakash, S., Kaushik, A., and Kumar Jana, S. (2021). Bio-Nanocomposite Based Highly Sensitive and Label-Free Electrochemical Immunosensor for Endometriosis Diagnostics Application. *Bioelectrochemistry* 139, 107740. doi:10.1016/j.bioelechem.2021.107740

Karaman, C., Karaman, O., Atar, N., and Yola, M. L. (2021). Electrochemical Immunosensor Development Based on Core-Shell High-Crystalline Graphitic Carbon Nitride@ Carbon Dots and Cd 0.5 Zn 0.5 S/d-Ti 3 C 2 T X MXene Composite for Heart-Type Fatty Acid–Binding Protein Detection. *Microchim. Acta* 188, 1–15. doi:10.1007/s00604-021-04838-6

Karimi-Maleh, H., Alizadeh, M., Orooji, Y., Karimi, F., Baghayeri, M., Rouhi, J., et al. (2021a). Guanine-based DNA Biosensor Amplified with Pt/SWCNTs Nanocomposite as Analytical Tool for Nanomolar Determination of Daunorubicin as an Anticancer Drug: A Docking/experimental Investigation. *Ind. Eng. Chem. Res.* 60, 816–823. doi:10.1021/acs.iecr.0c04698

Karimi-Maleh, H., Orooji, Y., Karimi, F., Alizadeh, M., Baghayeri, M., Rouhi, J., et al. (2021b). A Critical Review on the Use of Potentiometric Based Biosensors for Biomarkers Detection. *Biosens. Bioelectron.* 184, 113252. doi:10.1016/j.bios.2021.113252

Karimi-Maleh, H., Yola, M. L., Atar, N., Orooji, Y., Karimi, F., Senthil Kumar, P., et al. (2021c). A Novel Detection Method for Organophosphorus Insecticide Fenamiphos: Molecularly Imprinted Electrochemical Sensor Based on Core-Shell Co3O4@MOF-74 Nanocomposite. *J. Colloid Interf. Sci.* 592, 174–185. doi:10.1016/j.jcis.2021.02.066

Khandelwal, N., Dey, S. K., Chakravarty, S., and Kumar, A. (2019). miR-30 Family miRNAs Mediate the Effect of Chronic Social Defeat Stress on Hippocampal Neurogenesis in Mouse Depression Model. *Front. Mol. Neurosci.* 12, 188. doi:10.3389/fnmol.2019.00188

Liu, J., Yang, T., Xu, J., and Sun, Y. (2021). A New Electrochemical Detection Technique for Organic Matter Content in Ecological Soils. *Front. Chem.* 9, 488. doi:10.3389/fchem.2021.699368

Luo, H., Xia, X., Kim, G. D., Liu, Y., Xue, Z., Zhang, L., et al. (2021). Characterizing Dedifferentiation of Thyroid Cancer by Integrated Analysis. *Sci. Adv.* 7, eabf3657. doi:10.1126/sciadv.abf3657

Lv, H., Li, Y., Zhang, X., Gao, Z., Feng, J., Wang, P., et al. (2018). The Label-Free Immunosensor Based on Rhodium@palladium Nanodendrites/sulfo Group Functionalized Multi-Walled Carbon Nanotubes for the Sensitive Analysis of Carcino Embryonic Antigen. *Analytica Chim. Acta* 1007, 61–70. doi:10.1016/j.aca.2017.12.030

Mashima, T., Iwasaki, R., Kawata, N., Kawakami, R., Kumagai, K., Migita, T., et al. (2019). In Silico chemical Screening Identifies Epidermal Growth Factor Receptor as a Therapeutic Target of Drug-Tolerant CD44v9-Positive Gastric Cancer Cells. *Br. J. Cancer* 121, 846–856. doi:10.1038/s41416-019-0600-9

Medetalibeyoğlu, H., Beytur, M., Manap, S., Karaman, C., Kardaş, F., and Akyıldırım, O. (2020). Molecular Imprinted Sensor Including Au Nanoparticles/polyoxometalate/two-Dimensional Hexagonal boron Nitride Nanocomposite for Diazinon Recognition. *ECS J. Solid State. Sci. Technol.* 9, 101006. doi:10.1149/2162-8777/abbe6a

Mic, M., Varodi, C., Pogacean, F., Socaci, C., Coros, M., Stefan-van Staden, R.-I., et al. (2020). Sensing and Interaction of His-Tagged CA19-9 Antigen with Graphene-Modified Electrodes. *Chemosensors* 8, 112. doi:10.3390/chemosensors8040112

Naderi Asrami, P., Aberoomand Azar, P., Saber Tehrani, M., and Mozaffari, S. A. (2020). Glucose Oxidase/nano-ZnO/thin Film Deposit FTO as an Innovative Clinical Transducer: aA Sensitive Glucose Biosensor. *Front. Chem.* 8, 503. doi:10.3389/fchem.2020.00503

Pei, F., Wang, P., Ma, E., Yang, Q., Yu, H., Gao, C., et al. (2019). A Sandwich-Type Electrochemical Immunosensor Based on RhPt NDs/NH2-GS and Au NPs/PPy NS for Quantitative Detection Hepatitis B Surface Antigen. *Bioelectrochemistry* 126, 92–98. doi:10.1016/j.bioelechem.2018.11.008

Sheng, Q.-L., Zheng, J.-B., Shang-Guan, X.-D., Lin, W.-H., Li, Y.-Y., and Liu, R.-X. (2010). Direct Electrochemistry and Electrocatalysis of Heme-Proteins Immobilized in Porous Carbon Nanofiber/room-Temperature Ionic Liquid Composite Film. *Electrochimica Acta* 55, 3185–3191. doi:10.1016/j.electacta.2009.12.101

Su, C.-W., Tian, J.-H., Ye, J.-J., Chang, H.-W., and Tsai, Y.-C. (2021). Construction of a Label-free Electrochemical Immunosensor Based on Zn-Co-S/Graphene Nanocomposites for Carbohydrate Antigen 19-9 Detection. *Nanomaterials* 11, 1475. doi:10.3390/nano11061475

Timur, S., Anik, U., Odaci, D., and Gorton, L. (2007). Development of a Microbial Biosensor Based on Carbon Nanotube (CNT) Modified Electrodes. *Electrochemistry Commun.* 9, 1810–1815. doi:10.1016/j.elecom.2007.04.012

Wang, X., Wu, W. K. K., Gao, J., Li, Z., Dong, B., Lin, X., et al. (2019). Autophagy Inhibition Enhances PD-L1 Expression in Gastric Cancer. *J. Exp. Clin. Cancer Res.* 38, 140. doi:10.1186/s13046-019-1148-5

Yammouri, G., Mandli, J., Mohammadi, H., and Amine, A. (2017). Development of an Electrochemical Label-Free Biosensor for microRNA-125a Detection Using Pencil Graphite Electrode Modified with Different Carbon Nanomaterials. *J. Electroanalytical Chem.* 806, 75–81. doi:10.1016/j.jelechem.2017.10.012

Zhang, L., Ren, Z., Su, Z., Liu, Y., Yang, T., Cao, M., et al. (2021). Novel Recurrent Altered Genes in Chinese Patients with Anaplastic Thyroid Cancer. *J. Clin. Endocrinol. Metab.* 106, 988–998. doi:10.1210/clinem/dgab014

Conflict of Interest: The authors declare that the research was conducted in the absence of any commercial or financial relationships that could be construed as a potential conflict of interest.

Publisher's Note: All claims expressed in this article are solely those of the authors and do not necessarily represent those of their affiliated organizations, or those of the publisher, the editors and the reviewers. Any product that may be evaluated in this article, or claim that may be made by its manufacturer, is not guaranteed or endorsed by the publisher.

Advantages of publishing in Frontiers

OPEN ACCESS
Articles are free to read for greatest visibility and readership

FAST PUBLICATION
Around 90 days from submission to decision

HIGH QUALITY PEER-REVIEW
Rigorous, collaborative, and constructive peer-review

TRANSPARENT PEER-REVIEW
Editors and reviewers acknowledged by name on published articles

Frontiers
Avenue du Tribunal-Fédéral 34
1005 Lausanne | Switzerland

Visit us: www.frontiersin.org
Contact us: frontiersin.org/about/contact

REPRODUCIBILITY OF RESEARCH
Support open data and methods to enhance research reproducibility

DIGITAL PUBLISHING
Articles designed for optimal readership across devices

FOLLOW US
@frontiersin

IMPACT METRICS
Advanced article metrics track visibility across digital media

EXTENSIVE PROMOTION
Marketing and promotion of impactful research

LOOP RESEARCH NETWORK
Our network increases your article's readership